

**University of Alberta**

**DEVELOPMENTAL STUDIES OF THE MEDULLA  
AND RESPIRATORY RHYTHM  
GENERATING CENTRE IN RODENT MODELS**

by

SILVIA PAGLIARDINI



A thesis submitted to the Faculty of Graduate Studies and Research  
in partial fulfillment of the requirements for the degree of

Doctor of Philosophy

Department of Physiology

Edmonton, Alberta

Fall 2006



Library and  
Archives Canada

Bibliothèque et  
Archives Canada

Published Heritage  
Branch

Direction du  
Patrimoine de l'édition

395 Wellington Street  
Ottawa ON K1A 0N4  
Canada

395, rue Wellington  
Ottawa ON K1A 0N4  
Canada

*Your file* *Votre référence*

*ISBN: 978-0-494-23093-0*

*Our file* *Notre référence*

*ISBN: 978-0-494-23093-0*

#### NOTICE:

The author has granted a non-exclusive license allowing Library and Archives Canada to reproduce, publish, archive, preserve, conserve, communicate to the public by telecommunication or on the Internet, loan, distribute and sell theses worldwide, for commercial or non-commercial purposes, in microform, paper, electronic and/or any other formats.

The author retains copyright ownership and moral rights in this thesis. Neither the thesis nor substantial extracts from it may be printed or otherwise reproduced without the author's permission.

#### AVIS:

L'auteur a accordé une licence non exclusive permettant à la Bibliothèque et Archives Canada de reproduire, publier, archiver, sauvegarder, conserver, transmettre au public par télécommunication ou par l'Internet, prêter, distribuer et vendre des thèses partout dans le monde, à des fins commerciales ou autres, sur support microforme, papier, électronique et/ou autres formats.

L'auteur conserve la propriété du droit d'auteur et des droits moraux qui protègent cette thèse. Ni la thèse ni des extraits substantiels de celle-ci ne doivent être imprimés ou autrement reproduits sans son autorisation.

---

In compliance with the Canadian Privacy Act some supporting forms may have been removed from this thesis.

Conformément à la loi canadienne sur la protection de la vie privée, quelques formulaires secondaires ont été enlevés de cette thèse.

While these forms may be included in the document page count, their removal does not represent any loss of content from the thesis.

Bien que ces formulaires aient inclus dans la pagination, il n'y aura aucun contenu manquant.

  
**Canada**

## Abstract

The preBötzinger Complex (preBötC) is composed of a group of neurons located in the ventrolateral medulla that is necessary for the generation of mammalian respiratory rhythm. The main focus of this thesis was toward understanding preBötC and medullary development in normal and pathological conditions using rodent models. Four major studies were undertaken. I determined the birth date, the settlement, and the inception of preBötC formation in the developing embryonic rat. That fundamental study provides a key foundation for work examining the ontogeny of respiratory neural control. I then performed a comprehensive anatomical study of the developing brainstem in a *necdin* deficient mouse model of Prader-Willi Syndrome (PWS). These mice, and newborn children with PWS, have abnormal breathing patterns. The data revealed wide-spread anatomical defects, including nuclei and axonal tracts that provide modulatory synaptic input to the preBötC. A second mutant mouse model, lacking the gene for the homeodomain transcription factor *Lbx1*, was examined. This study initially focused on understanding the basis for the severe respiratory dysfunction at birth in the mice and subsequently expanded into a detailed study of *Lbx1* expression and its role in the developing medulla. I determined that *Lbx1* is a key regulator for determining neuronal cell fate and neurotransmitter phenotype in the medulla. Those data, in conjunction with previous studies of *Lbx1* in the spinal cord, provide a comprehensive understanding of *Lbx1* function in the developing neuraxis. Finally, I developed a novel experimental method that will allow for the precise targeting of preBötC neurons expressing neurokinin-1 receptors (NK1R), to which the neuropeptide Substance P binds. These

neurons have been hypothesized to be essential for respiratory rhythmogenesis. Specifically, I determined that the internalization of tetramethylrhodamine conjugated Substance P in rhythmically active medullary slice preparations provided clear visualization of NK1R-expressing neurons for subsequent whole-cell patch clamp recordings. This approach should greatly expedite studies necessary for elucidating the cellular mechanisms within the preBötC.

## Table of contents

<b>Chapter I: General Introduction.....</b>	<b>1</b>
1.1 Overview.....	2
1.2 Neural Control of Respiratory Activity.....	3
1.2.1 Brainstem Respiratory Centers .....	3
1.2.2 Ventral Respiratory Group.....	5
1.2.3 PreBötzinger Complex and Respiratory Rhythm Generation .....	6
1.2.4 Anatomical and Electrophysiological Properties of PreBötC Neurons.....	7
1.2.5 Role of preBötzinger Complex Neurons in Respiratory Rhythmogenesis .....	11
1.2.6 Neuromodulation of PreBötzinger Complex .....	13
a) Glutamate .....	14
b) GABA and Glycine.....	15
c) Noradrenaline and adrenaline.....	16
d) Serotonin.....	17
e) Substance P.....	18
f) Opioids.....	18
g) Tyrotropin releasing hormone.....	18
h) ATP.....	19
i) Somatostatin.....	20
1.3 Ontogeny of Respiratory Rhythms.....	21
1.4 Brainstem Development.....	24
a) Catecholaminergic Centers in the Brainstem.....	27
b) Serotonergic Centers in the Brainstem.....	27
c) Ventral Respiratory Group.....	28
1.5 Respiratory Defect Associated with Genetic Disorder.....	29
1.6 References.....	42
<b>Chapter II: Ontogeny of the preBötzinger Complex in Perinatal Rats.....</b>	<b>60</b>
2.1 Introduction .....	61

2.2	Material and Methods.....	63
2.2.1	Animal Handling.....	63
2.2.2	Immunohistochemistry.....	63
2.2.3	Neuronal Birth Date Assessment via BrdU Injections.....	65
2.2.4	Confocal Imaging.....	65
2.2.5	Cell Counting and Measurements.....	66
2.2.6	In Vitro Preparations.....	67
2.2.7	Recording and analysis of Inspiratory Discharge.....	67
2.3	Results.....	69
2.3.1	NK1R Immunolabeling in the Newborn Medulla.....	69
2.3.2	NK1R Immunolabeling in the Prenatal Medulla.....	70
2.3.3	NK1R and ChAT Expression in the Prenatal Ventrolateral Medulla.....	70
2.3.4	Birth Dating of Medullary Neurons.....	71
2.3.5	BrdU, NK1R, and ChAT in the Prenatal Ventrolateral Medulla.....	72
2.3.6	Somatostatin Expression in the Perinatal Ventrolateral Medulla.....	73
2.3.7	Electrophysiological Recordings from Perinatal Medullary Slice Preparations .....	74
2.4	Discussion.....	76
2.4.1	Anatomical and Immunohistochemical Data.....	76
2.4.2	Birth Dates of Medullary Neurons.....	77
2.4.3	Electrophysiological recordings.....	78
2.5	Summary.....	80
2.6	References.....	94

**Chapter III: Developmental abnormalities of neuronal structure and function in prenatal mice lacking the Prader-Willi syndrome gene *necdin*.....99**

3.1	Introduction .....	100
3.2	Material and Methods.....	102
3.2.1	Mouse Breeding and Genotyping.....	102
3.2.2	Animal Handling for Anatomical Studies.....	102
3.2.3	Immunohistochemistry.....	102

3.2.4 Confocal Imaging.....	103
3.2.5 Volumetric Measurements and Cell Counts.....	103
3.2.6 Electron Microscopy.....	104
3.2.7 Brainstem-Spinal Cord and Medullary Slice Preparations.....	105
3.2.8 Recording and Analysis.....	105
3.3 Results.....	106
3.3.1 General Cytoarchitectural Features in the Medulla of <i>Ndn<sup>tm2Stw</sup></i> Mice.....	106
3.3.2 Organization of Neuronal Subpopulations within the Medulla of <i>Ndn<sup>tm2Stw</sup></i> Mice.....	107
3.3.3 Abnormalities within Medullary Dorsal Column Structures of <i>Ndn<sup>tm2Stw</sup></i> Mice.....	109
3.3.4 Ontogeny of Medullary Cytoarchitecture in <i>Ndn<sup>tm2Stw</sup></i> Mice.....	112
3.3.5 General Cytoarchitectural Features in the Spinal Cord of <i>Ndn<sup>tm2Stw</sup></i> Mice..	112
3.3.6 Main Cytoarchitectural Features in <i>Ndn<sup>tm2Stw</sup></i> Mice Diaphragm.....	114
3.3.7 Electrophysiological Recordings of Respiratory Rhythm Generated by <i>Ndn<sup>tm2Stw</sup></i> Mice.....	115
3.4 Discussion.....	117
3.4.1 Respiratory Related Defects within the Medulla of <i>Ndn<sup>tm2Stw</sup></i> Mice.....	118
3.4.2 Defects within Gracile and Cuneate Nuclei .....	119
3.4.3 Spinal Cord and Diaphragm Defects.....	120
3.4.4 Potential Mechanisms Underlying Pathogenesis.....	121
3.4.5 Relevance to Prader-Willi Syndrome.....	121
3.5 References.....	139
<b>Chapter IV: Fluorescent Tagging of Rhythmically Active Respiratory Neurons within the Pre-Bötzinger Complex of Rat Medullary Slice Preparations.....</b>	<b>148</b>
4.1 Introduction.....	149
4.2 Material and Methods.....	150
4.2.1 Medullary Slice Preparation.....	150

4.2.2 Tetramethylrhodamine Conjugated-SubP Application in Living Medullary Slice.....	150
4.2.3 Immunohistochemistry.....	151
4.2.4 Confocal Imaging of Fixed Tissue.....	151
4.2.5 Recording and Analysis.....	152
4.3 Results.....	153
4.3.1 Diffusion and Internalization of TMR-SubP in medullary slices.....	153
4.3.2 Whole-Cell Recording from Fluorescently Tagged PreBötC Neurons.....	154
4.4 Discussion.....	156
4.5 References.....	163
<b>Chapter V: Role of Lbx1 in the Formation of Relay Somatic Sensory Neurons in the Developing Medulla.....</b>	<b>166</b>
5.1 Introduction.....	167
5.2 Material and Methods.....	170
5.2.1 Generation and Genotyping of <i>Lbx1</i> <sup>GFP/GFP</sup> Mice.....	170
5.2.2 Animal Handling.....	170
5.2.3 Immunohistochemistry .....	170
5.2.4 Bright Field and Confocal Imaging.....	171
5.2.5 In Vitro Embryonic Slice Preparation.....	172
5.2.5.1 Brainstem-Spinal Cord-Diaphragm Preparations.....	172
5.2.5.2 Medullary Slice Preparations.....	173
5.2.5 Recording and Analysis.....	173
5.3 Results.....	174
5.3.1 <i>Lbx1</i> Expression in the Prenatal Medulla.....	174
5.3.2 <i>Lbx1</i> Expression in the Medulla during Development .....	175
5.3.3 Cytoarchitectonical Abnormalities in the Brainstem of <i>Lbx1</i> <sup>GFP/GFP</sup> Mice. ....	176
5.3.4 Lbx1 Expression is Necessary for the Proper Development of Dorsal Interneuronal Population in the Developing Hindbrain.....	177

5.3.5 Inactivation of <i>Lbx1</i> Alters the Developmental Program of Inferior Olive Formation.....	180
5.3.6 Inactivation of <i>Lbx1</i> alters the Developmental Program of the Solitary Tract Nucleus.....	181
5.3.7 Analysis of the Respiratory Rhythm Generating Pattern Generated by <i>Lbx1</i> <sup>GFP/+</sup> and <i>Lbx1</i> <sup>GFP/GFP</sup> Mice.....	186
5.3.8 Structural Analysis of the Respiratory Rhythm Generating Centre in the Medulla of <i>Lbx1</i> <sup>GFP/+</sup> and <i>Lbx1</i> <sup>GFP/GFP</sup> Mice.....	187
5.4 Discussion.....	189
5.4.1 Expression of <i>Lbx1</i> in the Medulla and Cytoarchitectonical Abnormalities in <i>Lbx1</i> <sup>GFP/GFP</sup> Mice.....	189
5.4.2 Characterization of <i>Lbx1</i> <sup>+</sup> Neurons in the Medulla of <i>Lbx1</i> <sup>GFP/+</sup> and <i>Lbx1</i> <sup>GFP/GFP</sup> Mice.....	190
5.4.3 Analysis of the Ventrolateral Medulla and the Respiratory Function in <i>Lbx1</i> <sup>GFP/+</sup> and <i>Lbx1</i> <sup>GFP/GFP</sup> Mice.....	195
5.5 References.....	214
<b>Chapter VI: General Discussion.....</b>	<b>221</b>
6.1 Ontogeny of preBötzinger Complex Neurons in Perinatal Rats.....	222
6.2 Analysis of Developmental Abnormalities in the Medulla of <i>Ndn</i> <sup>tm2Stw</sup> Mouse.....	228
6.3 Tagging of NK1R <sup>+</sup> preBötzinger Complex Neurons with TMR-Substance P.....	232
6.4 Developmental Abnormalities in the Medulla of Mice Lacking the Expression of the homeodomain transcription factor <i>Lbx1</i> .....	236
6.5 Conclusions.....	238
6.6 References.....	239

## List of tables

<b>Table 1.1.</b> Transcription factor mutations affecting specific central respiratory neurons in mice and identified corresponding mutations in human respiratory syndromes.....	38
<b>Table 1.2</b> Abnormalities in the respiratory rhythms of mutant mice in the perinatal period.....	40
<b>Table 2.1</b> Characterization of inspiratory bursts recorded from the preBötzinger complex of rat medullary slice preparations isolated from perinatal rats.....	93
<b>Table 3.1</b> Antibodies utilized in the study.....	138

## List of figures

<b>Figure 1.1</b> Brainstem nuclei involved in the neural control of breathing.....	31
<b>Figure 1.2</b> Classes of medullary respiratory neurons spontaneously active in vitro.....	33
<b>Figure 1.3</b> Reconstruction of spatial distributions of inspiratory and expiratory neuron activity in ventrolateral reticular formation at medullary levels extending from the pyramidal decussation to the caudal pole of facial nucleus.....	34
<b>Figure 1.4</b> Rhombomeric blueprint for the hindbrain in the nervous system.....	35
<b>Figure 1.5</b> Transcription factor requirement in the development of respiratory hindbrain neurons.....	36
<b>Figure 1.6.</b> Expression of transcription factors in progenitor cells and differentiating neurons of the mice spinal cord.....	37
<b>Figure 2.1</b> Rostrocaudal distribution of NK1R <sup>+</sup> neurons within the ventrolateral medulla of perinatal rats.....	81
<b>Figure 2.2</b> Size distribution of NK1R <sup>+</sup> neurons located in the preBötC at different perinatal ages.....	82
<b>Figure 2.3</b> NK1R expression in medullary structures of P2 rats.....	83
<b>Figure 2.4</b> Colocalization of NK1R and ChAT is prominent in the nucleus ambiguus but mostly absent within the preBötC of prenatal rats.....	84
<b>Figure 2.5</b> NK1R <sup>+</sup> neurons within the preBötC are born 2 days later than those within the NA.....	85
<b>Figure 2.6</b> Most NK1R <sup>+</sup> neurons within the preBötC are born on E12.5 and E13.5.....	86
<b>Figure 2.7</b> Size of NK1R <sup>+</sup> neurons born on E12.5 and E13.5 located in the preBötC....	87
<b>Figure 2.8</b> Spatiotemporal distribution of the birth dates of NK1R <sup>+</sup> and ChAT <sup>+</sup> neurons in the ventrolateral medulla of prenatal rats (E15-E18) .....	88
<b>Figure 2.9</b> A subpopulation of neurons within the preBötC of perinatal rats expresses both SST and NK1R.....	89
<b>Figure 2.10</b> Size of SST <sup>+</sup> neurons within the preBötC .....	90
<b>Figure 2.11</b> Respiratory discharge patterns generated by perinatal medullary slice preparations.....	91
<b>Figure 2.12</b> Substance P causes a marked increase in the frequency of respiratory rhythm generated by E17 in vitro preparations.....	92

<b>Figure 3.1</b> Cytoarchitectural abnormalities in the medulla of <i>Ndn<sup>tm2Stw</sup></i> mice.....	123
<b>Figure 3.2</b> NK1R, NF and vimentin expression in wild-type and <i>Ndn<sup>tm2Stw</sup></i> mice at E18.....	124
<b>Figure 3.3</b> Expression of NK1R, ChAT, SubP, SST and 5HT in the ventral medulla of wild-type and <i>Ndn<sup>tm2Stw</sup></i> mice at E18.....	125
<b>Figure 3.4</b> Expression of TH in the medulla of wild-type and <i>Ndn<sup>tm2Stw</sup></i> mice.....	127
<b>Figure 3.5</b> Expression of NF and GAP43 in the dorsal column in <i>Ndn<sup>tm2Stw</sup></i> mice during development.....	128
<b>Figure 3.6</b> Calcium binding proteins in the medullary dorsal column in E18 wild-type and <i>Ndn<sup>tm2Stw</sup></i> mice.....	129
<b>Figure 3.7</b> Ultrastructural analysis of the dorsal column in wild-type and <i>Ndn<sup>tm2Stw</sup></i> mice.....	131
<b>Figure 3.8</b> GAP43 expression at different caudo-rostral level of the brainstem in wild-type and <i>Ndn<sup>tm2Stw</sup></i> mice at E11.....	132
<b>Figure 3.9</b> Expression of NF and GAP43 in the cervical spinal cord of wild-type and <i>Ndn<sup>tm2Stw</sup></i> mice.....	133
<b>Figure 3.10</b> Expression of TAG1, GAP43, NF and L1 in cervical spinal cord of wild-type and <i>Ndn<sup>tm2Stw</sup></i> mice at E10 and E11.....	134
<b>Figure 3.11</b> Diaphragm innervation of wild-type and <i>Ndn<sup>tm2Stw</sup></i> mice at E16.....	136
<b>Figure 3.12</b> Effects of excitatory neuromodulators on respiratory rhythm generated by <i>Ndn<sup>tm2Stw</sup></i> mouse brainstem-spinal cord preparations.....	137
<b>Figure 4.1</b> Bath application of TMR-SubP (500 nM) reversibly increases the frequency of endogenous inspiratory-related bursts generated by medullary slice preparations.....	159
<b>Figure 4.2</b> Internalization of TMR-SubP in living medullary slice preparations.....	160
<b>Figure 4.3</b> Whole–cell recording from fluorescently tagged preBötC neurons.....	161
<b>Figure 5.1</b> Expression of GFP in <i>Lbx1<sup>GFP/+</sup></i> Mice at E18.....	198
<b>Figure 5.2</b> GFP Expression in the Medulla of <i>Lbx1<sup>GFP/+</sup></i> and <i>Lbx1<sup>GFP/GFP</sup></i> Mice during Embryonic Development.....	199
<b>Figure 5.3</b> Cytoarchitectural Abnormalities in the Medulla of <i>Lbx1<sup>GFP/GFP</sup></i> Mice at E18.....	201

<b>Figure 5.4</b> GFP, <i>Pax2</i> and <i>Lmx1b</i> Expression in the Medulla of <i>Lbx1</i> <sup>GFP/+</sup> and <i>Lbx1</i> <sup>GFP/GFP</sup> Mice at E10, E11 and E12.....	202
<b>Figure 5.5</b> GFP and <i>Pax2</i> Expression in the Medulla of <i>Lbx1</i> <sup>GFP/+</sup> and <i>Lbx1</i> <sup>GFP/GFP</sup> Mice at E18.....	204
<b>Figure 5.6</b> GFP and <i>FoxP2</i> Expression in the Medulla of <i>Lbx1</i> <sup>GFP/+</sup> and <i>Lbx1</i> <sup>GFP/GFP</sup> Mice at E12, E13 and E17.....	205
<b>Figure 5.7</b> GFP, <i>Phox2b</i> and ChAT Expression in the Medulla of <i>Lbx1</i> <sup>GFP/+</sup> and <i>Lbx1</i> <sup>GFP/GFP</sup> Mice at E11, E12 and E13.....	206
<b>Figure 5.8</b> GFP and <i>Phox2b</i> Expression in the Medulla of <i>Lbx1</i> <sup>GFP/+</sup> and <i>Lbx1</i> <sup>GFP/GFP</sup> Mice at E18.....	208
<b>Figure 5.9</b> GFP, Calbindin and Calretinin Expression in the Medulla of <i>Lbx1</i> <sup>GFP/+</sup> and <i>Lbx1</i> <sup>GFP/GFP</sup> Mice at E18.....	209
<b>Figure 5.10</b> Calbindin and Calretinin Expression in the Medulla of <i>Lbx1</i> <sup>GFP/+</sup> and <i>Lbx1</i> <sup>GFP/GFP</sup> Mice at E11.5 and E13.5.....	210
<b>Figure 5.11</b> GFP and TH expression in the medulla of <i>Lbx1</i> <sup>GFP/+</sup> and <i>Lbx1</i> <sup>GFP/GFP</sup> mice at E18.....	211
<b>Figure 5.12</b> Respiratory Discharge Patterns Generated in the Brainstem-Spinal Cord-Diaphragm Preparations (top) and in the Medullary Slice Preparations of Wild-Type and Mutant Animals at E18.....	212
<b>Figure 5.13</b> GFP, NK1R, ChAT and SST Expression in the Ventrolateral Medulla of <i>Lbx1</i> <sup>GFP/+</sup> and <i>Lbx1</i> <sup>GFP/GFP</sup> Mice at E18.....	213

## List of symbols, nomenclature abbreviations

5HT	serotonin
VII	facial nucleus
X	dorsal motor nucleus of the vagus nerve
XII	hypoglossal nucleus
aCSF	artificial cerebrospinal fluid
AMPA	$\alpha$ -amino-5-hydroxy-3-methyl-4-isoxazole propionic acid
BötC	Böttinger Complex
BrdU	5-Bromo-2'deoxyuridine
BSA	bovine serum albumin
Ca <sup>2+</sup>	calcium ion
CB	calbindin 28kD
CCHS	congenital central hypoventilation syndrome
CR	calretinin
Cd <sup>2+</sup>	cadmium ion
ChAT	choline acetyl transferase
CNQX	6-cyano-7-nitroquinoxaline-2,3-dione
CO <sub>2</sub>	carbon dioxide
Cu/Cn	cuneate nucleus
cu/cn	cuneate funicle
cVRG	caudal Ventral Respiratory Group
DAM	donkey anti-mouse
DAR	donkey anti-rabbit
DAG	donkey anti-goat
DRG	Dorsal Respiratory Group
dI	dorsal interneuron
dIL	late-born dorsal interneurons
E	expiratory
EMG	Electromyography
FBMs	fetal breathing movements
<i>FoxP2</i>	<i>winged-helix/forkhead (Fox) P2</i> transcriptional repressor gene
FoxP2	<i>winged-helix/forkhead (Fox) P2</i> transcriptional repressor gene product
fp	floor plate
GABA	$\gamma$ -aminobutyric acid
GAP43	growth associated protein 43
GFP	green fluorescent protein
GH	growth hormone
Gr	gracile nucleus
gr	gracile funicle
I	inspiratory
I <sub>CAN</sub>	Ca <sup>2+</sup> -activated inward cationic current
I <sub>h</sub>	hyperpolarization-activated current
I <sub>NaP</sub>	Na <sup>+</sup> persistent current
IR-DIC	infrared - differential interference contrast

IRt	intermediate reticular nucleus
<i>Lmx1b</i>	LIM homeodomain-containing gene
Lmx1b	LIM homeodomain-containing gene product
<i>Lbx1</i>	<i>Ladybird1</i> homeodomain transcription factor gene
Lbx1	<i>Ladybird1</i> homeodomain transcription factor gene product
LHRH	luteinizing hormone-releasing hormone
LRN	lateral reticular nucleus
μOR	μ opioid receptors
MAP2	anti-microtubule associated protein2
MdD	dorsal medullary reticular formation
MdV	ventral medullary reticular formation
MN	motoneuron
Na <sup>+</sup>	sodium ion
NA	nucleus ambiguus
NAc	compact division of the nucleus ambiguus
NAI	nucleus ambiguus, loose formation
NAsc	semicompact division of the nucleus ambiguus
Ndn	neccdin
NF	neurofilament
NK1R	Neurokinin1 Receptor
NK1R <sup>+</sup>	NK1R expressing
NMDA	<i>N</i> -methyl-D-aspartic acid
np	neuroepithelium
nr	nerve root
O <sub>2</sub>	Oxygen
<i>Pax2</i>	paired box transcription factor gene
Pax2	paired box 2 transcription factor gene product
PB	phosphate buffer
PBS	saline phosphate buffer
PCRt/PR	parvocellular reticular nucleus
pFRG/RTN	para Facial Respiratory Group/RetroTrapezoid Nucleus
Phox2b	<i>homeodomain transcription factorPhox2b gene</i>
Phox2b	homeodomain transcription factorPhox2b gene product
preI	pre-inspiratory
preBötC /PBC	preBötzinger Complex
PR	parvicellular reticular formation
PRG	Pontine Respiratory Group
PV	parvalbumin
PWS	Prader-Willi Syndrome
RFN	retrofacial nucleus
rp	roof plate.
RP	raphe pallidus
RTN	retrotrapezoid nucleus
r	rhombomere
rVRG	rostral Ventral Respiratory Group
SD	standard deviation

SIDS	sudden infant death syndrome
Sl	sulcus limitans
sol	solitary tract
Sp5/ SpV	spinal trigeminal nucleus
SpVc	spinal trigeminal nucleus, subnucleus caudalis
SpVi	spinal trigeminal nucleus, subnucleus interpolaris
SpVo	spinal trigeminal nucleus, subnucleus oralis
SST	somatostatin
STN (Sol)	solitary tract nucleus
SubP	substance P
SubP-SAP	substance P conjugated to saporin
TF	transcription factor
TH	tyrosine hydroxylase
TMR-SubP	Tetramethylrhodamine conjugated-Substance P
TRH	tyrotropin releasing hormone
TSA	tyramide signal amplification
Ve	vestibular nucleus
VGLUT2	vesicular glutamate transporter 2
vml	ventral midline
VRG	Ventral Respiratory Group

# **CHAPTER I**

## **General Introduction**

## 1.1 OVERVIEW

Respiration is a necessary behavior for human and animal life. The fundamental function accomplished by respiration is to provide gas exchange in the lungs in order to maintain adequate levels of oxygen and carbon dioxide in the whole body to promote cell metabolism and regulate pH. This function is mediated by a mechanism of gas exchange at the interface between the alveolar epithelium and the pulmonary capillary endothelium within the lungs. In order to maintain constant levels of blood gasses, a coordinated contraction of respiratory muscles must occur continuously, from birth to the last breath. Further, respiratory muscle activity has to adapt through life to several challenges, such as development, aging, body weight variations, physical activity, pregnancy and pathological conditions. In every situation the respiratory system has to appropriately respond, either in the long or in the short term, in order to support gas homeostasis.

The fine regulation of respiratory activity is not a mere reflex but it is highly regulated by the nervous system. In particular, several regions in the brainstem are responsible for the precise control of respiratory rhythms and the coordination of muscle contractions. Among them, the preBötzinger Complex (preBötC) is a key component in inspiratory rhythmogenesis. A major aim of this thesis is to provide fundamental knowledge about the anatomical and physiological maturation of preBötC and the adjacent medullary structures in normal and pathological conditions.

By elucidating the crucial events involved in the development of respiratory rhythm generating center, it is hoped that the results of this thesis will enhance our basic knowledge in this important area, provide a fundamental ground work for future studies and potentially help to understand conditions in which breathing can be compromised in newborns and to develop pharmacological strategies to help normalize breathing.

## 1.2 NEURAL CONTROL OF RESPIRATORY ACTIVITY

### 1.2.1 BRAINSTEM RESPIRATORY CENTERS

Control of respiratory activity by the central nervous system occurs primarily at the level of the brainstem. In mammals respiratory control occurs in three major centers: pons (pontine respiratory group, PRG), dorsal medulla (dorsal respiratory group, DRG) and ventrolateral medulla (ventral respiratory group, VRG) (fig1.1).

The parabrachial (PB, lateral and medial) and the Kölliker–Fuse (KF) nuclei are the main components of the PRG; these structures have been proposed to be important centers for the sensory integration of adaptive behaviors in the respiratory system. PB and KF receive extensive somato and viscerosensory inputs from the solitary tract nucleus (STN), the spinal trigeminal nucleus (SpV) and indirectly from the upper and lower airways. These nuclei are thought to integrate and process the inputs they receive and send projections to the sensory nuclei and other respiratory center to modulate their activity. PB and KF nuclei contribute to neuromodulation of medullary centers and are involved in the diving reflex, vocalization, the Hering-Breuer reflex, and in the control of airway muscles during exercise and sleep (Dutschmann et al., 2004 Alheid et al., 2004; Chamberlin, 2004).

The ventrolateral region of the STN in the dorsal medulla is the principal component of the DRG. It contains neurons that fire during inspiration and it is an important relay station for inputs coming from the carotid bodies involved in peripheral chemoreception (reviewed in Nattie, 1999; Feldman et al., 2003).

The VRG is a columnar cluster of respiratory neurons located close to the ventral surface of the medulla. In this region, several inputs from higher level of the brain (responsible for controlling voluntary respiratory activity), peripheral and central chemoreception centers (responsible for maintaining appropriate blood levels of O<sub>2</sub>, and CO<sub>2</sub>) and other respiratory and non-respiratory centers within the brainstem (integrative centers in both pons and medulla) converge to coordinate and maintain appropriate respiratory patterns and frequency (Feldman et al., 2003). Ineed the VRG is the major

focus of research investigation because it is hypothesized, as outlined below, to contain the minimal circuit responsible for respiratory rhythmogenesis.

### 1.2.2 VENTRAL RESPIRATORY GROUP

The extension of the VRG within the medulla spans from the caudal end of the facial nucleus to the rostral end of the lateral reticular nucleus, ventral to the column of motoneurons (MNs) of the nucleus ambiguus (fig1.1). Within the VRG, several neurons with respiratory-related activity have been recorded and multiple classifications of neurons based upon their firing patterns, their membrane potential changes and their synaptic inputs have been proposed (Ezure et al., 1988; Ezure, 1990; Smith et al., 1990; Schwarzacher et al., 1995). Respiratory related neurons were thus classified as: pre-inspiratory, early inspiratory, late inspiratory, inspiratory, post-inspiratory and expiratory neurons according to their firing pattern in respect to the respiratory cycle (figs1.2, 1.3).

Neurons in the VRG column then project to specific MNs responsible for controlling contraction of respiratory muscle in the upper airways and the tongue (hypoglossal motor nucleus, glossopharyngeal vagal MNs in the nucleus ambiguus, NA), intercostal muscles (thoracic spinal MNs), diaphragm (phrenic spinal MNs at spinal cervical level) and abdominal muscles (lumbar spinal MNs).

Within the VRG, functionally different regions have been identified: caudal VRG (cVRG), rostral VRG (rVRG), the preBötC, the Böttinger complex (BötC) and the para facial respiratory group/retrotrapezoid nucleus (pFRG/RTN) (fig1.1). The caudal VRG contains neurons firing during expiration, rVRG contains mainly inspiratory premotor neurons, preBötC contains respiratory neurons that fire during inspiration and BötC neurons show primarily an inhibitory expiratory discharge pattern (Ezure et al., 1988; Ezure, 1990; Smith et al., 1990; Schwarzacher et al., 1995).

### **1.2.3 PREBÖTZINGER COMPLEX AND RESPIRATORY RHYTHM GENERATION**

In the last decade the region of the preBötC has been the major site for research in the field of respiratory neurobiology. This is the consequence of a seminal paper published by Smith and collaborators in the early 90s, in which they provided evidence to support the hypothesis that the preBötC is a key site for respiratory rhythm generation. Using the neonatal rat brainstem-spinal cord preparation and serial transverse microsectioning of the medulla, either starting from the pontomedullary junction or the spinomedullary junction, they identified a relatively small region within the ventrolateral medulla, that was able to generate a respiratory-like rhythmic activity similar to the oscillations generated in the brainstem spinal cord preparation (Smith et al., 1991).

The rostro-caudal extension of this region corresponds to the location of the preBötC, in which neurons with voltage dependent bursting properties were identified and further analyzed (Smith et al., 1991). Since reduction of synaptic inhibition by administration of GABAergic and glycinergic antagonists to in vitro preparations has little effect on rhythm generation and neurons with pacemaker properties were identified within the preBötC, the most likely hypothesis for respiratory rhythm generation was based on the key role of pacemaker neurons to drive rhythmogenesis rather than a network driven by recurrent inhibition (Feldman and Smith, 1989; Onumaru et al., 1989). However, this hypothesis has been recently challenged by the discovery of alternate sites for respiratory rhythm generation (pFRG/RTN) and by studies on electrophysiological properties of preBötC pacemaker neurons (reviewed in Feldman and Del Negro, 2006 and discussed below).

#### 1.2.4 ANATOMICAL AND ELECTROPHYSIOLOGICAL PROPERTIES OF PREBötC NEURONS

Following the initial study by Smith and collaborators, several studies focused their attention on the region, trying to identify specific properties of preBötC neurons. Initially, tract-tracing studies (Ellenberger and Feldman, 1990; Smith et al., 1991) demonstrated that the region corresponding to the preBötC was particularly abundant with propriobulbar neurons with contralateral projections (70% of neurons were propriobulbar in comparison to 40% in the adjacent regions of the VRG), neurons whose projections are restricted to the medulla and have no direct axonal projections to respiratory muscles. The majority of excitatory inputs received by the region of preBötC were originating from the solitary tract nucleus, the adjacent region of the VRG superficial to the facial nucleus (the region corresponding to pFRG/RTN), the medullary raphe nuclei and the parabrachial/Kolliker-Fuse nuclei (Ellenberger and Feldman, 1994).

Another critical advancement in the study of the preBötC neurons' properties was the identification of a specific marker for this region. Frequency of respiratory rhythm can be modified by several neuromodulators; one of them, substance P (SubP), causes an increase in frequency of endogenous respiratory related motor output, both *in vivo* and *in vitro*, when applied directly to the preBötC (Chen et al., 1990; Chen et al., 1991; Monteau et al., 1996). The physiological response to SubP is due to the expression of the high affinity receptor for SubP, neurokinin1 receptor (NK1R), in rhythm generating neurons located within the preBötC (Gray et al., 1999). The discovery led to the use of NK1R immunoreactivity as an anatomical marker for the region of preBötC.

Detailed analysis of NK1R expressing (NK1R<sup>+</sup>) neurons within the preBötC of adult rats in combination with electrophysiological recordings provided further information regarding the anatomical and electrophysiological properties of neurons located in the region:

i) Both type I and type II neurons within the preBötC (Rekling et al., 1996b) respond to SubP and express NK1R. Type I neurons present rhythmogenic properties, they respond to both thyrotropin releasing hormone (TRH) and opioids and they also express  $\mu$  opioid receptors ( $\mu$ OR). Type II neurons are respiratory neurons that do not

have rhythmogenic properties, they do not respond to opioids, and do not express  $\mu$ OR (Gray et al., 1999).

ii) A high percentage of NK1R<sup>+</sup> neurons in preBötC are indeed respiratory neurons with a pre-I neuron bursting pattern (11 of 32 pre-I neurons recorded *in vivo* in anesthetized rats were NK1R<sup>+</sup>; no NK1R immunoreactivity in 20 neurons with different recorded discharge pattern) (Guyenet and Wang, 2001).

iii) NK1R<sup>+</sup> neurons in the rat preBötC are predominantly propriobulbar glutamatergic interneurons (Wang et al., 2001; Guyenet et al., 2002) and they differ from other NK1R<sup>+</sup> neurons in other regions of the VRG by expressing high levels of somatostatin (SST) (Stornetta et al., 2003) along with vesicular glutamate transporter 2 (VGLUT2) (Liu et al., 2003) and by lacking markers for acetylcholine, catecholamines (Wang et al., 2001) and expression of preproenkephalin mRNA (Stornetta et al., 2003). Very few NK1R<sup>+</sup> preBötC neurons are GABAergic ( $\gamma$ -aminobutyric acid expressing) or glycinergic (Wang et al., 2001), whereas a small fraction of bulbospinal C1 catecholaminergic (5.3% of the total catecholaminergic cell in A1/C1 region) neurons also express NK1R (Makeham et al., 2001).

iv) NK1R<sup>+</sup> neurons in the preBötC receive synaptic inputs from GABAergic, glycinergic and glutamatergic neurons (Liu et al., 2002). SubP and enkephalin are also present in glutamatergic terminals, suggesting the presence of a dense network of projections, both excitatory and inhibitory, onto the preBötC neurons from several neuronal groups (Liu et al., 2004).

Analysis of electrical properties of preBötC neurons revealed that the region contains a large number of inspiratory and pre-inspiratory neurons (Ezure et al., 1988; Ezure, 1990; Smith et al., 1990; Schwarzacher et al., 1995). When properties of preBötC respiratory neurons were analyzed via extracellular recordings in neonatal rat medullary slice preparations, several neurons showed bursting properties, the majority of them fired during the inspiratory phase (41/63 recorded neurons) and only a few had properties of tonic expiratory neurons (4/63) or tonic neurons (18/63) (Johnson et al., 1994).

Amongst the currents that might sustain pacemaker properties in preBötC neurons of rats and mice, it has been shown that preBötC neurons express sodium (Na<sup>+</sup>)-

persistent current ( $I_{NaP}$ ), the hyperpolarization-activated current ( $I_h$ ) and a calcium ( $Ca^{2+}$ )-activated inward cationic current ( $I_{CAN}$ ) during the neonatal period (Thoby-Brisson et al., 2000; Del Negro et al., 2002; Pena et al., 2004; Del Negro et al., 2005). These currents are expressed in pacemaker and non-pacemaker neurons within the preBötC and may promote rhythmogenesis. Bursting activity of pacemaker neurons can be explained by a higher ratio of persistent  $Na^+$  conductance versus voltage-insensitive leak conductance in comparison to non-pacemaker neurons within the preBötC (Del Negro et al., 2002).

Thoby-Brisson and Ramirez (2001) identified two different classes of pacemaker neurons within the mouse preBötC: in one group of neurons the bursting behavior was cadmium ( $Cd^{2+}$ ) / flufenamic acid sensitive (evidence for expression of  $I_{CAN}$ ), hypoxia sensitive and riluzole insensitive whereas in a second group bursting behavior was characterized by opposite properties:  $Cd^{2+}$ / flufenamic acid insensitive, hypoxia insensitive and riluzole sensitive (evidence for expression of  $I_{NaP}$ ) (Thoby-Brisson and Ramirez, 2000, 2001). The two currents are differentially expressed during development (Del Negro et al., 2005) and may contribute to a different network configuration during eupnea and gasping both in vivo and in vitro (Lieske et al., 2000; Pena et al., 2004; Paton et al., 2006). It has also been shown that  $I_{NaP}$  may play an important role in stabilizing the membrane potential of pacemaker neurons in such a way that bursting and rhythmogenesis are safely maintained (Tryba and Ramirez, 2004).

Interestingly, when one current is pharmacologically eliminated the respiratory rhythm is maintained in vitro, but when both currents are eliminated, the rhythm can subsist by application of neuromodulators that increase neuronal excitability (Del Negro et al., 2005). These data support the hypothesis that pacemaker neurons in preBötC are likely to play a key role in respiratory rhythm generation, probably stabilizing network rhythmicity, but they are not the only mechanism underlying respiratory rhythms (see the following chapter).

It is important to note that  $NK1R^+$  neurons are only a subset of preBötC neurons. The anatomical properties of other neuronal subpopulations within the preBötC have not yet been investigated due to the complex cytoarchitecture of the ventrolateral medulla. In this region, neurons with various autonomic physiological functions coexist (cardiovascular, respiratory) making the analysis of respiratory-related neurons quite

challenging. A combined analysis of electrophysiological and anatomical properties on the same neurons would be the most informative approach to study the area. Up to now, very few studies used a combined approach (Gray et al., 1999; Guyenet and Wang, 2001; Pena and Ramirez, 2004), therefore the anatomical data focused mainly on the NK1R<sup>+</sup> expressing neurons within the preBötC, whereas the electrophysiological data were based on pacemaker properties of recorded neurons without identifying the recorded neurons according to their expression for NK1R or other identified anatomical markers.

### 1.2.5 ROLE OF PREBÖTZINGER COMPLEX NEURONS IN RESPIRATORY RHYTHMOGENESIS

Are preBötC NK1R<sup>+</sup> neurons necessary for respiratory rhythmogenesis in vivo? To test this hypothesis, a selective lesion of this neuronal population was conducted in adult rats and goats. The selective destruction of the preBötC NK1R<sup>+</sup> neurons was induced by local application of SubP conjugated to saporin (SubP-SAP), a toxin that is selectively internalized in cells that express the receptor for SubP and acts inside the cells as a ribosome-inactivating protein, causing cell death. SubP-SAP induced progressive cell death of NK1R<sup>+</sup> cells in the preBötC region, inducing an initial perturbation of respiratory activity during REM sleep (McKay et al., 2005), followed by ataxic breathing and altered responses to low O<sub>2</sub> or high CO<sub>2</sub> levels challenges when neuronal degeneration reached 80% of the total amount of preBötC NK1R<sup>+</sup> neurons (Gray et al., 2001; Wenninger et al., 2004a; Wenninger et al., 2004b).

Analyses of respiratory phenotype in absence of NK1R or SubP, either blocked pharmacologically or by means of a genetic deletion (NK1R and SubP knockout mice), revealed that rodents survive and do not show serious respiratory defects at rest in absence of expression of either SubP or NK1R (De Felipe et al., 1998; Telgkamp et al., 2002). These results provided the evidence for a necessary role of preBötC NK1R<sup>+</sup> neurons in regular breathing, whereas expression of NK1R and its ligand within the preBötC is not critical for quiet breathing.

Is the preBötC the only region critical for the generation of respiratory activity? Since the late 80s, an alternative site for respiratory rhythmogenesis was proposed (Onimaru et al., 1987, 1988, 1989). Neurons with a pre-inspiratory phenotype and voltage dependent bursting properties were identified rostral to the BötC, in a region partially overlapping with the chemosensitive region of the retrotrapezoid nucleus (RTN) and adjacent to the facial nucleus. Onimaru and colleagues named therefore the pFRG/RTN (Ballanyi et al., 1999; Onimaru and Homma, 2003).

Recent data have suggested that the pFRG/RTN may have a role in respiratory rhythm generation in combination with preBötC in particular physiological conditions (Janczewski et al., 2002; Mellen et al., 2003; Onimaru and Homma, 2003; Janczewski

and Feldman, 2006; Onimaru et al., 2006a). Anatomical and physiological data showed that preBötC neurons express NK1R and  $\mu$ OR (Gray et al., 1999). pFRG/RTN preI neurons respond to SubP but not to opioids (Yamamoto et al., 1992; Mellen et al., 2003). When DAMGO, a  $\mu$ OR agonist, is applied to medullary slice preparation (containing preBötC but not RTN/pFRG) it causes a gradual increase in respiratory periods (Mellen et al., 2003). In the *en bloc* preparation, where both pFRG/RTN and preBötC are present, opioid agonists cause a step-like lengthening of respiratory period that correspond to exact increments of respiratory periods (quantal slowing). Therefore a quantal slowing of respiratory rhythm occurs when preBötC neurons are inactivated following  $\mu$ OR activation (Mellen et al., 2003).

This phenomenon occurs also when fentanyl, another opioid receptor agonist, is administered to juvenile anesthetized and vagotomized rats (Janczewski and Feldman, 2006). In vivo, inspiratory activity is quantally reduced, but expiratory frequency is not affected unless a transection caudal to the region corresponding to pFRG/RTN eliminates expiratory activity.

When a similar transection was performed in *en bloc* preparations, Onimaru and colleagues were able to obtain respiratory related recordings from the region corresponding to pFRG/RTN, rostral to the transection and the preBötC, caudal to the transection (Onimaru et al., 2006a).

Collectively, these data can be interpreted in two alternative ways, as discussed in a point-counterpoint article format recently published in the Journal of Applied Physiology (Onimaru et al., 2006b): one hypothesis is that pFRG/RTN is the respiratory rhythm generator and preBötC is instead the inspiratory pattern generator. PreBötC is directly activated and modulated by pre-inspiratory neurons located in the pFRG/RTN region. An alternative view is that the preBötC has a fundamental role in generating inspiratory rhythms and the pFRG/RTN, rather than being an alternative site for respiratory rhythm generation, has a key role in expiratory rhythm generation. In physiological conditions, when the preBötC is intact, it is the driving force for respiratory rhythms; when the preBötC is depressed or absent, the pFRG/RTN may overcome the respiratory depression and drive respiratory rhythms favoring an active expiration and passive inspiration (Feldman and Del Negro, 2006).

### 1.2.6 NEUROMODULATION OF PREBÖTZINGER COMPLEX

Major aims in the field of respiratory neurobiology are to comprehend how respiratory rhythms are generated, how they maintain homeostasis and how they are modulated in different physiological and pathological conditions.

Different challenges can affect respiratory activity under acute or chronic circumstances. Variation in oxygen requirements due to physiological challenges (development, exercise, pregnancy, altitude variation) or pathological conditions (weight gain or loss, ageing, heart and lung diseases) can induce adaptive responses in the respiratory system that are mediated by changes in frequency of respiratory activity or in intensity in the contraction of respiratory muscle and both changes ultimately affect respiratory parameters (i.e. minute ventilation, tidal volume).

Since the main purpose of the respiratory system is to provide O<sub>2</sub> to the whole body, O<sub>2</sub> blood levels have a very potent effect on respiratory regulation. O<sub>2</sub> levels are detected in the periphery within specialized structures, the carotid bodies. Variations of O<sub>2</sub> in the blood will modulate activity of the carotid body neurons that will project to the solitary tract nucleus and induce an excitatory or inhibitory effect on the respiratory centers (reviewed in Lahiri et al., 2006; Prabhakar, 2006).

CO<sub>2</sub> levels and pH are also very important for energy regulation and homeostasis. Several neuronal groups within the brainstem continuously monitor CO<sub>2</sub> and pH levels, providing a potent drive to the respiratory rhythm-generating center under normal condition and in response to small changes in CO<sub>2</sub> and pH blood levels (Feldman et al., 2003; Nattie and Li, 2006). Further, at the level of the lung, pulmonary stretch receptors, if activated or inhibited, send vagal afferent projections to the solitary tract nucleus and can modulate the respiratory center via a reflex loop called Hering-Breuer reflex to prevent overinflation or collapse of the lungs.

In general, the modulatory actions induced by mechanical or chemical stimulations act via receptors in specialized cells that then activate or inhibit neuronal populations within the respiratory centers by releasing specific neurotransmitters or neuropeptides.

A variation in respiratory frequency is generated when modulatory inputs act directly or indirectly on the central rhythm generator, therefore at the level of the preBötC and/or pFRG/RTN. A variation in muscle contraction can be generated when neuromodulatory agents act directly or indirectly on firing properties and burst amplitude of premotor neurons and MNs that innervate respiratory muscle in the upper airways and in the chest.

Neuromodulatory effects on a specific neuronal population can vary according to the expression of specific receptors that are present on the target cells: these effects can be further influenced by the stage of development or interactions with other neuromodulators. Development has a critical role in the efficacy of several neuromodulators, since during development several receptors can be expressed at different levels, the affinity for specific ligands varies or different signal pathways can be activated. Recent studies have reported the expression of major receptors expressed by preBötC neurons within the neonatal period (Liu and Wong-Riley, 2002, 2003, 2005; Wong-Riley and Liu, 2005). These data provide useful information for the possible neurotransmitters and receptors involved in respiratory rhythm generation and modulation that are mainly studied in the perinatal period thanks to the development of reduced preparation that maintain respiratory rhythmic activity (brainstem spinal cord preparation, *en bloc* preparation and medullary slice preparation).

These data can also provide important insights regarding the stage of development of respiratory neuronal networks in the perinatal period, when the respiratory system is most susceptible to failure and it can induce life-threatening situations for the newborn (apnea of prematurity, sudden infant death syndrome).

The effects of several neurotransmitters on the activity of preBötC have been reported in the literature. Amongst the neurotransmitters that act on the activity of the preBötC, glutamate, GABA, glycine, serotonin, noradrenaline, neuropeptides (TRH, SubP, SST) and ATP will be described below.

#### **a) Glutamate**

Glutamate is the major excitatory neurotransmitter in the central nervous system. PreBötC neurons are mainly glutamatergic and glutamate sustains

rhythmogenesis and excitability within the network, mainly via activation of AMPA ( $\alpha$ -amino-5-hydroxy-3-methyl-4-isoxazole propionic acid) receptors (Greer et al., 1991; Funk et al., 1993). Inactivation of AMPA receptors in rats and mice medullary slice preparation and in brainstem spinal cord preparation, with a specific antagonist (6-cyano-7-nitroquinoxaline-2,3-dione, CNQX) slows and eventually eliminates inspiratory synaptic drive to hypoglossal and phrenic motoneurons. NMDA (*N*-methyl-D-aspartic acid) receptors are also present in the preBötC and other respiratory structures. Their activation can strongly stimulate respiratory drive but is not critical for respiratory rhythmogenesis per se (Greer et al., 1991; Funk et al., 1993; Ling et al., 1994).

### **b) GABA and Glycine**

Inhibitory inputs are not essential for respiratory rhythmogenesis in neonatal rodents, since the respiratory rhythms are not induced by reciprocal inhibition of respiratory neurons and respiratory rhythms continue after blocking GABAergic and glycinergic transmission (Feldman and Smith, 1989; Onimaru et al., 1990; Ramirez and Richter, 1996). However, GABA and glycine can influence respiratory rhythmogenesis and the pattern of respiratory motor output at cranial and spinal levels.

GABA activates two receptors: GABA<sub>A</sub>, a chloride channel, and GABA<sub>B</sub>, a metabotropic receptor. Their activation has in general a hyperpolarizing effect on the target cell. Glycine receptor is a chloride channel and it has a hyperpolarizing effect.

In brainstem-spinal cord and medullary slice preparations of postnatal rats and mice, GABA and glycine decrease respiratory frequency by modulating chloride conductance via specific ionic channels (Brockhaus and Ballanyi, 1998; Ren and Greer, 2006). In the respiratory network, similarly to other regions in the nervous system, GABA and glycine have a depolarizing effect during the early embryonic period up to E18 in rats (Ren and Greer, 2006). This phenomenon is determined by the presence of high intracellular Cl<sup>-</sup> concentration in the developing neurons; the high levels of intracellular Cl<sup>-</sup> may be explained by the high expression and activity in the early stages of development of the Na<sup>+</sup>/K<sup>+</sup>/2Cl<sup>-</sup> cotransporter that acts to promote entrance of Cl<sup>-</sup> in the cells. Once the second cotransporter for potassium and chloride (KCC2) is expressed and becomes functional, the concentration of intracellular Cl<sup>-</sup> decreases and activation of

GABA<sub>A</sub> and glycine receptors promote hyperpolarization in rhythmogenic neurons and as a consequence, the respiratory frequency is depressed (Ren and Greer, 2006).

### **c) Noradrenaline and Adrenaline**

Adrenaline and noradrenaline are produced by several brainstem neuronal groups that directly project to the preBötC and other respiratory related structures. Among these structures, the effects on respiratory modulation of adrenaline and noradrenaline released by A5 group, noradrenergic cells in the locus ceruleus (A6) have been studied in detail.

The A5 noradrenergic group in the caudal pons has an inhibitory effect on respiratory rhythms; this effect appears to be more potent in neonatal mice than in neonatal rats (Errchidi et al., 1990; Errchidi et al., 1991; Jean-Charles and Gerard, 2002). When A5 neurons are pharmacologically or electrically inactivated in ponto-medullary preparations of neonatal mice and rats, respiratory frequency increases. The inhibitory effect on the preBötC is mediated by activation of  $\alpha$ 2-adrenoreceptors (Errchidi et al., 1991; Al-Zubaidy et al., 1996; Hilaire et al., 2004).

In addition, in medullary slice preparations, noradrenaline application induces opposing effects in neonatal mice versus neonatal rats: noradrenaline induces a reduction in respiratory frequency in rats possibly via activation of  $\alpha$ 2 receptors within the preBötC, and an increase in respiratory frequency in mice, possibly via activation of  $\alpha$ 1 preBötC receptors (Jean-Charles and Gerard, 2002).

A6 noradrenergic neurons are located in the locus ceruleus and they project to the ventrolateral medulla. Noradrenaline released by A6 neurons has a facilitatory effect on respiratory frequency mediated by  $\alpha$ 1 adrenoreceptors (Viemari et al., 2004).

In addition, noradrenaline application in brainstem-spinal cord preparations of both mice and rats facilitates phrenic MN firing via activation of  $\alpha$ 1 receptors at spinal level (Jean-Charles and Gerard, 2002). This noradrenaline stimulatory effect could originate from noradrenergic neurons in the locus ceruleus or the A2/C2 region of the solitary tract nucleus. Recent data also suggest that A1/C1 neurons within the ventrolateral medulla may modulate respiratory rhythmogenesis. In particular, noradrenaline release from A1/C1 neurons may depress respiratory rhythms (Zanella et al., 2005).

#### **d) Serotonin**

Serotonin (5HT) is produced and endogenously released by specialized cells within the brainstem raphe nuclei and it has a potent modulatory effect at the level of several nervous structures responsible for respiratory control (Al-Zubaidy et al., 1996; Onimaru et al., 1998; Pena and Ramirez, 2002; Manzke et al., 2003; Richter et al., 2003). A subset of raphe 5-HT neurons has also been postulated to be involved in chemosensory regulation of respiratory activity (reviewed and discussed in Richerson, 2004; Richerson et al., 2004; 2005).

5HT has a complex modulatory effect on the respiratory network, with effects that vary according to the location of 5HT release and the activation of specific receptor subtype (reviewed in Richter et al., 2003). Activation of the 5HT<sub>1A</sub> receptor, either at presynaptic or postsynaptic sites, causes the inhibition of adenylate cyclase activity, activation of K<sup>+</sup> channels and closure of Ca<sup>2+</sup> channels. When applied to the respiratory centers, both in vivo and in vitro 5HT<sub>1A</sub> agonists cause depression of the network and agonists have proven to be useful pharmacological tools to overcome respiratory disturbances during apneusis, an abnormal respiratory pattern characterized by prolonged inspiration (reviewed in Richter et al., 2003)

Activation of 5HT<sub>2A,B</sub> and 5HT<sub>2C</sub> receptors induce a facilitatory action on both preBötC and pFRG/RTN neurons of neonatal rats and mice, possibly via activation of protein kinase C signaling pathway and I<sub>NaP</sub> current on pacemaker neurons (Al-Zubaidy et al., 1996; Onimaru et al., 1998; Pena and Ramirez, 2002).

Activation of 5HT<sub>4</sub> receptors promotes adenylate cyclase activity and specific 5HT<sub>4</sub> receptor agonists promote a facilitatory effect on the respiratory network. In particular, 5HT<sub>4A</sub> receptor subunit is present in NK1<sup>+</sup>/μOR<sup>+</sup> respiratory neurons within the preBötC and its activation has a potent stimulatory effect on respiratory rhythms, both in basal conditions and during opioid-induced respiratory depression (Manzke et al., 2003). 5HT has a potent modulatory role also at the level of phrenic and hypoglossal MNs, where it acts both postsynaptically, in a facilitatory mode, and presynaptically, inhibiting the respiratory drive to phrenic MNs from upper levels (reviewed in Hilaire and Duron, 1999).

### **e) Substance P**

SubP has a major excitatory activity on the respiratory network from early stages of development, acting at the level of preBötC (Gray et al., 1999; Ptak et al., 1999), and at the level of phrenic and hypoglossal MNs (Ptak et al., 1999; Ptak et al., 2000; Yasuda et al., 2001). Bath application of SubP in medullary slice and brainstem spinal cord preparations generates a slow depolarization of membrane potential in respiratory neurons and an increase in inspiratory burst frequency. Within the preBötC region, SubP acts via NK1R and induces a slow depolarization via activation of a low threshold tetrodotoxin-insensitive Na<sup>+</sup> channel (Pena and Ramirez, 2004). In preBötC non-pacemaker neurons, SubP causes a slow depolarization that induces the generation of spontaneous action potentials. In Cd<sup>2+</sup> sensitive pacemaker neurons, SubP causes a slow depolarization accompanied by an increase in burst duration and amplitude without affecting burst frequency. SubP in Cd<sup>2+</sup> insensitive neurons causes an increase in burst frequency in addition to the increase in burst duration and amplitude (Pena and Ramirez, 2004). SubP is released by fibers possibly originating from solitary tract nucleus, the raphe nuclei or the parapyramidal region (Holtman and Speck, 1994; Agassandian et al., 2002).

### **f) Opioids**

Respiratory activity in both neonatal and adult rats and cats is highly perturbed by opioids. Opioids depress respiratory frequency and tidal volume in *in vivo* adult rats (Morin-Surun et al., 1984; Pazos and Florez, 1984; Manzke et al., 2003) and determine respiratory depression in neonatal rodents via activation of  $\mu$ OR (Greer et al., 1995; Ballanyi et al., 1997). The selective inhibition on preBötC neurons generates in *en bloc* preparation the phenomenon of quantal slowing previously described (Mellen et al., 2003).

### **g) Thyrotropin releasing hormone**

TRH has a potent stimulatory effect both in adult rabbit *in vivo* (Homma et al., 1984) and in neonatal rat brainstem spinal cord and medullary slice preparations when applied directly to the preBötC (Greer et al., 1996; Rekling et al., 1996a). The presence of

TRH immunoreactive fibres have been identified in the medulla of rats and rabbits (Iwase et al., 1988; Iwase et al., 1991; Sun et al., 1996) but the specific receptor subtype, localization and the mechanism of action for TRH within the VRG have not yet been investigated.

#### **h) ATP**

ATP is not only an essential intracellular energy source, but it is also considered an important extracellular signaling molecule via interaction with two classes of receptors: ionotropic purinergic (P2X) and metabotropic purinergic (P2Y) receptors. In respiratory neurobiology, ATP is an important mediator in peripheral and central chemosensitivity (Gourine et al., 2004, 2005; Spyer et al., 2004) and may mediate respiratory frequency and motor output amplitude in respiratory MNs (Funk et al., 1997; Miles et al., 2002; Lorier et al., 2004). Blockade of ATP receptors attenuates CO<sub>2</sub> responses *in vivo*, while ATP receptor activation excites pre-I and inspiratory neuronal activity *in vivo* (Thomas et al., 1999; Thomas and Spyer, 2000).

ATP is released by type I glomus cells in the carotid bodies upon hypoxic stimulation which activates afferent nerve fibers of the carotid sinus that then stimulate the chemosensitive relay station in the CNS (STN). P2X<sub>2</sub> may have a key role in modulation of peripheral chemosensitivity at the level of the carotid bodies, since P2X<sub>2</sub> receptors are expressed in the afferent terminal of the sinus nerve and knockout mice for P2X<sub>2</sub> do not respond to peripheral hypoxia (Rong et al., 2003). ATP is also released by chemosensitive areas on the surface of the medulla oblongata upon hypercapnia in *in vivo* and *in vitro* rat preparations, providing evidence for a role of ATP in central chemoreception, possibly mediated by activation of P2X receptors on the chemosensitive neurons (Gourine et al., 2005). This hypothesis has been recently challenged by a series of experiments in juvenile rats in which chemosensitivity responses within RTN neurons have been examined; from these data it appears that P2X and P2Y receptors can modulate excitability of RTN neurons (indirect inhibition and direct excitation, respectively) but they are not responsible for the pH sensitivity mechanisms (Mulkey et al., 2006).

ATP may also be involved in direct or indirect stimulation of preBötC neurons, since several purinergic receptors subtypes are expressed in the region (Thomas et al.,

2001) and local application of ATP induces an increase in respiratory frequency in rat brainstem-spinal cord and medullary preparations (Lorier et al., 2004).

#### **i) Somatostatin**

SST and its receptors are highly expressed and developmentally regulated in NK1R<sup>+</sup> preBötC neurons (Stornetta et al., 2003; Wong-Riley and Liu, 2005). Exogenous application of SST in adult rats *in vivo* and in neonatal brainstem-preparation has a potent inhibitory effect on respiratory rhythms and can counteract the excitatory effect caused by SubP administration (Suzue, 1984; Chen et al., 1991). The mechanisms underlying the inhibitory action on the respiratory system have not been yet investigated.

### 1.3 ONTOGENY OF RESPIRATORY RHYTHMS

During early stages of gestation, nonrespiratory movements can be recorded in both human and ovine fetuses; they are characterized by tonic contractions of thoracic muscles and diaphragms. Fetal breathing movements (FBMs) start in utero after the third trimester of gestation (10-20 weeks of gestation in humans; Cosmi et al., 2003) and at 147 days of gestation in fetal lambs (Jansen and Chernick, 1991). Initially, FBMs are periodic and irregular abdominal contractions; they are characterized by abdominal body wall movements, associated with intrathoracic pressure change and movements of amniotic fluids in the trachea. FBMs are mainly caused by abrupt onsets and endings of diaphragm contractions. With progression of gestation, FBMs become more regular and frequent, and they are characterized by rhythmic and coordinated contractions of respiratory muscles (diaphragm, intercostals and upper airways muscle), occurring mainly during the REM-like state of sleep (Rigatto, 1992; Cosmi et al., 2003; Peirano et al., 2003).

Interestingly, the frequency and occurrence of FBMs can be modified by several chemical stimuli, such as O<sub>2</sub> and CO<sub>2</sub> blood levels, cold cutaneous stimulation of the fetus, blood pH changes, alcohol and nicotine (Polin and Fox, 1998) suggesting the existence of functional regulatory mechanisms from early stages of development.

Since effective respiration does not occur until after delivery, the presence of active movements in the chest and the rhythmic expansion of the lungs during fetal development are quite surprising. It has been proposed that FBMs and the pulmonary stretch associated with them, are important for the proper development of the lungs (Kitterman, 1996; Sanchez-Esteban et al., 2001; Sanchez-Esteban et al., 2002). Further, the primordial activity of the respiratory rhythm generator and the structures responsible for respiratory pattern generation may be important for shaping and refining the developing respiratory network during gestation, in order to be fully functional at birth (Chatonnet et al., 2002; Borday et al., 2003; Chatonnet et al., 2003).

In rodents, a similar developmental pattern occurs: FBMs have been recorded in the last week of gestation, initially as episodic events (E16) and then they become progressively more frequent and regular (E18-20) (Kobayashi et al., 2001).

Prior to the occurrence of FBMs (<E16 in rats), a spontaneous pattern of neuronal activity with slow frequency occurs within the nervous system. This activity can be recorded in several regions of the CNS and it is also present in the spinal cord and hindbrain (Hanson and Landmesser, 2003; Ren and Greer, 2003; Chatonnet et al., 2006). It has been proposed that spontaneous rhythmic activity is likely generated by developing neuronal networks and gap junction coupling, although the presence of functional pacemaker neurons has not been investigated, they may be present. Several experimental studies suggest that the spontaneous rhythmic activity may be important in developmental processes such as neuronal wiring, synapse formation and elimination, target muscle innervation and gene expression (Buonanno and Fields, 1999; Hanson and Landmesser, 2003, 2004).

Close to birth, respiratory activity in humans and rodents become more regular and increasingly responsive to several neuromodulators and chemical stimuli (Moss and Inman, 1989; Hilaire and Duron, 1999).

Newborn babies and pups usually breathe irregularly in the first neonatal period, with frequent episodic breathing events, represented by brief interruptions in respiratory activity (periodic breathing). In preterm infants, periodic breathing can exacerbate into prolonged respiratory interruptions defined as apneas. These events can be classified as obstructive, central or mixed apneas. Obstructive apnea is characterized by recurrent apneic episodes caused by the obstruction of the upper airways, whereas central apnea is an interruption of breathing in which there is no central respiratory effort. Central apnea is therefore considered the result of a central defect in the respiratory rhythm generating center or within the central network. Mixed apneas present both obstructive and central components (Martin et al., 2004; Martin and Abu-Shaweesh, 2005). Apneic events occur most often during sleep, when neuromodulatory inputs are low, and prolonged or recurrent apneic events can seriously endanger the neurodevelopment of the newborn and potentially cause irreversible hypoxic events, leading to neuronal cell death (Martin et al., 2004; Martin and Abu-Shaweesh, 2005).

In general, it is believed that apnea of prematurity is the consequence of an immature neural respiratory center or the neuromodulatory mechanisms that constantly

regulate the efficiency of the respiratory systems (Martin et al., 2004). Understanding how neuromodulatory mechanisms operate in the perinatal period is of critical importance if we are to manipulate the system in pathological conditions or in the intensive care units where the survival of premature babies is at risk in the first weeks of postnatal life. Further, understanding the genetic determinants of brainstem and respiratory network development is now becoming a focus of study.

## 1.4 BRAINSTEM DEVELOPMENT

The hindbrain originates from the rhombencephalon, the central portion of the neural tube that differentiates into a segmental structure consisting of 8 metameric units called rhombomeres (r1 to r8). Each rhombomere contains progenitor cells that will acquire a specific identity according to their relative location within the anterior-posterior axis (reviewed in Jacobson and Rao, 2005).

The process of hindbrain segmentation is initially under the influence of several extrinsic factors (e.g. myelin basic proteins, sonic hedgehog, retinoids, fibroblast growth factors) that promote a developmental program along the anterior-posterior axis and the expression of specific transcription factors (TFs) in both progenitor cells and developing neurons. At this initial stage of brainstem development, the products of the *Hox* family genes, *Kreisler* and *Krox20* genes, ephrin receptors and their ligands have a fundamental role in determining the extension of each segmental unit and the specification of position and neuronal identity of progenitor cells within each unit (Fig.1.4).

Each rhombomeric unit is identifiable along the rostro-caudal extension of the rhombencephalon by the expression of a unique pattern of expression of TFs during its development. When the TF machinery is experimentally altered, either by a gene deletion or by rhombomeric misplacements during development, an abnormal developmental program occurs and specific mutations are generated (reviewed in Schneider-Maunoury et al., 1998; Pasqualetti and Rijli, 2001; Borday et al., 2004). Therefore a deletion of a gene necessary for the specification of a rhombomeric unit will generate a mutation in a specific region of the rhombencephalon and may also influence the proper development of adjacent rhombomeres and alter the overall anatomical structures of the developing embryo (Pasqualetti and Rijli, 2001). For example, inactivation *Hoxb1* or *Hoxb2*, two of the *Hox* family of TF genes, leads to partial respecification of neuronal populations in r4 into a r2 phenotype, whereas ectopic expression of *Hoxa1* leads to transformation of r2 into a r4 phenotype (reviewed in Schneider-Maunoury et al., 1998; Pasqualetti and Rijli, 2001).

Developmental defects in the early stages of hindbrain segmentation, just before hindbrain neurogenesis occurs, can consequently alter the identity and the connectivity of

neurons within the respiratory centers (reviewed in Chatonnet et al., 2002; Borday et al., 2004; Chatonnet et al., 2006).

Mutant mice for *Hoxa1*, *Kreisler* and *Krox20* have been generated; consequently, the anatomy and the physiological properties of both early spontaneous rhythms in the embryos and respiratory activity in the newborn have been analyzed.

*Hoxa1* is normally expressed from the caudal end of the neural tube till the boundary between r3 and r4 (fig1.4). Mice with inactivation of *Hoxa1* show a severe reduction in the extension of r4 and r5 and their derived structures (VII and pFRG/RTN). Interestingly, *Hoxa1* mutants develop a supranumerary neuronal circuit originating from r2-4 that connects to the VRG and reconfigures the respiratory network. Pups die within the first 24 hours due to irregular breathing activity and apneic episodes (del Toro et al., 2001).

*Kreisler* gene is expressed in r5 and r6, its inactivation determines a reduction of r5, r6 extension and a consequent severe hypoplasia of the pontine reticular formation. The defects do not affect respiratory rhythm generation, although chemosensory control is altered and delayed responses to hypoxia and hyperoxia are eliminated (Chatonnet et al., 2002).

*Krox20* is transiently expressed in the putative regions corresponding to r3 and r5 prior to hindbrain segmentation (fig1.4). In *Krox20* mutants the hindbrain regions corresponding to r3 and r5 are eliminated. As a result, *Krox20*<sup>-/-</sup> newborn die at birth due to prolonged apneas, perhaps because of an inactivation of a caudal pontine “anti-apneic” center derived from r3-r4, likely the pFRG region (fig1.5; table 1.1 and 1.2)(Schneider-Maunoury et al., 1993; Jaquin et al., 1996; Borday et al., 2004).

The results of these studies on the early hindbrain segmentation and patterning suggest that respiratory defects in *Krox20*<sup>-/-</sup> and *Hoxa1* mice are caused by defects in development of r3/r4 progenitors, that will likely project to the central pattern generators in the VRG.

Within each level of the neural tube, precursor cells are distributed in the proliferating region of the neural tube (ventricular zone). When they exit the cell cycle they migrate out of the ventricular zone onto the mantle layer and then they start their differentiation program. Once again, a combinatorial code of different TFs is involved in

the determination of the dorsal ventral patterning of progenitor cells and their differentiation into neurons with a unique phenotype, patterns of connectivity and therefore a unique function within the central nervous system.

A major effort in the field of developmental neurobiology focuses on the identification of a complete combinatorial code of TFs necessary for the proper development of each neuronal population. A significant amount of research has produced substantial data regarding the development of the spinal cord, where at least 11 neuronal progenitor domains can be identified along the dorso-ventral axis according to their function, origin and TFs combinatorial code: 6 domains of dorsal interneurons (dI 1-6), 4 domains of ventral interneurons (V0-3) and 1 domain of motoneurons (MN) (fig1.6; reviewed in Goulding et al., 2002). In comparison, only a limited amount of information is at present available on TFs expressed by brainstem neuronal populations.

Although different patterns of TF expression exist between spinal cord and brainstem, it is conceivable to postulate that similar mechanisms occurs in the hindbrain and that TFs have a similar role during development if expressed in both hindbrain and spinal cord. For example, hindbrain MNs express a pattern of TFs genes responsible for the acquisition of the motoneuronal phenotype that is similar to those expressed by spinal cord MNs. The TFs *MNR2*, *Lhx3*, *Isl1/2*, *Pax3*, *Pax6* and *HB9* are in fact important in determining a motoneuronal phenotype and their specific characteristics, such as neurotransmitter and vesicle machinery expression, axonal exit from the central nervous system (CNS) and contacts with muscle cells (Eisen, 1999). Other TFs are instead specific to the hindbrain. For example *Phox2a* and *Phox2b* TFs are required for the formation of all hindbrain branchiomotor and visceral MNs, but not the somatic MNs (Pattyn et al., 2000).

In the brainstem, the neuronal organization into specific nuclei with a selective function and connectivity requires an even more complex spatiotemporal contribution of TFs during embryonic development. Several brainstem nuclei that have been related to respiratory function control have been investigated in order to find genes responsible for their development and correlate the mutation of specific genes to respiratory defects (fig1.5; reviewed in Bianchi and Sieweke, 2005; Gaultier and Gallego, 2005).

### **a) Catecholaminergic centers in the brainstem**

(Nor)adrenergic centers in the pons (A6 group within the locus ceruleus and A5 group in the ventral pons) and medulla (A2/C2 adjacent to the solitary tract nucleus in the dorsal medulla, A1/C1 group in the ventrolateral medulla) have been shown to be responsible for the release of (nor)adrenaline which affects activity of respiratory VRG, DRG and respiratory MNs in brainstem and spinal cord via  $\beta$  (DRG; (Huang et al., 2000)),  $\alpha 1$  and  $\alpha 2$  noradrenergic receptors (DRG, VRG and phrenic Mns (Al-Zubaidy et al., 1996; Jean-Charles and Gerard, 2002; Hilaire et al., 2004; Hilaire, 2006).

*Mash-1*, *Phox2b*, *Phox2a* and *Rnx* are TF genes involved in the specification of (nor)adrenergic phenotype in one or more brainstem groups (fig1.5); (Tiveron et al., 1996; Bianchi and Sieweke, 2005). Genetic mutation for any of these genes determines a neurodevelopmental defect in the noradrenergic groups with death at birth from respiratory defect (see tables 1.1 and 1.2 for details of the associated defects) (Errchidi et al., 1990; Errchidi et al., 1991; Arata et al., 1998; Shirasawa et al., 2000; Qian et al., 2001; Viemari and Hilaire, 2003; Viemari et al., 2004; Zanella et al., 2005; Hilaire, 2006).

### **b) Serotonergic centers in the brainstem**

Neuromodulation of respiratory activity also arises from 5HT neurons in the raphe nuclei. 5HT neurons project to VRG and to respiratory motoneurons in the brainstem and spinal cord to provide neuromodulatory inputs to the respiratory centers (Connelly et al., 1989; Di Pasquale et al., 1992; Di Pasquale et al., 1994; Al-Zubaidy et al., 1996; Schwarzacher et al., 2002). Several TFs important for the development of raphe nuclei have been identified: *Pet-1*, *Lmx1b*, *Gata-2*, *Gata-3* and *Nkx2.2* are important for the acquisition of serotonergic phenotype. Selective mutations of one of these genes determines the loss of most of the 5HT neurons in the raphe nuclei and mutant animals die during embryonic development because of the important role of 5HT in promoting neuronal development (fig 1.5; see tables 1.1 and 1.2 for details of the associated defects) (Cheng et al., 2003; Gaspar et al., 2003; Gaspar, 2004; Scott et al., 2005).

### **c) Ventral Respiratory Group**

Fewer TFs have been identified in the region of the VRG. *Mafb* has been implicated in the development of preBötC neurons. Mutants for *Mafb* show abnormalities in the ventral respiratory group, in particular in the region of preBötC. The embryos develop until the end of gestation but only produce intermittent gasps at birth and die within a few minutes (fig 1.5; see tables 1.1 and 1.2 for details of the associated defects (Blanchi et al., 2003)).

## 1.5 RESPIRATORY DEFECTS ASSOCIATED WITH GENETIC DISORDERS

A combinatorial code of TFs that identifies preBötC neurons or other respiratory neurons within the VRG is still not available. This novel area of research is being pursued in an effort to identify possible genetic defects associated with respiratory insufficiency diseases. For example, congenital central hypoventilation syndrome (CCHS) or Ondine's curse has been recently associated with mutations in the *Phox2b* gene (Amiel et al., 2003; Sasaki et al., 2003). CCHS is generally considered a rare autonomic disorder disease in which severe hypoventilation occurs particularly during quiet sleep (non REM-sleep). This condition is evident since the newborn period and it is associated with absence of ventilatory responses under hypercapnic or hypoxemic challenges (reviewed in Chen and Keens, 2004; Weese-Mayer et al., 2005). Polyalanine expansion mutations is the most common genetic defect in determining the disease, but other defects in the *Phox2b* gene sequence and expression have been identified in CCHS patients, such as frameshift mutations, nonsense and missense mutation of the gene (Weese-Mayer et al., 2005).

Rett syndrome is another genetically determined disease in which mental retardation, growth failure, speech impairment and limited social interaction skills are often associated with an autonomic defect at both cardiovascular and respiratory levels (Glaze, 2005; Segawa and Nomura, 2005; Bienvenu and Chelly, 2006). Rett syndrome is caused by a mutation in the gene encoding methyl-CpG-binding protein 2 (*MeCP2*) (Amir et al., 1999). Respiratory defects in Rett syndrome patients are present only during wakefulness and they are associated with respiratory pattern variability in which breath holding and hyperventilation events are frequent (Julu et al., 2001). *MeCP2* mutant mice have been generated and respiratory activity has been investigated in the postnatal period (Viemari et al., 2005). Mice show a normal respiratory activity in the first month of life. After that, an irregular respiratory activity pattern develops, in which a high variability of respiratory cycles and apneas occur till animals die for respiratory arrest. Abnormalities in the catecholaminergic system have been proposed to be associated with the respiratory defects (Viemari et al., 2005).

No clear association with a genetic defect has been proven in the occurrence of sudden infant death syndrome (SIDS). SIDS seems to be caused by a multifactorial condition associated with congenital or acquired vulnerability, intrinsic vulnerability of the neonatal period and an acute stressor (Filiano and Kinney, 1994). Several factors can contribute to death in SIDS cases: rebreathing asphyxia, central, obstructive or mixed apneic events, failure of neuronal mechanisms involved in the process of arousal from sleep, ability to recover from an hypoxic event (reviewed in Thach, 2005).

Prader-Willi Syndrome (PWS) is a neurodevelopmental disorder characterized by mental retardation, sensory and motor skills impairment, failure to thrive at birth and obesity in the later stages of development (Goldstone, 2004; Stevenson et al., 2004). Occurrence of sleep apnea and blunted chemosensitivity have been reported in several PWS patients (Arens et al., 1994; Clift et al., 1994; Gozal et al., 1994; Wharton and Loechner, 1996; Schluter et al., 1997; Menendez, 1999; Manni et al., 2001; Nixon and Brouillette, 2002; Stevenson et al., 2004). PWS is caused by the inactivation of a set of genes located on chromosome 15 (reviewed in Nicholls and Knepper, 2001). Among them, the expression of the *Necdin* gene seems to play a key role in the phenotype of the disease. Our laboratory analyzed the respiratory phenotype and the neurodevelopmental defects of a mice in which *Necdin* has been genetically inactivated (Ren et al., 2003; Pagliardini et al., 2005) and part of the results of these studies will be reported in chapter III of this thesis.

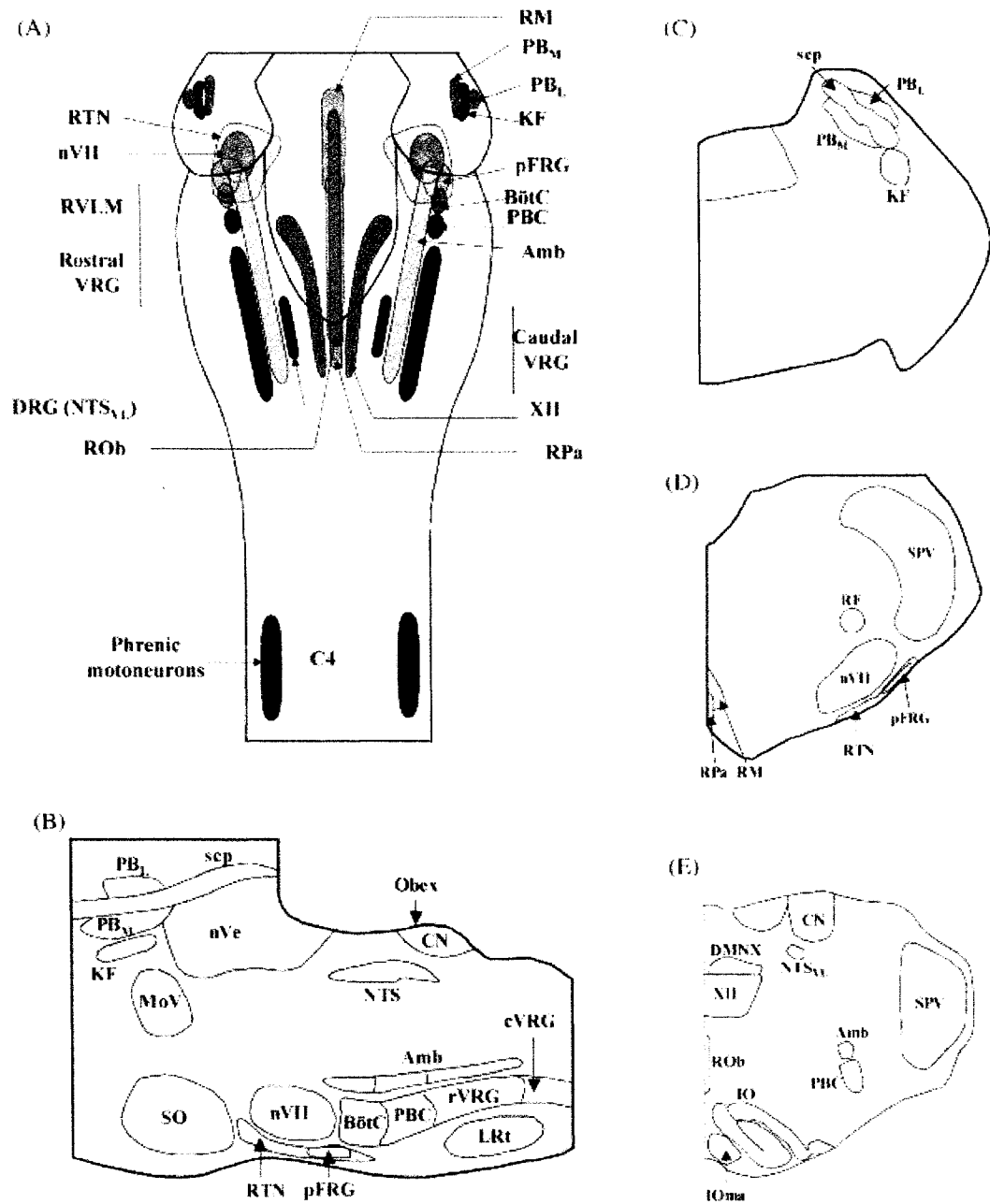


**Figure 1.1 Brainstem nuclei involved in the neural control of breathing.** (A) Schematic longitudinal representation of brain stem nuclei associated with respiratory neural control. (B) Schematic parasagittal representation of brain stem respiratory nuclei. (C)–(E) Schematic representation of coronal sections of the rat brain stem at pontine (C), rostral medullary (D), and caudal medullary (E) levels. Amb, nucleus ambiguus; BötC, Bötzinger complex; DRG, dorsal respiratory group; KF, Kölliker-Fuse nucleus; LRt, lateral reticular nucleus; NTS, nucleus tractus solitarius; PBC, preBötzinger complex;

PB<sub>L</sub>, lateral parabrachial nucleus; PB<sub>M</sub>, medial parabrachial nucleus; pFRG, para-facial respiratory group; RM, raphé magnus; ROb, raphé obscurus; RPa, raphé pallidus; RTN, retrotrapezoid nucleus; RVLM, rostroventrolateral medulla; VRG, ventral respiratory group; XII, hypoglossal nucleus. For landmark reference: CN, cuneate nucleus; C4, cervical 4 level; DMNX, dorsal motor nucleus of the vagus nerve; IO, inferior olivary nucleus; IOma, medial accessory olivary nucleus; MoV, motor nucleus of trigeminal nerve; nVe, vestibular nuclei; nVII, facial nucleus; RF, retrofacial nucleus; scp, superior cerebellar peduncle; SO, superior olivary nucleus; SPV, spinal nucleus of trigeminal nerve [from Wong-Riley and Liu, 2005]

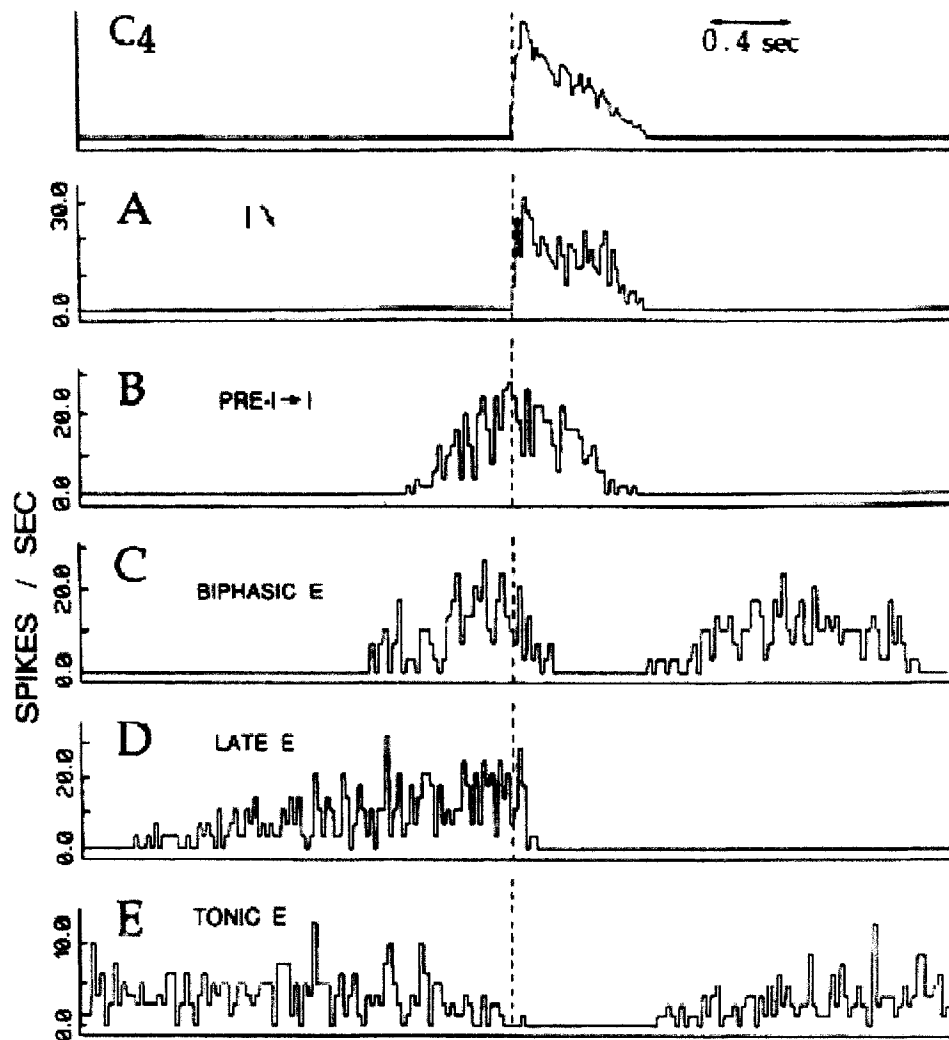


**Figure 1.2 Classes of medullary respiratory neurons spontaneously active in vitro.** Cycle-triggered histograms show temporal discharge patterns of representative inspiratory (I) and expiratory (E) phase units in relation to C4 phrenic inspiratory discharge. Neuron types shown are (A) I neuron with decrementing spike discharge pattern (I $\searrow$  neuron) with spiking onset coincident with phrenic motoneuronal discharge; (B) I neuron with spike onset -500 ms before C4 discharge with spiking continuing through the I phase (pre-I $\rightarrow$ I neuron); (C) expiratory-phase neurons with both late E- and early E-phase spike discharge (biphasic E neurons); (D) expiratory neurons with late E-phase spike discharge (late E neuron), and (E) expiratory neurons with tonic discharge throughout E phase (tonic E neurons). [from Smith et al., 1990]

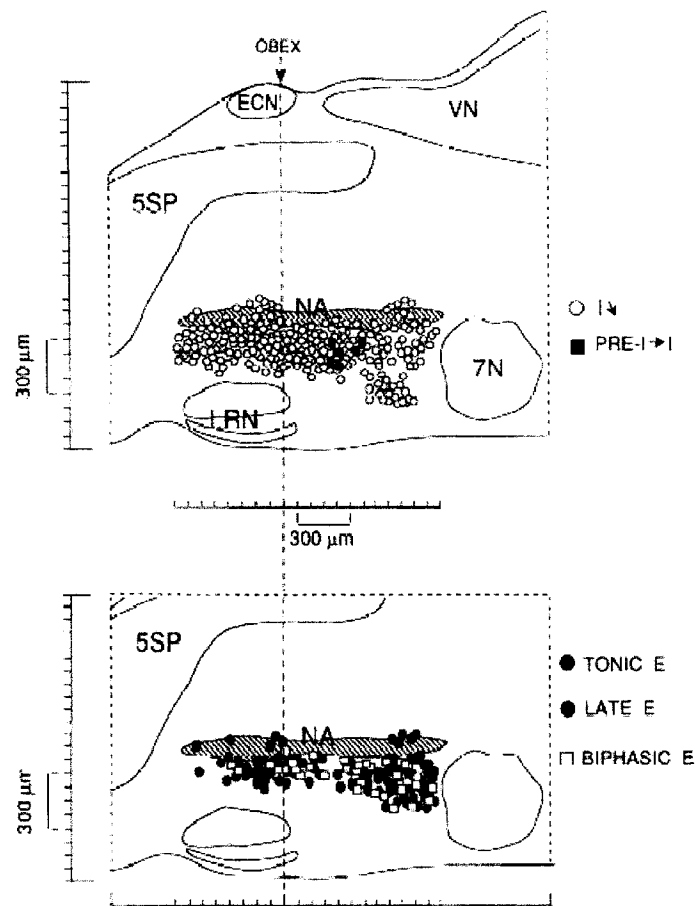


**Figure 1.3 Reconstruction of spatial distributions of inspiratory (top) and expiratory neuron (bottom) activity in ventrolateral reticular formation at medullary levels extending from the pyramidal decussation to the caudal pole of facial nucleus.** Cell positions indicated by symbols represent locations of 229 I phase cells and 123 E-phase cells projected onto a composite sagittal plane passing through the approximate center of the locus of mapped cell activity at each level. Dimensions indicated represent average dimensions for this plane computed from the histology from 47 preparations; Standard deviation for dimensions is  $\pm 7\%$ . Each symbol indicates point of maximum extracellular field potential of unit recorded along a single-electrode tract. Cell locations were reconstructed from dye marks on histological sections at recording sites. Abbreviations: NA, nucleus ambiguus; LRN, lateral reticular nucleus; 7N, facial nucleus; VN, vestibular nucleus; ECN, external cuneate nucleus; and BP, spinal trigeminal nucleus. [from Smith et al., 1990]

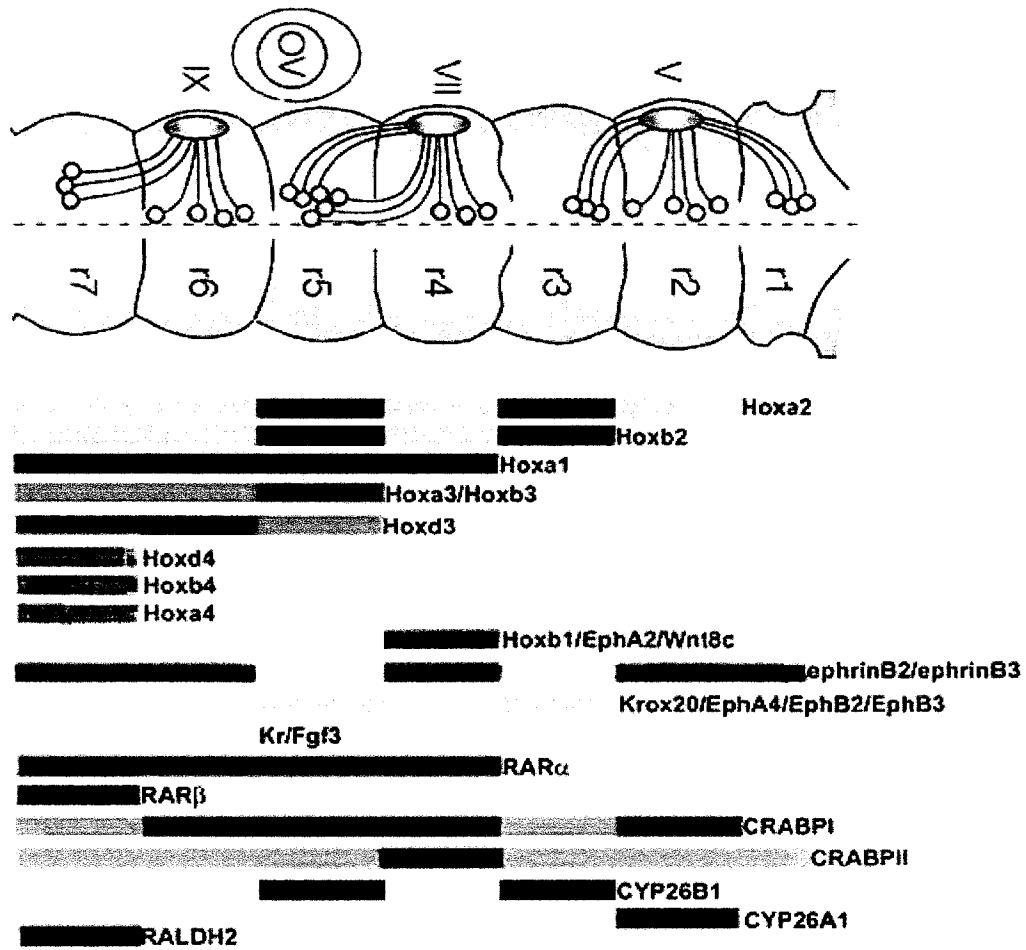


**Figure 1.4. Rhombomeric blueprint for the hindbrain and nervous system.** The hindbrain is segmented into seven cell lineage restricted units called rhombomeres (r) which exert a profound influence on brain and nervous system patterning. There is a clear correlation between individual rhombomeres and the spatial distribution of the cranial nerves (V, trigeminal; VII, facial; IX, glosso-pharyngeal), the axons of which leave the neural tube only from exits points contained within the even numbered rhombomeres. Concomitant with hindbrain segmentation is the establishment of sharp domains of gene expression within individual rhombomeres, or pairs of rhombomeres or alternating rhombomere segments. The domains of expression are incredibly dynamic during the 7.5-10.5dpc of embryonic development and only the principal domain of expression is represented here. The combinatorial gene expression exhibited by an individual

rhombomere, ultimately determines its identity and fate and removing specific genes such as *Hoxb1* can transform r4 into an r2 like identity and fate. [From Melton et al., 2004].

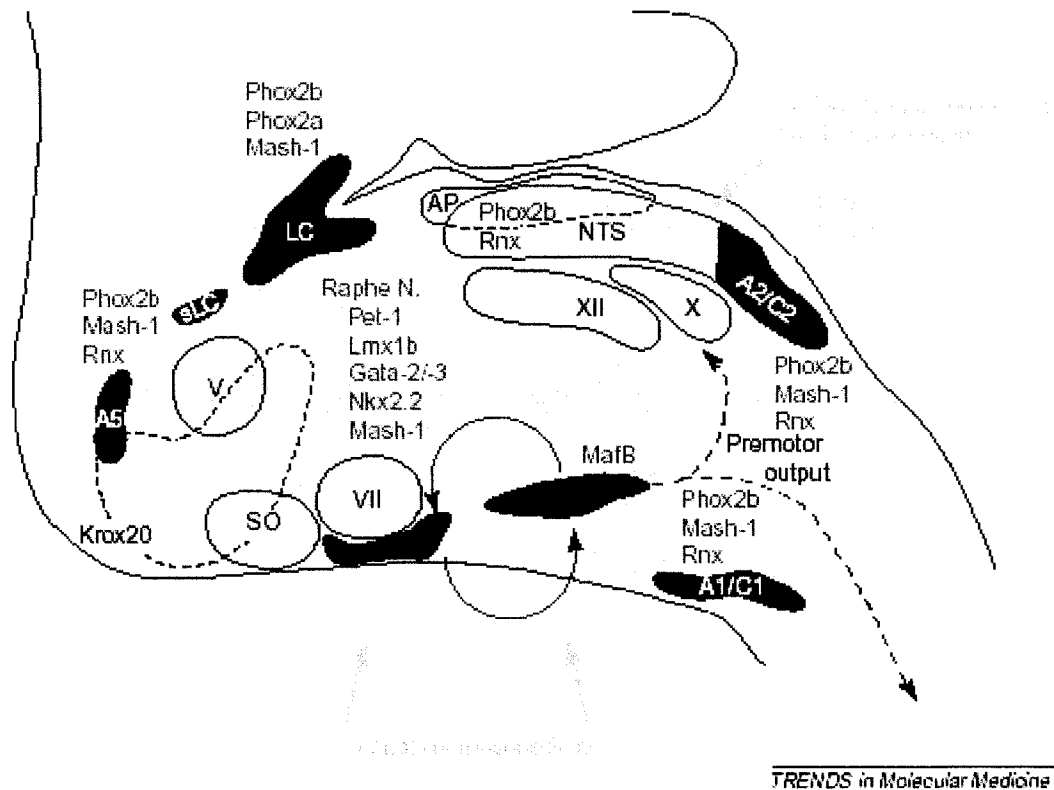


**Figure 1.5 Transcription factor requirement in the development of respiratory hindbrain neurons.** Schematic representation of respiratory groups of neurons in the sagittal view of the brainstem (forebrain, left; spinal cord, right). Rhythmogenic groups of neurons in red (PBC, preBötzinger complex; pFRG, parafacial respiratory group). (Nor)adrenergic groups of neurons in blue (A1/C1; A2/C2; A5; LC, locus coeruleus; sLC, sub-locus coeruleus). Nucleus tractus solitarius (NTS), in light orange; Raphe nuclei (Raphe N.) in brown hatching (AP, area postrema; SO, superior olive; V, VII, X, XII, motor nuclei). Central and peripheral chemoreception and mechanoreception represented by orange arrows. Transcription factors required for correct development of each group of neurons are indicated next to the affected groups. *Krox20* deletion leads to rostral medulla hypoplasia and the loss of neurons of the reticular formation close to the A5 [from Blanche and Sieweke, 2005].

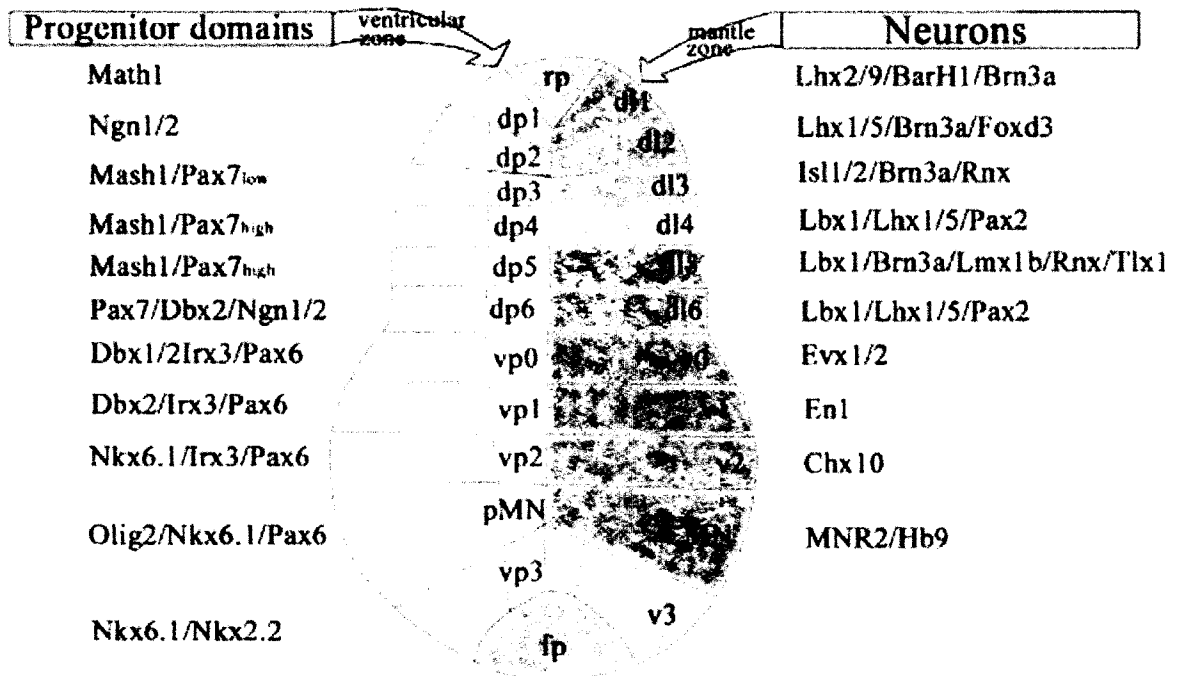


**Figure 1.6 Expression of transcription factors in progenitor cells and differentiating neurons of the mice spinal cord.** A combinatorial code of transcription factors divides the ventricular zone in 6 dorsal progenitors (dp1 to dp6), 4 ventral progenitors (vp0 to vp3) and a domain of progenitor motoneurons (pMN). A different set of transcription factors identifies neuronal population in the mantle zone: 6 dorsal interneuronal populations (dI1 to dI6), 4 ventral interneuronal populations (v1 to v3) and 1 motoneuronal population (MN).

Gene	Overall phenotype of knockout mice	Associated cell disorder in the nervous system	Mutation in human respiratory syndrome
<b><i>MafB</i></b>	-Death within 2 hrs after birth -Gaspings <i>in vivo</i> (Blanchi et al., 2003) -Severely reduced respiratory rhythm; no response to electrical peptidergic stimuli and hypoxia in <i>in vitro</i> preparations (Blanchi et al., 2003)	-Loss of cellularity and organization in the preBötC (Blanchi et al., 2003)	-Not determined
<b><i>Phox2b</i></b>	-Death during embryonic development (Pattyn et al., 2000) - +/-: altered response to hypercapnia and hypoxia (Dauger et al., 2003)	-Loss of NA neurons, NTS and visceral neurons (Pattyn et al., 2000; Dauger et al., 2003)	-polyAla expansion /mutation /deletion in 106 CCHS cases (Amiel et al., 2003; Sasaki et al., 2003)
<b><i>Phox2a</i></b>	-Death within the first day after birth (Morin et al., 1997) -Reduced respiratory frequency and <i>in vitro</i> response to hypoxia (Viemari et al., 2004)	-Loss of LC and subsets of visceral neurons (Morin et al., 1997)	-One mutation in 77 CCHS cases (Sasaki et al., 2003; Weese-Mayer et al., 2003) -One mutation in 92 SIDS cases (Weese-Mayer et al., 2004)
<b><i>Rnx</i></b>	-Death within the first day after birth (Shirasawa et al., 2000) -Alternation of tachypnea and apnea periods (Shirasawa et al., 2000)	-Loss of NTS and NA groups neurons except rostral LC (Qian et al., 2002)	-No mutation found in CCHS patients (Amiel et al., 2003) -One mutation in 92 SIDS cases (Weese-Mayer et al., 2004)
<b><i>Mash-1</i> <i>Hash-1</i></b>	-Death within the first day after birth -Increased breathing frequency (Dauger et al., 2001)	-Loss of groups of NA and 5-HT neurons and subsets of ANS ganglia (Hirsch et al., 1998; Pattyn et al., 2004)	-Mutation or polyAla deletion found in 6/107 CCHS cases, (3/107 also had polyAla expansion in <i>Phox2b</i> ) (Sasaki et al., 2003; Weese-Mayer et al., 2003; Gaultier et al., 2004) -No mutation found in 92 SIDS cases (Weese-Mayer et al., 2004)

<b>Gene</b>	<b>Overall phenotype of knockout mice</b>	<b>Associated cell disorder in the nervous system</b>	<b>Mutation in human respiratory syndrome</b>
<i>Pet-1</i>	-30% death during the first week after birth (Hendricks et al., 2003)	-Loss of most 5-HT neurons (Hendricks et al., 2003)	-Not determined
<i>Lmx1b</i>	-Death within the first week after birth (Chen et al., 1998)	-Loss of 5-HT neurons (Ding et al., 2003)	-Not determined
<i>Gata-2</i>	-Death during embryonic development (Tsai et al., 1994)	-Loss of 5-HT neurons (Craven et al., 2004)	-Not determined
<i>Gata-3</i>	-Death during embryonic development (Lim et al., 2000)	-Loss of most 5-HT neurons in caudal raphe nuclei (Pattyn et al., 2004)	-Not determined
<i>Krox20</i>	- 70% death during the first day after birth (Jacquin et al., 1996) -Decreased in vivo respiratory rhythm normal in vitro rhythm in medulla preparations -Decreased in vitro rhythm in preparations containing the pons	-Hypoplasia and loss of non NA neurons with potential rhythm-promoting function in the rostral medulla (Jacquin et al., 1996)	-Not determined

### Previous Page and this page

**Table 1.1 Transcription factor mutations affecting specific central respiratory neurons in mice and identified corresponding mutations in human respiratory syndromes.** Pink shadowed boxes: TF mutation affecting the preBötC region. Blue shadowed boxes: TF mutation affecting the noradrenergic system and the solitary tract nucleus. Yellow shadowed boxes: TF mutation affecting the serotonergic neurons. Green shadowed boxes: TF mutation generating hypoplasia of the rostral medulla. [adapted from Bianchi and Sieweke, 2005].

Gene	Respiratory movement or diaphragmic EMG profile <sup>a</sup>	<i>In vitro</i> respiratory-like rhythm <sup>b</sup>
<i>MafB</i>	<p>from <b>Blanchi et al., 2003</b></p>	
<i>Phox2b</i>	<p>from <b>Dauger et al., 2003</b></p>	<ul style="list-style-type: none"> <li>• Not determined</li> </ul>
<i>Phox2a</i>	<p>from <b>Viemari et al., 2004</b></p>	
<i>RNX</i>	<p>from <b>Shirasawa et al., 2000</b></p>	
<i>Mash-1</i> <i>Hes1-1</i>	<p>from <b>Dauger et al., 2001</b></p>	<ul style="list-style-type: none"> <li>• Not determined</li> </ul>
<i>Krox20f</i>	<p>from <b>Jacquin et al., 1996</b></p>	

## Previous Page

**Table 1.2 Abnormalities in the respiratory rhythms of mutant mice in the perinatal period.** (Left panel) *In vivo* respiratory rhythms measured by whole-body plethysmography recording (*MafB*, *Phox2b*, *Phox2a*, *Mash-1*, *Krox20*) or diaphragmic electromyogram EMG (*Rnx*) on surgically delivered E18.5 embryos (*MafB*, *Phox2a*), P0 (*Mash-1*, *Rnx*), P0 to P4 (*Krox20*) or P2 mice (*Phox2b*) (bars: 2 s). (Right panel) *In vitro* respiratory-like rhythms were recorded on brainstem preparations of E18.5 embryos (*MafB*, *Phox2a*), P0 (*Rnx*) or P0 to P4 mice (*Krox20*), at the C4 phrenic root (*MafB*, *Phox2a*, *Rnx*) or the XIIth cranial nerve (*Krox20*) (bars: 10 s). [From Blanche and Sieweke, 2005].

## 1.5 REFERENCES

- Agassandian K, Fazan VP, Adanina V, Talman WT (2002) Direct projections from the cardiovascular nucleus tractus solitarius to pontine preganglionic parasympathetic neurons: a link to cerebrovascular regulation. *J Comp Neurol* 452:242-254.
- Al-Zubaidy ZA, Erickson RL, Greer JJ (1996) Serotonergic and noradrenergic effects on respiratory neural discharge in the medullary slice preparation of neonatal rats. *Pflugers Arch* 431:942-949.
- Alheid GF, Milsom WK, McCrimmon DR (2004) Pontine influences on breathing: an overview. *Respir Physiol Neurobiol* 143:105-114.
- Amiel J, Laudier B, Attie-Bitach T, Trang H, de Pontual L, Gener B, Trochet D, Etchevers H, Ray P, Simonneau M, Vekemans M, Munnich A, Gaultier C, Lyonnet S (2003) Polyalanine expansion and frameshift mutations of the paired-like homeobox gene PHOX2B in congenital central hypoventilation syndrome. *Nat Genet* 33:459-461.
- Amir RE, Van den Veyver IB, Wan M, Tran CQ, Francke U, Zoghbi HY (1999) Rett syndrome is caused by mutations in X-linked MECP2, encoding methyl-CpG-binding protein 2. *Nat Genet* 23:185-188.
- Arata A, Onimaru H, Homma I (1998) The adrenergic modulation of firings of respiratory rhythm-generating neurons in medulla-spinal cord preparation from newborn rat. *Exp Brain Res* 119:399-408.
- Arens R, Gozal D, Omlin KJ, Livingston FR, Liu J, Keens TG, Ward SL (1994) Hypoxic and hypercapnic ventilatory responses in Prader-Willi syndrome. *J Appl Physiol* 77:2224-2230.
- Ballanyi K, Onimaru H, Homma I (1999) Respiratory network function in the isolated brainstem-spinal cord of newborn rats. *Prog Neurobiol* 59:583-634.
- Ballanyi K, Lalley PM, Hoch B, Richter DW (1997) cAMP-dependent reversal of opioid- and prostaglandin-mediated depression of the isolated respiratory network in newborn rats. *J Physiol* 504 ( Pt 1):127-134.
- Bienvenu T, Chelly J (2006) Molecular genetics of Rett syndrome: when DNA methylation goes unrecognized. *Nat Rev Genet* 7:415-426.

- Blanchi B, Sieweke MH (2005) Mutations of brainstem transcription factors and central respiratory disorders. *Trends Mol Med* 11:23-30.
- Blanchi B, Kelly LM, Viemari JC, Lafon I, Burnet H, Bevençut M, Tillmanns S, Daniel L, Graf T, Hilaire G, Sieweke MH (2003) MafB deficiency causes defective respiratory rhythmogenesis and fatal central apnea at birth. *Nat Neurosci* 6:1091-1100.
- Borday C, Abadie V, Chatonnet F, Thoby-Brisson M, Champagnat J, Fortin G (2003) Developmental molecular switches regulating breathing patterns in CNS. *Respir Physiol Neurobiol* 135:121-132.
- Borday C, Wrobel L, Fortin G, Champagnat J, Thaeron-Antono C, Thoby-Brisson M (2004) Developmental gene control of brainstem function: views from the embryo. *Prog Biophys Mol Biol* 84:89-106.
- Brockhaus J, Ballanyi K (1998) Synaptic inhibition in the isolated respiratory network of neonatal rats. *Eur J Neurosci* 10:3823-3839.
- Buonanno A, Fields RD (1999) Gene regulation by patterned electrical activity during neural and skeletal muscle development. *Curr Opin Neurobiol* 9:110-120.
- Chamberlin NL (2004) Functional organization of the parabrachial complex and intertrigeminal region in the control of breathing. *Respir Physiol Neurobiol* 143:115-125.
- Chatonnet F, Thoby-Brisson M, Abadie V, Dominguez del Toro E, Champagnat J, Fortin G (2002) Early development of respiratory rhythm generation in mouse and chick. *Respir Physiol Neurobiol* 131:5-13.
- Chatonnet F, Dominguez del Toro E, Thoby-Brisson M, Champagnat J, Fortin G, Rijli FM, Thaeron-Antono C (2003) From hindbrain segmentation to breathing after birth: developmental patterning in rhombomeres 3 and 4. *Mol Neurobiol* 28:277-294.
- Chatonnet F, Borday C, Wrobel L, Thoby-Brisson M, Fortin G, McLean H, Champagnat J (2006) Ontogeny of central rhythm generation in chicks and rodents. *Respir Physiol Neurobiol*.

- Chen H, Lun Y, Ovchinnikov D, Kokubo H, Oberg KC, Pepicelli CV, Gan L, Lee B, Johnson RL (1998) Limb and kidney defects in *Lmx1b* mutant mice suggest an involvement of LMX1B in human nail patella syndrome. *Nat Genet* 19:51-55.
- Chen Z, Hedner J, Hedner T (1990) Substance P in the ventrolateral medulla oblongata regulates ventilatory responses. *J Appl Physiol* 68:2631-2639.
- Chen ZB, Engberg G, Hedner T, Hedner J (1991) Antagonistic effects of somatostatin and substance P on respiratory regulation in the rat ventrolateral medulla oblongata. *Brain Res* 556:13-21.
- Cheng L, Chen CL, Luo P, Tan M, Qiu M, Johnson R, Ma Q (2003) *Lmx1b*, *Pet-1*, and *Nkx2.2* coordinately specify serotonergic neurotransmitter phenotype. *J Neurosci* 23:9961-9967.
- Clift S, Dahlitz M, Parkes JD (1994) Sleep apnoea in the Prader-Willi syndrome. *J Sleep Res* 3:121-126.
- Connelly CA, Ellenberger HH, Feldman JL (1989) Are there serotonergic projections from raphe and retrotrapezoid nuclei to the ventral respiratory group in the rat? *Neurosci Lett* 105:34-40.
- Cosmi EV, Anceschi MM, Cosmi E, Piazzè JJ, La Torre R (2003) Ultrasonographic patterns of fetal breathing movements in normal pregnancy. *Int J Gynaecol Obstet* 80:285-290.
- Craven SE, Lim KC, Ye W, Engel JD, de Sauvage F, Rosenthal A (2004) *Gata2* specifies serotonergic neurons downstream of sonic hedgehog. *Development* 131:1165-1173.
- Dauger S, Pattyn A, Lofaso F, Gaultier C, Goridis C, Gallego J, Brunet JF (2003) *Phox2b* controls the development of peripheral chemoreceptors and afferent visceral pathways. *Development* 130:6635-6642.
- Dauger S, Guimiot F, Renolleau S, Levacher B, Boda B, Mas C, Nepote V, Simonneau M, Gaultier C, Gallego J (2001) MASH-1/RET pathway involvement in development of brain stem control of respiratory frequency in newborn mice. *Physiol Genomics* 7:149-157.

- De Felipe C, Herrero JF, O'Brien JA, Palmer JA, Doyle CA, Smith AJ, Laird JM, Belmonte C, Cervero F, Hunt SP (1998) Altered nociception, analgesia and aggression in mice lacking the receptor for substance P. *Nature* 392:394-397.
- Del Negro CA, Koshiya N, Butera RJ, Jr., Smith JC (2002) Persistent sodium current, membrane properties and bursting behavior of pre-botzinger complex inspiratory neurons in vitro. *J Neurophysiol* 88:2242-2250.
- Del Negro CA, Morgado-Valle C, Hayes JA, Mackay DD, Pace RW, Crowder EA, Feldman JL (2005) Sodium and calcium current-mediated pacemaker neurons and respiratory rhythm generation. *J Neurosci* 25:446-453.
- del Toro ED, Borday V, Davenne M, Neun R, Rijli FM, Champagnat J (2001) Generation of a novel functional neuronal circuit in *Hoxa1* mutant mice. *J Neurosci* 21:5637-5642.
- Di Pasquale E, Monteau R, Hilaire G (1994) Endogenous serotonin modulates the fetal respiratory rhythm: an in vitro study in the rat. *Brain Res Dev Brain Res* 80:222-232.
- Di Pasquale E, Morin D, Monteau R, Hilaire G (1992) Serotonergic modulation of the respiratory rhythm generator at birth: an in vitro study in the rat. *Neurosci Lett* 143:91-95.
- Ding YQ, Marklund U, Yuan W, Yin J, Wegman L, Ericson J, Deneris E, Johnson RL, Chen ZF (2003) *Lmx1b* is essential for the development of serotonergic neurons. *Nat Neurosci* 6:933-938.
- Dutschmann M, Morschel M, Kron M, Herbert H (2004) Development of adaptive behaviour of the respiratory network: implications for the pontine Kolliker-Fuse nucleus. *Respir Physiol Neurobiol* 143:155-165.
- Eisen JS (1999) Patterning motoneurons in the vertebrate nervous system. *Trends Neurosci* 22:321-326.
- Ellenberger HH, Feldman JL (1990) Subnuclear organization of the lateral tegmental field of the rat. I: Nucleus ambiguus and ventral respiratory group. *J Comp Neurol* 294:202-211.
- Ellenberger HH, Feldman JL (1994) Origins of excitatory drive within the respiratory network: anatomical localization. *Neuroreport* 5:1933-1936.

- Errchidi S, Hilaire G, Monteau R (1990) Permanent release of noradrenaline modulates respiratory frequency in the newborn rat: an in vitro study. *J Physiol* 429:497-510.
- Errchidi S, Monteau R, Hilaire G (1991) Noradrenergic modulation of the medullary respiratory rhythm generator in the newborn rat: an in vitro study. *J Physiol* 443:477-498.
- Ezure K (1990) Synaptic connections between medullary respiratory neurons and considerations on the genesis of respiratory rhythm. *Prog Neurobiol* 35:429-450.
- Ezure K, Manabe M, Yamada H (1988) Distribution of medullary respiratory neurons in the rat. *Brain Res* 455:262-270.
- Feldman JL, Smith JC (1989) Cellular mechanisms underlying modulation of breathing pattern in mammals. *Ann N Y Acad Sci* 563:114-130.
- Feldman JL, Del Negro CA (2006) Looking for inspiration: new perspectives on respiratory rhythm. *Nat Rev Neurosci* 7:232-242.
- Feldman JL, Mitchell GS, Nattie EE (2003) Breathing: rhythmicity, plasticity, chemosensitivity. *Annu Rev Neurosci* 26:239-266.
- Filiano JJ, Kinney HC (1994) A perspective on neuropathologic findings in victims of the sudden infant death syndrome: the triple-risk model. *Biol Neonate* 65:194-197.
- Funk GD, Smith JC, Feldman JL (1993) Generation and transmission of respiratory oscillations in medullary slices: role of excitatory amino acids. *J Neurophysiol* 70:1497-1515.
- Funk GD, Kanjhan R, Walsh C, Lipski J, Comer AM, Parkis MA, Housley GD (1997) P2 receptor excitation of rodent hypoglossal motoneuron activity in vitro and in vivo: a molecular physiological analysis. *J Neurosci* 17:6325-6337.
- Gaspar P (2004) [Genetic models to understand how serotonin acts during development]. *J Soc Biol* 198:18-21.
- Gaspar P, Cases O, Maroteaux L (2003) The developmental role of serotonin: news from mouse molecular genetics. *Nat Rev Neurosci* 4:1002-1012.
- Gaultier C, Amiel J, Dager S, Trang H, Lyonnet S, Gallego J, Simonneau M (2004) Genetics and early disturbances of breathing control. *Pediatr Res* 55:729-733.
- Glaze DG (2005) Neurophysiology of Rett syndrome. *J Child Neurol* 20:740-746.

- Goldstone AP (2004) Prader-Willi syndrome: advances in genetics, pathophysiology and treatment. *Trends Endocrinol Metab* 15:12-20.
- Goulding M, Lanuza G, Sapir T, Narayan S (2002) The formation of sensorimotor circuits. *Curr Opin Neurobiol* 12:508-515.
- Gourine AV, Dale N, Spyer KM (2004) Chemosensory control of the respiratory function. Working towards understanding the role of ATP-mediated purinergic signalling. *Adv Exp Med Biol* 551:31-38.
- Gourine AV, Llaudet E, Dale N, Spyer KM (2005) ATP is a mediator of chemosensory transduction in the central nervous system. *Nature* 436:108-111.
- Gozal D, Arens R, Omlin KJ, Ward SL, Keens TG (1994) Absent peripheral chemosensitivity in Prader-Willi syndrome. *J Appl Physiol* 77:2231-2236.
- Gray PA, Rekling JC, Bocchiario CM, Feldman JL (1999) Modulation of respiratory frequency by peptidergic input to rhythmogenic neurons in the preBotzinger complex. *Science* 286:1566-1568.
- Gray PA, Janczewski WA, Mellen N, McCrimmon DR, Feldman JL (2001) Normal breathing requires preBotzinger complex neurokinin-1 receptor-expressing neurons. *Nat Neurosci* 4:927-930.
- Greer JJ, Smith JC, Feldman JL (1991) Role of excitatory amino acids in the generation and transmission of respiratory drive in neonatal rat. *J Physiol* 437:727-749.
- Greer JJ, Carter JE, al-Zubaidy Z (1995) Opioid depression of respiration in neonatal rats. *J Physiol* 485 ( Pt 3):845-855.
- Greer JJ, al-Zubaidy Z, Carter JE (1996) Thyrotropin-releasing hormone stimulates perinatal rat respiration in vitro. *Am J Physiol* 271:R1160-1164.
- Guyenet PG, Wang H (2001) Pre-Botzinger neurons with preinspiratory discharges "in vivo" express NK1 receptors in the rat. *J Neurophysiol* 86:438-446.
- Guyenet PG, Sevigny CP, Weston MC, Stornetta RL (2002) Neurokinin-1 receptor-expressing cells of the ventral respiratory group are functionally heterogeneous and predominantly glutamatergic. *J Neurosci* 22:3806-3816.
- Hanson MG, Landmesser LT (2003) Characterization of the circuits that generate spontaneous episodes of activity in the early embryonic mouse spinal cord. *J Neurosci* 23:587-600.

- Hanson MG, Landmesser LT (2004) Normal patterns of spontaneous activity are required for correct motor axon guidance and the expression of specific guidance molecules. *Neuron* 43:687-701.
- Hendricks TJ, Fyodorov DV, Wegman LJ, Lelutiu NB, Pehk EA, Yamamoto B, Silver J, Weeber EJ, Sweatt JD, Deneris ES (2003) Pet-1 ETS gene plays a critical role in 5-HT neuron development and is required for normal anxiety-like and aggressive behavior. *Neuron* 37:233-247.
- Hilaire G (2006) Endogenous noradrenaline affects the maturation and function of the respiratory network: Possible implication for SIDS. *Auton Neurosci* 126-127:320-331.
- Hilaire G, Duron B (1999) Maturation of the mammalian respiratory system. *Physiol Rev* 79:325-360.
- Hilaire G, Viemari JC, Coulon P, Simonneau M, Bevenut M (2004) Modulation of the respiratory rhythm generator by the pontine noradrenergic A5 and A6 groups in rodents. *Respir Physiol Neurobiol* 143:187-197.
- Hirsch MR, Tiveron MC, Guillemot F, Brunet JF, Goridis C (1998) Control of noradrenergic differentiation and Phox2a expression by MASH1 in the central and peripheral nervous system. *Development* 125:599-608.
- Holtman JR, Jr., Speck DF (1994) Substance P immunoreactive projections to the ventral respiratory group in the rat. *Peptides* 15:803-808.
- Homma I, Oouchi M, Ichikawa S (1984) Facilitation of inspiration by intracerebroventricular injection of thyrotropin-releasing hormone in rabbits. *Neurosci Lett* 44:265-269.
- Huang ZG, Subramanian SH, Balnave RJ, Turman AB, Moi Chow C (2000) Roles of periaqueductal gray and nucleus tractus solitarius in cardiorespiratory function in the rat brainstem. *Respir Physiol* 120:185-195.
- Iwase M, Homma I, Shioda S, Nakai Y (1988) Thyrotropin-releasing hormone-like immunoreactive neurons in rabbit medulla oblongata. *Neurosci Lett* 92:30-33.
- Iwase M, Shioda S, Nakai Y, Homma I (1991) Immunocytochemistry of thyrotropin-releasing hormone in the rabbit medulla oblongata. *Brain Res Bull* 26:49-57.

- Jacobson M, Rao MS (2005) *Developmental neurobiology*. New York: Kluwer Academic/Plenum.
- Jacquin TD, Borday V, Schneider-Maunoury S, Topilko P, Ghilini G, Kato F, Charnay P, Champagnat J (1996) Reorganization of pontine rhythmogenic neuronal networks in Krox-20 knockout mice. *Neuron* 17:747-758.
- Janczewski WA, Feldman JL (2006) Distinct rhythm generators for inspiration and expiration in the juvenile rat. *J Physiol* 570:407-420.
- Janczewski WA, Onimaru H, Homma I, Feldman JL (2002) Opioid-resistant respiratory pathway from the preinspiratory neurones to abdominal muscles: in vivo and in vitro study in the newborn rat. *J Physiol* 545:1017-1026.
- Jansen AH, Chernick V (1991) Fetal breathing and development of control of breathing. *J Appl Physiol* 70:1431-1446.
- Jean-Charles V, Gerard H (2002) Noradrenergic receptors and in vitro respiratory rhythm: possible interspecies differences between mouse and rat neonates. *Neurosci Lett* 324:149-153.
- Johnson SM, Smith JC, Funk GD, Feldman JL (1994) Pacemaker behavior of respiratory neurons in medullary slices from neonatal rat. *J Neurophysiol* 72:2598-2608.
- Julu PO, Kerr AM, Apartopoulos F, Al-Rawas S, Engerstrom IW, Engerstrom L, Jamal GA, Hansen S (2001) Characterisation of breathing and associated central autonomic dysfunction in the Rett disorder. *Arch Dis Child* 85:29-37.
- Kitterman JA (1996) The effects of mechanical forces on fetal lung growth. *Clin Perinatol* 23:727-740.
- Kobayashi K, Lemke RP, Greer JJ (2001) Ultrasound measurements of fetal breathing movements in the rat. *J Appl Physiol* 91:316-320.
- Lahiri S, Roy A, Baby SM, Hoshi T, Semenza GL, Prabhakar NR (2006) Oxygen sensing in the body. *Prog Biophys Mol Biol* 91:249-286.
- Lieske SP, Thoby-Brisson M, Telgkamp P, Ramirez JM (2000) Reconfiguration of the neural network controlling multiple breathing patterns: eupnea, sighs and gasps [see comment]. *Nat Neurosci* 3:600-607.

- Lim KC, Lakshmanan G, Crawford SE, Gu Y, Grosveld F, Engel JD (2000) Gata3 loss leads to embryonic lethality due to noradrenaline deficiency of the sympathetic nervous system. *Nat Genet* 25:209-212.
- Ling L, Karius DR, Speck DF (1994) Role of N-methyl-D-aspartate receptors in the pontine pneumotaxic mechanism in the cat. *J Appl Physiol* 76:1138-1143.
- Liu Q, Wong-Riley MT (2002) Postnatal expression of neurotransmitters, receptors, and cytochrome oxidase in the rat pre-Botzinger complex. *J Appl Physiol* 92:923-934.
- Liu Q, Wong-Riley MT (2003) Postnatal changes in cytochrome oxidase expressions in brain stem nuclei of rats: implications for sensitive periods. *J Appl Physiol* 95:2285-2291.
- Liu Q, Wong-Riley MT (2005) Postnatal developmental expressions of neurotransmitters and receptors in various brain stem nuclei of rats. *J Appl Physiol* 98:1442-1457.
- Liu YY, Wong-Riley MT, Liu JP, Jia Y, Liu HL, Jiao XY, Ju G (2002) GABAergic and glycinergic synapses onto neurokinin-1 receptor-immunoreactive neurons in the pre-Botzinger complex of rats: light and electron microscopic studies. *Eur J Neurosci* 16:1058-1066.
- Liu YY, Wong-Riley MT, Liu JP, Jia Y, Liu HL, Fujiyama F, Ju G (2003) Relationship between two types of vesicular glutamate transporters and neurokinin-1 receptor-immunoreactive neurons in the pre-Botzinger complex of rats: light and electron microscopic studies. *Eur J Neurosci* 17:41-48.
- Liu YY, Wong-Riley MT, Liu JP, Wei XY, Jia Y, Liu HL, Fujiyama F, Ju G (2004) Substance P and enkephalinergic synapses onto neurokinin-1 receptor-immunoreactive neurons in the pre-Botzinger complex of rats. *Eur J Neurosci* 19:65-75.
- Lorier AR, Peebles K, Brosenitsch T, Robinson DM, Housley GD, Funk GD (2004) P2 receptors modulate respiratory rhythm but do not contribute to central CO<sub>2</sub> sensitivity in vitro. *Respir Physiol Neurobiol* 142:27-42.
- Makeham JM, Goodchild AK, Pilowsky PM (2001) NK1 receptor and the ventral medulla of the rat: bulbospinal and catecholaminergic neurons. *Neuroreport* 12:3663-3667.

- Manni R, Politini L, Nobili L, Ferrillo F, Livieri C, Veneselli E, Biancheri R, Martinetti M, Tartara A (2001) Hypersomnia in the Prader Willi syndrome: clinical-electrophysiological features and underlying factors. *Clin Neurophysiol* 112:800-805.
- Manzke T, Guenther U, Ponimaskin EG, Haller M, Dutschmann M, Schwarzacher S, Richter DW (2003) 5-HT<sub>4</sub>(a) receptors avert opioid-induced breathing depression without loss of analgesia. *Science* 301:226-229.
- Martin RJ, Abu-Shaweesh JM (2005) Control of breathing and neonatal apnea. *Biol Neonate* 87:288-295.
- Martin RJ, Abu-Shaweesh JM, Baird TM (2004) Apnoea of prematurity. *Paediatr Respir Rev* 5 Suppl A:S377-382.
- McKay LC, Janczewski WA, Feldman JL (2005) Sleep-disordered breathing after targeted ablation of preBotzinger complex neurons. *Nat Neurosci* 8:1142-1144.
- Mellen NM, Janczewski WA, Bocchiario CM, Feldman JL (2003) Opioid-induced quantal slowing reveals dual networks for respiratory rhythm generation. *Neuron* 37:821-826.
- Melton KR, Iulianella A, Trainor PA (2004) Gene expression and regulation of hindbrain and spinal cord development. *Front Biosci* 9:117-138.
- Menendez AA (1999) Abnormal ventilatory responses in patients with Prader-Willi syndrome. *Eur J Pediatr* 158:941-942.
- Miles GB, Parkis MA, Lipski J, Funk GD (2002) Modulation of phrenic motoneuron excitability by ATP: consequences for respiratory-related output in vitro. *J Appl Physiol* 92:1899-1910.
- Monteau R, Ptak K, Broquere N, Hilaire G (1996) Tachykinins and central respiratory activity: an in vitro study on the newborn rat. *Eur J Pharmacol* 314:41-50.
- Morin-Surun MP, Boudinot E, Gacel G, Champagnat J, Roques BP, Denavit-Saubie M (1984) Different effects of mu and delta opiate agonists on respiration. *Eur J Pharmacol* 98:235-240.
- Morin X, Cremer H, Hirsch MR, Kapur RP, Goridis C, Brunet JF (1997) Defects in sensory and autonomic ganglia and absence of locus coeruleus in mice deficient for the homeobox gene Phox2a. *Neuron* 18:411-423.

- Moss IR, Inman JG (1989) Neurochemicals and respiratory control during development. *J Appl Physiol* 67:1-13.
- Mulkey DK, Mistry AM, Guyenet PG, Bayliss DA (2006) Purinergic P2 receptors modulate excitability but do not mediate pH sensitivity of RTN respiratory chemoreceptors. *J Neurosci* 26:7230-7233.
- Nattie E (1999) CO<sub>2</sub>, brainstem chemoreceptors and breathing. *Prog Neurobiol* 59:299-331.
- Nattie E, Li A (2006) Central chemoreception 2005: A brief review. *Auton Neurosci* 126-127:332-338.
- Nicholls RD, Knepper JL (2001) Genome organization, function, and imprinting in Prader-Willi and Angelman syndromes. *Annu Rev Genomics Hum Genet* 2:153-175.
- Nixon GM, Brouillette RT (2002) Sleep and breathing in Prader-Willi syndrome. *Pediatr Pulmonol* 34:209-217.
- Onimaru H, Homma I (2003) A novel functional neuron group for respiratory rhythm generation in the ventral medulla. *J Neurosci* 23:1478-1486.
- Onimaru H, Arata A, Homma I (1987) Localization of respiratory rhythm-generating neurons in the medulla of brainstem-spinal cord preparations from newborn rats. *Neurosci Lett* 78:151-155.
- Onimaru H, Arata A, Homma I (1988) Primary respiratory rhythm generator in the medulla of brainstem-spinal cord preparation from newborn rat. *Brain Res* 445:314-324.
- Onimaru H, Arata A, Homma I (1989) Firing properties of respiratory rhythm generating neurons in the absence of synaptic transmission in rat medulla in vitro. *Exp Brain Res* 76:530-536.
- Onimaru H, Arata A, Homma I (1990) Inhibitory synaptic inputs to the respiratory rhythm generator in the medulla isolated from newborn rats. *Pflugers Arch* 417:425-432.
- Onimaru H, Shamoto A, Homma I (1998) Modulation of respiratory rhythm by 5-HT in the brainstem-spinal cord preparation from newborn rat. *Pflugers Arch* 435:485-494.

- Onimaru H, Kumagawa Y, Homma I (2006a) Respiration-related rhythmic activity in the rostral medulla of newborn rats. *J Neurophysiol*.
- Onimaru H, Homma I, Feldman JL, Janczewski WA (2006b) Point:Counterpoint: The parafacial respiratory group (pFRG)/pre-Botzinger complex (preBotC) is the primary site of respiratory rhythm generation in the mammal. *J Appl Physiol* 100:2094-2098.
- Pagliardini S, Ren J, Wevrick R, Greer JJ (2005) Developmental abnormalities of neuronal structure and function in prenatal mice lacking the prader-willi syndrome gene *necdin*. *Am J Pathol* 167:175-191.
- Pasqualetti M, Rijli FM (2001) Homeobox gene mutations and brain-stem developmental disorders: learning from knockout mice. *Curr Opin Neurol* 14:177-184.
- Paton JF, Abdala AP, Koizumi H, Smith JC, St-John WM (2006) Respiratory rhythm generation during gasping depends on persistent sodium current. *Nat Neurosci* 9:311-313.
- Pattyn A, Goridis C, Brunet JF (2000) Specification of the central noradrenergic phenotype by the homeobox gene *Phox2b*. *Mol Cell Neurosci* 15:235-243.
- Pattyn A, Simplicio N, van Doorninck JH, Goridis C, Guillemot F, Brunet JF (2004) *Ascl1/Mash1* is required for the development of central serotonergic neurons. *Nat Neurosci* 7:589-595.
- Pazos A, Florez J (1984) A comparative study in rats of the respiratory depression and analgesia induced by mu- and delta-opioid agonists. *Eur J Pharmacol* 99:15-21.
- Peirano P, Algarin C, Uauy R (2003) Sleep-wake states and their regulatory mechanisms throughout early human development. *J Pediatr* 143:S70-79.
- Pena F, Ramirez JM (2002) Endogenous activation of serotonin-2A receptors is required for respiratory rhythm generation in vitro. *J Neurosci* 22:11055-11064.
- Pena F, Ramirez JM (2004) Substance P-mediated modulation of pacemaker properties in the mammalian respiratory network. *J Neurosci* 24:7549-7556.
- Pena F, Parkis MA, Tryba AK, Ramirez JM (2004) Differential contribution of pacemaker properties to the generation of respiratory rhythms during normoxia and hypoxia. *Neuron* 43:105-117.
- Polin RA, Fox WW (1998) Fetal and neonatal physiology. Philadelphia Saunders Editor.

- Prabhakar NR (2006) O<sub>2</sub> sensing at the mammalian carotid body: why multiple O<sub>2</sub> sensors and multiple transmitters? *Exp Physiol* 91:17-23.
- Ptak K, Di Pasquale E, Monteau R (1999) Substance P and central respiratory activity: a comparative in vitro study on foetal and newborn rat. *Brain Res Dev Brain Res* 114:217-227.
- Ptak K, Konrad M, Di Pasquale E, Tell F, Hilaire G, Monteau R (2000) Cellular and synaptic effect of substance P on neonatal phrenic motoneurons. *Eur J Neurosci* 12:126-138.
- Qian Y, Shirasawa S, Chen CL, Cheng L, Ma Q (2002) Proper development of relay somatic sensory neurons and D2/D4 interneurons requires homeobox genes *Rnx/Tlx-3* and *Tlx-1*. *Genes Dev* 16:1220-1233.
- Qian Y, Fritsch B, Shirasawa S, Chen CL, Choi Y, Ma Q (2001) Formation of brainstem (nor)adrenergic centers and first-order relay visceral sensory neurons is dependent on homeodomain protein *Rnx/Tlx3*. *Genes Dev* 15:2533-2545.
- Ramirez JM, Richter DW (1996) The neuronal mechanisms of respiratory rhythm generation. *Curr Opin Neurobiol* 6:817-825.
- Rekling JC, Champagnat J, Denavit-Saubie M (1996a) Thyrotropin-releasing hormone (TRH) depolarizes a subset of inspiratory neurons in the newborn mouse brain stem in vitro. *J Neurophysiol* 75:811-819.
- Rekling JC, Champagnat J, Denavit-Saubie M (1996b) Electroresponsive properties and membrane potential trajectories of three types of inspiratory neurons in the newborn mouse brain stem in vitro. *J Neurophysiol* 75:795-810.
- Ren J, Greer JJ (2003) Ontogeny of rhythmic motor patterns generated in the embryonic rat spinal cord. *J Neurophysiol* 89:1187-1195.
- Ren J, Greer JJ (2006) Modulation of respiratory rhythmogenesis by chloride-mediated conductances during the perinatal period. *J Neurosci* 26:3721-3730.
- Ren J, Lee S, Pagliardini S, Gerard M, Stewart CL, Greer JJ, Wevrick R (2003) Absence of *Ndn*, encoding the Prader-Willi syndrome-deleted gene *necdin*, results in congenital deficiency of central respiratory drive in neonatal mice. *J Neurosci* 23:1569-1573.

- Richerson GB (2004) Serotonergic neurons as carbon dioxide sensors that maintain pH homeostasis. *Nat Rev Neurosci* 5:449-461.
- Richerson GB, Wang W, Hodges MR, Dohle CI, Diez-Sampedro A (2005) Homing in on the specific phenotype(s) of central respiratory chemoreceptors. *Exp Physiol* 90:259-266; discussion 266-259.
- Richter DW, Manzke T, Wilken B, Ponimaskin E (2003) Serotonin receptors: guardians of stable breathing. *Trends Mol Med* 9:542-548.
- Rigatto H (1992) Maturation of breathing. *Clin Perinatol* 19:739-756.
- Rong W, Gourine AV, Cockayne DA, Xiang Z, Ford AP, Spyer KM, Burnstock G (2003) Pivotal role of nucleotide P2X2 receptor subunit of the ATP-gated ion channel mediating ventilatory responses to hypoxia. *J Neurosci* 23:11315-11321.
- Sanchez-Esteban J, Wang Y, Cicchiello LA, Rubin LP (2002) Cyclic mechanical stretch inhibits cell proliferation and induces apoptosis in fetal rat lung fibroblasts. *Am J Physiol Lung Cell Mol Physiol* 282:L448-456.
- Sanchez-Esteban J, Cicchiello LA, Wang Y, Tsai SW, Williams LK, Torday JS, Rubin LP (2001) Mechanical stretch promotes alveolar epithelial type II cell differentiation. *J Appl Physiol* 91:589-595.
- Sasaki A, Kanai M, Kijima K, Akaba K, Hashimoto M, Hasegawa H, Otaki S, Koizumi T, Kusuda S, Ogawa Y, Tuchiya K, Yamamoto W, Nakamura T, Hayasaka K (2003) Molecular analysis of congenital central hypoventilation syndrome. *Hum Genet* 114:22-26.
- Schluter B, Buschatz D, Trowitzsch E, Aksu F, Andler W (1997) Respiratory control in children with Prader-Willi syndrome. *Eur J Pediatr* 156:65-68.
- Schneider-Maunoury S, Topilko P, Seitandou T, Levi G, Cohen-Tannoudji M, Pournin S, Babinet C, Charnay P. (1993) Disruption of Krox-20 results in alteration of rhombomeres 3 and 5 in the developing hindbrain. *Cell* 75(6):1199-214.
- Schneider-Maunoury S, Gilardi-Hebenstreit P, Charnay P (1998) How to build a vertebrate hindbrain. Lessons from genetics. *C R Acad Sci III* 321:819-834.
- Schwarzacher SW, Smith JC, Richter DW (1995) Pre-Botzinger complex in the cat. *J Neurophysiol* 73:1452-1461.

- Schwarzacher SW, Pestean A, Gunther S, Ballanyi K (2002) Serotonergic modulation of respiratory motoneurons and interneurons in brainstem slices of perinatal rats. *Neuroscience* 115:1247-1259.
- Scott MM, Krueger KC, Deneris ES (2005) A differentially autoregulated Pet-1 enhancer region is a critical target of the transcriptional cascade that governs serotonin neuron development. *J Neurosci* 25:2628-2636.
- Segawa M, Nomura Y (2005) Rett syndrome. *Curr Opin Neurol* 18:97-104.
- Shirasawa S, Arata A, Onimaru H, Roth KA, Brown GA, Horning S, Arata S, Okumura K, Sasazuki T, Korsmeyer SJ (2000) Rnx deficiency results in congenital central hypoventilation. *Nat Genet* 24:287-290.
- Smith JC, Greer JJ, Liu GS, Feldman JL (1990) Neural mechanisms generating respiratory pattern in mammalian brain stem-spinal cord in vitro. I. Spatiotemporal patterns of motor and medullary neuron activity. *J Neurophysiol* 64:1149-1169.
- Smith JC, Ellenberger HH, Ballanyi K, Richter DW, Feldman JL (1991) Pre-Botzinger complex: a brainstem region that may generate respiratory rhythm in mammals. *Science* 254:726-729.
- Spyer KM, Dale N, Gourine AV (2004) ATP is a key mediator of central and peripheral chemosensory transduction. *Exp Physiol* 89:53-59.
- Stevenson DA, Anaya TM, Clayton-Smith J, Hall BD, Van Allen MI, Zori RT, Zackai EH, Frank G, Clericuzio CL (2004) Unexpected death and critical illness in Prader-Willi syndrome: report of ten individuals. *Am J Med Genet A* 124:158-164.
- Stornetta RL, Rosin DL, Wang H, Sevigny CP, Weston MC, Guyenet PG (2003) A group of glutamatergic interneurons expressing high levels of both neurokinin-1 receptors and somatostatin identifies the region of the pre-Botzinger complex. *J Comp Neurol* 455:499-512.
- Sun QJ, Llewellyn-Smith I, Minson J, Arnolda L, Chalmers J, Pilowsky P (1996) Thyrotropin-releasing hormone immunoreactive boutons form close appositions with medullary expiratory neurons in the rat. *Brain Res* 715:136-144.

- Suzue T (1984) Respiratory rhythm generation in the in vitro brain stem-spinal cord preparation of the neonatal rat. *J Physiol* 354:173-183.
- Telgkamp P, Cao YQ, Basbaum AI, Ramirez JM (2002) Long-term deprivation of substance P in PPT-A mutant mice alters the anoxic response of the isolated respiratory network. *J Neurophysiol* 88:206-213.
- Thach BT (2005) The role of respiratory control disorders in SIDS. *Respir Physiol Neurobiol* 149:343-353.
- Thoby-Brisson M, Ramirez JM (2000) Role of inspiratory pacemaker neurons in mediating the hypoxic response of the respiratory network in vitro. *J Neurosci* 20:5858-5866.
- Thoby-Brisson M, Ramirez JM (2001) Identification of two types of inspiratory pacemaker neurons in the isolated respiratory neural network of mice. *J Neurophysiol* 86:104-112.
- Thoby-Brisson M, Telgkamp P, Ramirez JM (2000) The role of the hyperpolarization-activated current in modulating rhythmic activity in the isolated respiratory network of mice. *J Neurosci* 20:2994-3005.
- Thomas T, Spyer KM (2000) ATP as a mediator of mammalian central CO<sub>2</sub> chemoreception. *J Physiol* 523 Pt 2:441-447.
- Thomas T, Ralevic V, Gadd CA, Spyer KM (1999) Central CO<sub>2</sub> chemoreception: a mechanism involving P<sub>2</sub> purinoceptors localized in the ventrolateral medulla of the anaesthetized rat. *J Physiol* 517 ( Pt 3):899-905.
- Thomas T, Ralevic V, Bardini M, Burnstock G, Spyer KM (2001) Evidence for the involvement of purinergic signalling in the control of respiration. *Neuroscience* 107:481-490.
- Tiveron MC, Hirsch MR, Brunet JF (1996) The expression pattern of the transcription factor Phox2 delineates synaptic pathways of the autonomic nervous system. *J Neurosci* 16:7649-7660.
- Tryba AK, Ramirez JM (2004) Background sodium current stabilizes bursting in respiratory pacemaker neurons. *J Neurobiol* 60:481-489.

- Tsai FY, Keller G, Kuo FC, Weiss M, Chen J, Rosenblatt M, Alt FW, Orkin SH (1994) An early haematopoietic defect in mice lacking the transcription factor GATA-2. *Nature* 371:221-226.
- Viemari JC, Hilaire G (2003) Monoamine oxidase A-deficiency and noradrenergic respiratory regulations in neonatal mice. *Neurosci Lett* 340:221-224.
- Viemari JC, Bevengut M, Burnet H, Coulon P, Pequignot JM, Tiveron MC, Hilaire G (2004) Phox2a gene, A6 neurons, and noradrenaline are essential for development of normal respiratory rhythm in mice. *J Neurosci* 24:928-937.
- Viemari JC, Roux JC, Tryba AK, Saywell V, Burnet H, Pena F, Zanella S, Bevengut M, Barthelemy-Requin M, Herzing LB, Moncla A, Mancini J, Ramirez JM, Villard L, Hilaire G (2005) Mecp2 deficiency disrupts norepinephrine and respiratory systems in mice. *J Neurosci* 25:11521-11530.
- Wang H, Stornetta RL, Rosin DL, Guyenet PG (2001) Neurokinin-1 receptor-immunoreactive neurons of the ventral respiratory group in the rat. *J Comp Neurol* 434:128-146.
- Weese-Mayer DE, Berry-Kravis EM, Marazita ML (2005) In pursuit (and discovery) of a genetic basis for congenital central hypoventilation syndrome. *Respir Physiol Neurobiol* 149:73-82.
- Weese-Mayer DE, Berry-Kravis EM, Zhou L, Maher BS, Silvestri JM, Curran ME, Marazita ML (2003) Idiopathic congenital central hypoventilation syndrome: analysis of genes pertinent to early autonomic nervous system embryologic development and identification of mutations in PHOX2b. *Am J Med Genet A* 123:267-278.
- Weese-Mayer DE, Berry-Kravis EM, Zhou L, Maher BS, Curran ME, Silvestri JM, Marazita ML (2004) Sudden infant death syndrome: case-control frequency differences at genes pertinent to early autonomic nervous system embryologic development. *Pediatr Res* 56:391-395.
- Wenninger JM, Pan LG, Klum L, Leekley T, Bastastic J, Hodges MR, Feroah T, Davis S, Forster HV (2004a) Small reduction of neurokinin-1 receptor-expressing neurons in the pre-Botzinger complex area induces abnormal breathing periods in awake goats. *J Appl Physiol* 97:1620-1628.

- Wenninger JM, Pan LG, Klum L, Leekley T, Bastastic J, Hodges MR, Feroah TR, Davis S, Forster HV (2004b) Large lesions in the pre-Botzinger complex area eliminate eupneic respiratory rhythm in awake goats. *J Appl Physiol* 97:1629-1636.
- Wharton RH, Loechner KJ (1996) Genetic and clinical advances in Prader-Willi syndrome. *Curr Opin Pediatr* 8:618-624.
- Wong-Riley MT, Liu Q (2005) Neurochemical development of brain stem nuclei involved in the control of respiration. *Respir Physiol Neurobiol* 149:83-98.
- Yamamoto Y, Onimaru H, Homma I (1992) Effect of substance P on respiratory rhythm and pre-inspiratory neurons in the ventrolateral structure of rostral medulla oblongata: an in vitro study. *Brain Res* 599:272-276.
- Yasuda K, Robinson DM, Selvaratnam SR, Walsh CW, McMorland AJ, Funk GD (2001) Modulation of hypoglossal motoneuron excitability by NK1 receptor activation in neonatal mice in vitro. *J Physiol* 534:447-464.
- Zanella S, Roux JC, Viemari JC, Hilaire G (2005) Possible modulation of the mouse respiratory rhythm generator by A1/C1 neurones. *Respir Physiol Neurobiol*.

## **\*CHAPTER II**

### **Ontogeny of the preBötzinger Complex in Perinatal Rat**

---

\* Previously published paper:

Pagliardini S, Ren J, Greer JJ (2003) Ontogeny of the preBötzinger Complex in the perinatal rats. *J Neurosci* 23: 9575-9584. Copyright 2003 by the Society for Neuroscience  
My contribution to this study consisted in the planning and execution of the anatomical studies and birthdating of neurons. Electrophysiological recordings and analysis were performed by Dr. J. Ren.

## 2.1 INTRODUCTION

The preBötC is composed of a group of neurons located in the ventrolateral medulla that are essential for the generation of the mammalian respiratory rhythm (for review, see Rekling and Feldman, 1998; Feldman et al., 2003). Given the functional importance of this region, it has become a major focus of research in the field of respiratory neural control. This study is the first to examine the ontogeny of the preBötC. Immunohistochemical and electrophysiological techniques were used to discern when the preBötC forms and how its anatomical organization and rhythmic neuronal activity change during the perinatal period in rats. Collectively, these data provide the necessary foundation for understanding critical stages of mammalian respiratory center development.

The preBötC, originally identified in a seminal study published by Smith et al. (1991), is located ventral to the semicompact division of the nucleus ambiguus (NA), caudal to the compact division of the NA and rostral to the lateral reticular nucleus (LRN) formation. Subsequent experiments using electrophysiological recordings, pharmacological manipulations, and lesions, both in vitro and in vivo, confirmed that the preBötC is critically involved in the generation of the respiratory rhythm (Smith et al., 1991; Ramirez et al., 1998; Solomon et al., 1999; Gray et al., 2001; Sun et al., 2001).

Gray et al. (1999) proposed that preBötC neurons could be identified by immunolabeling for NK1Rs. Although demonstrating that NK1R-immunopositive neurons were also present outside the preBötC, subsequent studies supported the idea that there is a population of small fusiform neurons expressing NK1Rs in the preBötC that have characteristics consistent with their being involved in respiratory rhythmogenesis (Pilowsky and Feldman, 2001; Wang et al., 2001; Guyenet et al., 2002). Further support came from experiments demonstrating that bilateral destruction of NK1R<sup>+</sup> neurons within the preBötC by SubP conjugated to saporin results in ataxic breathing (Gray et al., 2001). Collectively, the data indicates that NK1R immunolabeling is a useful tool for demarcating the proposed region underlying respiratory rhythmogenesis and thus was used in this study. Recent evidence suggests that SST immunolabeling may also be a

marker of neurons within the preBötC (Stornetta et al., 2003) and thus was incorporated into this study.

5-Bromo-2'deoxyuridine (BrdU) labeling was used to examine the birth dates of respiratory nuclei in the medulla. If NK1R-positive neurons within the preBötC neurons are truly distinct, as hypothesized, then we expected this to be reflected by differences in the relative birth dates of respiratory neurons within the ventrolateral medulla.

Recordings from spinal ventral roots of embryonic brainstem-spinal cord preparations had demonstrated that respiratory discharge commenced within the cervical spinal cord at E17 in the rat (Greer et al., 1992; DiPasquale et al., 1996). Confirmative data were derived from ultrasound recordings of FBMs in utero from unanesthetized dams (Kobayashi et al., 2001). However, those data demonstrate the commencement of inspiratory drive transmission within spinal MN populations. Whether this reflected the onset of activity within the preBötC is unknown and therefore is addressed in the current study.

## **2.2 MATERIAL AND METHODS**

### **2.2.1 ANIMAL HANDLING**

Sprague Dawley rats were bred at the University of Alberta and all procedures were approved by the Animal Welfare Committee of the institution. The timing of pregnancies was determined from the appearance of sperm plugs in the breeding cages, and the embryonic age of rats was confirmed by measuring crown-rump length (Angulo y González, 1932). E0 was considered the day of vaginal plug detection. Fetal rats were delivered from timed pregnant rats anesthetized with halothane (1.25-1.5% delivered in 95% O<sub>2</sub> and 5% CO<sub>2</sub>) and maintained at 37°C by radiant heat. Newborn rats were anesthetized by inhalation of metofane (2-3%).

### **2.2.2 IMMUNOHISTOCHEMISTRY**

We examined the distribution of NK1R-, SST-, and choline acetyl transferase (ChAT)-immunoreactive neurons within the ventrolateral medulla from ages E15 to postnatal day 7 (P7). The rabbit polyclonal antibody to rat NK1R (residues 393-407) was previously characterized (Vigna et al., 1994; Mantyh et al., 1997). Transverse and sagittal sections (50 µm) were serially collected and immunoreacted. Single- and double-labeling experiments for NK1R (Advanced Targeting Systems, San Diego, CA), ChAT (Chemicon, Temecula, CA), and SST (Immunostar, Hudson, WI) were performed on free-floating sections according to the following protocol. Sections were rinsed in PBS and incubated with 1.0% bovine serum albumin (BSA; Sigma, St. Louis, MO) and 0.3% Triton X-100 in PBS for 60 min to reduce nonspecific staining and to increase antibody penetration. Sections were incubated overnight with primary antibodies (rabbit polyclonal anti-NK1R and anti-SST, diluted 1:1000; goat polyclonal anti-ChAT, diluted 1:400) diluted in PBS containing 0.1% BSA and 0.3% Triton X-100. After several washes in PBS, sections were incubated with secondary antibodies conjugated to the fluorescent probes Cy3-conjugated donkey anti-rabbit (Cy3-DAR, 1:200; Jackson ImmunoResearch, West Grove, PA) and Cy5-conjugated donkey anti-goat (Cy5-DAG, 1:200; Jackson

ImmunoResearch) diluted in PBS and 0.1% BSA for 2 hr. Sections were further washed in PBS and mounted and coverslipped with Fluorsave mounting medium (Calbiochem, San Diego, CA).

In a subset of experiments, sections were labeled using a peroxidase method. After overnight incubation with primary antibodies and several washes in PBS, sections were incubated with biotinylated secondary antibodies (DAR, 1:200; Jackson ImmunoResearch; DAG, 1:200; Sigma) for 2 hr, washed in PBS, and then incubated with standard peroxidase-conjugated ABC (1:100, Vector Laboratories, Toronto, Ontario, Canada). The reaction was then detected with 0.08% DAB and 0.007% H<sub>2</sub>O<sub>2</sub> in Tris-HCl buffer. Adjacent sections were counterstained with Thionin (1%) to visualize the cytoarchitecture of the tissue.

To detect very low expression of NK1R, serial sagittal sections were immunoreacted according to the tyramide signal amplification (TSA) protocol. Briefly, sections were pretreated in 3% H<sub>2</sub>O<sub>2</sub> in PBS, washed in TNT buffer (0.1 M Tris-HCl, pH 7.5, 0.15 M NaCl, and 0.05% Tween 20) and incubated in TNB-T (0.1 M Tris-HCl, pH 7.5, 0.15 M NaCl, 0.5% blocking reagent, and 0.3% Triton X-100). Sections were incubated with NK1R antibody diluted 1:30,000 in TNB-T overnight. With this dilution, no signal for NK1R receptor-like immunoreactivity was detected unless amplified with the TSA kit. After several washes in TNT, sections were incubated for 2 hr in biotinylated DAR (1:200). Biotin was revealed using the TSA kit (PerkinElmer Life Sciences, Boston, MA). Sections were incubated with Streptavidin-HRP (1:150) for 30 min followed by tyramide conjugated to fluorescein (1:75) for 10 min, diluted in amplification diluent.

If sections were immunoreacted for NK1R and SST, the tyramide amplification system was used. After NK1R immunolabeling, the sections were extensively washed in TNT and incubated for 30 min in TNB-T followed by anti-SST antibody (1:1000) in TNB-T overnight. The following day, sections were incubated with DAR-Cy3 (1:200) in TNB for 2 hr, washed, mounted on slides, and coverslipped with Fluorsave solution.

Double and triple labeling for ChAT, NK1R, and BrdU were performed on tissue obtained from embryonic and postnatal rats that had been previously treated with BrdU. Sections were pretreated with 2N HCl for 60 min to separate the double-stranded DNA

and to allow interaction of the primary anti-BrdU antibody with incorporated BrdU. After the acid treatment, the pH was restored using 0.1 M Na<sub>2</sub>B<sub>4</sub>O<sub>7</sub> for 10 min, and the sections were incubated with 1.0% BSA and 0.3% Triton X-100 in PBS. A mixture of primary antibodies (anti-NK1R, 1:1000; anti-ChAT, 1:400; and mouse monoclonal anti-BrdU, 1:100; BD Biosciences, San Jose, CA) diluted in PBS with 0.1% BSA and 0.3% Triton X-100 was applied overnight. Sections were then washed with PBS and incubated with a mixture of fluorescent or biotin-conjugated secondary antibodies diluted 1:200 in 0.1% BSA and PBS [Cy5-DAG, Cy3-DAR, and biotinylated donkey anti-mouse (DAM; Jackson ImmunoResearch)]. After a 2 hr incubation, sections were washed and incubated with streptavidin-488 (1:200; Molecular Probes, Eugene, OR) in 0.1% BSA and PBS for a further 2 hr.

### **2.2.3 NEURONAL BIRTH DATE ASSESSMENT VIA BRDU INJECTIONS**

Single pulses of BrdU (Roche Molecular Biochemicals, Indianapolis, IN; 50 mg/kg of maternal body weight) were injected intraperitoneally into pregnant rats on different gestational ages from E9.5 to E16.5 (at 12 P.M.). BrdU-treated and control pregnant rats or postnatal (P0-P7) rats were anesthetized with halothane or metofane, and the embryos or pups were perfused with phosphate buffer (PB) followed by a solution of 4% formaldehyde (Sigma) in PB. Brainstems were dissected and postfixed in the same fixative solution, and the tissue was either embedded in agar and cut on a vibrating microtome (VT1000S; Leica, Nussloch, Germany) for single and double labeling or dehydrated, embedded in paraffin, and cut on a microtome (8 μm thickness) for cell counting.

### **2.2.4 CONFOCAL IMAGING**

Immunostained sections were scanned with a Zeiss (Oberkochen, Germany) Axioplan microscope (10, 20, or 40x, 1.3 oil objective) using a Zeiss LSM 510 NLO laser configured to a computer running LSM 510 software. For FITC and Alexafluor 488 fluorescence, excitation (argon, 40 mV) was set to 488 nm, and emissions were collected

with a 505 nm long-pass filter. For Cy3 fluorescence, excitation (HeNe, 1 mV) was set to 543 nm, and emissions were collected using a 560 nm long-pass filter. For Cy5 fluorescence, excitation (HeNe, 1 mV) was set to 633 nm, and emissions were collected using a 630 nm long-pass filter. Thin sections and multiple sectioning acquisitions along the z-plane were performed to obtain a better signal through the depth of the section. Acquired images were then exported in JPEG format, and figure panels were obtained with Photoshop 6.0 (Adobe Systems, Mountain View, CA).

### **2.2.5 CELL COUNTING AND MEASUREMENTS**

Paraffin transverse sections from P7 rats were double-immunolabeled for NK1R and BrdU according to the following protocol. Sections were dewaxed in xylenes and rehydrated in descending alcohols, and antigene retrieval was performed in citrate buffer (0.01 M Na citrate, pH 6.0; Sigma) in a microwave oven (750 W) for 5 min. Sections were pretreated in 2N HCl as described above for the fluorescent triple-labeling staining protocol, and a mixture of the two primary antibodies was applied overnight (anti-NK1R, diluted 1:700; anti-BrdU, diluted 1:75). The following day, slides were washed in PBS, and sections were incubated with alkaline phosphatase-conjugated goat anti-rabbit antibody (1:50; Sigma) diluted in PBS and 0.1% BSA for 3 hr. NK1R immunoreactivity was then revealed with fast red substrate (Sigma). Sections were extensively washed and incubated with bDAM (1:200) and standard ABC (1:100) in PBS and 0.1% BSA. BrdU staining was revealed with 0.08% DAB, 0.05% nickel ammonium sulfate, and 0.007% H<sub>2</sub>O<sub>2</sub>. Sections were then washed, dehydrated, and coverslipped.

Three to four animals per BrdU treatment were analyzed. Sections from the caudal end of the facial nucleus (VII) to the rostral end of the LRN were immunoreacted. One in every four sections in the preBötC area was captured with a Nikon (Melville, NY) 990 digital camera mounted on a Leica DMRBE microscope with a 20x objective. NK1R-positive neurons in a 400 x 540  $\mu$ m box, centered below the NA and touching its ventral border, were considered during the counting process. NK1R-positive neurons with or without BrdU-labeled nuclei were counted, and statistical analysis of the results was performed as reported in Figure 6.

Measurements of cell area were obtained from confocal acquired images using LSM 510 software. NK1R-, SST-, and BrdU-positive cells were identified in the z-stack planes, and the area was calculated for each cell. Statistics were calculated using Prism 3.0 software (GraphPad Inc., San Diego, CA). Values given are means and SE, and the raw data and medians are plotted in Figures 2, 7, and 10.

### **2.2.6 IN VITRO PREPARATIONS**

Immediately on delivery, the neuraxis was isolated from embryonic rats, leaving the diaphragm attached for EMG recordings (Smith et al., 1991). To prepare medullary slice preparations, the brain stem-spinal cord was pinned down, ventral surface-upward, on a paraffin-coated block. The block was mounted in the vise of a Leica VT1000S vibratome. A single transverse slice containing the preBötC and more caudal reticular formation regions was then cut, transferred to a recording chamber, and pinned down onto a Sylgard elastomer. The cytoarchitecture was observed under infrared differential interference contrast (IR-DIC) optics (Leica Axioskop) to confirm that a similar rostral level of the medulla was recorded from at each age. The medullary slice was continuously perfused (5 ml/min) at  $27 \pm 1^\circ\text{C}$  (chamber volume, 1.5 ml) with a solution containing (in mM): 128 NaCl, 9.0 KCl, 1.5 CaCl<sub>2</sub>, 1.0 MgSO<sub>4</sub>, 24 NaHCO<sub>3</sub>, 0.5 NaH<sub>2</sub>PO<sub>4</sub>, and 30 D-glucose equilibrated with 95% O<sub>2</sub> and 5% CO<sub>2</sub>.

### **2.2.7 RECORDING AND ANALYSIS OF INSPIRATORY DISCHARGE**

Recordings of diaphragm EMG or hypoglossal (XII) nerve roots were made with suction electrodes. Furthermore, suction electrodes were placed into XII nuclei and the preBötC under visual guidance using an IR-DIC microscope to record extracellular neuronal population discharge from the medullary slice. Signals were amplified, rectified, low-pass-filtered, and recorded using an analog-to-digital converter (Digidata 1200; Axon Instruments, Foster City, CA) and data acquisition software (Axoscope). The effects of adding SubP (100 nM) were evaluated using E17 preparations. Values given

are means, SD, and coefficients of variability (SD/mean). Statistical significance was tested using paired difference Student's t test; significance was accepted at  $p < 0.05$ .

## 2.3 RESULTS

### 2.3.1 NK1R IMMUNOLABELING IN THE NEWBORN MEDULLA

The initial stage of the study examined the spatiotemporal profile of NK1R expression in the medulla of newborn rats (P2 and P4;  $n = 4$  for each age). Sagittal sectioning provided a clear view of NK1R labeling within key respiratory nuclei located along the rostrocaudal axis of the ventrolateral medulla (Fig. 2.1). Figure 1, B and C, shows examples of NK1R labeling in sagittal sections of the ventrolateral medulla at P4 and P2, respectively. The areas of particular interest, from rostral to caudal levels, included the facial nucleus, RTN, pFRG, retrofacial nucleus, compact division of the nucleus ambiguus (NAc), preBötC, semicompact division of the nucleus ambiguus (NAsc), and rVRG. NK1R was present in several brainstem nuclei during the first postnatal week. Intense immunoreactivity was present in the cell bodies of the NAc, RTN, pFRG, and retrofacial nucleus, whereas the NAsc showed weaker immunostaining. In the pre-BötC, cell bodies were strongly immunolabeled for NK1R at all postnatal ages studied. NK1R<sup>+</sup> neurons within the preBötC area were generally small with prominent dendrites orientated in the dorsoventral axis (P2,  $149.7 \pm 8.5 \mu\text{m}^2$ ; P4,  $183.9 \pm 8.4 \mu\text{m}^2$ ).

Figure 2.2 shows the population data for NK1R-positive neuronal areas at all perinatal ages studied. The rostrocaudal extents of the preBötC were 350-700 and 400-800  $\mu\text{m}$  caudal to the facial nucleus at P2 and P4, respectively. Neither the BötC region, located rostral to the preBötC, nor the rVRG were immunoreactive for NK1R.

Although the ventrolateral medulla was the primary focus of the study, we did note the pattern of NK1R labeling within other medullary structures (Fig. 2.3). Intense labeling for NK1R was present on processes extending out of the dorsal side of the hypoglossal nucleus and along the midline. Several cell bodies and processes in the STN were strongly immunoreactive for NK1R, and sparse numbers of immunolabeled cells were present in the spinal trigeminal nucleus as well as large cells in the gigantocellular reticular nucleus and the paramedian reticular nucleus. The neuropil in the inferior olive

was lightly immunoreactive, whereas intense cellular labeling was present at the level of the raphe pallidus.

### **2.3.2 NK1R IMMUNOLABELING IN THE PRENATAL MEDULLA**

The second stage of our study examined NK1R expression in the medulla during prenatal development (Figs. 2.1D-F, 2.2). At E15 (n = 19), strong NK1R expression was evident in the NA, the solitary tract, midline structures, and spinal trigeminal nuclei (data not shown). Weak staining was also present in the RTN, pFRG, medial neuroepithelium, and rhombic lip. The intensity of NK1R immunolabeling within medullary nuclei expressing NK1R at E15 increased markedly at E16 (n = 15) and older embryonic ages. There was no obvious NK1R labeling in the region of the preBötC at E15. By E16, there was weak neuropilar staining within the preBötC. It was not until E17 (n = 14) that NK1R expression was clearly detectable in cell bodies within the preBötC. Most NK1R-positive neurons at E17 were small ( $99.9 \pm 2.2 \mu\text{m}^2$ ). From ages E18 to E20 (n = 12), the intensity of the NK1R immunostaining and cell area increased (E18,  $103.2 \pm 3.13 \mu\text{m}^2$ ; E20,  $132.9 \pm 4.1 \mu\text{m}^2$ ). The rostrocaudal extents of the preBötC were 300-550 and 325-650  $\mu\text{m}$  caudal to the facial nucleus at E17 and E18, respectively.

### **2.3.3 NK1R AND CHAT EXPRESSION IN THE PRENATAL VENTROLATERAL MEDULLA**

Past studies of the adult medulla had demonstrated that ChAT<sup>+</sup> neurons in the ventrolateral medulla also express NK1R. Thus, it was important to differentiate between those neurons, which include MNs from the pharyngeal branch of the vagus nerve (Bieger and Hopkins, 1987), and ChAT<sup>+</sup> preBötC neurons. We performed double labeling for ChAT and NK1R in transverse sections of medullas isolated from ages E16 to E20 (n = 4-7 for each age; Fig. 2.4). Colocalization for NK1R and ChAT expression was evident at the level of the NAc at every perinatal age investigated. No MNs in the external formation of the NA expressed NK1R.

As mentioned above, there was no clear staining for NK1R in the preBötC at E16, although MNs in the compact formation of the NA were intensely stained for NK1R and ChAT. At this early stage, the MNs were located somewhat ventral to the position observed in the newborn and adult. Furthermore, several NK1R<sup>+</sup>/ ChAT<sup>+</sup> expressing MNs extended processes toward the ventral surface of the medulla. The first clear indication of NK1R immunoreactivity in ChAT<sup>+</sup> neurons within the region of the preBötC was evident at E17 and increased through to E20 (Fig. 2.4).

### **2.3.4 BIRTH DATING OF MEDULLARY NEURONS**

Cells undergoing their final stages of division before migration from the ventricular zone to medullary nuclei were labeled by exposure to BrdU at different gestational ages (E10.5-E16.5). BrdU is a thymidine analog used to determine cell proliferation, migration, and genesis of cells in different nervous structures (del Rio and Soriano, 1989; Nowakowski et al., 1989). BrdU is incorporated in actively dividing cells when they enter the S-phase of the cell cycle and can be detected by means of a BrdU antibody. We performed double labeling for BrdU and NK1R on transverse sections from P7 rats (n = 40; Fig. 2.5) to identify NK1R<sup>+</sup> neurons born at different developmental times. At P7, NK1R<sup>+</sup> neurons located in the preBötC were spherical, fusiform, or irregularly shaped ( $213.6 \pm 2.9 \mu\text{m}^2$ ).

Presumptive NA MNs that were NK1R<sup>+</sup> incorporated a high amount of BrdU after injections on E10.5 and to a lesser extent after injections on E11.5. Other structures labeled intensely after E10.5 BrdU injections included regions containing VII, X, and XII MNs. After injection on E11.5, BrdU-positive nuclei were intensely labeled in the RTN, pFRG, STN, and spinal trigeminal nucleus (Sp5), gigantocellular, intermediate reticular, and vestibular (Ve) nuclei. Only a few nuclei were detected in the VRG. BrdU injections on E12.5 labeled several nuclei throughout the medulla, including the STN and Sp5, intermediate reticular, parvocellular reticular (PCRt), and raphe nuclei.

Peak BrdU incorporation within NK1R<sup>+</sup> preBötC neurons resulted from injections on E12.5 and E13.5 (Fig. 2.6). Cell counts of NK1R<sup>+</sup> neurons within the preBötC demonstrated that peak birth dates at E12.5 ( $33.1 \pm 5.3\%$ ) and E13.5 ( $38.0 \pm 6.1\%$ ). A

small population of NK1R<sup>+</sup> neurons in the region of the preBötC was born before (E11.5, 10.1 ± 4.6%) and after (E14.5, 2.0 ± 1.6%) that period. Other nuclei labeled by injections on E13.5 included the rVRG, gigantocellular reticular nucleus, PCRt, Sp5, Ve, area postrema, external cuneate, and inferior olive nuclei. Injections on E15.5 and E16.5 labeled a small number of NK1R<sup>-</sup> cells distributed along the dorsal and lateral medulla.

Cell size distribution analysis of NK1R<sup>+</sup> neurons generated at different times (Fig. 2.7) indicated that larger neurons were generated earlier (E11.5, 269.8 ± 15.21 μm<sup>2</sup>), whereas most of the small neurons were labeled with BrdU during the peak generation of preBötC neurons (E12.5, 211.5 ± 5.8 μm<sup>2</sup>; E13.5, 205 ± 7.2 μm<sup>2</sup>).

### **2.3.5 BRDU, NK1R AND CHAT IN THE PRENATAL VENTROLATERAL MEDULLA**

To further characterize the birth date and timing of migration of NK1R-positive neurons in the preBötC, we injected single pulses of BrdU on E10.5, E11.5, E12.5, and E13.5 and collected the embryos at different gestational ages (E15-E18). Triple labeling for NK1R, BrdU, and ChAT allowed us to identify different neuronal populations in the ventrolateral medulla (Fig. 2.8).

Figure 2.8A-C illustrates the distribution of cells within the E15 ventrolateral medulla (n = 12) labeled for BrdU at ages E10.5, E11.5, and E12.5, respectively. There was a high concentration of ChAT<sup>+</sup> / NK1R<sup>+</sup> neurons in the NA and facial nucleus at E15 that were born at E10.5. Furthermore, some ChAT<sup>+</sup>, NK1R<sup>-</sup> neurons born at E10.5 appeared along their putative migratory pathway from the dorsal neuroepithelium to the ventrolateral medulla (Fig. 2.8A). Cells born at E11.5 were distributed more diffusely in the ventrolateral medulla at E15, with a pronounced cluster in the ventrolateral medulla spanning rostrocaudally from the facial nucleus to the rVRG. Injection of BrdU on E12.5 labeled a large population of cells dorsal to the NA (Fig. 2.8C).

Figure 2.8D-F illustrates the distribution of cells within the E16 ventrolateral medulla (n = 14) labeled for BrdU at ages E11.5, E12.5, and E13.5, respectively. Cells born at E11.5, E12.5, and E13.5 were distributed both dorsally and ventrally to the NA at E16. There were very few BrdU<sup>+</sup> cells among the NK1R<sup>+</sup> / ChAT<sup>+</sup> neurons.

Figure 2.8, G and H, illustrates the distribution of cells within the E17 ventrolateral medulla (n = 9) labeled for BrdU at ages E12.5 and E13.5, respectively. Figure 2.8I illustrates the distribution of cells labeled for BrdU at E13.5 within the E18 ventrolateral medulla (n = 3). By E17, a large number of neurons within the preBötC area expressed NK1R. Many of the NK1R<sup>+</sup> neurons found within the preBötC at E17 were born at E12.5 (Fig. 2.8G). In contrast, most NK1R<sup>+</sup> neurons within the preBötC born on E13.5 were not detected in the area until E18 (Figs. 2.8H-I).

### **2.3.6 SOMATOSTATIN EXPRESSION IN THE PERINATAL VENTRO-LATERAL MEDULLA**

We analyzed SST immunolabeling in the developing ventrolateral medulla during embryonic and perinatal development as a further means of examining preBötC ontogenesis (Fig. 2.9; n = 21). In the perinatal medulla, SST was present in a high number of neurons located dorsal and ventral to the NA. Intense labeling for SST was detected within the VRG, including some, but not all, NK1R-positive neurons in the preBötC area. In postnatal rats, expression for SST was particularly intense at the level of the preBötC, at which several neurons expressed both NK1R and SST. On P7, 33.3% of SST<sup>+</sup> neurons expressed NK1R, and 34.4% of NK1R<sup>+</sup> neurons colocalized with SST (n = 65). The average cell area of SST<sup>+</sup> neurons was  $176.4 \pm 5.13 \mu\text{m}^2$  (Fig. 2.10). It should be noted that we detected a high number of SST<sup>+</sup> cells within the preBötC and in the adjacent respiratory areas (both the Bötzing complex and rVRG) that did not coexpress NK1R. Neurons expressing high levels of NK1R located in the RTN, pFRG, NAc, and retrofacial nucleus did not coexpress SST at any age examined (E15-P4). SST expression in the ventrolateral medulla increased during the developmental period studied. At E15, expression of SST was strongly detectable in tangential fibers, whereas neuronal cell bodies within the ventrolateral medulla expressed a very low amount of the neuropeptide. By E17, when NK1R-positive neurons within the preBötC area were detectable, expression of SST was present in both NK1R<sup>+</sup> and NK1R<sup>-</sup> neurons. On E18 and E20, respectively, 38.9% (n = 117) and 38.8% (n = 225) of SST<sup>+</sup> neurons expressed NK1R, whereas 35.9 and 52.0% of NK1R<sup>+</sup> neurons coexpressed SST. Double-labeling

experiments for ChAT and SST showed a number of MNs in the rostral part of the external formation of the NA that also expressed SST. Few scattered MNs in the facial nucleus were positive for SST.

The mean cell area of SST<sup>+</sup> neurons in the preBötC was slightly less on average than in NK1R<sup>+</sup> neurons. The average cell area was  $94.07 \pm 5.7$  and  $97.9 \pm 3.8 \mu\text{m}^2$  on E17 and E18, respectively. The average area of SST<sup>+</sup> neurons increased to  $115.9 \pm 4.7 \mu\text{m}^2$  on E20.

### **2.3.7. ELECTROPHYSIOLOGICAL RECORDINGS FROM PERINATAL MEDULLARY SLICE PREPARATIONS**

To determine when inspiratory motor discharge commences in the medulla, suction electrode recordings were made from the regions of the preBötC and hypoglossal motor pool from ages E15 to P2 (Fig. 2.11, Table 1). A clear inspiratory discharge was observed in all medullary preparations isolated at ages E17 and beyond. An apparent inspiratory rhythmic discharge recorded from both the preBötC and hypoglossal motor pool was present in 5 of 10 medullary slice preparations isolated at E16.5. At earlier developmental ages, we occasionally observed a robust rhythmic discharge with characteristics different from inspiratory bursts. The burst duration (2 sec) and interburst interval (40 sec) were significantly longer than inspiratory rhythmic motor patterns. This nonrespiratory rhythmic activity was very characteristic of the spontaneous motor discharge generated at multiple sites along the embryonic rat neuraxis (Ren and Greer, 2003) (for review, see Ben-Ari, 2001). With advancing embryonic age, there were significant increases in the frequency and amplitude of inspiratory motor discharge. Furthermore, the delay between the onset of XII motor discharge and preBötC population discharge decreased.

Given that the immunohistochemical data had demonstrated the inception of NK1R expression within preBötC neurons at E17, we examined the effects of endogenously applied SubP. As shown in Figure 2.12A, there was a pronounced increase in the respiratory rhythm frequency generated by the medullary slice with application of 100 nM SubP to the bathing medium ( $360 \pm 78\%$  of control;  $n = 3$ ). These results differ

from those reported in an earlier study (Ptak et al., 1999) reporting no modulatory action of applied SubP on the respiratory rhythm before E20 in the brainstem-spinal cord preparation. To determine whether the difference could be accounted for by the different types of *in vitro* preparations, we repeated the SubP application to the medium bathing brainstem-spinal cord preparations with the diaphragm muscle attached. As shown in Figure 2.12B, there was also marked stimulation of respiratory frequency at E17 ( $419 \pm 92\%$  of control; n=3).

## 2.4 DISCUSSION

The immunohistochemical and electrophysiological data from this study indicate that a key component of the respiratory rhythm-generating center, the preBötC, forms and becomes functional at E16.5-E17 in the rat. Furthermore, the NK1R<sup>+</sup> neurons that populate the area of the preBötC during late E16-E18 are born at E12.5-E13.5, approximately 2 days later than adjacent NK1R<sup>+</sup> neurons in the ventrolateral medulla.

### 2.4.1 ANATOMICAL AND IMMUNOHISTOCHEMICAL DATA

The NK1R has proven to be a valuable marker for identifying neurons within the preBötC (Gray et al., 1999, 2001; Guyenet and Wang, 2001; Liu et al., 2001; Wang et al., 2001; Guyenet et al., 2002). This is the first use of NK1R expression to discern the ontogenesis of the preBötC throughout the perinatal period. Postnatally, the pattern of NK1R expression in the medulla found in the current study is similar to that reported for the adult. The exceptions are that we did not see significant labeling in the postnatal rVRG (Makeham et al., 2001). We also did not observe a marked decrease in NK1R expression at P4 in the neonate, as reported previously (Liu and Wong-Riley, 2002). SST expression has also been proposed as a marker for preBötC neurons in the adult rat (Stornetta et al., 2003). Most SST<sup>+</sup>, fusiform-shaped neurons within the adult preBötC are NK1R<sup>+</sup> and glutamatergic and project to the contralateral preBötC and thus fit the profile of respiratory rhythmogenic neurons. We also found clear SST expression in small fusiform-shaped neurons within the perinatal preBötC. However, the degree of overlap between SST and NK1R immunoreactivity within preBötC neurons was not as prominent as in the adult. Furthermore, the distribution of SST immunolabeling was more extensive in regions adjacent to the preBötC. These differences could reflect age-dependent changes in expression, the immunohistochemical methods used, or both.

The NK1R and SST immunohistochemical data provide for a general view of the anatomical inception of the preBötC. However, although the preBötC contains neurons involved directly in respiratory rhythmogenesis, the population is not homogeneous. The region is thought to contain respiratory rhythmogenic pacemaker neurons and

propriobulbar interneurons as well as nonrespiratory neurons. Furthermore, unlike in the adult, there is likely a significant population of bulbospinal neurons within the preBötC during the perinatal period (Ellenberger, 1999). Those neurons may have made up part of the small population of larger NK1R neurons found in the perinatal preBötC. It is currently not possible to delineate clearly between specific neuronal subtypes within the preBötC using molecular markers. Thus, a more precise understanding of the intricate details of preBötC internal ontogeny derived from immunohistochemical labeling is presently unobtainable.

The region located ventral to the facial nucleus is also of considerable importance to the neural control of respiration. We found intense NK1R labeling in that region from E16 onward. This region includes the RTN, a cluster of NK1R<sup>+</sup> neurons located ventral to the caudal portions of the facial nucleus that are chemosensitive and connected to respiratory nuclei in the dorsal and ventral medulla (Cream et al., 2002). Furthermore, recent evidence from optical recordings in newborn rat brainstem-spinal cord preparations suggests that neurons located ventral to the facial nucleus are involved in primary rhythm generation (Onimaru and Homma, 2003). The area has been referred to as the pFRG. The anatomical differentiation between the RTN and pFRG is not clear because there appears to be some overlap, particularly in the caudal regions of the RTN. The pFRG contains a significant population of neurons that discharge during the preinspiratory phase (pre-I neurons). This class of neurons has been implicated in rhythm generation (Onimaru et al., 1989) and may be coupled to rhythm-generating neurons within the preBötC (Janczewski et al., 2002; Mellen et al., 2003). Interestingly, pre-I neurons respond to SubP (Yamamoto et al., 1992) and thus may make up a portion of the neurons labeled in the current study. Single-cell recordings in conjunction with immunohistochemical labeling will be required to assess this clearly.

#### **2.4.2 BIRTH DATES OF MEDULLARY NEURONS**

Previous [<sup>3</sup>H]thymidine studies demonstrated that the genesis of medullary neurons in the rat occurs between E10 and E16 (Altman and Bayer, 1980; Bourrat and Sotelo, 1990, 1991; Phelps et al., 1990). To delineate specifically the birth date of NK1R<sup>+</sup>

medullary neurons, we injected BrdU at various embryonic ages (E10-E16) in combination with NK1R and BrdU immunolabeling at P7 (i.e., when the preBötC is well demarcated by NK1R expression). Consistent with previous reports (Altman and Bayer, 1980; Phelps et al., 1990), we found that NA, XII, X, and XII motoneuron pools were the first nuclei generated in the medulla (peak birth at E10.5). The NK1R-positive neurons in the region of the RTN and pFRG had peak birth dates at E11.5. Most cells within the preBötC were born on E12.5 and E13.5. The only other NK1R<sup>+</sup> neurons born on a date similar to that of the preBötC neurons were located in the retrofacial nucleus, an area not associated with respiratory neuronal activity.

The second series of BrdU experiments performed used a combination of BrdU injections from E10 to E13 with immunolabeling for NK1R and BrdU at developmental periods E15-E18. This provided some insight regarding the time of settlement of NK1R<sup>+</sup> medullary neurons during embryonic development. We observed ChAT<sup>+</sup> neurons born on E10 and E11 that appeared to be migrating toward the NAc at E15. However, we did not see any evidence of NK1R expression in those neurons before their reaching the NAc. Nor did we observe any NK1R expression in any of the medullary neurons before their reaching nuclei from origins in the ventricular zone. Within the preBötC, a population of NK1R<sup>+</sup> neurons born on E12 was evident at E17, and another population born on E13 was detected at E18. Our interpretations of these data are that (1) neurons within the medullary nuclei, including the preBötC, do not begin to express NK1R until their migratory phase is complete; and (2) the migration to the preBötC by the majority of NK1R<sup>+</sup> neurons born on E12 and E13 is completed by E17 and E18, respectively.

### **2.4.3 ELECTROPHYSIOLOGICAL RECORDINGS**

The recordings made from embryonic medullary slice preparations were critical for providing supportive data for the immunohistochemical and birth-dating studies. The lack of a well defined preBötC before E17 based on the NK1R and SST immunolabeling could reflect the fact that the critical neurons in the preBötC simply do not express those proteins at earlier ages. However, strong NK1R and SST labeling was observed in other medullary structures at earlier ages. The onset of rhythmic respiratory activity from the

preBötC region at late E16 and E17 strongly supports the contention that the preBötC forms at that time. The increase in the amplitude and frequency of the rhythm at E18 is also consistent with an increase in NK1R<sup>+</sup> neurons within the preBötC at that age. Our data demonstrating an increase in the amplitude and frequency of inspiratory discharge with advancing embryonic age are consistent with previous data derived from the brainstem-spinal cord preparation (Greer et al., 1992; DiPasquale et al., 1996; Onimaru and Homma, 2002; Viemari et al., 2003). The decrease in the delay between the onsets of XII motor discharge relative to that recorded in the preBötC could reflect increases in axonal diameter, myelination of projecting premotor axons, or both.

The marked increase in the frequency of respiratory discharge generated by medullary slice preparations at E17 in response to exogenous application of SubP is informative in two regards. First, it indicates that functional NK1Rs are expressed by preBötC neurons regulating respiratory rhythmogenesis by E17. Second, it corroborates results from an earlier study of TRH effects, demonstrating that the frequency of rhythmic respiratory discharge in the embryo can be increased toward neonatal levels by conditioning neuromodulation (Greer et al., 1996). Our studies did not assess the role of endogenously released SubP in modulating respiratory rhythmogenesis. However, endogenous SubP expression is present as early as E13 within the medulla (Horie et al., 2000). Thus, although SubP is not necessary for generating a respiratory rhythm (Ptak et al., 2000), along with serotonin and TRH released from raphe neurons, it may play an important role in modulating perinatal respiratory drive.

Collectively, the data from in vitro nerve recordings and in vivo ultrasonography indicate that the neuronal network generating FBMs commences activity in a coordinated manner at E17 in the rat. Specifically, the following occurs: (1) the preBötC forms and commences respiratory rhythmogenesis; (2) bulbospinal projections extend to the cervical spinal cord (Lakke, 1997); and (3) diaphragm innervation and primary myogenesis are complete (Allan and Greer; 1997; Babiuk et al., 2003).

## **2.5 SUMMARY**

These novel data provide the necessary foundation for future work on the development of the preBötC, including the analyses of cell lineages and the transcriptional control of respiratory neuronal development and electrophysiological and pharmacological properties of the preBötC during the prenatal period. Furthermore, when extended to the murine model, this approach will allow for the determination of anatomical and functional anomalies within the preBötC of genetically engineered models with central apnea phenotypes (Shirasawa et al., 2000; Berry et al., 2003; Ren et al., 2003).

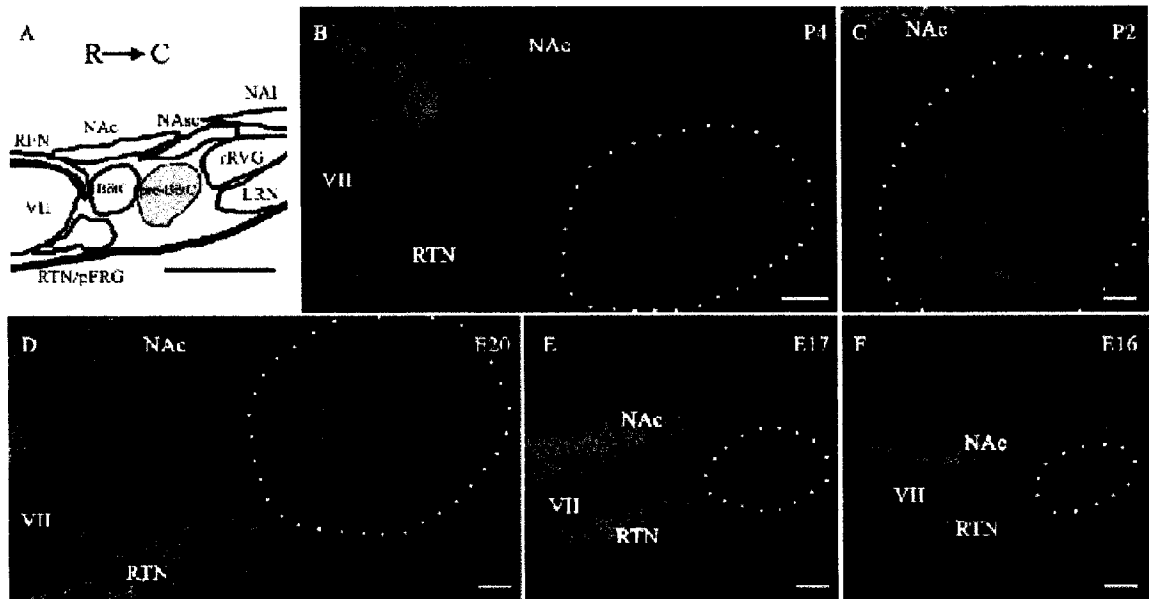


**Figure 2.1 Rostrocaudal distribution of NK1R<sup>+</sup> neurons within the ventrolateral medulla of perinatal rats.** (A), Primary structures in the ventrolateral medulla, which include VII, NAc, NAsc, nucleus ambiguus, loose formation (NAI), RTN, pFRG, RFN, BötC, preBötC, rVRG, and LRN. R, Rostral; C, caudal. (B-F), Representative examples of immunolabeling for NK1R (green) in P4, P2, E20, E17, and E16 sagittal sections of the ventrolateral medulla. The dashed circle demarcates the approximate area of the preBötC. Scale bars: A, 700  $\mu$ m; B, E, F, 100  $\mu$ m; C, D, 50  $\mu$ m.

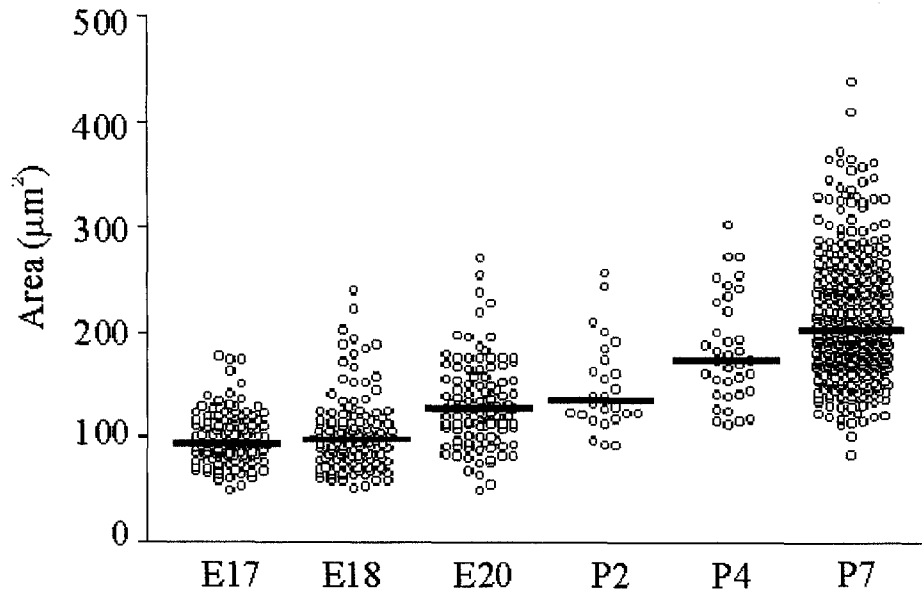


**Figure 2.2 Size distribution of NK1R<sup>+</sup> neurons located in the preBötC at different perinatal ages.** A plot of individual somal areas of NK1R-positive cells located within the preBötC is shown. Horizontal lines show the median of the population data for each age.

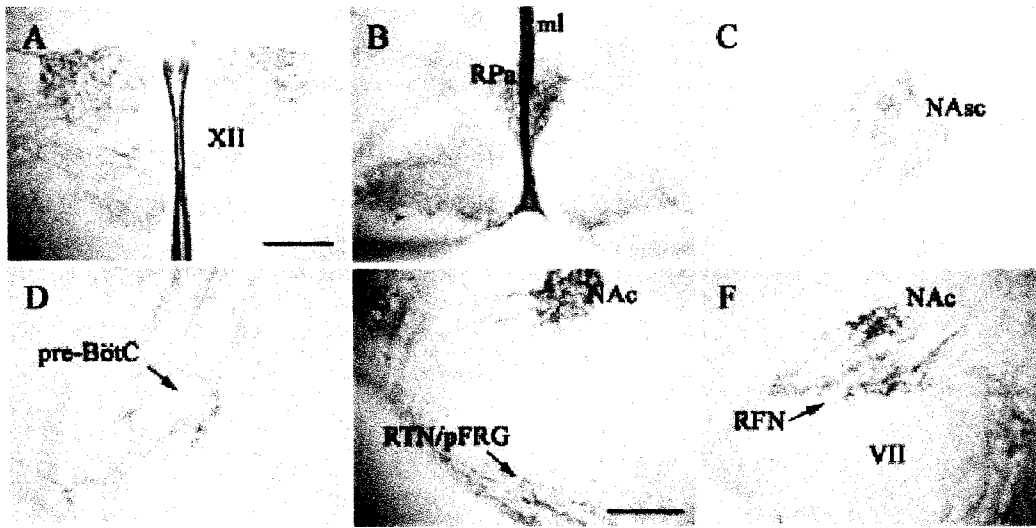


**Figure 2.3 NK1R expression in medullary structures of P2 rats.** Photomicrographs from transverse medullary sections illustrate the pattern of NK1R labeling in various medullary nuclei, including XII, midline (ml), raphe pallidus (Rpa), NAc, NAsc, preBötC, RTN, pFRG, and RFN. Scale bars: A-D, 200  $\mu$ m; E, F, 200  $\mu$ m.

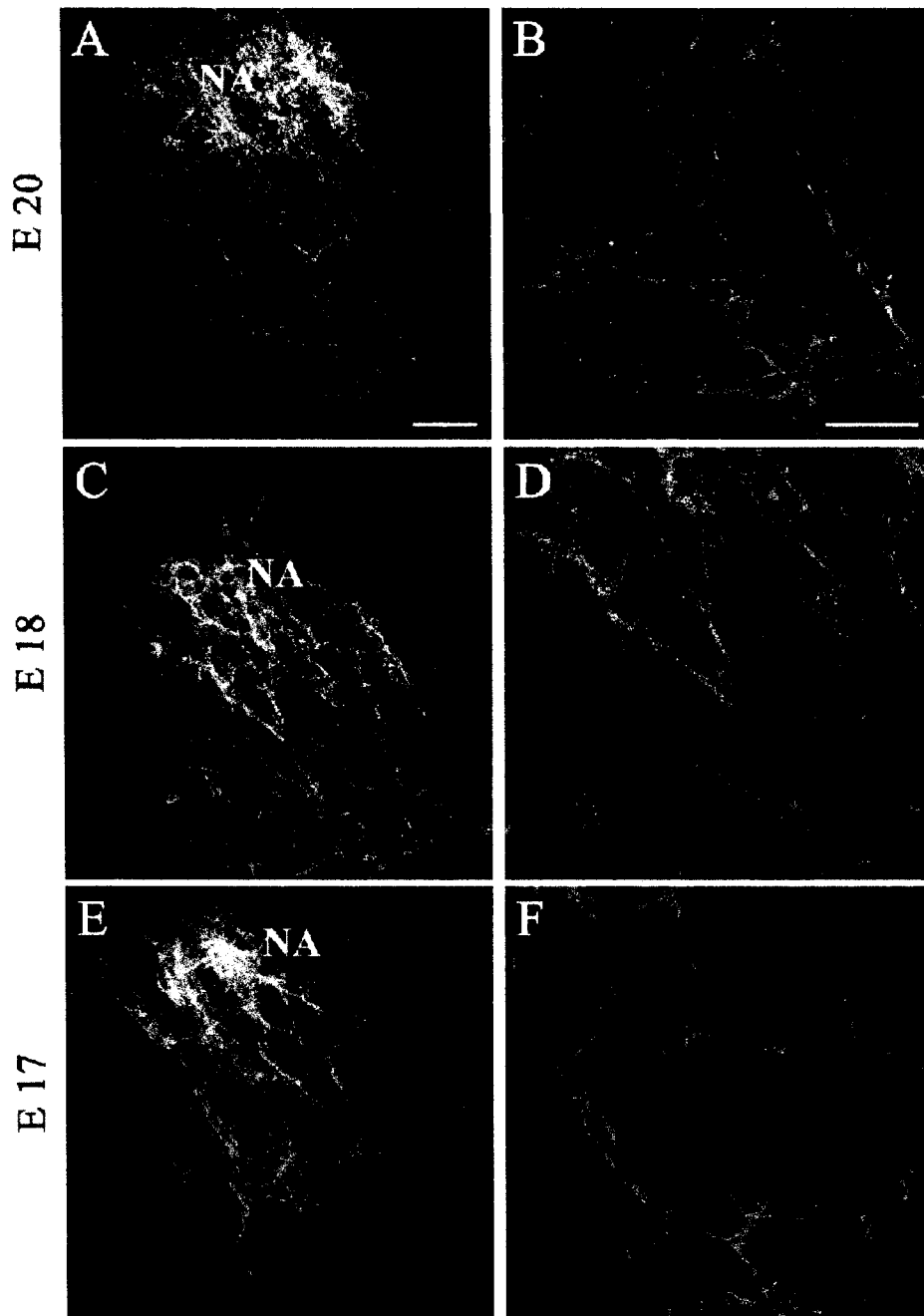


**Figure 2.4 Colocalization of NK1R and ChAT is prominent in the nucleus ambiguus but mostly absent within the preBötC of prenatal rats. (A,B,C)** Immunoreactivity for ChAT (red) and NK1R (green) is shown in transverse sections at the level of the NA and preBötC at E20 (A), E18 (C), and E17 (E). **(B, D, F)** Higher magnification views of the preBötC from A, C, E, respectively. Double-labeled cells appear yellow. Scale bars, 50  $\mu\text{m}$ .

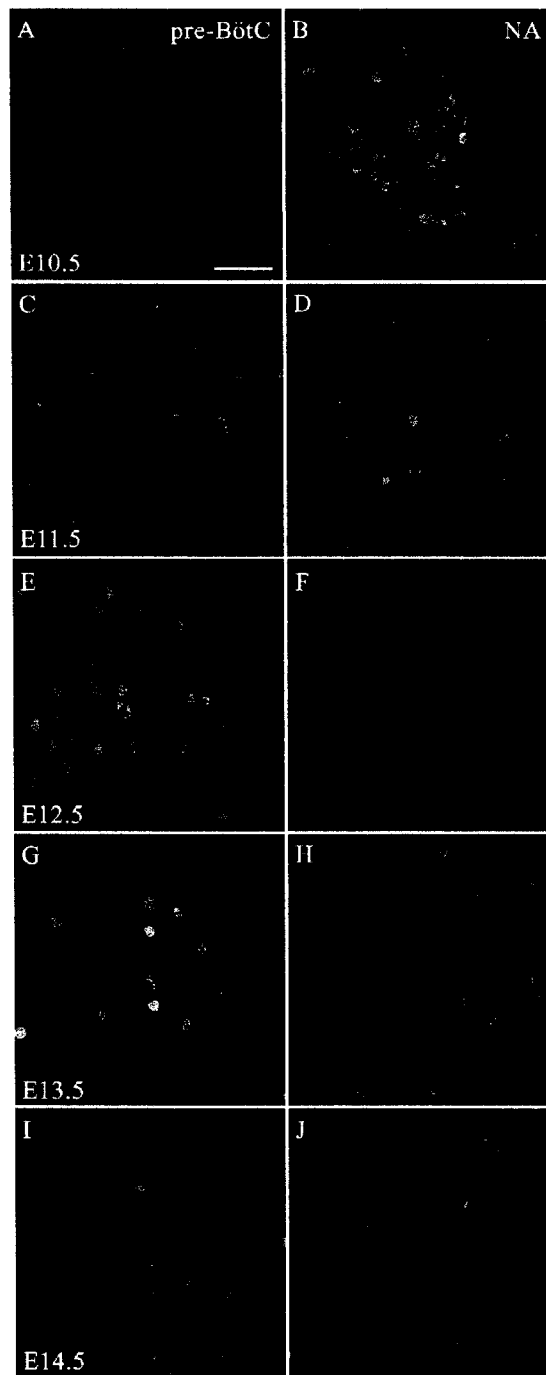


**Figure 2.5** NK1R<sup>+</sup> neurons within the preBötC are born 2 days later than those within the NA. (A, C, E, G, I) Representative immunolabeling for NK1R (red) and BrdU (green) within the preBötC of transverse sections of P7 rats. (B, D, F, H, J) Representative immunolabeling for NK1R (red) and BrdU (green) within the NA of transverse sections of P7 rats. The BrdU was injected on different days ranging from E10.5 to E14.5. Scale bar, 50  $\mu$ m.

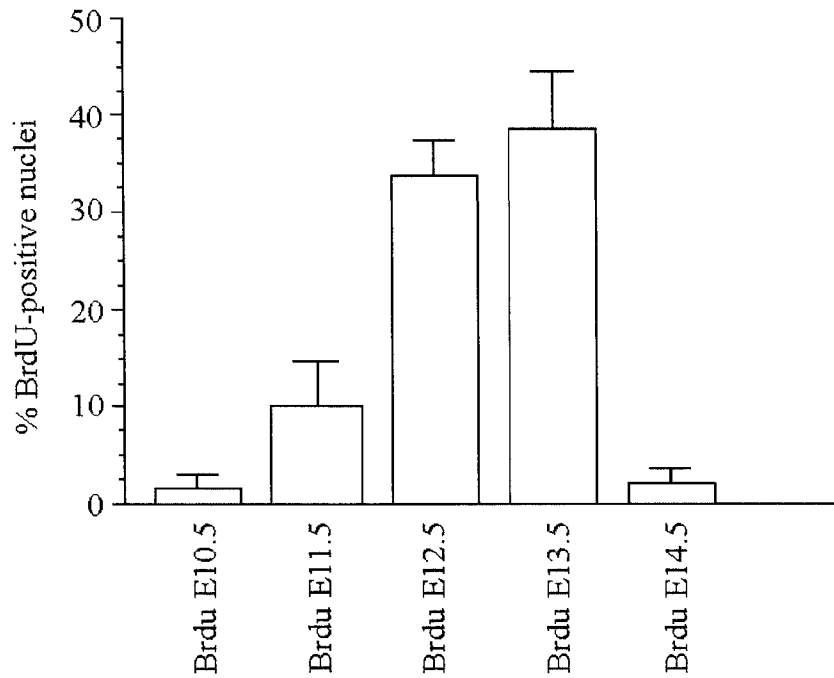


**Figure 2.6 Most NK1R<sup>+</sup> neurons within the preBötC are born on E12.5 and E13.5.** The plot shows the percentages of NK1R<sup>+</sup> neurons in the region of the preBötC that have BrdU<sup>+</sup> nuclei after injections on different days ranging from E10.5 to E14.5.

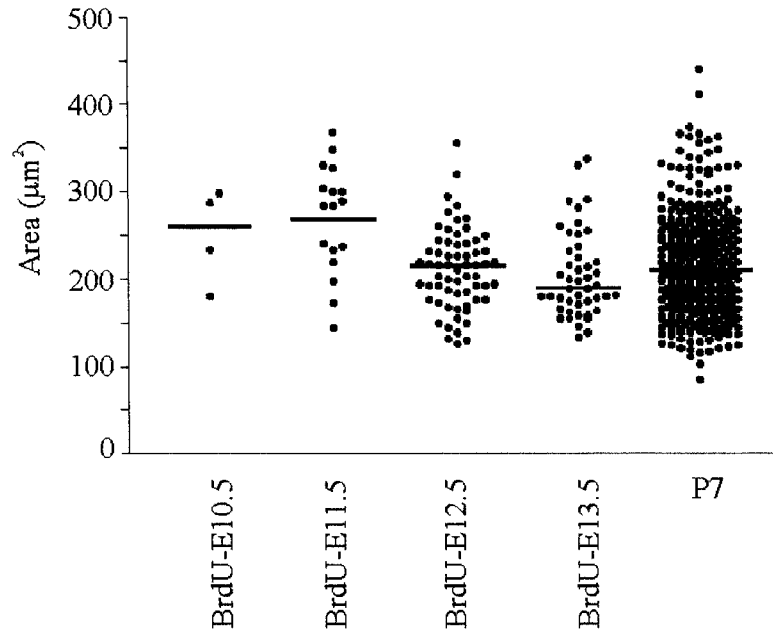


**Figure 2.7 Size of NK1R<sup>+</sup> neurons born on E12.5 and E13.5 located in the preBötC.** The plot shows individual somal areas of cells located within the preBötC that are labeled for both NK1R and BrdU on P7. The BrdU was injected on different days ranging from E10.5 to E13.5. Horizontal lines show the median of the population data for each age.

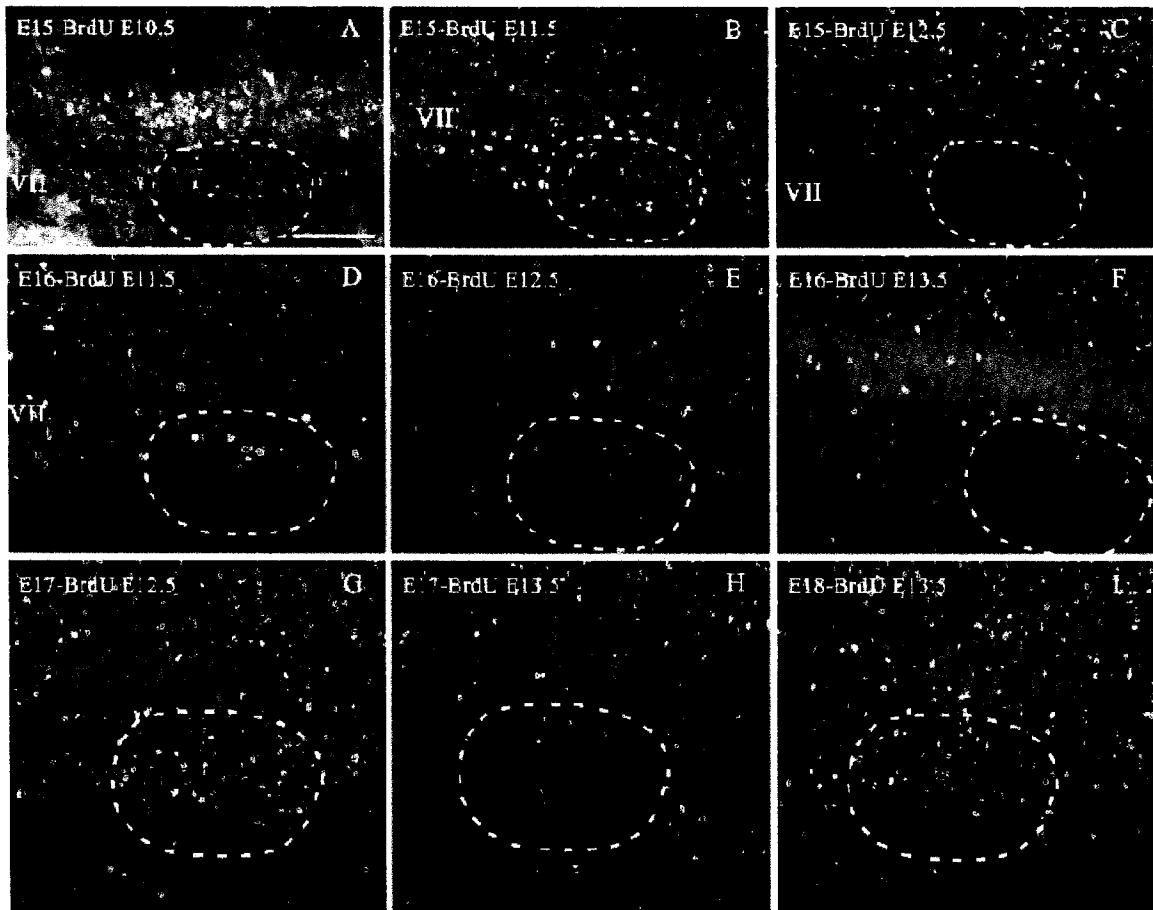


**Figure 2.8** Spatiotemporal distribution of the birth dates of NK1R<sup>+</sup> and ChAT<sup>+</sup> neurons in the ventrolateral medulla of prenatal rats (E15-E18). Sagittal sections were immunolabeled for NK1R (red), ChAT (blue), and BrdU (green). Cells expressing both NK1R and ChAT appear magenta. (A-C) Labeling patterns at E15 after BrdU injections on E10.5, E11.5, and E12.5, respectively. (D-F) Labeling patterns at E16 after BrdU injections on E11.5, E12.5, and E13.5, respectively. (G, H) Labeling patterns at E17 after BrdU injections on E12.5 and E13.5, respectively. (I) Labeling pattern at E18 after BrdU injections on E13.5. The dashed circles demarcate the approximate area of the preBötC. Scale bar, 100  $\mu$ m.

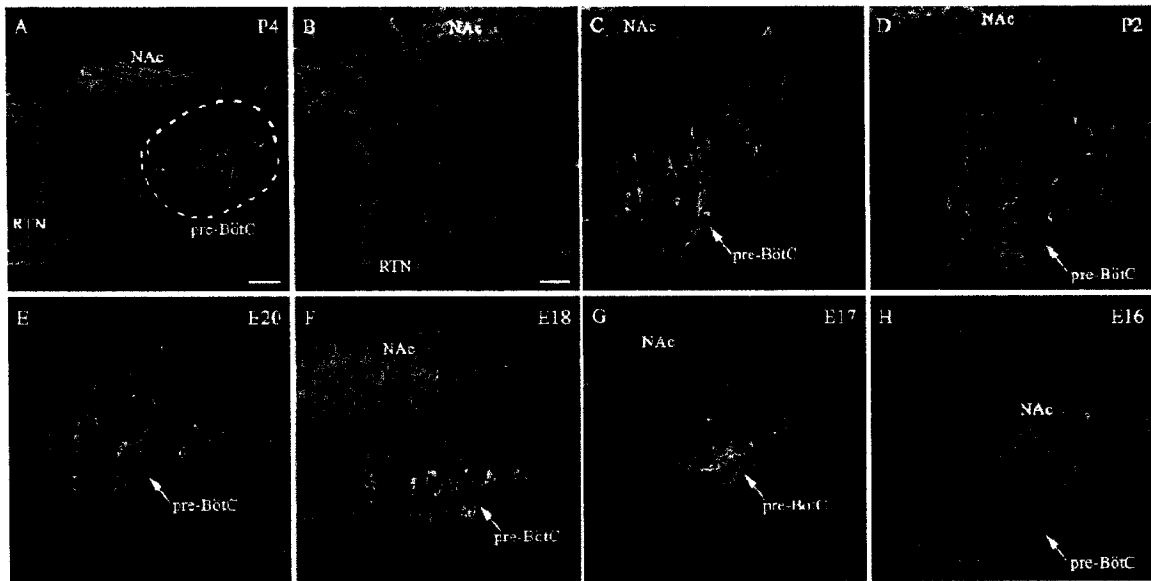


**Figure 2.9 A subpopulation of neurons within the preBötC of perinatal rats expresses both SST and NK1R.** (A) Representative examples of immunolabeling for NK1R (green) and SST (red) in a sagittal section of a P4 ventrolateral medulla. Double-labeled neurons appear yellow. (B) Higher-magnification view of A showing the area immediately rostral to the facial nucleus. (C) Higher-magnification view of A showing the preBötC region. (D-H) Region of the preBötC in transverse sections from animals aged P2, E20, E18, E17, and E16. The dashed circle demarcates the approximate area of the preBötC. Scale bars: A, 700  $\mu\text{m}$ ; B, E, F, 100  $\mu\text{m}$ ; C, D, 50  $\mu\text{m}$ .

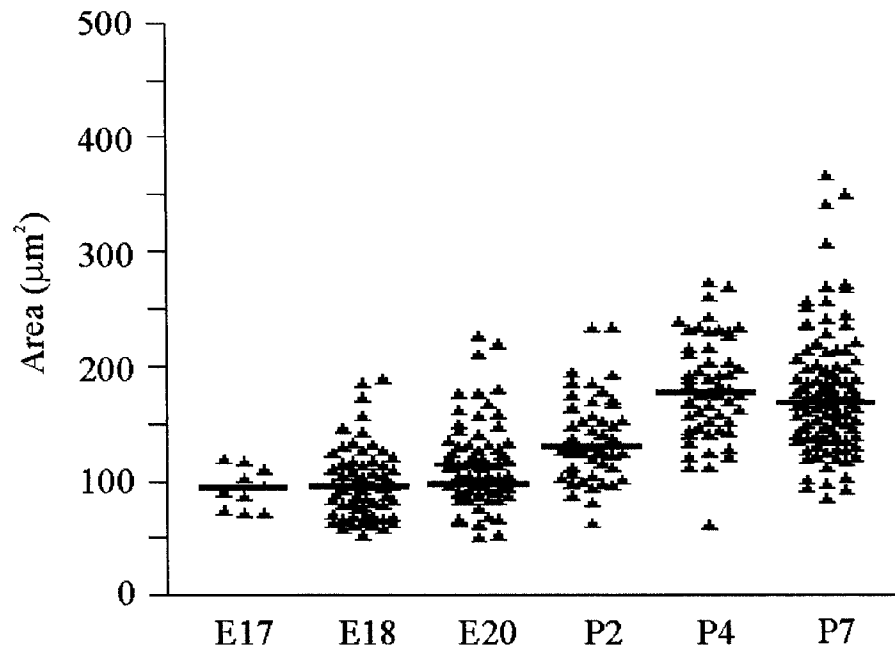


**Figure 2.10 Size of SST<sup>+</sup> neurons within the preBötC.** The plot shows of individual somal areas of SST<sup>+</sup> cells within the region of the preBötC at ages E17-P7. Horizontal lines show the median of the population data for each age.

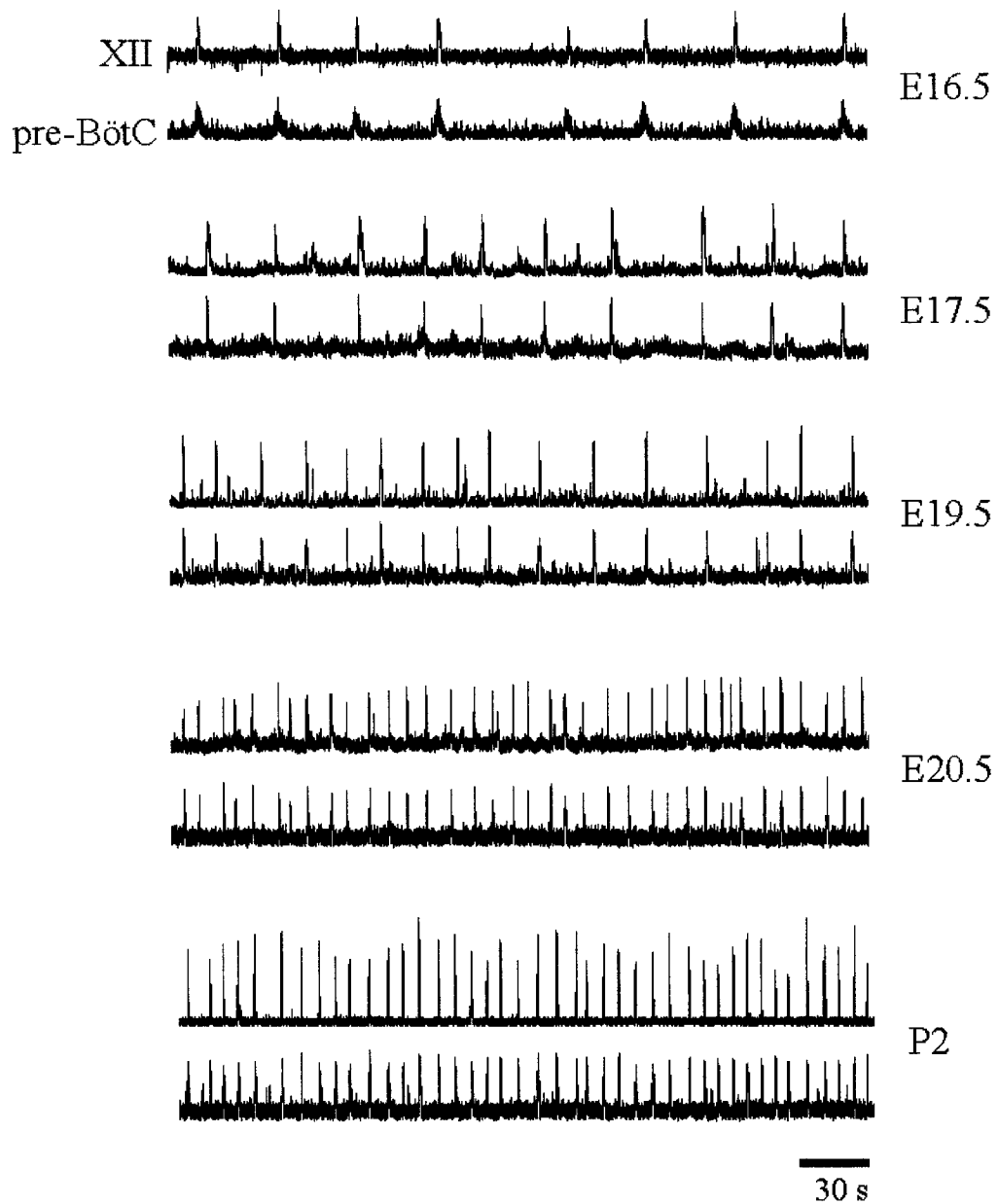


**Figure 2.11 Respiratory discharge patterns generated by perinatal medullary slice preparations.** Sample rectified and integrated suction electrode recordings were made from neurons located within the XII nucleus and preBötC in medullary slice preparations isolated from E16.5-P2 perinatal rats.

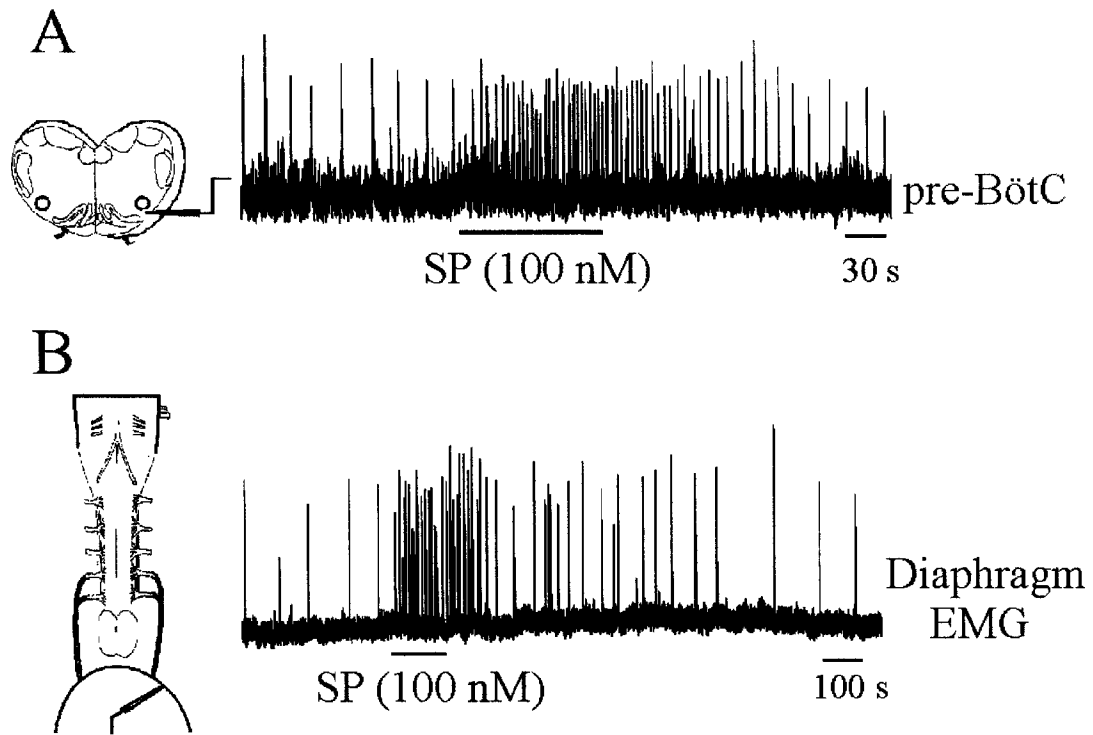


**Figure 2.12 Substance P causes a marked increase in the frequency of respiratory rhythm generated by E17 in vitro preparations. (A)** Rectified and integrated suction electrode recordings made from the preBötC of an E17 medullary slice preparation. **(B)** Rectified and integrated suction electrode recordings of diaphragm EMG activity from an E17 brainstem-spinal cord preparation. SubP was added to the perfusate during the period demarcated by the horizontal lines.

Age (day)	n	Interval (sec)	Duration (sec)	Amplitude (mV)	Coefficient of variation of burst interval	Delay onset (sec)
E16.5	5	40±15*	1.3±0.14*	11±6.1*	0.38	0.72±0.15*
E17.5	8	24±8.7*	1.0±0.12*	19±5.7*	0.36	0.45±0.11*
E18.5	4	18±7.0*	0.9±0.13*	23±6.9	0.39	0.34±0.12*
E19.5	4	14±5.1*	0.82±0.10	21±7.9	0.36	0.21±0.09*
E20.5	5	8.8±3.1	0.74±0.09	25±6.4	0.35	0.12±0.07
P2	5	6.7±2.3	0.72±0.10	27±7.2	0.34	0.10±0.07

**Table 2.1. Characterization of inspiratory bursts recorded from the preBötzing complex of rat medullary slice preparations isolated from perinatal rats.** The mean interburst interval, duration and amplitude of inspiratory bursts were calculated from suction electrode recordings of population inspiratory discharge within the region of the preBötC of medullary slice preparations from perinatal rats. The delay onset refers to the relative timing of the onset of inspiratory bursts recorded from the XII nucleus inspiratory discharge relative to that recorded within the preBötC. Results are means±SD; n is the number of preparations examined. \* p<0.05 compared with P2; Students's t-test.

## 2.6 REFERENCES

- Allan DW, Greer JJ (1997) Embryogenesis of the phrenic nerve and diaphragm in the fetal rat. *J Comp Neurol* 382: 459-468.
- Altman J, Bayer SA (1980) Development of the brain stem in the rat. I. Thymidine-radiographic study of the time of origin of neurons of the lower medulla. *J Comp Neurol* 194: 1-35.
- Angulo y González AW (1932) The prenatal growth of the albino rat. *Anat Rec* 52: 117-138.
- Babiuk RP, Zhang W, Clugston R, Allan DW, Greer JJ (2003) Embryological origins and development of the rat diaphragm. *J Comp Neurol* 455: 477-487.
- Ben-Ari Y (2001) Developing networks play a similar melody. *Trends Neurosci* 24: 353-360.
- Berry GT, Wu S, Buccafusca R, Ren J, Gonzales L, Ballard P, Golden J, Greer JJ (2003) Lethal neonatal myo-inositol deficiency and central apnea in mice lacking the Na<sup>+</sup>/myo-inositol cotransporter (SLC5A3) gene. *J Biol Chem* 278: 18297-18302.
- Bieger D, Hopkins DA (1987) Viscerotopic representation of the upper alimentary tract in the medulla oblongata in the rat: the nucleus ambiguus. *J Comp Neurol* 262: 546-562.
- Bourrat F, Sotelo C (1990) Migratory pathways and selective aggregation of the lateral reticular neurons in the rat embryo: a horseradish peroxidase in vitro study, with special reference to migration patterns of the precerebellar nuclei. *J Comp Neurol* 294: 1-13.
- Bourrat F, Sotelo C (1991) Relationships between neuronal birthdates and cytoarchitecture in the rat inferior olivary complex. *J Comp Neurol* 313: 509-521.
- Cream C, Li A, Nattie E (2002) The retrotrapezoid nucleus (RTN): local cytoarchitecture and afferent connections. *Respir Physiol Neurobiol* 130: 121-137.
- del Rio JA, Soriano E (1989) Immunocytochemical detection of 5'-bromodeoxyuridine incorporation in the central nervous system of the mouse. *Brain Res Dev Brain Res* 49: 311-317.

- DiPasquale E, Tell F, Monteau R, Hilaire G (1996) Perinatal developmental changes in respiratory activity of medullary and spinal neurons: an in vitro study on fetal and newborn rats. *Brain Res Dev Brain Res* 91: 121-130.
- Ellenberger HH (1999) Nucleus ambiguus and bulbospinal ventral respiratory group neurons in the neonatal rat. *Brain Res Bull* 50: 1-13.
- Feldman JL, Mitchell GS, Nattie EE (2003) Breathing: rhythmicity, plasticity, chemosensitivity. *Annu Rev Neurosci* 26: 239-266.
- Gray PA, Rekling JC, Bocchiaro CM, Feldman JL (1999) Modulation of respiratory frequency by peptidergic input to rhythmogenic neurons in the pre-Bötzinger complex. *Science* 286: 1566-1568.
- Gray PA, Janczewski WA, Mellen N, McCrimmon DR, Feldman JL (2001) Normal breathing requires pre-Bötzinger complex neurokinin-1 receptor-expressing neurons. *Nat Neurosci* 4: 927-930.
- Greer JJ, Smith JC, Feldman JL (1992) Generation of respiratory and locomotor patterns by an in vitro brainstem-spinal cord fetal rat preparation. *J Neurophysiol* 67: 996-999.
- Greer JJ, Al-Zubaidy ZA, Carter JE (1996) Thyrotropin releasing hormone (TRH) stimulates perinatal rat respiration in vitro. *Am J Physiol* 40: R1160-R1164.
- Guyenet PG, Wang H (2001) Pre-Botzinger neurons with preinspiratory discharges "in vivo" express NK1 receptors in the rat. *J Neurophysiol* 86: 438-446.
- Guyenet PG, Sevigny CP, Weston MC, Stornetta RL (2002) Neurokinin-1 receptor-expressing cells of the ventral respiratory group are functionally heterogeneous and predominantly glutamatergic. *J Neurosci* 22: 3806-3816.
- Horie M, Miyashita T, Watabe K, Takeda Y, Kawamura K, Kawano H (2000) Immunohistochemical localization of Substance P receptors in the midline glia of the developing rat medulla oblongata with special reference to the formation of raphe nuclei. *Brain Res Dev Brain Res* 121: 197-207.
- Janczewski WA, Onimaru H, Homma I, Feldman JL (2002) Opioid-resistant respiratory pathway from the preinspiratory neurones to abdominal muscles: in vivo and in vitro study in the newborn rat. *J Physiol (Lond)* 545: 1017-1026.

- Kobayashi K, Lemke RP, Greer JJ (2001) Ultrasound measurements of fetal breathing movements in the rat. *J Appl Physiol* 91: 316-320.
- Lakke EA (1997) The projections to the spinal cord of the rat during development: a timetable of descent. In: *Advances in anatomy, embryology and cell biology*, Vol 135, pp 1-43. New York: Springer.
- Liu Q, Wong-Riley MT (2002) Postnatal expression of neurotransmitters, receptors, and cytochrome oxidase in the rat pre-Botzinger complex. *J Appl Physiol* 92: 923-934.
- Liu YY, Ju G, Wong-Riley MT (2001) Distribution and colocalization of neurotransmitters and receptors in the pre-Botzinger complex of rats. *J Appl Physiol* 91: 1387-1395.
- Makeham JM, Goodchild AK, Pilowsky PM (2001) NK1 receptor and the ventral medulla of the rat: bulbospinal and catecholaminergic neurons. *NeuroReport* 12: 3663-3667.
- Mantyh PW, Rogers SD, Honore P, Allen BJ, Ghilardi JR, Li J, Daughters RS, Lappi DA, Wiley RG, Simone DA (1997) Inhibition of hyperalgesia by ablation of lamina I spinal neurons expressing the substance P receptor. *Science* 278: 275-279.
- Mellen NM, Janczewski WA, Bocchiaro CM, Feldman JL (2003) Opioid-induced quantal slowing reveals dual networks for respiratory rhythm generation. *Neuron* 37: 821-826.
- Nowakowski RS, Lewin SB, Miller MW (1989) Bromodeoxyuridine immunohistochemical determination of the lengths of the cell cycle and the DNA-synthetic phase for an anatomically defined population. *J Neurocytol* 18: 311-318.
- Onimaru H, Homma I (2002) Development of the rat respiratory neuron network during the late fetal period. *Neurosci Res* 42: 209-218.
- Onimaru H, Homma I (2003) A novel functional neuron group for respiratory rhythm generation in the ventral medulla. *J Neurosci* 23: 1478-1486.
- Onimaru H, Arata A, Homma I (1989) Firing properties of respiratory rhythm generating neurons in the absence of synaptic transmission in rat medulla in vitro. *Exp Brain Res* 76: 530-536.

- Phelps PE, Brennan LA, Vaughn JE (1990) Generation patterns of immunocytochemically identified cholinergic neurons in rat brainstem. *Brain Res Dev Brain Res* 56: 63-74.
- Pilowsky PM, Feldman JL (2001) Identifying neurons in the pre-Bötzinger complex that generate respiratory rhythm: visualizing the ghost in the machine. *J Comp Neurol* 434: 125-127.
- Ptak K, DiPasquale E, Monteau R (1999) Substance P and central respiratory activity: a comparative in vitro study on foetal and newborn rat. *Brain Res Dev Brain Res* 114: 217-227.
- Ptak K, Hunt SP, Monteau R (2000) Substance P and central respiratory activity: a comparative in vitro study in NK1 receptor knockout and wild-type mice. *Pflügers Arch* 440: 446-451.
- Ramirez JM, Schwarzacher SW, Pierrefiche O, Olivera BM, Richter DW (1998) Selective lesioning of the cat pre-Bötzinger complex in vivo eliminates breathing but not gasping. *J Physiol (Lond)* 507: 895-907.
- Rekling JC, Feldman JL (1998) Pre-Bötzinger complex and pacemaker neurons: hypothesized site and kernel for respiratory rhythm generation. *Annu Rev Physiol* 60: 385-405.
- Ren J, Greer JJ (2003) Ontogeny of rhythmic motor patterns generated in the embryonic rat spinal cord. *J Neurophysiol* 89: 1187-1195.
- Ren J, Lee S, Pagliardini S, Gerard M, Stewart CL, Greer JJ, Wevrick R (2003) Absence of Ndn, encoding the Prader-Willi syndrome deleted gene neccdin, results in congenital deficiency of central respiratory drive in neonatal mice. *J Neurosci* 23: 1569-1573.
- Shirasawa S, Arata A, Onimaru H, Roth KA, Brown GA, Horning S, Arata S, Okumura K, Sasazuki T, Korsmeyer SJ (2000) Rnx deficiency results in congenital central hypoventilation. *Nat Genet* 24: 287-290.
- Smith JC, Ellenberger HH, Ballanyi K, Richter DW, Feldman JL (1991) Pre-Bötzinger complex: a brainstem region that may generate respiratory rhythm in mammals. *Science* 254: 726-729.

- Solomon IC, Edelman NH, Neubauer JA (1999) Patterns of phrenic motor output evoked by chemical stimulation of neurons located in the pre-Bötzinger complex in vivo. *J Neurophysiol* 81: 1150-1161.
- Stornetta RL, Rosin DL, Wang H, Sevigny CP, Weston MC, Guyenet PG (2003) A group of glutamatergic interneurons expressing high levels of both neurokinin-1 receptors and somatostatin identifies the region of the pre-Bötzinger complex. *J Comp Neurol* 455: 499-512.
- Sun Q, Goodchild AK, Pilowsky PM (2001) Firing patterns of pre-Bötzinger and Böttinger neurons during hypocapnia in the adult rat. *Brain Res* 903: 198-206.
- Viemari JC, Burnet H, Bevendig M, Hilaire G (2003) Perinatal maturation of the mouse respiratory rhythm-generator: in vivo and in vitro studies. *Eur J Neurosci* 17: 1233-1244.
- Vigna SR, Bowden JJ, McDonald DM, Fisher J, Okamoto A, McVey DC, Payan DG, Bunnett NW (1994) Characterization of antibodies to the rat substance P (NK-1) receptor and to a chimeric substance P receptor expressed in mammalian cells. *J Neurosci* 14: 834-845.
- Wang H, Stornetta RL, Rosin DL, Guyenet PG (2001) Neurokinin-1 receptor-immunoreactive neurons of the ventral respiratory group in the rat. *J Comp Neurol* 434: 128-146.
- Yamamoto Y, Onimaru H, Homma I (1992) Effect of substance P on respiratory rhythm and pre-inspiratory neurons in the ventrolateral structure of rostral medulla oblongata: an in vitro study. *Brain Res* 599: 272-276.

## **\*CHAPTER III**

### **Developmental abnormalities of neuronal structure and function in prenatal mice lacking the Prader-Willi syndrome gene *necdin***

---

\*Previously published paper:

Pagliardini S, Ren J, Wevrick R, Greer JJ (2003) Developmental abnormalities of neuronal structure and function in prenatal mice lacking the Prader-Willi syndrome gene *necdin*. *Am J Pathol* 167: 175-191. Copyright 2005 by American Society for Investigative Pathology

My contribution to this study consisted in the planning and execution of the anatomical study. Electrophysiological recordings and analyses were performed by Dr. J. Ren.

### 3.1 INTRODUCTION

Prader-Willi syndrome (PWS) is a contiguous gene deletion syndrome that occurs at a frequency of approximately 1:15,000 births. Symptoms are variable and include transient infantile hypotonia, failure to thrive, hyperphagia leading to severe obesity, somatosensory deficits, behavioral problems and mild to moderate mental retardation (Goldstone, 2004; Stevenson et al., 2004). Further, PWS is associated with respiratory instability in the newborn period that is manifest as apneas and blunted chemosensitivity (Arens et al., 1994; Clift et al., 1994; Gozal et al., 1994; Wharton and Loechner, 1996; Schluter et al., 1997; Menendez, 1999; Manni et al., 2001; Nixon and Brouillette, 2002; Stevenson et al., 2004).

The genetic defect in PWS patients (paternal deletions, maternal disomy or imprinting mutations) results in the inactivation of paternally expressed genes on chromosome 15q11-q13 (reviewed in Nicholls and Knepper, 2001). To gain a better understanding of the function of individual genes within the loci, mouse models with a deficiency of paternal gene expression in the orthologous 7C chromosomal region have been generated. This has included mice deficient in *necdin*, one of four known protein coding genes that are deficient in PWS (Jay et al., 1997; MacDonald and Wevrick, 1997; Sutcliffe et al., 1997). Three *necdin*-deficient mouse strains were independently generated with two of the strains demonstrating neonatal lethality of variable penetrance (Tsai et al., 1994; Gerard et al., 1999; Muscatelli et al., 2000). Death of *Ndn* null mouse pups occurred during the immediate neonatal period due to severe hypoventilation (Gerard et al., 1999; Muscatelli et al., 2000). The source of the respiratory dysfunction was traced to abnormal respiratory neuronal activity within the preBötC, a key medullary structure responsible for respiratory rhythmogenesis (Ren et al., 2003). Here, we extend upon that work by addressing two fundamental questions. First, are there anatomical abnormalities within neuronal structures of the developing medulla and spinal cord in *Ndn<sup>tm2Srw</sup>* mice that could account for respiratory and other CNS related dysfunction? Second, is the abnormal breathing pattern in *Ndn<sup>tm2Srw</sup>* mice due to intrinsic defects within preBötC or can it be accounted for by abnormalities of modulatory neuronal inputs that regulate respiratory rhythmogenesis? These data demonstrate abnormalities in respiratory related

nuclei and further widespread developmental anomalies that may account for other sensory, motor and behavioral deficits associated with PWS.

## 3.2 METHODS

### 3.2.1 MOUSE BREEDING AND GENOTYPING

Procedures for animal care were approved by the Animal Welfare Committee at the University of Alberta. *Ndn*<sup>tm2Stw</sup> mice were bred through the maternal line with C57BL/6J male mice. Male offspring carrying a maternally inherited *Ndn*<sup>tm2Stw</sup> are phenotypically normal and were bred to C57BL/6J females to produce experimental embryos and offspring. In these litters, one-half of the mice are wild type and one-half carry a paternally inherited neccdin deficiency and are functionally null. The timing of pregnancies was determined from the appearance of sperm plugs in the breeding cages, and the embryonic age of mice was confirmed by measuring crown-rump length (Kaufman, 1994).

Identification of mutant offspring was performed by histochemical detection of  $\beta$ -galactosidase activity and by PCR genotyping of snap frozen tissue with *lacZ* oligonucleotide primers (LACZ1942F, 5'GTGTCGTTGCTGCATAAA CC; and LACZ2406R, 5'TCGTCTGCTCATCCATGACC).

### 3.2.2 ANIMAL HANDLING FOR ANATOMICAL STUDIES

Fetal mice were delivered from timed pregnant animals anaesthetized with halothane (1.5% delivered in 95% O<sub>2</sub> and 5% CO<sub>2</sub>) and transcardially perfused with 4% paraformaldehyde or 4% paraformaldehyde-2.5% gluteraldehyde in PB at pH 7.2. Brainstems, spinal cords and diaphragms were dissected out and post-fixed in the same fixative solution; tissue was embedded in agar and cut on a vibratome (VT1000S; Leica) for single and double labeling immuno-histochemistry.

### 3.2.3 IMMUNOHISTOCHEMISTRY

In order to examine the detailed neuroanatomy of *Ndn*<sup>tm2Stw</sup> mice, we analyzed brainstem and spinal cord distribution of several anatomical and neuronal markers (see

table 1 for antibodies used and their references) from E10 to E18. Mutant and wild type mice within the same litter were processed together for comparisons. Transverse and sagittal sections (50  $\mu$ m) were serially collected in PBS and immunoreacted according to the following protocol. Free-floating sections were incubated with 1.0% BSA (Sigma) and 0.2-0.3% Triton X-100 in PBS for 60 minutes to reduce non-specific staining and to increase antibody penetration. Sections were incubated overnight with primary antibodies diluted in PBS containing 0.1% BSA and 0.2-0.3% Triton X-100. The following day, sections were washed in PBS and incubated with specific secondary antibodies diluted in PBS and 0.1% BSA for 2 hours (biotin-, Cy3-, Cy5 or Cy2-conjugated donkey anti-rabbit, donkey anti-goat, donkey anti-rat, donkey anti-mouse IgG or donkey anti-mouse IgM; 1:200; all purchased from Jackson ImmunoResearch). Sections were further washed in PBS and those immunoreacted with fluorescent conjugated secondary antibodies were mounted and coverslipped with Fluorsave mounting medium (Calbiochem). In some experiments, sections were counterstained with Hoechst 33342 (Molecular Probes). When biotin conjugated secondary antibodies were used, sections were labeled using a peroxidase method. After washes in PBS, sections were incubated with standard peroxidase-conjugated ABC kit (1:100, Vector Laboratories) for a further 2 hours. The reaction was detected with 0.08% DAB and 0.007% H<sub>2</sub>O<sub>2</sub> in Tris-HCl buffer. Adjacent sections were counterstained with Thionin (1%) to visualize tissue cytoarchitecture. DAB-immunostained sections were analyzed with an Olympus BX40 microscope and images were taken with a SPOTdigital Microscope camera (Carsen) connected to a computer running Image-Pro-Plus software (Media Cybernetics Inc). Acquired images were exported in TIFF format, and brightness and contrast adjusted in Adobe Photoshop 7.0.

### **3.2.4 CONFOCAL IMAGING**

Immunostained sections were examined and processed using a Zeiss100M microscope, LSM510 NLO laser and LSM510 software. For Cy2, Cy3 and Cy5 fluorescence, excitation was set to 488, 543 and 633 nm and emissions were collected with 505, 560 and 630 nm long-pass filters, respectively. For Hoechst 33342

fluorescence, a two-photon laser was used with the excitation set at 780 nm and emissions collected using a 390-465 nm band pass filter. Thin sections and multiple sectioning acquisitions along the z-plane were performed to obtain a suitable signal through the depth of the section. Acquired images were then exported in JPEG format, and brightness and contrast adjusted in Photoshop 7.0.

### **3.2.5 SURFACE AREA MEASUREMENTS AND CELL COUNTS**

Measurements of cross sectional areas of motoneuronal pools, dorsal fasciculus and anterolateral funiculus were obtained from confocal acquired images of serial sections of brainstem and spinal cord (E11 to E18). Cross sectional area of vagus, ambiguus and hypoglossal nuclei was measured bilaterally for each section and an average area was calculated for each animal by means of LSM510 software. For motoneuronal pools of E18 brainstems and cervical spinal cords, a cell count was also performed and an average cell density (# cells/surface area) was determined for each pool. Varicosities immunolabeled for serotonin, substance P and tyrosine hydroxylase and the dystrophic structures were analyzed by means of LSM510 software and an average area of the varicosities determined. Paired t-tests comparing *Ndn<sup>tm2Snv</sup>* mice to wild type litter mates were applied to determine statistical significance at  $p < 0.05$ .

### **3.2.6 ELECTRON MICROSCOPY**

For electron microscopy immunohistochemistry, 50  $\mu\text{m}$  free-floating sections were processed with pre-embedding immunoperoxidase. Sections were permeabilized by freeze-thawing at  $-80^{\circ}\text{C}$  (Pinault et al., 1997), rinsed in PBS, treated with 1%  $\text{H}_2\text{O}_2$  in PBS, and incubated with 1.0% BSA to mask non-specific absorption sites. Sections were incubated with the primary anti-NF antibody, biotinylated secondary antibody (DAM), and ABC complex as specified above. Peroxidase staining was obtained by incubating the sections in 0.048% DAB, 0.024%  $\text{CoCl}_2$ , 0.019% NAS and 0.003%  $\text{H}_2\text{O}_2$  in 0.1 M PB. All sections were extensively washed, osmicated in 1%  $\text{OsO}_4$  in 0.1 M PB for 20 minutes, dehydrated in ethanol and flat embedded in TAAB812 Epon. Ultrathin sections (60-

90nm) were counterstained with uranyl acetate and lead citrate and examined using a Philips 410 transmission electron microscope.

### **3.2.7 BRAINSTEM- SPINAL CORD AND MEDULLARY SLICE PREPARATIONS**

Fetal mice (E18) were decerebrated and the brain stem-spinal cord with or without the ribcage and diaphragm muscle attached was dissected following procedures similar to those established previously (Smith et al., 1990; Greer et al., 1992). The neuraxis was continuously perfused at  $27\pm 1^\circ\text{C}$  (perfusion rate 5 ml/minute, chamber volume of 1.5 ml) with mock cerebral spinal fluid (CSF) that contained (mM): 128 NaCl, 3.0 KCl, 1.5 CaCl<sub>2</sub>, 1.0 MgSO<sub>4</sub>, 24 NaHCO<sub>3</sub>, 0.5 NaH<sub>2</sub>PO<sub>4</sub>, and 30 D-glucose equilibrated with 95%O<sub>2</sub> - 5%CO<sub>2</sub>. Details of the medullary slice preparation have been previously described (Smith et al., 1991). Briefly, the brain stem was sectioned serially using a Leica vibratome in the transverse plane starting from the rostral medulla to within ~150 μm of the rostral boundary of the preBötC, as judged by the appearance of the inferior olive. A single transverse slice containing the preBötC and more caudal reticular formation regions was then cut (~500 μm thick), transferred to a recording chamber and pinned down onto a Sylgard elastomer.

### **3.2.8 RECORDING AND ANALYSIS**

Recordings of XII cranial nerve roots, cervical (C4) ventral roots and diaphragm Electromyography (EMG) were made with suction electrodes. Further, suction electrodes were placed into XII nuclei and the preBötC to record extracellular neuronal population discharge from medullary slice preparations. Signals were amplified, rectified, low-passed filtered and recorded on computer using analog-digital converter (Digidata 1200, Axon Instruments) and data acquisition software (Axoscope, Axon Instruments).

### 3.3 RESULTS

Results were obtained from *Ndn*<sup>tm2Stw</sup> and wild type mice to elucidate the i) cytoarchitectural features of the medulla and spinal cord at various embryonic developmental stages, ii) innervation pattern of the diaphragm muscle and iii) modulation of respiratory neuronal discharge of in vitro preparations in response to exogenous application of neurotransmitter receptor agonists.

#### 3.3.1 GENERAL CYTOARCHITECTURAL FEATURES IN THE MEDULLA OF *NDN*<sup>TM2STW</sup> MICE

*Ndn*<sup>tm2Stw</sup> mice weighed ~17% less than wild type mice on average (0.94±0.04, n=12 versus 1.13±0.05 grams, n=11). As shown in Fig. 3.1, the general appearance of the cytoarchitecture of *Ndn*<sup>tm2Stw</sup> mice at different levels of the medulla is similar to wild type mice from the same litters at E18. No significant differences in the location of major nuclei were observed. However, upon closer examination, it was apparent that clearly identifiable motoneuronal nuclei in the brainstem including the nucleus ambiguus (NA), dorsal motor nucleus of the vagus (X), and hypoglossal nucleus (XII) were reduced in size. Statistical analysis of the surface extension of the nuclei determined that the size of the nuclei is significantly different at E18 between control and mutant animals (n=4). Specifically, the average area of the hypoglossal, vagus and ambiguus nuclei at E18 were reduced by 66±6.6%, 20±4.5% and 32±3.3%, respectively, in mutant versus wild type mice. We did not note any statistical difference in cell density in any of the nuclei. Further, the nuclei were clearly smaller at ages E12-E14, prior to the major period of neuronal cell death (Friedland et al., 1995a, b). The medial, dorsal and principal subnuclei of the inferior olive were present, but their general shape was less organized and delineated in all of the *Ndn*<sup>tm2Stw</sup> mice examined relative to the wild type.

Immunostaining for neurofilament (NF, both monoclonal and polyclonal antibody) in transverse sections of the medulla at E18 revealed further abnormalities in *Ndn*<sup>tm2Stw</sup> mice (Fig. 3.2). First, throughout the medulla, the reticular formation had an irregular pattern. Cross sections of rostrocaudally extending axonal bundles of both

sensory and motor pathways (e.g. medial lemniscus in Fig. 3.2D,G) were reduced in size. Further, the axonal tracts were not as tightly fasciculated and the characteristic lattice-work like pattern present in wild type mice was disorganized. Contralateral fibers running in the medulla, internal arcuate fibers and cervical nerve roots, while present and positioned correctly were reduced in size and number.

In the dorsal medulla, NF labeling showed a reduced size and an irregular distribution of fibers in the solitary tract (Fig. 3.2E,H). The most striking feature observed was at the level of the dorsal column where sensory fibers in the cuneate and gracile nuclei were swollen and enlarged. Similar staining was observed at the level of the external cuneate nuclei and, to a minor extent, in the spinal trigeminal nucleus and in the cerebellum (data not shown).

We also examined the anatomical organization of radial glia in the developing medulla via immunolabeling for vimentin (Dupouey et al., 1985). We were particularly interested in determining whether the abnormal bundling of axonal tracts described above could be related to disruptions in the normal pattern of radial glia that provide the major scaffolding system for neurite extension in the developing CNS (Rakic, 1971). While vimentin expression was evident in radial glia in *Ndn<sup>tm2Stw</sup>* mice, the typically precisely organized pattern was misplaced and the neuronal extensions were intermingled with the radial glia in a highly disorganized manner throughout the medulla (Fig. 3.2B,C,F,I). Along the midline, where fibers were compact and highly organized in a dorsoventral pattern in wild type mice, the immunolabeling for both vimentin (Fig. 3.2B,C) and NK1R (Fig. 3.2D,G) showed an irregular and less compact organization of the midline in *Ndn<sup>tm2Stw</sup>* mice. Figures 3.2F,I further illustrate the abnormal organization of the radial glia in the ventrolateral medulla.

### **3.3.2 ORGANIZATION OF NEURONAL SUBPOPULATIONS WITHIN THE MEDULLA OF *NDN<sup>TM2STW</sup>* MICE**

The lethal hypoventilation present in *Ndn<sup>tm2Stw</sup>* mice was shown previously to be due to abnormal neuronal activity within the preBötC, a major site of inspiratory rhythmogenesis within the medulla (Ren et al., 2003). NK1R expression has been used as

a marker for the preBötC in both adult and perinatal animals (Gray et al., 1999; Wang et al., 2001; Guyenet et al., 2002; Blachi et al., 2003; Pagliardini et al., 2003; Thoby-Brisson et al., 2003). Immunolabeling for NK1R in the ventrolateral medulla showed no obvious differences between wild type and *Ndn<sup>tm2Stw</sup>* mice (Fig. 3.3A-D, red). As shown in both sagittal and transverse sections, there was a reduction in size and extension of the NA (as already noted in thionin-stained sections in Fig. 3.1), but the cluster of neurons ventral to the caudal end of the compact formation of the NA, the putative location of the preBötC, appeared normal.

A further immunohistochemical marker for preBötC neurons is SST (Stornetta et al., 2003). The SST expression was similar in both wild type and *Ndn<sup>tm2Stw</sup>* mice at the level of the preBötC (Fig. 3.3E,F). Thus, collectively, based on the current criteria for immunohistochemical classification of the preBötC area, there were no obvious anatomical abnormalities within this critical site for inspiratory rhythmogenesis in *Ndn<sup>tm2Stw</sup>* mice.

We then turned our attention toward examining the organization of synaptic input from neuromodulatory systems that project to the preBötC and regulate inspiratory rhythmogenesis. Immunolabeling for SubP within the preBötC area was clearly present in both sagittal (Fig. 3.3A,B, green) and transverse (Fig. 3.3C,D, green; I-K, red) sections. SubP<sup>+</sup> fibers in the wild type mice were fine and evenly distributed in the ventrolateral medulla (Fig. 3.3A,C,I) with several synaptic boutons in the preBötC areas. In *Ndn<sup>tm2Stw</sup>* mice, SubP<sup>+</sup> fibers were present, but they were enlarged and irregularly oriented within the ventrolateral medulla (Fig. 3.3B,D,J,K).

Immunolabeling for 5HT identified 5HT<sup>+</sup> neurons of the raphe nuclei (magnus, pallidus and oralis) in the medulla and the pons. No major differences in the neuronal distribution or in the size of the different nuclei were observed (Fig. 3.3 G,H), although 5HT<sup>+</sup> fibers within the ventrolateral medulla were also swollen and enlarged in mutants (Fig. 3.3E,F red, L-N). In order to better characterize the abnormalities in the distribution and morphology of SubP and 5HT fibers, we measured the areas of varicosities. The average area in control animals at E18 was  $1.57 \pm 0.9 \mu\text{m}^2$  for 5HT fibers and  $2.64 \pm 0.15 \mu\text{m}^2$  for SubP fibers. In *Ndn<sup>tm2Stw</sup>* mice, the average area was significantly increased to  $3.14 \pm 0.14 \mu\text{m}^2$  for 5HT fibers and  $3.28 \pm 0.32 \mu\text{m}^2$  for SubP fibers.

Noradrenergic neurons located within the pons and medulla modulates the activity of the respiratory rhythm-generating center (Hilaire et al., 1989; Errchidi et al., 1991; Huang et al., 2000; Viemari et al., 2004). We analyzed the distribution of immunoreactivity for tyrosine hydroxylase (TH), a marker for adrenergic and noradrenergic neurons (Pickel et al., 1975). The number of neurons and positive fibers in A2 and C2 groups (Fig. 3.4A,B), although slightly increased, were not significantly different in *Ndn<sup>tm2Stw</sup>* and wild type mice. However, the distribution and appearance of TH<sup>+</sup> neurons were clearly abnormal in other medullary regions. The abnormalities included aberrant TH<sup>+</sup> neurons located along the midline (C3 group), in the ventral noradrenergic bundle (Fig. 3.4C-F) and in the A1/C1 group in the ventrolateral medulla (Fig. 3.4G,H). Cell counts of TH<sup>+</sup> neurons demonstrated significant increases in A1/C1, ventral bundle and C3/midline populations of 42±9.5%, 133±2.4% and 230±32.7%, respectively, in mutant versus wild type animals (Fig. 3.4K). Further, TH<sup>+</sup> fibers in several nuclei and within the ventral noradrenergic bundle were enlarged and dystrophic with some neurons having processes with a complex arborisation (data not shown). The abnormal morphology of TH<sup>+</sup> fibers located in the ventral bundle was quantified by measuring their cross sectional area in both control and mutant animals. The average size of TH<sup>+</sup> fibers in control mice was 2.09±0.10 μm<sup>2</sup>, whereas in the mutant mice the average size was significantly increased to 5.92± 0.41 μm<sup>2</sup>. At more rostral levels, noradrenergic cell bodies in A5 group were more numerous and irregularly distributed and the fibers running along the ventral bundle and the contralateral fibers in the locus ceruleus were swollen, irregular and dystrophic (data not shown).

### **3.3.3 ABNORMALITIES WITHIN MEDULLARY DORSAL COLUMN STRUCTURES OF *NDN<sup>TM2STW</sup>* MICE**

As shown in Fig. 3.2, the most marked abnormalities were observed at the level of the cuneate and gracile nuclei. To further elucidate the nature of the abnormal staining detected within those regions, double labeling experiments with antibodies against NF and the growth associated protein 43 (GAP43) (Fig. 3.5A-C) were performed. There was no co-localization between NF and GAP43 within the spheroids, although very clear

double labeling was present in adjacent fibers running in the fasciculi and through the brainstem, suggesting that dystrophic structures are not present in the still extending axons of the dorsal root ganglion neurons. These results suggest that dystrophic structures start appearing in the developing medulla after GAP43 is down regulated and thus after axonal extension is completed.

To determine the timing of spheroids formation, we analyzed brainstem sections immunolabeled with NF during earlier stages of development (Fig. 3.5D-F). Spheroids were present as early as E15 and they were clearly distinguishable from the growth cones of sensory afferents (arrows in Fig. 3.5E). In the putative area of the developing dorsal column, there were no NF<sup>+</sup> spheroids at earlier stages of development (E13; Fig. 3.5F) and they progressively developed between E13 and E15. The nature of the spheroids was further investigated by means of specific neuroanatomical markers used to identify neuronal populations within the cuneate and gracile nuclei (Celio, 1990; Crockett et al., 1996). Immunolabeling of sections from the dorsal motor column with antibodies against the calcium binding proteins parvalbumin (PV), calretinin (CR) and calbindin 28kD (CB) was performed (Fig. 3.6). In wild type mice, PV immunoreactivity was present in cell bodies and fibers within both gracile and cuneate nuclei (Fig. 3.6B). Intense fine and punctate staining (~5µm diameter) was also present at the level of the vestibular nuclei and in scattered immunopositive cells within the ventrolateral medulla. In *Ndn<sup>tm2Stw</sup>* mice, PV immunostaining was present in a similar pattern, but, notably, the abnormal structures immunolabeled with neurofilament were immunopositive for PV as well (Fig. 3.6E,F). Double labeling experiments with neurofilament showed that the majority of NF aggregates were also PV positive (Fig. 3.6J).

In both wild type and *Ndn<sup>tm2Stw</sup>* mice, CR and CB immunoreactivity within the cuneate and gracile nuclei was present in several cells and in some fibers, the majority of which were small in size (Fig. 3.6C,D,G,H); CR labeling was present in small caliber fibers and only occasionally in large NF positive spheroids in *Ndn<sup>tm2Stw</sup>* mice (Fig. 3.6K). A few intensely CB<sup>+</sup> spheroids were present at the dorsal surface of the nucleus in *Ndn<sup>tm2Stw</sup>* mice but they did not colocalize with NF (Fig. 3.6L). Further, transverse sections labeled for NF and counterstained with Hoechst 33342 showed that, where NF

accumulation occurred, no sign of neuronal degeneration was present and the abnormal staining was not associated with degenerated neuronal nuclei (Fig. 3.6I).

A more detailed analysis of these spheroid structures at the electron microscope (Fig. 3.7) showed that NF labeling was present in several small caliber axons that had similar morphology in wild type and *Ndn<sup>tm2Stw</sup>* mice (Fig. 3.7A,B). Intense immunolabeling was also present in abnormal structures exclusively identified in the *Ndn<sup>tm2Stw</sup>* mice. These structures were larger than primary sensory afferents (5 to 10  $\mu\text{m}$ ) and contained several mitochondria that were swollen, dysmorphic and embedded in large vacuoles (Fig. 3.7D-G, arrowheads). These structures were rarely associated with synaptic terminals (Fig. 3.7G, asterisk).

Gracile and cuneate nuclei receive PV<sup>+</sup> primary afferents from the dorsal root ganglia through gracile and cuneate fasciculi and subsequently project to the thalamus and cortex through the medial lemniscus pathway to process proprioceptive information. As previously shown in Fig. 3.2, the area of the medial lemniscus showed a reduced density of longitudinal fibers through the medulla. To further investigate the specificity of the defect in this system, we analyzed NF immunoreactivity in the dorsal root ganglia and in the thalamus. There was disarrangement of fibers and the presence of few dystrophic structures also in the dorsal root ganglia of *Ndn<sup>tm2Stw</sup>* mice (data not shown). At the level of the thalamus, dystrophic structures were present in the mutants, not only at the level of the ventral posterior thalamic nucleus, where the majority of the proprioceptive pathway from the cuneate and gracile nuclei project, but also in several other thalamic nuclei. The cross sectional area of the dystrophic structures in *Ndn<sup>tm2Stw</sup>* mice was  $16.06 \pm 0.32 \mu\text{m}^2$  compared to the normal cross sectional area of  $3.61 \pm 0.49 \mu\text{m}^2$  in wild type animals. We did not perform a systematic study of other CNS structures, but did note similar defects within other brain structures in the vicinity of the thalamus (i.e. septum, stria medullaris, anterior commissure and dorsolateral geniculate nucleus).

### **3.3.4 ONTOGENY OF MEDULLARY CYTOARCHITECTURE IN *NDN<sup>TM2STW</sup>* MICE**

In order to determine if the abnormalities observed at E18 were due to a neurodegenerative process or a consequence of abnormal cell migration and axonal extension, we examined the expression of NF and GAP43 during early stages of development in the brainstem (Fig.3.8). At E14, NF<sup>+</sup> fibers and GAP43<sup>+</sup> growing axons were reduced in size throughout the medulla in *Ndn<sup>tm2Stw</sup>* mice (data not shown). Longitudinal ascending and descending axon bundles were shrunk, disarranged and defasciculated as observed at later developmental stages. The defects were also apparent in *Ndn<sup>tm2Stw</sup>* mice at E10 (data not shown) and E11 (Fig. 3.8). These results are consistent with *necln* having a critical role in axonal organization and fasciculation and that its absence affects very early stages of neural development at the level of the brainstem.

### **3.3.5 GENERAL CYTOARCHITECTURAL FEATURES IN THE SPINAL CORD OF *NDN<sup>TM2STW</sup>* MICE**

In order to further assess the extent of anatomical abnormalities within the developing CNS, we analyzed the main cytoarchitectural and anatomical features of the cervical spinal cord from E10 to E18 in *Ndn<sup>tm2Stw</sup>* mice. In the E18 cervical spinal cord, spheroids were evident in lamina II and III and in the region ventral to the cuneate and gracile fasciculi and a few dystrophic structures were present in the ventral horn. The spheroids were similar to those detected at the level of the dorsal column in the brainstem (Fig. 3.9A,B) and they were detectable as early as E15 (Fig. 3.9D). However, spheroids directly within the cuneate and gracile fasciculi were very rare. At E18, there was also a reduction in thickness of the anterolateral funiculus and the gracile and cuneate fasciculi (Fig. 3.9 and 3.10). This phenomenon was present at earlier stages of development (E15 and E13) where NF<sup>+</sup> funiculi were reduced in size in *Ndn<sup>tm2Stw</sup>* mice in comparison to wild type mice (Fig. 3.9D,H, arrows) and several irregular bundles in the laminae IV-VII of the spinal cord were observed (Fig. 3.9D). GAP43 immunolabeling showed a similar pattern of fibers distribution in *Ndn<sup>tm2Stw</sup>* mice; a reduced size of longitudinal oriented

funiculi (Fig 3.9F, arrow) and several immunopositive bundles in the central laminae (Fig. 3.9F). Further analysis on spinal cord structures was performed: both anterolateral funiculus and the cuneate and gracile fasciculi were analyzed and their areas measured at the cervical level of spinal cord. At E18, there was a significant reduction in the size of the cross sectional area for both anterolateral funiculus ( $38\pm 2.2\%$ ) and dorsal fasciculus ( $18\pm 2.7\%$ ) in the *Ndn<sup>tm2Snw</sup>* mice. We also obtained measurements of the cross sectional area of the anterolateral funiculus during development and the reduction in this area was present at E13 ( $44\pm 2.7\%$ ), E14 ( $41\pm 2.1\%$ ) and E15 ( $38\pm 2.1\%$ ). The dorsal fasciculus was reduced also at E15 ( $40\pm 13.7\%$ ).

Fig. 3.10 illustrates the organization of the developing spinal cord at the early stages of development (E10 and E11). To test the hypothesis that *necln* deficiency could affect axonal extension and fasciculation in the spinal cord, we analyzed the development of commissural neurons and their axonal extension in the cervical spinal cord, a system that has been well studied and characterized (reviewed in Jessell, 2000; Dickson, 2002; Strahle et al., 2004). Commissural neurons are generated in the dorsal spinal cord and send projections ventrally towards the floor plate. Subsequently they cross the midline and run longitudinally to their final targets along the ventral and lateral funiculi. This process is highly regulated by several chemoattractant and chemorepellant cues produced by the floor plate that interact with their specific receptors temporally expressed by the growth cone of commissural neurons (Kennedy et al., 1994; Charron et al., 2003; Long et al., 2004). In their initial growth towards the midline a subset of commissural axons express TAG1 (Stoeckli and Landmesser, 1995); once the axons crossed the midline, TAG1 is down-regulated and they start expressing high levels of the adhesion molecule L1 (Dodd et al., 1988). We therefore analyzed this subset of commissural axons during their extension process. At E10, TAG1 antibody labeled dorsal commissural neurons and commissural axons as they grew ventrally toward the floor plate and as they crossed to the contralateral side (Fig. 3.10A,C). GAP43 was up-regulated at the level of the floor plate and the nerves extending out from the spinal cord. No major differences were detected between wild type and *Ndn<sup>tm2Snw</sup>* mice both at the level of the dorsal commissural neurons and the floor plate (Fig. 3.10B,D).

At E11, NF antibody labeled the numerous axons and cell bodies present in the spinal cord and the dorsal root ganglia. The ventral and lateral funiculi were compact and strongly immunoreactive for NF in wild type animals. In *Ndn<sup>tm2Stw</sup>* mice funiculi were thinner than in wild type mice and the extension of the lateral funiculi was reduced towards the dorsal spinal cord (Fig. 3.10E,I, arrow). At this stage of development, most of the commissural axons have crossed the midline and the expression of TAG1 was clearly down-regulated in both wild type and *Ndn<sup>tm2Stw</sup>* mice (Fig. 3.10F,J); GAP43 was strongly expressed in the ventral and lateral funiculi in wild type mice (Fig. 3.10G). L1, the adhesion molecule expressed by commissural axons upon crossing the midline (Stoeckli and Landmesser, 1995), was expressed along the ventral and lateral funiculi in wild type mice whereas both L1<sup>+</sup> and GAP43<sup>+</sup> fibers in *Ndn<sup>tm2Stw</sup>* mice were reduced in the ventral funiculus and almost absent at the dorsal level of the lateral funiculus (Fig. 3.10K,L, arrows).

These results suggest that as early as E13/15 there are major defects in the spinal cord within the longitudinally oriented fibers of neurons generated at either rostral or caudal locations of the CNS (mainly at the level of the anterolateral funiculus) or at the level of dorsal root ganglia (dorsal fasciculus and anterolateral system).

### **3.3.6 MAIN CYTOARCHITECTURAL FEATURES IN *NDN<sup>TM2STW</sup>* MICE DIAPHRAGM**

To determine if the abnormalities present in subsets of axonal bundles within the medulla and spinal cord were also present peripherally, we compared the phrenic branching pattern in wild type and *Ndn<sup>tm2Stw</sup>* mice. The intramuscular branching of the phrenic nerve within the perinatal rodent diaphragm muscle is very regular with a characteristic trifurcating pattern (Greer et al., 1999) and thus particularly suitable for such analysis. As shown in Fig. 3.11, NF labeling shows the phrenic innervation in the diaphragm of wild type and *Ndn<sup>tm2Stw</sup>* mice. The phrenic nerve successfully innervated the diaphragm in the *Ndn<sup>tm2Stw</sup>* mice an EMG signal could be recorded from the diaphragm muscle (shown in Fig. 3.12). However, the orientation of the secondary intramuscular branches in *Ndn<sup>tm2Stw</sup>* mouse diaphragms was clearly irregular in comparison to the

orderly pattern observed in the wild type. This included abnormalities in the orientation and extent of axon trajectories (Fig. 3.11A,B, asterisk) within the muscle and the tightness of axon fasciculation (Fig 3.11C,D).

### **3.3.7 ELECTROPHYSIOLOGICAL RECORDINGS OF RESPIRATORY RHYTHM GENERATED BY *NDN<sup>TM2STW</sup>* MICE**

The respiratory rhythm generated by in vitro preparations isolated from *Ndn<sup>tm2Stw</sup>* mice is unstable (Fig. 3.12). There were prominent bouts of respiratory depression and apneas during which the frequency of inspiratory bursts was typically less than one per minute. The bouts of suppressed respiratory rhythmic discharge (lasting  $16 \pm 7$  min,  $n=13$ ) were interspersed with periods of inspiratory motor bursts close to frequencies observed in wild type preparations (lasting  $7.5 \pm 3.4$  min,  $n=13$ ). As shown by the long duration recording in Fig. 3.12 (~ 2 hours), there was a clear periodicity to the fluctuations between slow and fast rhythms that was prominent in all brainstem-spinal cord preparations examined.

We tested the hypothesis that the respiratory rhythm could be normalized in the presence of endogenously applied neurotransmitter agonists (SubP and TRH) known to excite neurons within the preBötC region (Ptak and Hilaire, 1999) (Greer et al., 1996). As shown in Fig. 3.12, addition of SubP (1  $\mu$ M) and TRH (1  $\mu$ M) significantly modulated the rhythm generated by *Ndn<sup>tm2Stw</sup>* mouse brainstem-spinal cord preparations. The frequency of discharge during the previously slow periods was increased markedly and the incidence of apneas diminished. However, the fluctuations in respiratory frequency between slow and fast rhythmogenesis persisted. The application of SubP (1  $\mu$ m) to medullary slice preparations had similar modulatory effects (data not shown). Further, exogenous application of 5HT (25  $\mu$ M) or noradrenaline (3-30  $\mu$ M) resulted in the same excitatory response (data not shown). Thus, we concluded that addition of appropriate neuromodulatory drive to the preBötC region could alleviate the long periods of slow respiratory rhythms and apnea, however, the overall respiratory rhythm instability persisted.

We also tested the actions of growth hormone (GH) due to the fact that it is effective in alleviating apnea in Prader-Willi syndrome infants (Menendez, 1999). The stimulatory effects of GH observed clinically are likely not due to direct stimulation of the preBötC as exogenous application (1-15nM) did not affect respiratory frequency in either wild type or mutant *in vitro* preparations. Neither did insulin-like growth factor (IGF-1; 10-40 nM), an intermediate effector of GH action, have any noticeable effect on respiratory neural discharge *in vitro*.

### 3.4 DISCUSSION

Mouse models with selective gene deletions in chromosomal region 7C have been generated for analyses of the pathogenesis underlying PWS. Despite some variability in the phenotype among the different generated neccdin null mouse models (Gerard et al., 1999; Tsai et al., 1999; Muscatelli et al., 2000), correspondence with clinical manifestations of PWS are present. The neuronal mechanisms underlying the defects in genetic models have been elusive. Past studies using general histological markers of brain sections revealed no obvious differences in neccdin null mice outside of a reduction of oxytocin- and luteinizing hormone-releasing hormone (LHRH)- expressing neurons in the hypothalamus (Muscatelli et al., 2000). In this study, we performed a more detailed examination to determine if there were widespread developmental abnormalities of CNS structure. Particular attention was initially directed to the developing medulla due to its importance in generating respiratory rhythm, an aspect that is severely compromised in *Ndn<sup>tm2Srw</sup>* mice (Ren et al., 2003) and which may be of relevance to neonatal central apneas associated with PWS. We extended the investigation to the spinal cord, diaphragm and sensory pathways to further elucidate the extent of the developmental anomalies.

Thionin staining and immunolabeling for NF demonstrated anatomical abnormalities within the medulla. The defects included defasciculation of axonal tracts, aberrant neurite processes, a reduced size of the some motoneuronal pools (X, XII and NA) and, most notably, a major defect in the cytoarchitecture of the cuneate/gracile nuclei and their fasciculi. Further, NF immunolabeling demonstrated that the majority of axonal tracts within the medulla were abnormal in *Ndn<sup>tm2Srw</sup>* mice. Axonal bundles were reduced in size, they appeared defasciculated and distributed in an irregular pattern. The differences in axonal patterning between wild type and *Ndn<sup>tm2Srw</sup>* mice were present from the time when the first axonal tracts generated from postmitotic neurons migrated towards their targets. Further, the reduction in the size of motor nuclei appeared very early in development and thus could not be explained simply by an increase in apoptosis. The presence of disarrangement of the radial glia during the development of the brainstem may suggest a larger role for neccdin in axonal patterning and orientation. Further studies will be necessary to address the relative role and interactions between

radial glia and extending axons in *Ndn<sup>tm2Stw</sup>* mice. Defects in axonal fasciculation and extension were also present in a subset of spinal neurons and within phrenic nerve intramuscular branches. These results suggest that the anatomical defects in *Ndn<sup>tm2Stw</sup>* mice are more widespread than previously appreciated.

### **3.4.1 RESPIRATORY RELATED DEFECTS WITHIN THE MEDULLA OF *NDN<sup>TM2STW</sup>* MICE**

An area of particular interest within the medulla was the preBötC, the putative site for rhythmogenesis of inspiratory drive (reviewed in (Feldman et al., 2003)). A detailed understanding of the cellular mechanisms underlying rhythm and pattern generation with the preBötC is a major focus of ongoing studies. To date, there are data to support a pacemaker-network hypothesis which states that the kernel for rhythm generation consists of a population of neurons with intrinsic pacemaker properties that are embedded within, and modulated by, a neuronal network (Rekling and Feldman, 1998; Smith et al., 2000). The primary conditioning excitatory drive that maintains the oscillatory state arises from activation of glutaminergic receptors (Greer et al., 1991; Funk et al., 1993). Additional conditioning synaptic drive is provided by a diverse group of neuromodulators including GABA, 5HT, TRH, noradrenaline, opioids, prostaglandins, SubP and acetylcholine (Lagercrantz, 1987; Moss and Inman, 1989; Ballanyi et al., 1999). Contrary to our initial hypothesis, the gross structure of the preBötC was normal in *Ndn<sup>tm2Stw</sup>* mice, as shown by the presence of NK1R and SST immunopositive neurons within the putative region of the preBötC. Rather, there were clear anatomical abnormalities in surrounding medullary structures that provide conditioning synaptic input to respiratory rhythmogenic neurons. Several TH<sup>+</sup> neurons within the medulla were swollen and irregularly distributed in ectopic areas. Further, TH<sup>+</sup> fibers in the ventral bundles and in the ventral medulla were enlarged. Abnormal morphology and orientation of fibers within the ventrolateral medulla was also observed within incoming axons labeled for SubP and 5HT. The abnormal morphology of neuronal fibers expressing various neurotransmitters suggests that the absence of neccdin determines a defect in the formation and the

morphology of axonal tracts and fibers within the medulla in different neuronal phenotypes that regulate preBötC function.

Brainstem-spinal cord and medullary slice preparations from *Ndn<sup>tm2Srw</sup>* mice showed irregular respiratory activity associated with several periods of apneas and respiratory depression. The frequency of the respiratory rhythm could be increased and periods of apnea alleviated by the administration of SubP, TRH, 5-HT and noradrenaline. However, the fluctuations in the respiratory frequency continued in the *Ndn<sup>tm2Srw</sup>* mice. Our interpretation is that the endogenous application of neuromodulators overcame much of the deficit resulting from the abnormalities in medullary structures that normally provide conditioning drive to the preBötC. An abnormality in the function of the preBötC *per se* remains, however. The functional defect could reflect changes in neuronal properties or abnormalities in the preBötC network connectivity due to problems with axon guidance and fasciculation.

### 3.4.2 DEFECTS WITHIN GRACILE AND CUNEATE NUCLEI

The most remarkable anatomical medullary defects in *Ndn<sup>tm2Srw</sup>* mice were observed in the gracile and cuneate nuclei. Enlarged, dystrophic structures, identified via NF and PV immunolabeling, were abundant in the area. There was no evidence of neuronal cell death or reactive astrocytes in the dystrophic region. Rather, the dystrophic structures were similar in appearance to those previously reported for degenerating primary afferents (Fujisawa and Shiraki, 1978; Mukoyama et al., 1989; Ohara et al., 2004). Further, the dystrophic structures were similar to what has been reported in association with defects in kinesin-mediated axonal transport and outgrowth within the *Drosophila* CNS (Gho et al., 1992; Gindhart et al., 2003). Similar phenomena have been previously identified in normal aging rodents (Johnson et al., 1975; Fujisawa and Shiraki, 1978) and in the early postnatal life of animal models for Niemann-Pick disease (Ong et al., 2001; Ohara et al., 2004) and for gracile axonal dystrophy (Ohara et al., 2004). In those models, degenerating primary afferent fibers are the consequence of either a deficit in lipid storage metabolism (Cruz and Chang, 2000) or abnormal transport and protein accumulation of amyloid beta-protein and ubiquitin-positive deposits (Ichihara et al.,

1995; Saigoh et al., 1999). Ultrastructural analysis of the dorsal column via electron microscopy demonstrated that the abnormal structures were packed with neurofilament and mitochondria, some of which had an abnormal morphology. The abnormalities detected in the dorsal column may represent the initial steps of axonal degeneration in the distal ends of primary ascending afferent axons or the consequence of an abnormal axonal function that disrupts axonal outgrowth and homeostasis. This hypothesis is supported by the fact that dystrophic structures were consistently more evident at the level of the medulla rather than along the dorsal funiculi in the spinal cord and in the dorsal root ganglia. Further studies will be necessary for clarifying the mechanism of this phenomenon and the role that *neccin* plays.

Given the specific distribution of dystrophic structures and the differences in size from other enlarged fibers immunopositive for SubP and 5HT in the ventrolateral medulla, we also propose that these phenomena are different, even though they are both determined by the absence of *neccin* during development.

### **3.4.3 SPINAL CORD AND DIAPHRAGM DEFECTS**

An analysis of spinal cord development indicated that in *Ndn<sup>tm2Stw</sup>* mice most of the axonal tracts initially formed normally. However, there were indications of abnormalities in the dorsal column and in the anterolateral funiculus. The reduced size of these axonal tracts and the presence of dystrophic structures in the dorsal horn correlated with the defects observed in the upper structures (gracile and cuneate nuclei and reticular formation) and suggest a deficiency in the proper development of longitudinally projecting axons in the dorsal column and the anterolateral funiculus. Further studies (e.g. dye tracing) will be necessary to clarify if specific tracts in the anterolateral funiculus are affected or if more general defect is present in these fibers. Further, anterograde dye tracing could clarify if the reduced extension is proportionally related to either a reduction in number of neurons that send projections to different levels of the spinal cord or a reduction in the number of fibers extending to the spinal cord, or both.

Axons exiting the spinal cord within ventral roots appeared grossly normal although motoneuron pools were reduced in size (data not shown). Further, there were

clear abnormalities of the fine intramuscular branching pattern of the phrenic nerve within the diaphragm muscle. Previous preliminary data (Kozlov et al., 2001) reported abnormalities in the density and localization of acetylcholine receptors in the diaphragm of *Ndn<sup>tm2Srw</sup>* mice. These subtle, yet significant, abnormalities in the motor system may be associated with the prominence of hypotonia in infants with PWS.

### **3.4.4 POTENTIAL MECHANISMS UNDERLYING PATHOGENESIS**

The functional roles of neccdin, which is expressed widely within the developing CNS, remain to be clearly delineated. However, potential regulatory actions of neccdin have been derived from in vitro studies where neccdin expression was induced in proliferative cell lines or blocked by antisense-oligonucleotides in cultured dorsal root ganglion neurons (Yoshikawa, 2000; Takazaki et al., 2002; Taniura and Yoshikawa, 2002; Kuwako et al., 2004). Collectively, those data suggest that neccdin interacts with cytoplasmic and nuclear proteins to control cell growth, proliferation and apoptosis. More recent studies using heterologous expression systems have demonstrated an interaction between neccdin and fasciculation and elongation (*Fez*) proteins implicated in centrosome-mediated cytoskeletal rearrangement after neuronal differentiation and in axonal outgrowth (Lee et al., 2005). These data support a model whereby up-regulation of neccdin in post-mitotic neurons stabilizes *Fez* proteins to facilitate centrosome-mediated cytoskeletal rearrangements required for axonal outgrowth and kinesin mediated transport. The abnormalities in neuronal migration and the extension, arborization and fasciculation of axons during early stages of development reported here in the detailed analysis of *Ndn<sup>tm2Srw</sup>* mice are consistent with the hypothesized roles for neccdin. However, it is important to note that only certain axonal tracts and neuronal populations are clearly affected whereas others appear normal in the mouse model.

### **3.4.5 RELEVANCE TO PRADER-WILLI SYNDROME**

Dysfunction of various hypothalamic systems, as evident from histological examination of postmortem brain tissue, may be the basis of a number of symptoms in

Prader-Willi syndrome (reviewed in (Swaab, 1997). Other reported CNS deficits within PWS patients include enlarged lateral ventricles, hypoplasia of the corpus callosum, abnormal cortical development and some irregularities in the structures of inferior olive, dentate nucleus and cerebellum (Hayashi et al., 1992; Yoshii et al., 2002; L'Hermine et al., 2003). In light of the results from this current study it will be important to perform more extensive and detailed examinations of the CNS in PWS patients for evidence of the types of more subtle defects demonstrated in the *necdin* null model. Axonal defasciculations, abnormalities of neurite extension and reduced numbers of neurons within specific nuclei could be involved in some of the cognitive, behavioral, somatosensory and respiratory deficits associated with Prader-Willi syndrome.

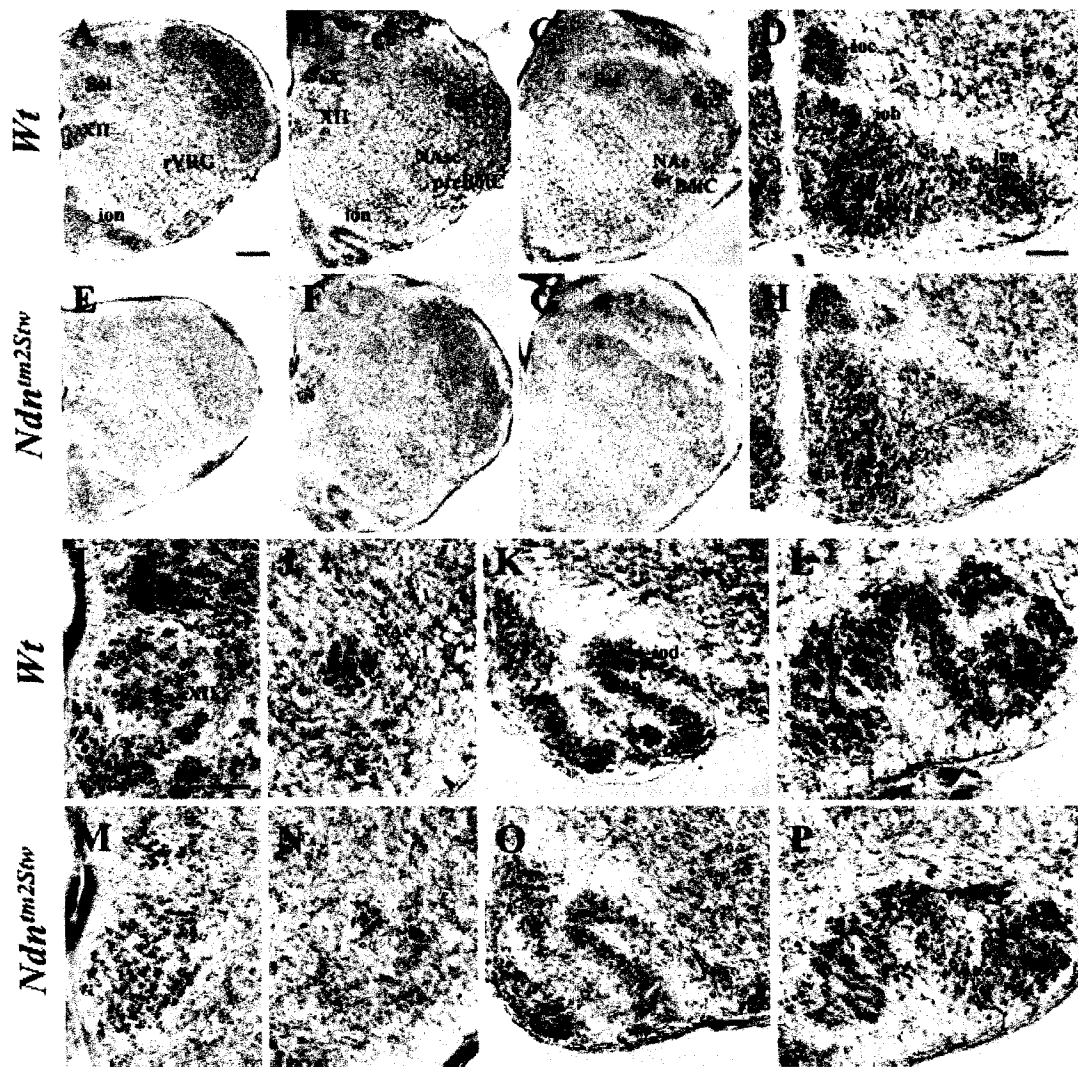


**Figure 3.1 Cytoarchitectural abnormalities in the medulla of *Ndn*<sup>tm2Stw</sup> mice.** Transverse sections of the medulla stained with thionin from wild type (**A-D**; **I-L**) and *Ndn*<sup>tm2Stw</sup> mice (**E-H**; **M-P**) at the level of the rVRG (**A,D,E,H,I,M**), the preBötC, (**B,F,J,K,N,O**), the BötC, (**C-G**) and the VII (**L,P**). (**D,H**). There are no major defects in the three subnuclei (**A,B,C**) of the caudal region of the inferior olive (ioa,iob,ioc). XII nucleus (**I,M**), dorsal motor nucleus of the vagus nerve, NAc, NAsc (**J,N**) are smaller in *Ndn*<sup>tm2Stw</sup> mice in comparison to wild type mice. (**K,O**) Medial, principal and dorsal nuclei of the inferior olive (iom, iop, iod) are less finely organized in *Ndn*<sup>tm2Stw</sup> mice in comparison to wild type mice. (**L,P**) VII is similar in wild type and *Ndn*<sup>tm2Stw</sup> mice. Scale bars: A-C,E-G=200  $\mu$ m; D,H,J-L,N-P=100  $\mu$ m; I,M=100  $\mu$ m.

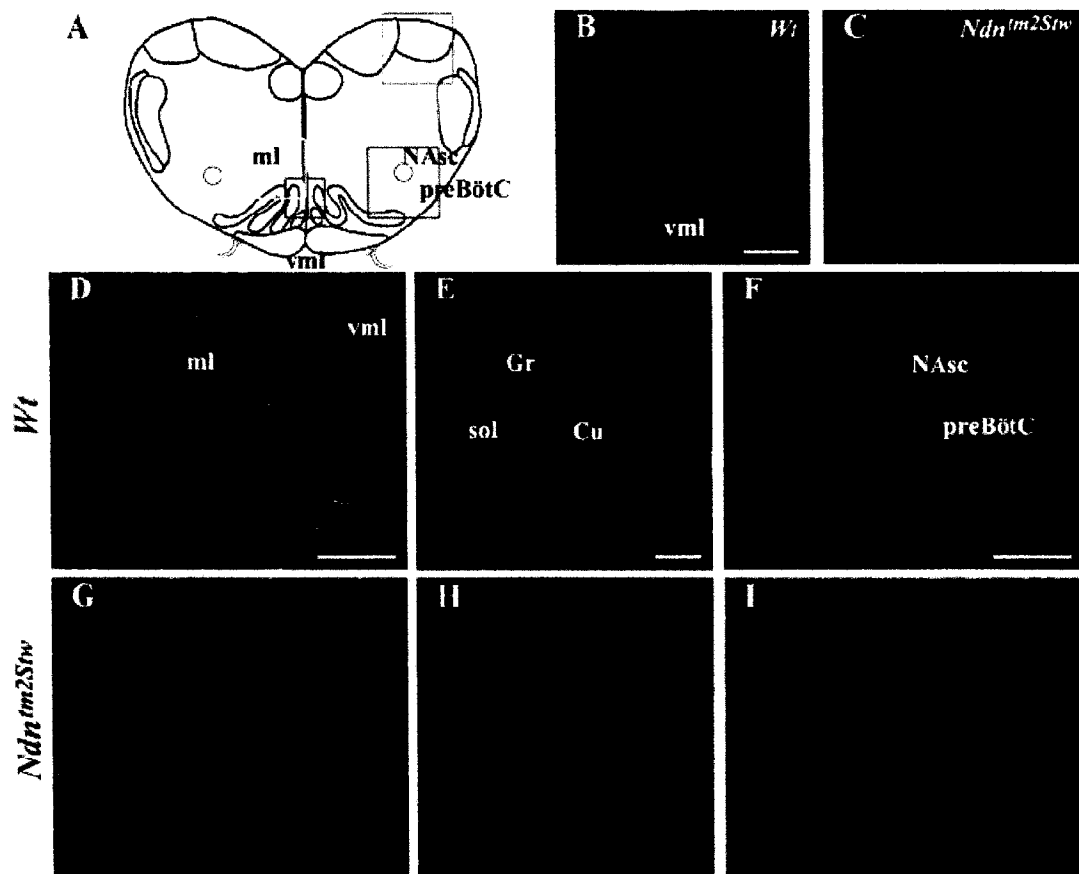
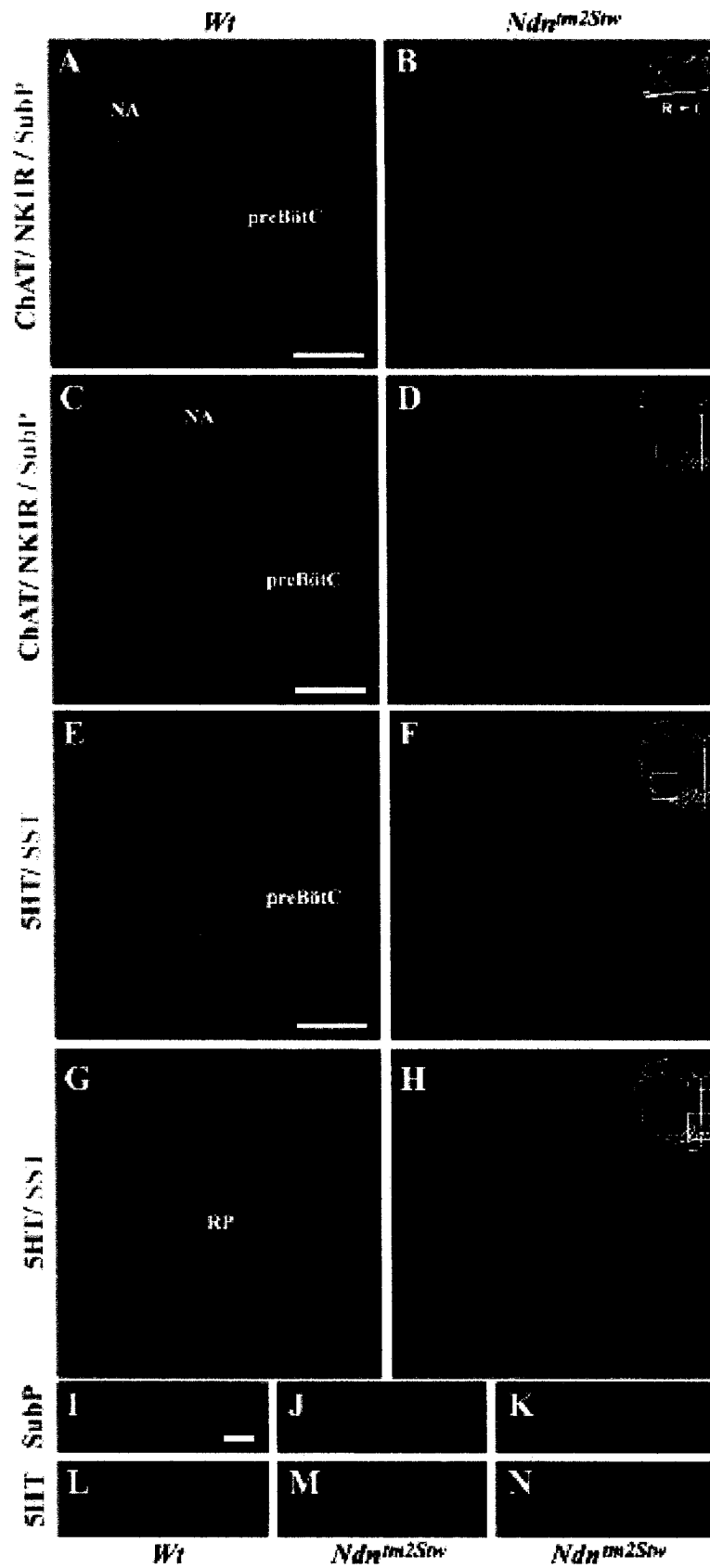


**Figure 3.2 NK1R, NF and vimentin expression in wild type (B,D-F) and *Ndn<sup>tm2Stw</sup>* mice (C,G-I) at E18.** (A) Schematic drawing of the medulla at the level of the preBötC. The colored squares delineate different areas of the medulla shown in the figure panels. Red: B,C; yellow: D,G; green: E,H; blue: F,I. (B,C) Vimentin expression shows a clear disarrangement in the organization of the ventral midline (vml) in *Ndn<sup>tm2Stw</sup>* in comparison to wild type mice. (D,G) NF (green) and NK1R (red) expression in the medial lemniscus (ml) lateral to vml. (G) Note the reduced size and the defasciculation of axonal bundles through the ventral medulla in *Ndn<sup>tm2Stw</sup>* mice. (E,H) At the level of the gracile (Gr) and cuneate (Cu) nuclei and fasciculi, NF labels dystrophic structures in *Ndn<sup>tm2Stw</sup>* mice. (F,I) Disarrangement of the radial glia in *Ndn<sup>tm2Stw</sup>* mice is shown by vimentin immunolabeling in the ventrolateral medulla. Scale bars: B,C,D,G,E,H,F,I=100  $\mu$ m.



### Previous page

**Figure 3.3 Expression of NK1R, ChAT, SubP, SST and 5HT in the ventral medulla of wild type (A,C,E,G,I,L) and *Ndn<sup>tm2Stw</sup>* mice (B,D,F,H,J,K,M,N) at E18.** In each set of figures (from A to H), a yellow square in the drawing indicates where the image was acquired. Sagittal (A,B) and transverse (C,D) sections immunoreacted for ChAT (blue), NK1R (red) and SubP (green) at the level of the preBötC show the reduced extension of the NA in *Ndn<sup>tm2Stw</sup>* mice. NK1R<sup>+</sup> neurons in the preBötC area are present in both wild type and *Ndn<sup>tm2Stw</sup>* mice. Transverse sections immunoreacted for SST (green) 5HT (red) at the level of the preBötC (E,F) and the raphe pallidus (RP; G,H) show no gross abnormalities in the SST positive neurons at the level of the preBötC and in the 5HT positive neurons of the caudal raphe nucleus. (I-N) Details of abnormalities within SubP (I-K) and 5HT (L-N) immunopositive fibers in the preBötC region. Note the presence of enlarged varicosities in the irregularly oriented fibers. Scale bars: A,B=200 μm; C,D=50 μm; E-H=100 μm; I-N=10 μm. C, caudal; R, rostral.

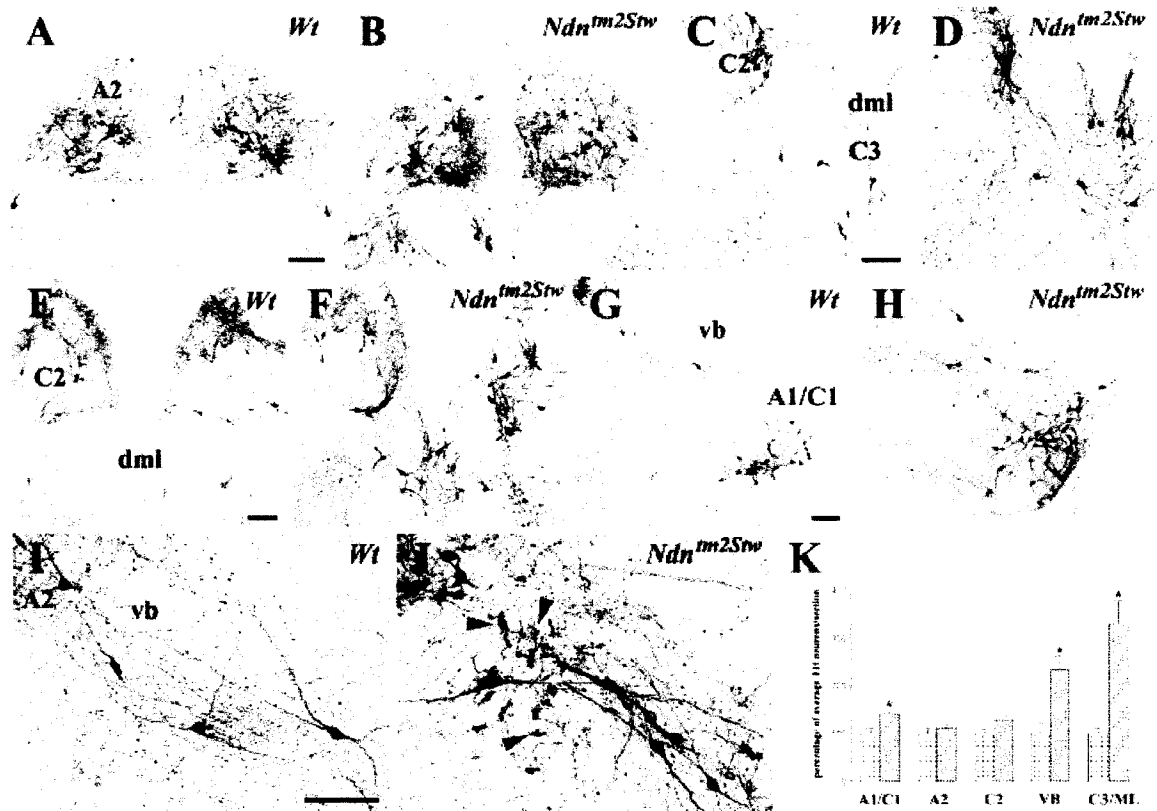


**Figure 3.4** Expression of TH in the medulla of wild type (A,C,E,G,I) and *Ndn<sup>tm2Stw</sup>* mice at E18 (B,D,F,H,J). (A-F) No major differences in cell number at the level of A2 noradrenergic and C2 adrenergic neurons are present between wild type and *Ndn<sup>tm2Stw</sup>* mice, although the TH immunoreactive neuropil appears stronger in *Ndn<sup>tm2Stw</sup>* mice. (C-F) C3 adrenergic neurons in the dorsal midline of the medulla of *Ndn<sup>tm2Stw</sup>* mice are more numerous than in wild type mice. Note the presence of several TH<sup>+</sup> neurons along the dorsal midline (dml; D,F). C and D are taken at more caudal level than E and F. (G,H) The A1/C1 noradrenergic group also contains a larger number of TH positive neurons in *Ndn<sup>tm2Stw</sup>* mice in comparison to wild type. (I-J) Ventral noradrenergic bundle in the reticular formation of the medulla. In *Ndn<sup>tm2Stw</sup>* mice, the noradrenergic bundle contains a higher number of cell bodies and fibers. (K) Relative percentage of adrenergic and noradrenergic neurons in the medulla of wild type (dotted bars) and *Ndn<sup>tm2Stw</sup>* mice (striped bars). Asterisks show differences that are statistically significant (p < 0.05). Scale bars: A-J = 100 μm.

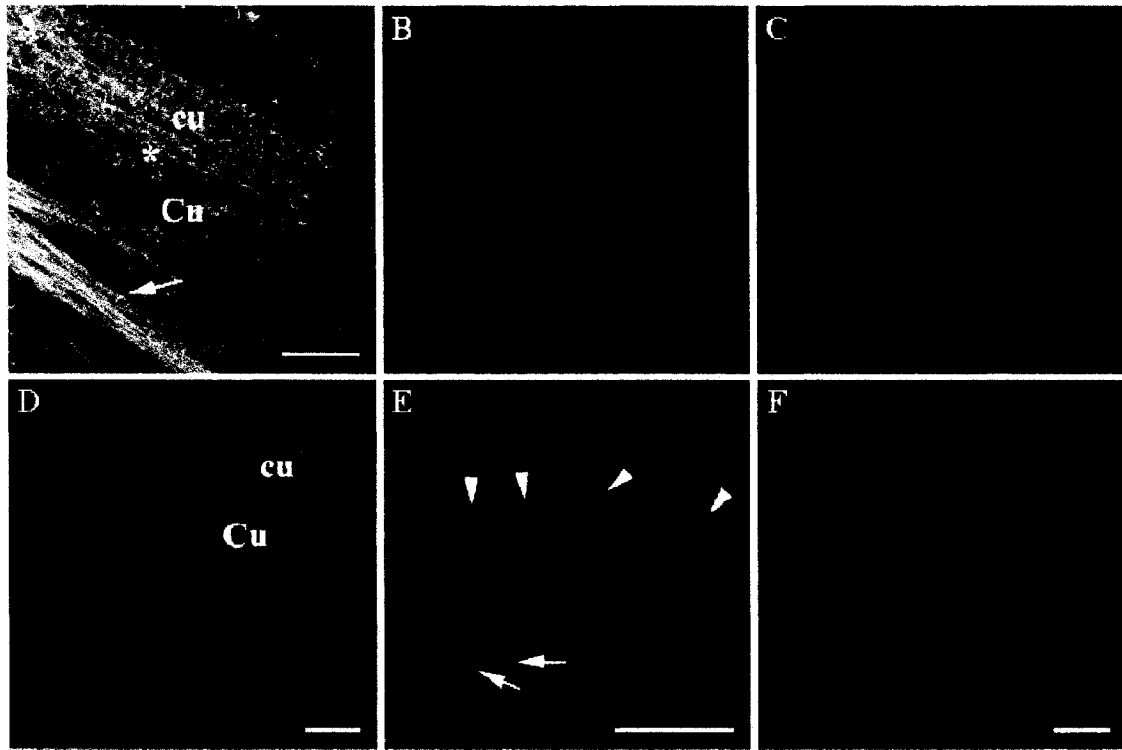
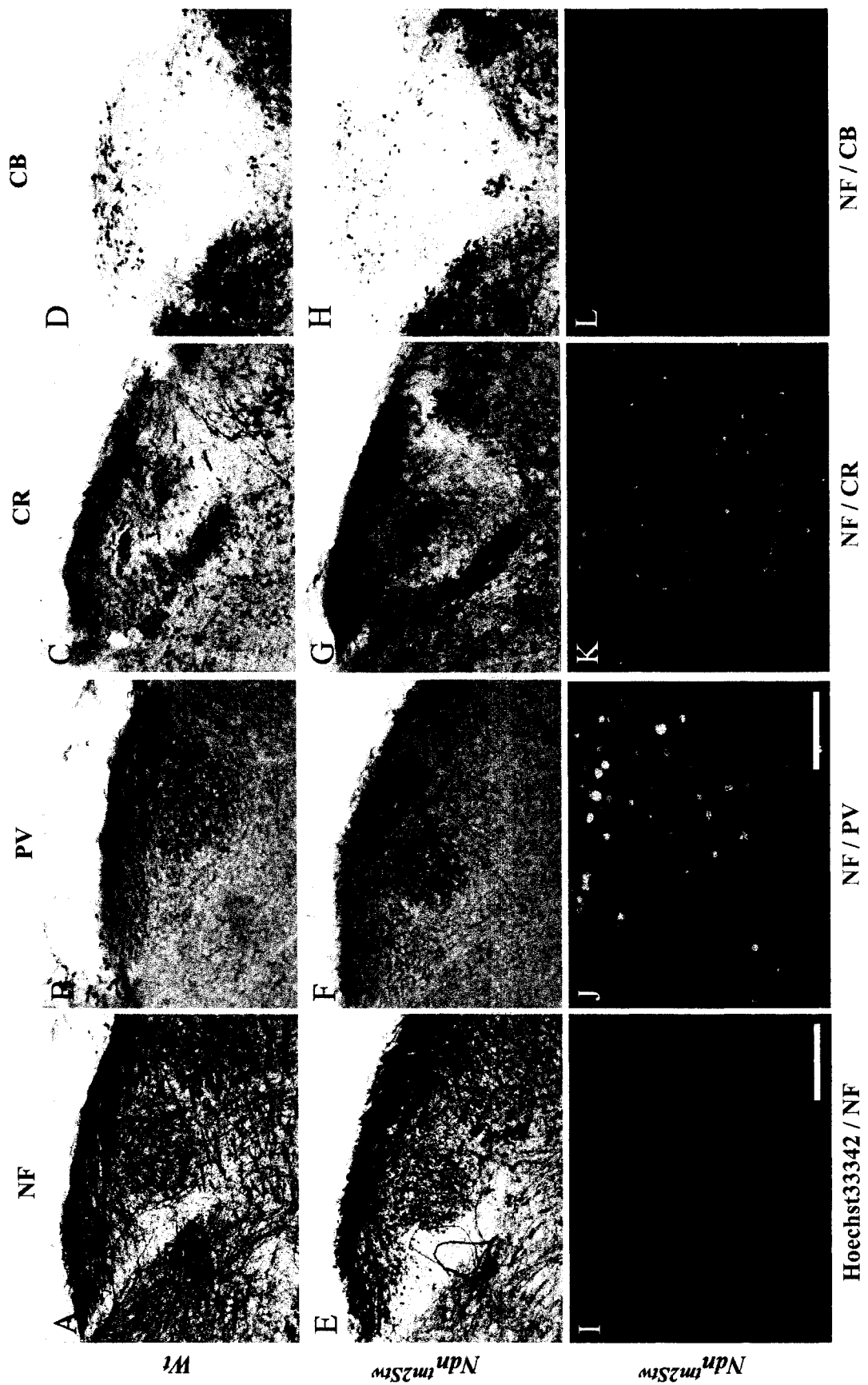


**Figure 3.5** Expression of NF (green, A-F) and GAP43 (red, A-C) in the dorsal column in *Ndn<sup>tm2Stw</sup>* mice during development. (A-C) Sagittal section of E18 cuneate nucleus (Cu) and fasciculus (cu). Note the lack of colocalization within the dystrophic structures in the dorsal column (asterisk) and the complete colocalization in the tangential axons ventral to the Cu (arrow). (D,E) Transverse section of Cu at E15 (E, detail from D). Dystrophic structures are present as early as E15 in Cu. Note that dystrophic structures (arrowheads) are larger than axonal growth cones (arrows). (F) Transverse section of the putative area of the Cu at E13. There is no evidence of dystrophic structures at this time of development. Scale bars: A-F=50  $\mu$ m.



### Previous Page

**Figure 3.6 Calcium binding proteins in the medullary dorsal column in E18 wild type (A-D) and *Ndn*<sup>tm2Stw</sup> mice (E-L).** Immunolabeling for NF (A,E), PV (B,F), CR (C,G) and CB (D,H) in the dorsal column. Double immunolabeling for NF/Hoechst 33342 (I), NF/PV (J), NF/CR (K) and NF/CB (L) in the Cu of *Ndn*<sup>tm2Stw</sup> mice. Dystrophic structures are identified by immunolabeling with NF and PV (J); they rarely express CB or CR (K,L). No Hoechst 33342 positive nuclei are present in the dystrophic structures. Scale bars: A-H=100  $\mu$ m; I-L=50  $\mu$ m.

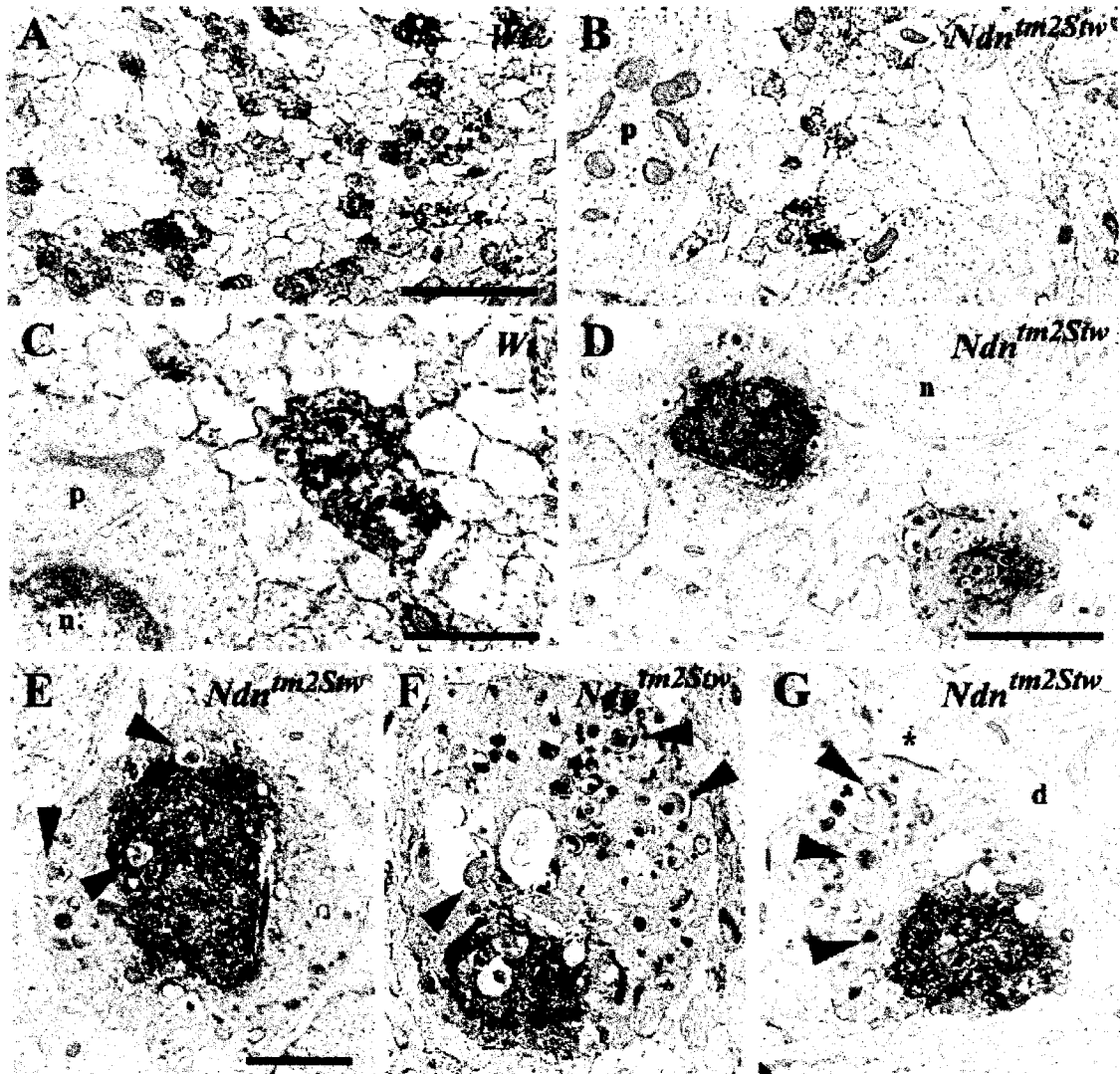


**Figure 3.7 Ultrastructural analysis of the dorsal column in wild type (A,C) and *Ndn<sup>tm2Stw</sup>* mice (B, D-G).** In both wild type and *Ndn<sup>tm2Stw</sup>* mice, small calibre axons are immunopositive for NF (A-C). In *Ndn<sup>tm2Stw</sup>* mice, NF immunolabeling is also present in enlarged fibers, in which there is accumulation of neurofilament, a large number of mitochondria and dark vesicles. Mitochondria are often swollen, dysmorphic and embedded in large vacuoles (arrowheads). Note the presence of a synaptic terminal in G (asterisk). Scale bars: A,B,E-G=2  $\mu$ m; C=1  $\mu$ m; D=5  $\mu$ m. d, dendrite; n, nucleus; p, perykarion.

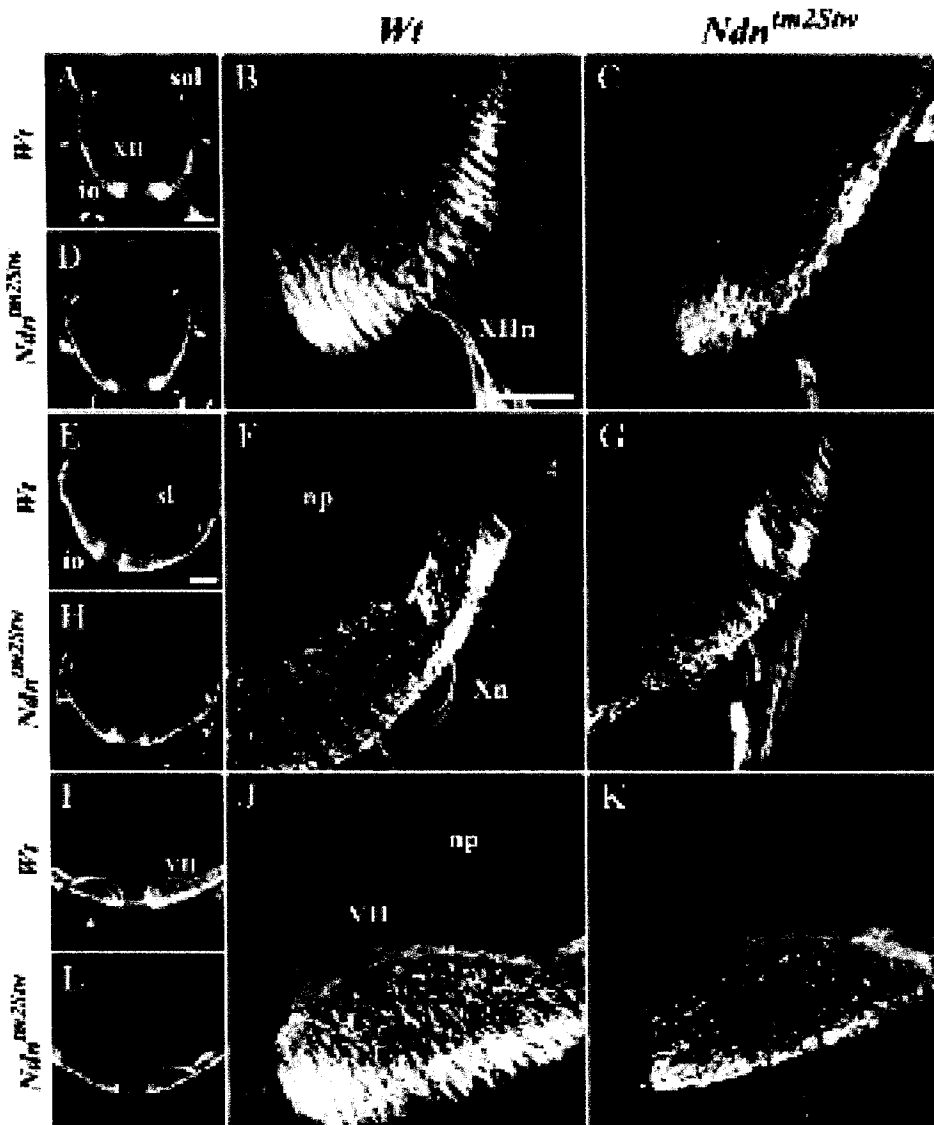


**Figure 3.8** GAP43 expression at different caudo-rostral level of the brainstem in wild type (A,B,E,F,I,J) and *Ndn<sup>tm2Stw</sup>* mice (C,D,G,H,K,L) at E11. (A-D) Caudal medulla at the level of the caudal inferior olive (io) domain and hyoglossal nucleus and nerve root (XII, XIIIn). B and C are details from A and D, respectively. (E-H) rostral medulla at the rostral level of the inferior olive domain. F and G are details from E and H respectively. (I-L) Rostral medulla, K and L are details from I and J, respectively. Note the reduction in number of GAP43 immunopositive axons through the brainstem in *Ndn<sup>tm2Stw</sup>* mice. Scale bars: A,D,E,H,I,L=200  $\mu$ m; B,C,F,G,J,K=100  $\mu$ m. Xn, vagus nerve root; np, neuroepithelium; sl, sulcus limitans; sol, solitary tract.

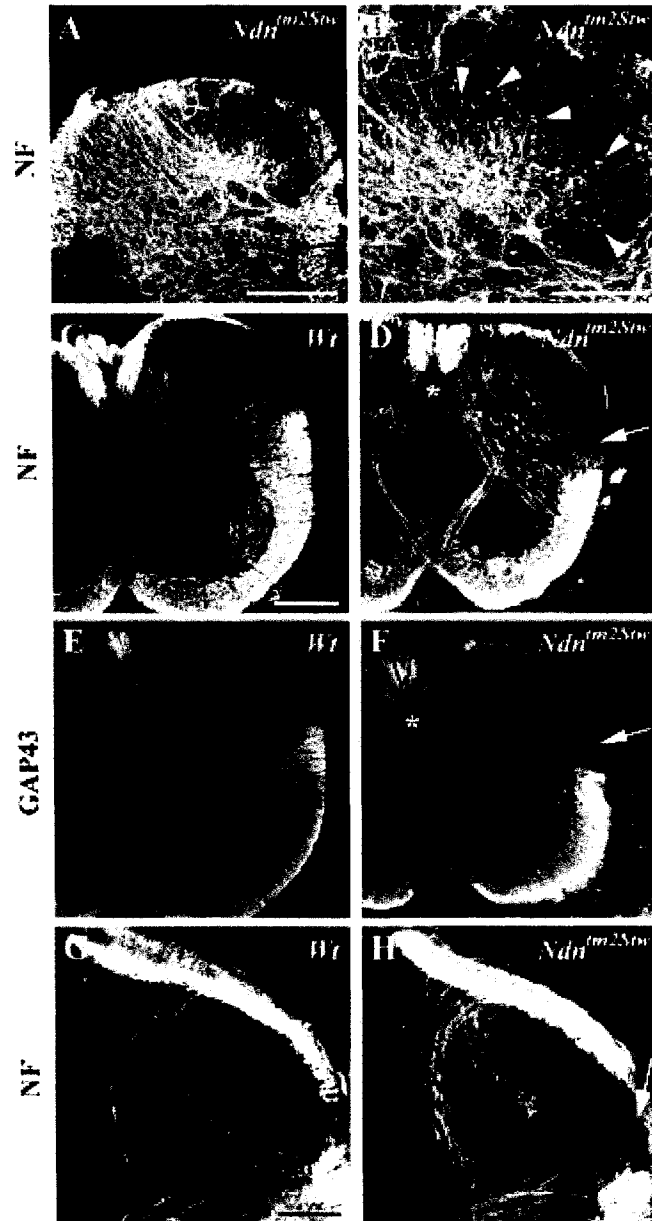


**Figure 3.9** Expression of NF (A-D; G, H) and GAP43 (E-F) in the cervical spinal cord of wild type (C,E,G) and *Ndn*<sup>tm2Stw</sup> mice (A,B,D,F,H). (A,B) NF expression in the dorsal horn of E18 *Ndn*<sup>tm2Stw</sup> mice shows dystrophic structures in laminae II and III of the spinal cord (arrowheads). (C-F) NF and GAP43 expression in wild type and *Ndn*<sup>tm2Stw</sup> mice at E15. Note the reduction in size of the gracile and cuneate fasciculi in the dorsal spinal cord (asterisks) and the limited extension of the lateral funiculus in *Ndn*<sup>tm2Stw</sup> mice (arrows). (G,H) NF expression in dorsal horn of wild type and *Ndn*<sup>tm2Stw</sup> mice at E13. Scale bars: A,C-F=200  $\mu$ m; B,G,H=100  $\mu$ m.

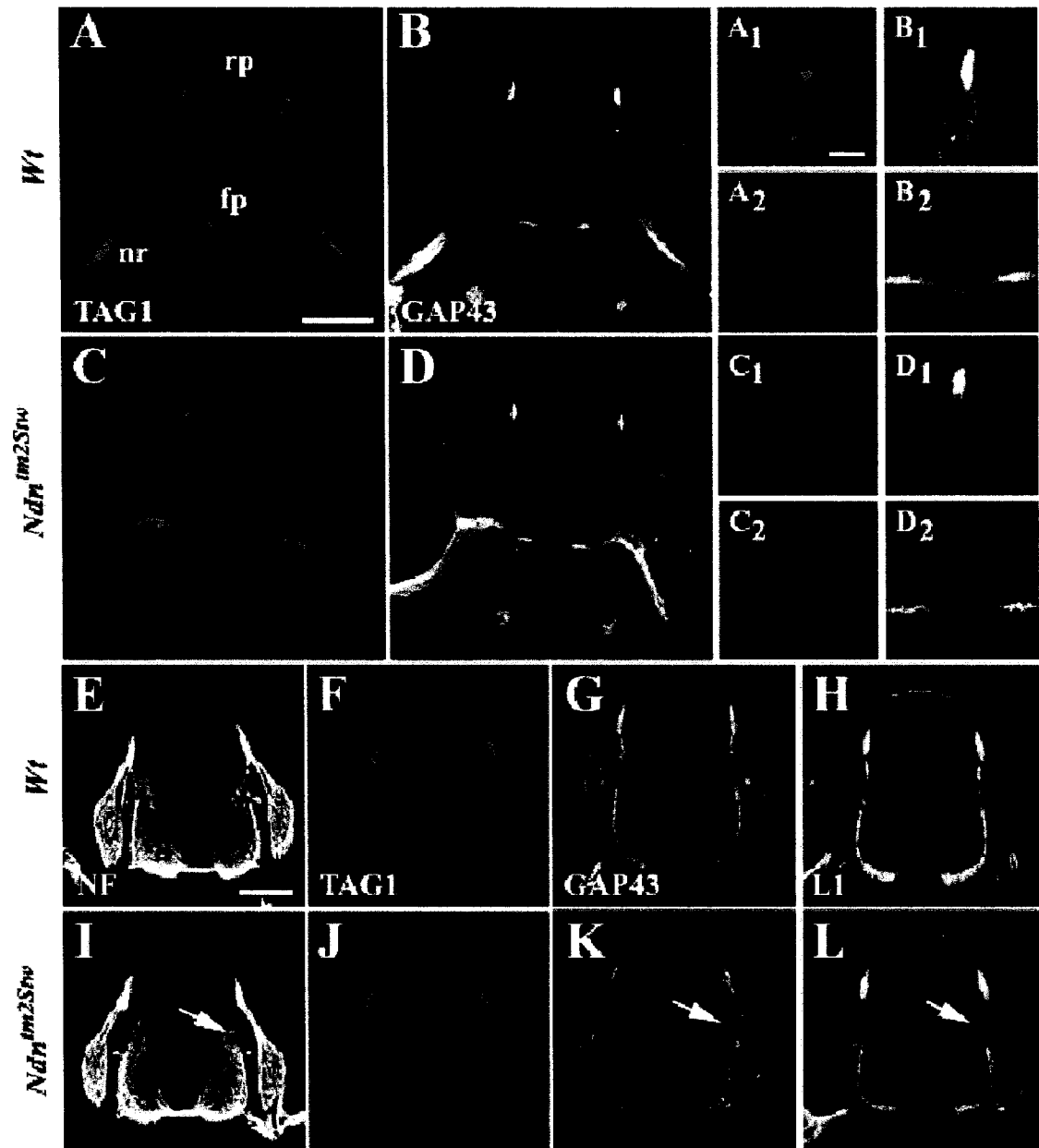


**Figure 3.10** Expression of TAG1, GAP43, NF and L1 in cervical spinal cord of wild type (A,B, E-H) and *Ndn<sup>tm2Stw</sup>* (C,D;I-L) mice at E10 (A-D) and E11 (E-L). (A,C,F,J) TAG1 expression in cervical spinal cord at E10 and E11. A1,A2 and C1,C2 are details of commissural neurons and ventral midline from A and C respectively. (B,D, G,K,) GAP43 expression in cervical spinal cord at E10 and E11. B1,B2 and D1,D2 are details of commissural neurons and ventral midline from B and D respectively. (E,I) NF expression in cervical spinal cord at E11. (H,L) L1 expression in cervical spinal cord at E11. No major differences between wild type and *Ndn<sup>tm2Stw</sup>* mice were identified by

TAG1 and GAP43 immunolabeling at E10. At E11, TAG1 immunolabeling does not show any major differences between wild type and *Ndn<sup>tm2Stw</sup>* mice through the spinal cord; NF, GAP43 and L1 immunopositive axons are reduced in *Ndn<sup>tm2Stw</sup>* mice at the level of the lateral funiculus (arrows). Scale bars: A-D,E-L=200  $\mu$ m; A1-D2=50  $\mu$ m. fp, floor plate; rp, roof plate; nr, nerve root.

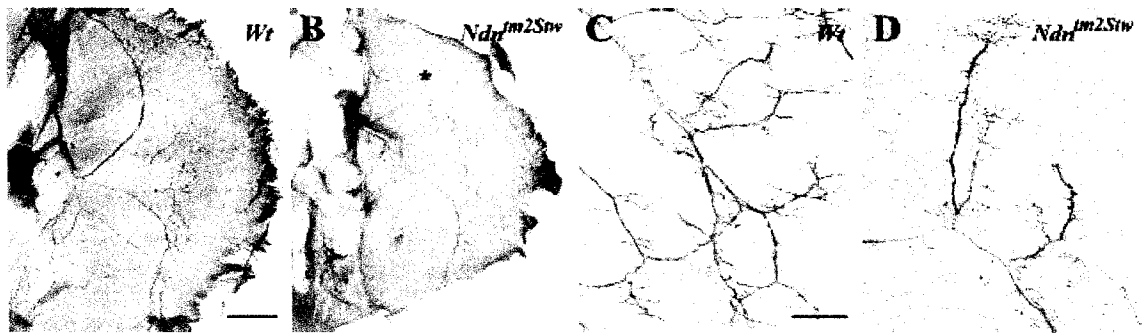


**Figure 3.11 Diaphragm innervation of wild type (A,C) and *Ndn*<sup>tm2Stw</sup> mice (B,D) at E16.** NF immunolabeling shows the reduced extension (asterisk in **B**) and innervation of the phrenic nerve intramuscular branching within the diaphragm of mutant mice. There was no evidence of swollen axons or dystrophic structures at phrenic nerve terminals. Scale bars: A,B=2 mm; C,D=200  $\mu$ m.

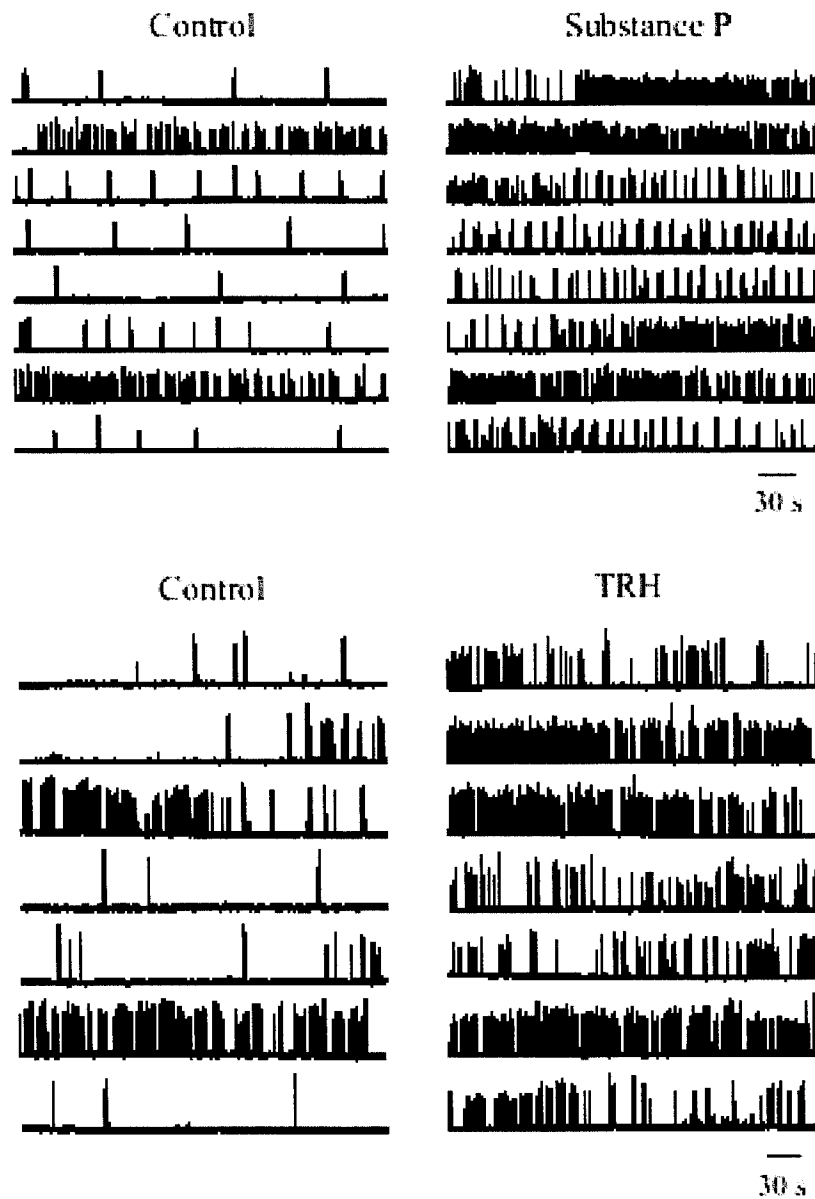


**Figure 3.12** Effects of excitatory neuromodulators on respiratory rhythm generated by *Ndn<sup>tm2Stw</sup>* mouse brainstem-spinal cord preparations. Rectified and integrated suction electrode recordings of diaphragm EMG from E18.5 *Ndn<sup>tm2Stw</sup>* mice in control solution (left) and in response to the addition of SubP (1  $\mu$ m) and TRH (1  $\mu$ m) to the bathing medium (right). Both neuromodulators increased the overall frequency of respiratory rhythm but the instabilities in the frequency remained.

Antigen	Dilution	Antibody	Source	References
Neurofilament -2H3 (NF)	1:2000	Monoclonal (Mouse IgG)	Dev. Studies Hybridoma Bank, IA	(Dodd et al., 1988)
Neurofilament 150kD	1:2000	Polyclonal (Rabbit)	Chemicon, Temecula, CA	(Albers et al., 1994)
Growth Associated Protein 43 (GAP43)	1:2000	Monoclonal (Mouse IgG)	Sigma, St. Louis, MO	(Meiri et al., 1991)
Vimentin 40E-C (VIM)	1:200	Monoclonal (Mouse IgM)	Dev. Studies Hybridoma Bank, IA	(Alvarez-Buylla et al., 1987)
Transiently expressed Axonal Glycoprotein clone 4D7 (TAG1)	1:200	Monoclonal (Mouse IgM)	Dev. Studies Hybridoma Bank, IA	(Yamamoto et al., 1986; Dodd et al., 1988)
Substance P receptor (NK1R)	1:1000	Polyclonal (Rabbit)	Advanced Targeting Systems, San Diego, CA	(Vigna et al., 1994; Mantyh, 2002)
Cell adhesion molecule L1 (L1)	1:200	Monoclonal (Rat)	Chemicon, Temecula, CA	(Dodd et al., 1988)
Choline Acetyl Transferase (ChAT)	1:300	Polyclonal (Goat)	Chemicon, Temecula, CA	(Shiromani et al., 1990)
Substance P (SubP)	1:500	Monoclonal (Rat)	Chemicon, Temecula, CA	(Cuello et al., 1979)
Serotonin (5HT)	1:1000	Polyclonal (Goat)	Chemicon, Temecula, CA	(Millhorn et al., 1988)
Somatostatin (SST)	1:1000	Polyclonal (Rabbit)	Immunostar, Hudson, WI	(Stornetta et al., 2003)
Tyrosine Hydroxylase (TH)	1:2000	Polyclonal (Rabbit)	Chemicon, Temecula, CA	(Albers et al., 1994)

**Table 3.1. Antibodies utilized in the study.**

### 3.5 REFERENCES

- Albers KM, Wright DE, Davis BM (1994) Overexpression of nerve growth factor in epidermis of transgenic mice causes hypertrophy of the peripheral nervous system. *J Neurosci* 14:1422-1432.
- Alvarez-Buylla A, Buskirk DR, Nottebohm F (1987) Monoclonal antibody reveals radial glia in adult avian brain. *J Comp Neurol* 264:159-170.
- Arens R, Gozal D, Omlin KJ, Livingston FR, Liu J, Keens TG, Ward SL (1994) Hypoxic and hypercapnic ventilatory responses in Prader-Willi syndrome. *J Appl Physiol* 77:2224-2230.
- Ballanyi K, Onimaru H, Homma I (1999) Respiratory network function in the isolated brainstem-spinal cord of newborn rats. *Prog Neurobiol* 59:583-634.
- Blanchi B, Kelly LM, Viemari JC, Lafon I, Burnet H, Bevingut M, Tillmanns S, Daniel L, Graf T, Hilaire G, Sieweke MH (2003) MafB deficiency causes defective respiratory rhythmogenesis and fatal central apnea at birth. *Nat Neurosci* 6:1091-1100.
- Celio MR (1990) Calbindin D-28k and parvalbumin in the rat nervous system. *Neuroscience* 35:375-475.
- Charron F, Stein E, Jeong J, McMahon AP, Tessier-Lavigne M (2003) The morphogen sonic hedgehog is an axonal chemoattractant that collaborates with netrin-1 in midline axon guidance. *Cell* 113:11-23.
- Clift S, Dahlitz M, Parkes JD (1994) Sleep apnoea in the Prader-Willi syndrome. *J Sleep Res* 3:121-126.
- Crockett DP, Maslany S, Egger MD (1996) Synaptophysin immunoreactivity and distributions of calcium-binding proteins highlight the functional organization of the rat's dorsal column nuclei. *Brain Res* 707:31-46.
- Cruz JC, Chang TY (2000) Fate of endogenously synthesized cholesterol in Niemann-Pick type C1 cells. *J Biol Chem* 275:41309-41316.
- Cuello AC, Galfre G, Milstein C (1979) Detection of substance P in the central nervous system by a monoclonal antibody. *Proc Natl Acad Sci U S A* 76:3532-3536.
- Dickson BJ (2002) Molecular mechanisms of axon guidance. *Science* 298:1959-1964.

- Dodd J, Morton SB, Karagogeos D, Yamamoto M, Jessell TM (1988) Spatial regulation of axonal glycoprotein expression on subsets of embryonic spinal neurons. *Neuron* 1:105-116.
- Dupouey P, Benjelloun S, Gomes D (1985) Immunohistochemical demonstration of an organized cytoarchitecture of the radial glia in the CNS of the embryonic mouse. *Dev Neurosci* 7:81-93.
- Errchidi S, Monteau R, Hilaire G (1991) Noradrenergic modulation of the medullary respiratory rhythm generator in the newborn rat: an in vitro study. *J Physiol* 443:477-498.
- Feldman JL, Mitchell GS, Nattie EE (2003) Breathing: rhythmicity, plasticity, chemosensitivity. *Annu Rev Neurosci* 26:239-266.
- Friedland DR, Eden AR, Laitman JT (1995a) Naturally occurring motoneuron cell death in rat upper respiratory tract motor nuclei: a histological, fast DiI and immunocytochemical study of the nucleus ambiguus. *J Neurobiol* 26:563-578.
- Friedland DR, Eden AR, Laitman JT (1995b) Naturally occurring motoneuron cell death in rat upper respiratory tract motor nuclei: a histological, fast DiI and immunocytochemical study in the hypoglossal nucleus. *J Neurobiol* 27:520-534.
- Fujisawa K, Shiraki H (1978) Study of axonal dystrophy. I. Pathology of the neuropil of the gracile and the cuneate nuclei in ageing and old rats: a stereological study. *Neuropathol Appl Neurobiol* 4:1-20.
- Funk GD, Smith JC, Feldman JL (1993) Generation and transmission of respiratory oscillations in medullary slices: role of excitatory amino acids. *J Neurophysiol* 70:1497-1515.
- Gerard M, Hernandez L, Wevrick R, Stewart CL (1999) Disruption of the mouse necdin gene results in early post-natal lethality. *Nat Genet* 23:199-202.
- Gho M, McDonald K, Ganetzky B, Saxton WM (1992) Effects of kinesin mutations on neuronal functions. *Science* 258:313-316.
- Gindhart JG, Chen J, Faulkner M, Gandhi R, Doerner K, Wisniewski T, Nandlestadt A (2003) The kinesin-associated protein UNC-76 is required for axonal transport in the *Drosophila* nervous system. *Mol Biol Cell* 14:3356-3365.

- Goldstone AP (2004) Prader-Willi syndrome: advances in genetics, pathophysiology and treatment. *Trends Endocrinol Metab* 15:12-20.
- Gozal D, Arens R, Omlin KJ, Ward SL, Keens TG (1994) Absent peripheral chemosensitivity in Prader-Willi syndrome. *J Appl Physiol* 77:2231-2236.
- Gray PA, Rekling JC, Bocchiaro CM, Feldman JL (1999) Modulation of respiratory frequency by peptidergic input to rhythmogenic neurons in the preBotzinger complex. *Science* 286:1566-1568.
- Greer JJ, Smith JC, Feldman JL (1991) Role of excitatory amino acids in the generation and transmission of respiratory drive in neonatal rat. *J Physiol* 437:727-749.
- Greer JJ, Smith JC, Feldman JL (1992) Respiratory and locomotor patterns generated in the fetal rat brain stem-spinal cord in vitro. *J Neurophysiol* 67:996-999.
- Greer JJ, al-Zubaidy Z, Carter JE (1996) Thyrotropin-releasing hormone stimulates perinatal rat respiration in vitro. *Am J Physiol* 271:R1160-1164.
- Greer JJ, Allan DW, Martin-Caraballo M, Lemke RP (1999) An overview of phrenic nerve and diaphragm muscle development in the perinatal rat. *J Appl Physiol* 86:779-786.
- Guyenet PG, Sevigny CP, Weston MC, Stornetta RL (2002) Neurokinin-1 receptor-expressing cells of the ventral respiratory group are functionally heterogeneous and predominantly glutamatergic. *J Neurosci* 22:3806-3816.
- Hayashi M, Itoh M, Kabasawa Y, Hayashi H, Satoh J, Morimatsu Y (1992) A neuropathological study of a case of the Prader-Willi syndrome with an interstitial deletion of the proximal long arm of chromosome 15. *Brain Dev* 14:58-62.
- Hilaire G, Monteau R, Errchidi S (1989) Possible modulation of the medullary respiratory rhythm generator by the noradrenergic A5 area: an in vitro study in the newborn rat. *Brain Res* 485:325-332.
- Huang ZG, Subramanian SH, Balnave RJ, Turman AB, Moi Chow C (2000) Roles of periaqueductal gray and nucleus tractus solitarius in cardiorespiratory function in the rat brainstem. *Respir Physiol* 120:185-195.
- Ichihara N, Wu J, Chui DH, Yamazaki K, Wakabayashi T, Kikuchi T (1995) Axonal degeneration promotes abnormal accumulation of amyloid beta-protein in

- ascending gracile tract of gracile axonal dystrophy (GAD) mouse. *Brain Res* 695:173-178.
- Jay P, Rougeulle C, Massacrier A, Moncla A, Mattei MG, Malzac P, Roeckel N, Taviaux S, Lefranc JL, Cau P, Berta P, Lalande M, Muscatelli F (1997) The human necdin gene, NDN, is maternally imprinted and located in the Prader-Willi syndrome chromosomal region. *Nat Genet* 17:357-361.
- Jessell TM (2000) Neuronal specification in the spinal cord: inductive signals and transcriptional codes. *Nat Rev Genet* 1:20-29.
- Johnson JE, Mehler WR, Miquel J (1975) A fine structural study of degenerative changes in the dorsal column nuclei of aging mice. Lack of protection by vitamin E. *J Gerontol* 30:395-411.
- Kaufman M (1994) *The atlas of mouse development*. London: Academic Press.
- Kennedy TE, Serafini T, de la Torre JR, Tessier-Lavigne M (1994) Netrins are diffusible chemotropic factors for commissural axons in the embryonic spinal cord. *Cell* 78:425-435.
- Kozlov SV, Gerard M, Stewart CL (2001) Morphological analysis of the respiratory pathway in perinatal mice deficient for necdin: a component of the pathology of Prader-Willi syndrome. In: *Soc Neurosci Abs* 694:10.
- Kuwako K, Taniura H, Yoshikawa K (2004) Necdin-related MAGE proteins differentially interact with the E2F1 transcription factor and the p75 neurotrophin receptor. *J Biol Chem* 279:1703-1712.
- L'Hermine AC, Aboura A, Brisset S, Cuisset L, Castaigne V, Labrune P, Frydman R, Tachdjian G (2003) Fetal phenotype of Prader-Willi syndrome due to maternal disomy for chromosome 15. *Prenat Diagn* 23:938-943.
- Lagercrantz H (1987) Neuromodulators and respiratory control in the infant. *Clin Perinatol* 14:683-695.
- Lee S, Walker CL, Karten B, Kuny SL, Tennese AA, O'Neill MA, Wevrick R (2005) Essential role for the Prader-Willi syndrome protein necdin in axonal outgrowth. *Hum Mol Genet* 14:627-637.

- Long H, Sabatier C, Ma L, Plump A, Yuan W, Ornitz DM, Tamada A, Murakami F, Goodman CS, Tessier-Lavigne M (2004) Conserved roles for Slit and Robo proteins in midline commissural axon guidance. *Neuron* 42:213-223.
- MacDonald HR, Wevrick R (1997) The *necdin* gene is deleted in Prader-Willi syndrome and is imprinted in human and mouse. *Hum Mol Genet* 6:1873-1878.
- Manni R, Politini L, Nobili L, Ferrillo F, Livieri C, Veneselli E, Biancheri R, Martinetti M, Tartara A (2001) Hypersomnia in the Prader Willi syndrome: clinical-electrophysiological features and underlying factors. *Clin Neurophysiol* 112:800-805.
- Mantyh PW (2002) Neurobiology of substance P and the NK1 receptor. *J Clin Psychiatry* 63 Suppl 11:6-10.
- Meiri KF, Bickerstaff LE, Schwob JE (1991) Monoclonal antibodies show that kinase C phosphorylation of GAP-43 during axonogenesis is both spatially and temporally restricted in vivo. *J Cell Biol* 112:991-1005.
- Menendez AA (1999) Abnormal ventilatory responses in patients with Prader-Willi syndrome. *Eur J Pediatr* 158:941-942.
- Millhorn DE, Hokfelt T, Seroogy K, Verhofstad AA (1988) Extent of colocalization of serotonin and GABA in neurons of the ventral medulla oblongata in rat. *Brain Res* 461:169-174.
- Moss IR, Inman JG (1989) Neurochemicals and respiratory control during development. *J Appl Physiol* 67:1-13.
- Mukoyama M, Yamazaki K, Kikuchi T, Tomita T (1989) Neuropathology of gracile axonal dystrophy (GAD) mouse. An animal model of central distal axonopathy in primary sensory neurons. *Acta Neuropathol (Berl)* 79:294-299.
- Muscatelli F, Abrous DN, Massacrier A, Boccaccio I, Le Moal M, Cau P, Cremer H (2000) Disruption of the mouse *Necdin* gene results in hypothalamic and behavioral alterations reminiscent of the human Prader-Willi syndrome. *Hum Mol Genet* 9:3101-3110.
- Nicholls RD, Knepper JL (2001) Genome organization, function, and imprinting in Prader-Willi and Angelman syndromes. *Annu Rev Genomics Hum Genet* 2:153-175.

- Nixon GM, Brouillette RT (2002) Sleep and breathing in Prader-Willi syndrome. *Pediatr Pulmonol* 34:209-217.
- Ohara S, Ukita Y, Ninomiya H, Ohno K (2004) Axonal dystrophy of dorsal root ganglion sensory neurons in a mouse model of Niemann-Pick disease type C. *Exp Neurol* 187:289-298.
- Ong WY, Kumar U, Switzer RC, Sidhu A, Suresh G, Hu CY, Patel SC (2001) Neurodegeneration in Niemann-Pick type C disease mice. *Exp Brain Res* 141:218-231.
- Pagliardini S, Ren J, Greer JJ (2003) Ontogeny of the pre-Botzinger complex in perinatal rats. *J Neurosci* 23:9575-9584.
- Pickel VM, Joh TH, Reis DJ (1975) Ultrastructural localization of tyrosine hydroxylase in noradrenergic neurons of brain. *Proc Natl Acad Sci U S A* 72:659-663.
- Pinault D, Smith Y, Deschenes M (1997) Dendrodendritic and axoaxonic synapses in the thalamic reticular nucleus of the adult rat. *J Neurosci* 17:3215-3233.
- Ptak K, Hilaire G (1999) Central respiratory effects of substance P in neonatal mice: an in vitro study. *Neurosci Lett* 266:189-192.
- Rakic P (1971) Neuron-glia relationship during granule cell migration in developing cerebellar cortex. A Golgi and electronmicroscopic study in *Macacus Rhesus*. *J Comp Neurol* 141:283-312.
- Rekling JC, Feldman JL (1998) PreBotzinger complex and pacemaker neurons: hypothesized site and kernel for respiratory rhythm generation. *Annu Rev Physiol* 60:385-405.
- Ren J, Lee S, Pagliardini S, Gerard M, Stewart CL, Greer JJ, Wevrick R (2003) Absence of *Ndn*, encoding the Prader-Willi syndrome-deleted gene *necdin*, results in congenital deficiency of central respiratory drive in neonatal mice. *J Neurosci* 23:1569-1573.
- Saigoh K, Wang YL, Suh JG, Yamanishi T, Sakai Y, Kiyosawa H, Harada T, Ichihara N, Wakana S, Kikuchi T, Wada K (1999) Intragenic deletion in the gene encoding ubiquitin carboxy-terminal hydrolase in *gad* mice. *Nat Genet* 23:47-51.
- Schluter B, Buschatz D, Trowitzsch E, Aksu F, Andler W (1997) Respiratory control in children with Prader-Willi syndrome. *Eur J Pediatr* 156:65-68.

- Shiromani PJ, Lai YY, Siegel JM (1990) Descending projections from the dorsolateral pontine tegmentum to the paramedian reticular nucleus of the caudal medulla in the cat. *Brain Res* 517:224-228.
- Smith JC, Greer JJ, Liu GS, Feldman JL (1990) Neural mechanisms generating respiratory pattern in mammalian brain stem-spinal cord in vitro. I. Spatiotemporal patterns of motor and medullary neuron activity. *J Neurophysiol* 64:1149-1169.
- Smith JC, Ellenberger HH, Ballanyi K, Richter DW, Feldman JL (1991) Pre-Botzinger complex: a brainstem region that may generate respiratory rhythm in mammals. *Science* 254:726-729.
- Smith JC, Butera RJ, Koshiya N, Del Negro C, Wilson CG, Johnson SM (2000) Respiratory rhythm generation in neonatal and adult mammals: the hybrid pacemaker-network model. *Respir Physiol* 122:131-147.
- Stevenson DA, Anaya TM, Clayton-Smith J, Hall BD, Van Allen MI, Zori RT, Zackai EH, Frank G, Clericuzio CL (2004) Unexpected death and critical illness in Prader-Willi syndrome: report of ten individuals. *Am J Med Genet A* 124:158-164.
- Stoeckli ET, Landmesser LT (1995) Axonin-1, Nr-CAM, and Ng-CAM play different roles in the in vivo guidance of chick commissural neurons. *Neuron* 14:1165-1179.
- Stornetta RL, Rosin DL, Wang H, Sevigny CP, Weston MC, Guyenet PG (2003) A group of glutamatergic interneurons expressing high levels of both neurokinin-1 receptors and somatostatin identifies the region of the pre-Botzinger complex. *J Comp Neurol* 455:499-512.
- Strahle U, Lam CS, Ertzer R, Rastegar S (2004) Vertebrate floor-plate specification: variations on common themes. *Trends Genet* 20:155-162.
- Sutcliffe JS, Han M, Christian SL, Ledbetter DH (1997) Neuronally-expressed *necdin* gene: an imprinted candidate gene in Prader-Willi syndrome. *Lancet* 350:1520-1521.
- Swaab DF (1997) Prader-Willi syndrome and the hypothalamus. *Acta Paediatr Suppl* 423:50-54.

- Takazaki R, Nishimura I, Yoshikawa K (2002) Necdin is required for terminal differentiation and survival of primary dorsal root ganglion neurons. *Exp Cell Res* 277:220-232.
- Taniura H, Yoshikawa K (2002) Necdin interacts with the ribonucleoprotein hnRNP U in the nuclear matrix. *J Cell Biochem* 84:545-555.
- Thoby-Brisson M, Cauli B, Champagnat J, Fortin G, Katz DM (2003) Expression of functional tyrosine kinase B receptors by rhythmically active respiratory neurons in the pre-Botzinger complex of neonatal mice. *J Neurosci* 23:7685-7689.
- Tsai FY, Keller G, Kuo FC, Weiss M, Chen J, Rosenblatt M, Alt FW, Orkin SH (1994) An early haematopoietic defect in mice lacking the transcription factor GATA-2. *Nature* 371:221-226.
- Tsai TF, Armstrong D, Beaudet AL (1999) Necdin-deficient mice do not show lethality or the obesity and infertility of Prader-Willi syndrome. *Nat Genet* 22:15-16.
- Viemari JC, Bevingut M, Burnet H, Coulon P, Pequignot JM, Tiveron MC, Hilaire G (2004) Phox2a gene, A6 neurons, and noradrenaline are essential for development of normal respiratory rhythm in mice. *J Neurosci* 24:928-937.
- Vigna SR, Bowden JJ, McDonald DM, Fisher J, Okamoto A, McVey DC, Payan DG, Bunnnett NW (1994) Characterization of antibodies to the rat substance P (NK-1) receptor and to a chimeric substance P receptor expressed in mammalian cells. *J Neurosci* 14:834-845.
- Wang H, Stornetta RL, Rosin DL, Guyenet PG (2001) Neurokinin-1 receptor-immunoreactive neurons of the ventral respiratory group in the rat. *J Comp Neurol* 434:128-146.
- Wharton RH, Loechner KJ (1996) Genetic and clinical advances in Prader-Willi syndrome. *Curr Opin Pediatr* 8:618-624.
- Yamamoto M, Boyer AM, Crandall JE, Edwards M, Tanaka H (1986) Distribution of stage-specific neurite-associated proteins in the developing murine nervous system recognized by a monoclonal antibody. *J Neurosci* 6:3576-3594.
- Yoshii A, Krishnamoorthy KS, Grant PE (2002) Abnormal cortical development shown by 3D MRI in Prader-Willi syndrome. *Neurology* 59:644-645.

Yoshikawa K (2000) Cell cycle regulators in neural stem cells and postmitotic neurons.  
Neurosci Res 37:1-14.

## **\*CHAPTER IV**

### **Fluorescent Tagging of Rhythmically Active Respiratory Neurons within the PreBötzinger Complex of Rat Medullary Slice Preparations**

---

\*Previously published paper:

Pagliardini S<sup>+</sup>, Adachi T<sup>+</sup>, Ren J, Funk GD, Greer JJ (2005) Fluorescent tagging of rhythmically active respiratory neurons within the preBötzinger Complex of rat medullary slice preparations. *J Neurosci* 25(10):2591-6. Copyright 2005 by the Society for Neuroscience.<sup>+</sup> These authors contributed equally

My contribution to this study consisted in the proposal of the project, and the planning and execution of the anatomical results. Electrophysiological recordings and analyses were performed by Drs T. Adachi and J. Ren.

## 4.1 INTRODUCTION

The discovery of the preBötC as a critical site for mammalian respiratory rhythmogenesis was a seminal advancement in the field of the neural control of mammalian breathing (Smith et al., 1991). The preBötC resides in a restricted region of the ventrolateral medulla at the rostral end of a column of neurons known for decades to be involved in respiratory control. The development of thin medullary slice preparations containing the preBötC provided a focal point for study and the promise of rapid progress toward final resolution of the mechanisms underlying rhythm generation. Indeed this preparation has enabled application of varied fluorescent imaging techniques, made the whole-cell analysis of neurons in this region routine, and has contributed to significant advances in the field over the last decade (Smith et al., 1991; Frermann et al., 1999; Koshiya and Smith, 1999; Onimaru and Homma, 2003). In spite of this, the fact that the preBötC contains a functionally heterogeneous pool of neurons has been a major remaining impediment to progress. It will be critical to specifically demarcate the target preBötC neurons of interest within viable, rhythmically-active preparations.

Here we present an important advancement that provides for the rapid and precise targeting of this relatively small population of neurons. We have exploited the fact that NK1R expression identifies a subset of respiratory neurons within the preBötC that are hypothesized to play an important role in inspiratory rhythmogenesis (Gray et al., 1999; Gray et al., 2001; Pilowsky and Feldman, 2001; Guyenet et al., 2002; Stornetta, et al., 2003; Manzke et al., 2003). Targeted destruction of these cells with SubP-SAP completely disrupts breathing rhythm *in vivo* (Gray et al., 2001). We have used fluorescently conjugated SubP, which is internalized after binding to NK1R, in conjunction with fluorescent IR-DIC microscopy, to identify key neurons within the preBötC for subsequent whole-cell analysis. This approach markedly increases the probability of selecting precisely those neurons thought to be essential for mammalian respiratory rhythmogenesis.

## **4.2 MATERIAL AND METHODS**

### **4.2.1 MEDULLARY SLICE PREPARATION**

Sprague-Dawley rats were bred at the University of Alberta. The institution's Animal Welfare Committee approved all procedures. Newborn rats (postnatal day 1 to 4) were used. Animals were anesthetized by inhalation of halothane or isoflurane (2-3%) and the neuraxis was isolated. Rhythmically-active medullary slice preparations were produced as previously described (Smith et al., 1991). Briefly, the brainstem-spinal cord was pinned, ventral surface upward, on a paraffin-coated metal plate. The plate was mounted in the vise of a Leica VT1000S vibratome and sectioned serially. Upon visualization of appropriate landmarks, a single transverse slice containing the preBötC was cut (550-650  $\mu\text{m}$  thick), transferred to a chamber containing artificial cerebrospinal fluid (aCSF) containing (in mM) 128 NaCl, 8.0 KCl, 1.5 CaCl<sub>2</sub>, 1.0 MgSO<sub>4</sub>, 24 NaHCO<sub>3</sub>, 0.5 NaH<sub>2</sub>PO<sub>4</sub>, and 30 D-glucose equilibrated with 95% O<sub>2</sub> - 5% CO<sub>2</sub> at room temperature and equilibrated with 95% O<sub>2</sub> - 5% CO<sub>2</sub>.

### **4.2.2. TETRAMETHYLRHODAMINE CONJUGATED- SUBSTANCE P APPLICATION IN LIVING MEDULLARY SLICE**

In experiments designed to assess the effects of TMR-SubP on rhythmic network activity and long-term viability, slices were placed in a "flow-through" recording chamber (2 ml) perfused with aCSF (2 ml/min). Tetramethylrhodamine conjugated-SubP (TMR-SubP; 500 nM; Molecular probes, Inc. Eugene, OR) was administered to the perfusion solution for 5 minutes. To assess the extent of TMR-SubP internalization, or for labeling neurons for subsequent whole-cell analysis of respiratory neurons, slices were transferred to microcentrifuge tubes containing TMR-SubP (500nM) in aCSF (1 ml), and incubated in the dark for 5-8 minutes at 31°C under continuous delivery of 95% O<sub>2</sub> - 5% CO<sub>2</sub>. Slices were transferred to a recording chamber (0.5 ml) perfused with aCSF (2-3 ml/min) for whole-cell analysis (see electrophysiology) or fixed in 4% paraformaldehyde in phosphate buffer (0.1M, pH 7.2) for imaging. Our initial

experiments were performed with a similar protocol but using the fluorochrome Oregon Green 488 conjugated with SubP (Molecular probes, Inc. Eugene, OR).

#### **4.2.3. IMMUNOHISTOCHEMISTRY**

Fixed medullary slices were processed for NK1R immunolabelling according to the following protocol. Slices were sectioned (50  $\mu$ m) on a vibratome. Sections were rinsed in PBS and incubated with 1.0% BSA and 0.3% Triton X-100 in PBS for 90 min in order to reduce non-specific staining and increase antibody penetration. Sections were incubated overnight with primary antibody (1:1000; rabbit polyclonal anti-NK1R, Advanced Targeting Systems, San Diego, CA) diluted in PBS containing 0.1% BSA. After several washes in PBS, sections were incubated with Cy2-conjugated DAR (1:200; Jackson ImmunoResearch, West Grove, PA) diluted in PBS and 0.1% BSA for 2 hours. Sections were further washed in PBS, mounted and cover-slipped with Fluorsave mounting medium (Calbiochem, San Diego, CA). Alternatively, medullary slices were embedded in 6% agar and 100  $\mu$ m thick coronal sections were cut with a vibratome in order to analyze the depth of TMR-SubP labeling in the tissue slice.

#### **4.2.4. CONFOCAL IMAGING OF FIXED TISSUE**

Mounted sections were examined with a Zeiss 100M microscope (20X or 40X objective) using a LSM 510 NLO laser and LSM 510 software (Zeiss, Oberkochen, Germany). For Cy2 fluorescence, excitation was set to 488 nm and emissions collected with a 505 nm long-pass filter. For TMR-SubP fluorescence, excitation was set to 543 nm and emissions collected using a 560 nm long-pass filter. Multiple, thin sections were acquired along the Z axis to assess extent of TMR-SubP labeling and the degree to which it colocalized with NK1R immunolabelling. Acquired images were exported in JPEG format, and brightness and contrast adjusted in Adobe Photoshop 7.0 (Adobe Systems, Mountain View, CA).

#### 4.2.5 RECORDING AND ANALYSIS

Recordings of population inspiratory activity from XII nerve roots were made via suction electrodes. Signals were amplified, filtered (0.3-3 kHz), rectified, integrated ( $\tau=50$  msec) and recorded on computer using a Digidata 1322A A/D board and Axoscope software. Whole-cell recordings were made from slices placed in a recording chamber on the fixed stage of an upright microscope (Zeiss Axioskop II FS) equipped with IR-DIC optics and epifluorescence. Slices were continuously perfused (2-3 ml/min) at 27°C with aCSF equilibrated with 95% O<sub>2</sub> - 5% CO<sub>2</sub>. A delay of at least 30 minutes was allowed prior to recording to allow for stabilization of respiratory rhythm and removal of non-specific TMR-SubP fluorescence. TMR-SubP positive neurons were identified under epifluorescence using a CCD camera (Ikegami, ICD-47) and monitor (National Electronics M910), without any additional image intensification hardware or imaging software. We have since used a DAGE-MTI IR-1000 camera that provides for yet a better detection of the fluorescent signal. Whole-cell recordings were then obtained from TMR-SubP positive neurons under IR-DIC visualization using patch electrodes (resistance 3-4 M $\Omega$ ) pulled on a horizontal puller (Sutter Model P-97) from 1.2 mm o.d. filamented borosilicate glass (Clark/WPI). Fluorescent illumination was minimized by placing a blocking filter in the fluorescent light path as soon as a candidate TMR-SubP positive neuron was identified. Pipettes were filled with potassium gluconate solution containing (in mM): 122.5 potassium gluconate, 17.5 KCl, 9 NaCl, 1 MgCl<sub>2</sub>, 10 HEPES, 0.2 EGTA, 3 ATP-Mg, 0.3 GTP-Tris, pH adjusted to 7.3 with 5 N KOH. Intracellular signals were amplified and filtered (2-5 kHz low pass Bessel filter) with a multiclamp 700A amplifier (Axon Instruments, Foster City, CA, USA), and acquired via a Digidata 1322A A/D board and pClamp 9.0 software. Series resistance and whole-cell capacitance were estimated under voltage-clamp conditions using short voltage pulses (100 Hz, -10 mV, 3 ms). Series resistance was compensated by 75% and monitored throughout the experiments. In cases where permanent records of fluorescent and IR-DIC images of live neurons were acquired, we used a Zeiss Axiocam camera in conjunction with Axiovision software.

## 4.3. RESULTS

### 4.3.1 DIFFUSION AND INTERNALIZATION OF TMR-SUB P IN MEDULLARY SLICES

To assess the diffusion of TMR-SubP and its effects on network activity, we applied it to the solution bathing medullary slice preparations. Similar to unconjugated SubP (Murakoshi et al., 1985; Yamamoto et al., 1992; Johnson et al., 1996), 500 nM TMR-SubP elicited a marked stimulation of respiratory rhythm (Fig. 4.1). The potentiation was readily reversible upon washout. Moreover, TMR-SubP did not affect preparation viability as the medullary slices generated a robust inspiratory output for at least 4 hours. These data indicate that the fluorescently tagged SubP diffuses into the medullary slice and binds to NK1R on neurons that regulate respiratory rhythm without having toxic effects.

SubP internalization within cells is thought to occur within minutes (reviewed in Harrison and Geppetti, 2001; Mantyh, 2002). To assess the degree of internalization of TMR-SubP within the medullary slice preparation, we bathed slices in TMR-SubP (500 nM) for 5 minutes at 31°C. Slices were then fixed, sectioned in both the transverse and coronal planes and the distribution of the fluorescent signal assessed via confocal imaging. As shown in Fig. 4.2, the distribution of fluorescent signal resulting from the internalization of TMR-SubP was similar to that achieved by immunolabelling for NK1R. Punctate immunofluorescence in both transverse and coronal sections was detected in cell bodies and dendrites within all regions of the slice that express NK1R during the perinatal period: midline (Fig. 4.2b,e), raphe nucleus (Fig. 4.2e), nucleus ambiguus (Fig. 4.2c,f), and preBötC (Fig. 4.2d,g,h) (Horie et al., 2000; Liu and Wong-Riley, 2002; Pagliardini et al., 2003). To further correlate the internalization of TMR-SubP with NK1R expression, treated slices were processed for immunohistochemical detection of NK1R. Double labelling, as indicated by fine yellow puncta, was observed in dendrites and cell bodies at all depths of the slice. This included strong co-localization within the preBötC (Fig. 4.2i,j). It appeared that all NK1R<sup>+</sup> neurons had internalized SubP-TMR.

### 4.3.2. WHOLE-CELL RECORDING FROM FLUORESCENTLY TAGGED PREBötC NEURONS

We next combined TMR-SubP labeling procedure with IR-DIC optics to obtain whole-cell recordings of NK1R<sup>+</sup> respiratory neurons within the preBötC of rhythmically-active slice preparations. We targeted neurons located ventrolateral to the nucleus ambiguus in the rostral aspect of the medullary slices. Within a single field of view, there were typically a few neurons on the surface that had intense, diffuse staining. As is often the case for surface cells of vibratome prepared slices, these neurons showed evidence of fractured membranes, depolarized resting membrane potentials and were unable to fire action potentials. In neurons located 2-3 cell layers below the surface, labeling was punctate and outlined the surface of dendrites and somata.

Targeting of these neurons for whole-cell patch recording under IR-DIC visualization provided a very high yield of recordings from healthy inspiratory neurons. In total, we recorded 34 TMR-SubP positive preBötC neurons from 12 rhythmically active medullary slices (Fig.4.3). Eighty two percent (28/34) of neurons were rhythmically-active inspiratory neurons with overshooting action potentials. The remaining 6 neurons fired robust trains of action potentials in response to depolarizing current but did not receive inspiratory-related synaptic drive potentials (data not shown). We then determined whether any of the fluorescently tagged preBötC neurons had characteristics consistent with pacemaker neurons; fitting with a prominent hypothesis that NK1R<sup>+</sup> neurons are important in rhythm generation, and in turn that pacemaker neurons are involved in respiratory rhythmogenesis (Rekling and Feldman, 1998; Smith et al., 2000). Putative pacemaker neurons within the preBötC discharged in phase with inspiratory activity but their oscillation frequency increases with progressive depolarization (i.e. they generate ectopic bursts). More definitive is that they continue to burst following disruption of network activity, for example following the removal of inspiratory drive transmission by blocking ionotropic, non-NMDA glutamate receptors (Johnson et al., 1994; Butera et al., 1999). We used the latter criteria following the observation that in some neurons with voltage-dependent bursting properties,

spontaneous burst firing stopped after disruption of network activity with CNQX. Of the 12 inspiratory neurons examined before and after blockade of network activity in 5  $\mu$ M CNQX, 9 stopped firing and all rhythmic synaptic activity was abolished after ~15 minutes. CNQX-sensitive neurons that were depolarized via injection of DC current did not burst but fired tonically. The remaining 3 (25%) neurons continued to generate periodic bursting at a frequency and duration similar to the inspiratory-related motor output generated by the intact network in vitro (Fig. 4.3B, lower recording). We did not systematically confirm under voltage-clamp conditions that all rhythmic synaptic activity was blocked by CNQX in these 3 neurons. However, the same concentration of CNQX has been used successfully in a similar preparation to synaptically isolate pacemaker neurons (Del Negro et al., 2002). The neuron shown in Fig. 3c demonstrated voltage-dependent bursting in the presence of CNQX. Further confirmation that the fluorescently tagged neurons were NK1R<sup>+</sup> was achieved by applying the NK1R agonist, [Sar<sup>9</sup>,Met(O<sub>2</sub>)<sup>11</sup>]-SP (500 nM) in presence of TTX (400 nM). [Sar<sup>9</sup>,Met(O<sub>2</sub>)<sup>11</sup>]-SP produced a long-lasting depolarization in all CNQX-resistant neurons tested (n=3) (Fig. 4.3d).

#### 4.4. DISCUSSION

There is a concerted effort to elucidate the neuronal mechanisms operating within the preBötC due to its essential role for breathing in mammals. This includes an assessment of its ontogeny, cellular, network and neuropharmacological properties. Advancement will depend critically upon targeting of putative respiratory rhythmogenic neurons for intracellular recordings. Work in these areas has benefited greatly from the development of the brainstem-spinal cord preparation by Suzue (1984) and the subsequent use of 'blind' whole-cell recordings (Smith et al., 1988, 1992). Accessibility increased with the development of the medullary slice preparation and whole-cell yields were enhanced with development of IR-DIC microscopy (Smith et al., 1991; Stuart et al., 1993). Together, these techniques offered direct visualization and targeting of neurons within the ventrolateral medulla based on general morphological criteria. However, due to the functional heterogeneity of neurons within the region, which contains respiratory and non-respiratory neurons, there were no reliable distinguishing criteria for targeting. Smith and colleagues developed the approach of retrogradely labelling propriobulbar neurons with calcium-sensitive dyes to allow for real-time dynamic fluorescent imaging of neuronal activity, including those with pacemaker properties, within the preBötC (Koshiya and Smith, 1999). More recently, it has become apparent that immunohistochemical labelling for NK1R and SST in paraformaldehyde fixed tissue can help delineate respiratory neurons within the preBötC that are thought to play a critical role in respiratory rhythmogenesis (Gray et al., 1999; Gray et al., 2001; Pilowsky and Feldman, 2001; Guyenet et al., 2002; Stornetta, et al., 2003; Manzke et al., 2003). In this study, we provide a significant advancement by fluorescently tagging these neurons in viable, rhythmically active medullary slices.

SubP is a high affinity ligand for the G-protein coupled NK1R. Upon binding with NK1R, SubP recruits G-proteins to the receptor, which mediates an alteration of receptor distribution via internalization of the receptor-ligand complex followed by recycling of the receptor into cell membrane (Wang and Marvizon, 2002; Roosterman et al., 2004).

The SubP-induced internalization and recycling of NK1R has been well characterized (Roosterman et al., 2004; Wang and Marvizon, 2002). Several fluorochrome compounds conjugated to SubP have been developed (Bennett and Simmons, 2001; Turcatti et al., 1997). Our initial labelling experiments used the fluorochrome Oregon Green 488 conjugated with SubP. Despite the high specificity of binding with NK1R, the signal was unstable and bleached rapidly in living slices visualized with standard epifluorescence. TMR-SubP proved much more effective, providing a more intense, stable fluorescent signal. Moreover, comparing the pattern of TMR-SubP labelling with immunohistochemical labelling for NK1R receptors indicated that the fluorescent tag specifically labelled the entire complement of NK1R<sup>+</sup> neurons contained within the boundaries of the rhythmic slice.

The number of NK1R neurons within each bilateral preBötC has been estimated to be as few as 300 (Gray et al., 2001). Thus, the chances of patching onto those neurons without a means of precise targeting are very restricted. Granted, there has been considerable success in routinely obtaining recordings of respiratory neurons using 'blind' approaches. This has included recordings of neurons distributed within the ventrolateral medulla that demonstrate bursting properties in isolated preparations bathed in elevated extracellular potassium. However, the experimental approach described here allows one to target the specific population of NK1R<sup>+</sup> respiratory neurons within the preBötC that are hypothesized to be directly involved in rhythmogenesis; i.e. the population of neurons whose selective destruction in vivo with SubP-SAP causes breathing to stop (Gray et al., 2001). NK1R<sup>+</sup> neurons could be readily visualized and recorded using a standard IR-DIC microscope equipped for electrophysiology and epifluorescence. Moreover, visualization was achieved with a standard IR camera and monitor, and did not require elaborate image integration or processing. Data collected to date indicate that TMR-SubP labelled cells within the preBötC are a functionally heterogeneous population of neurons, a high percentage of which are active during the inspiratory cycle. Further, one quarter of those characterized in detail had properties consistent with pacemaker neurons and thus provides the first definitive evidence that bursting pacemaker neurons in preBötC have the NK1 receptor phenotype. The fluorescent tagging of neurons will also facilitate characterization of the molecular

properties that define their ontogenic and functional properties by allowing more precise neuronal targeting for single-cell RT-PCR or the collection of mRNA from multiple NK1R<sup>+</sup> neurons using laser-capture technologies. It may also prove advantageous to combine TMR-SubP labeling with the use of voltage- and calcium-sensitive dyes to examine population specific oscillatory behavior.

In summary, tagging of NK1R<sup>+</sup> neurons within the preBötC via internalization of TMR-SubP will accelerate acquisition of intracellular data (via conventional and perforated-patch whole cell recording) required for defining cellular and synaptic properties of the preBötC, and hasten progress toward understanding the processes underlying its role in the generation of respiratory rhythm.

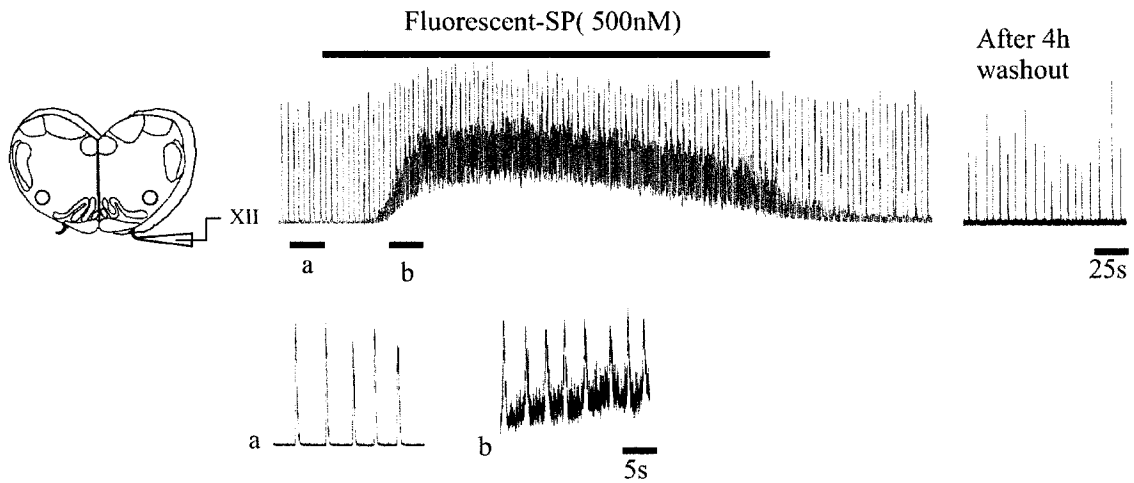


**Figure 4.1 Bath application of TMR-SubP (500 nM) reversibly increases the frequency of endogenous inspiratory-related bursts generated by medullary slice preparations.** Left panel depicts medullary slice. Right top panel shows rectified and integrated recordings of XII nerve activity from a P2 slice before, during and after bath application of TMR-SubP. Rhythmic activity persisted for at least 4 hours after application of TMR-SubP. Bottom traces show extended traces from times indicated by (a) and (b) in upper trace (i.e. prior to and during application of TMR-SubP).

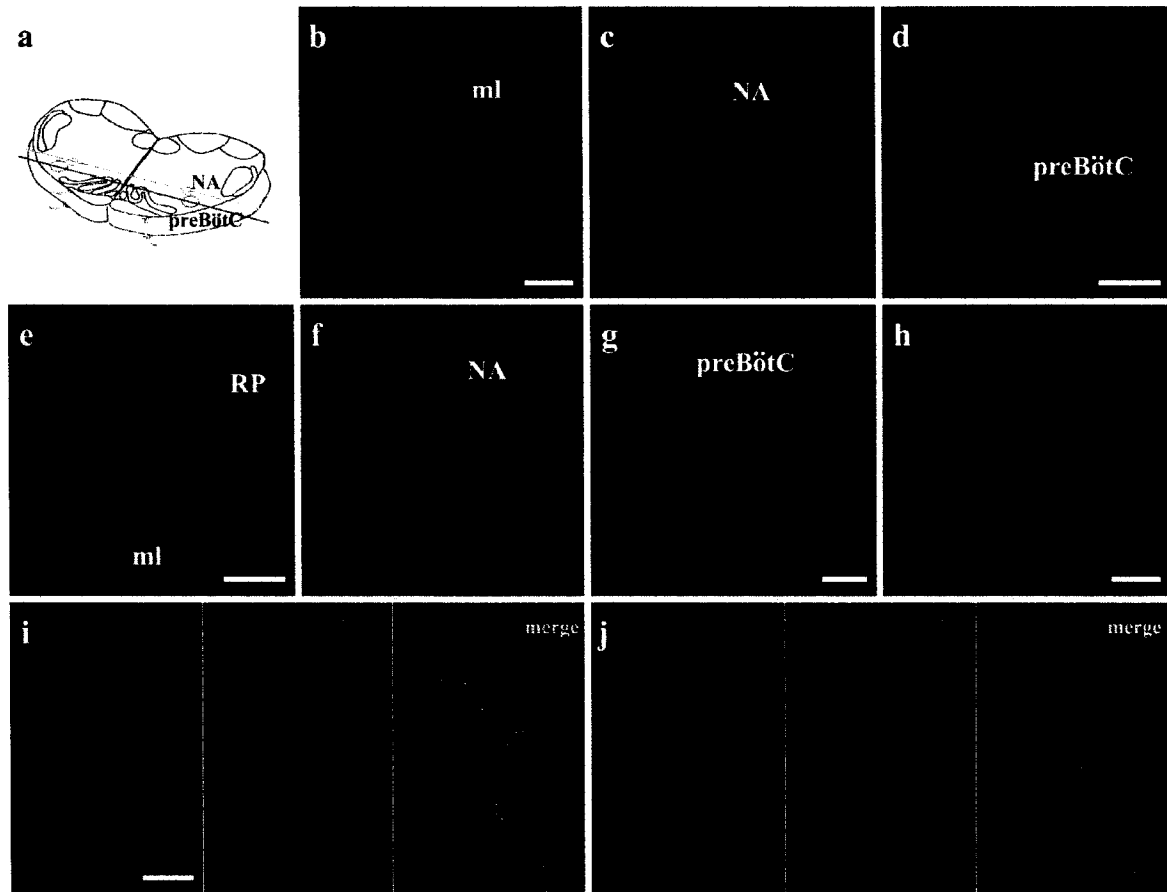


**Figure 4.2 Internalization of TMR-SubP in medullary slice preparations.** (a) Schematic drawing of medullary slices used for TMR-SubP internalization experiments. The green and red lines delineate the coronal plane from which images **b,c** (green) and **d** (red) were taken. (**b-d**) TMR-SubP internalization along the coronal plane at the midline (ml; **b**), more laterally at the nucleus ambiguus (NA; **c**) and more ventrolaterally at the preBötC (**d**). The upper part of the figures corresponds to the rostral surface of the slice. (**e-h**) TMR-SubP internalization in medullary slices along the transverse plane. A 5 min application of TMR-SubP (500 nM) results in robust internalization into neurons located in the midline, raphe pallidus (RP; **e**), nucleus ambiguus (**f**) and preBötC (**g,h**). (**i,j**) Colocalization of TMR-SubP fluorescence (red) and NK1R immunolabelling (green) in preBötC neurons. Fine and punctate staining for both NK1R and TMR-SubP is present in preBötC neurons. Note the high level of colocalization (yellow puncta) in the cell body and dendrites of preBötC neurons. Scale Bars: (**b,c; d; e,f; g**) 50  $\mu\text{m}$ ; (**h; i,j**), 20  $\mu\text{m}$ .

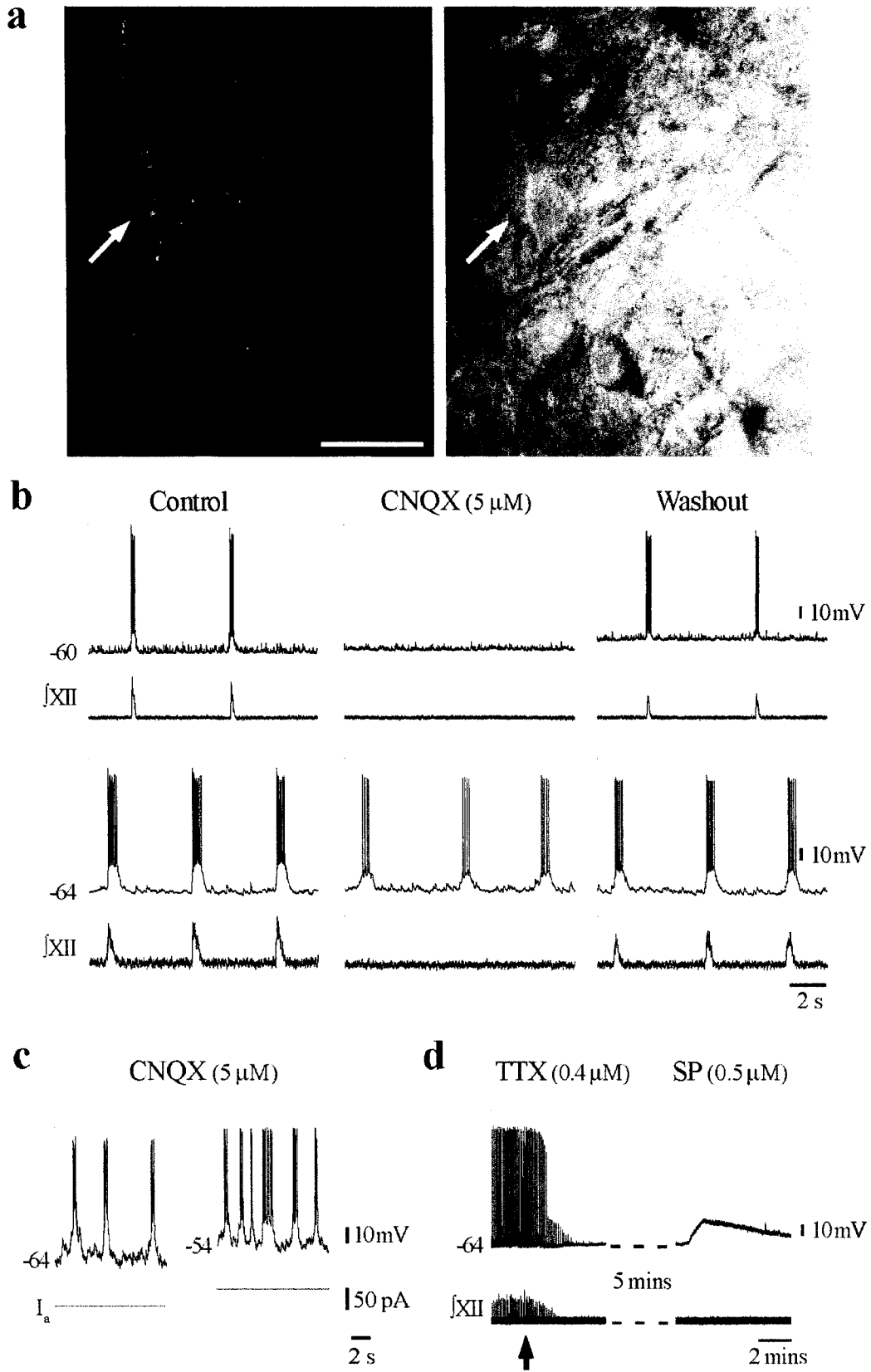


**Figure 4.3 Whole-cell recording from fluorescently tagged preBötC neurons.** (a) Fluorescent (left panel) and IR-DIC (right panel) image of a TMR-SubP labelled preBötC neuron (arrow). Note that only a subpopulation of preBötC neurons visible under IR-DIC are TMR-SubP<sup>+</sup>. Calibration bar, 25µm. (b) Whole-cell recording of membrane potential from two TMR-SubP positive neurons and simultaneous recording of integrated XII nerve inspiratory activity before, during and after block of rhythmic activity by bath application of CNQX. (c) Whole-cell recording from a TMR-SubP<sup>+</sup> neuron that bursts in a voltage-dependent manner in response to 37 pA depolarizing bias current injection ( $I_a$ ) after application of CNQX. (d) Whole-cell recording from a TMR-SubP<sup>+</sup>, CNQX-resistant, preBötC inspiratory neuron showing the membrane potential response evoked by local application of the NK1R agonist, [Sar<sup>9</sup>,Met(O<sub>2</sub>)<sup>11</sup>]-SP (500 nM) after block of rhythmic network activity by TTX (arrow indicates time of TTX application).

#### 4.4. REFERENCES

- Bennett VJ, Simmons MA (2001). Analysis of fluorescently labeled substance P analogs: binding, imaging and receptor activation. *BMC Chem Biol* 1(1), 1-12.
- Butera RJ, Rinzel J, Smith JC (1999). Models of respiratory rhythm generation in the pre-Bötzinger complex. I. Bursting pacemaker neurons. *J Neurophysiol* 82:382-97.
- Frermann D, Keller BU, Richter DW (1999). Calcium oscillations in rhythmically active respiratory neurones in the brainstem of the mouse. *J Physiol* 515:119-31.
- Gray PA, Rekling JC, Bocchiaro CM, Feldman JL (1999). Modulation of respiratory frequency by peptidergic input to rhythmogenic neurons in the pre-Bötzinger complex. *Science* 286:1566-8.
- Gray PA, Janczewski WA, Mellen N, McCrimmon DR, Feldman JL (2001). Normal breathing requires pre-Bötzinger complex neurokinin-1 receptor-expressing neurons. *Nat Neurosci* 4:927-30.
- Guyenet PG, Sevigny CP, Weston MC, Stornetta RL (2002). Neurokinin-1 receptor-expressing cells of the ventral respiratory group are functionally heterogeneous and predominantly glutamatergic. *J Neurosci* 22:3806-16.
- Harrison S, Geppetti P (2001). Substance P. *Int. J Biochem Cell Biol* 33(6):555-76.
- Horie M, Miyashita T, Watabe K, Takeda Y, Kawamura K, Kawano H. (2000). Immunohistochemical localization of substance P receptors in the midline glia of the developing rat medulla oblongata with special reference to the formation of raphe nuclei. *Brain Res Dev Brain Res* 121(2):197-207.
- Johnson SM, Smith JC, Funk GD, Feldman JL. (1994). Pacemaker behavior of respiratory neurons in medullary slices from neonatal rat. *J Neurophysiol* 72(6):2598-608.
- Johnson SM, Smith JC, Feldman JL (1996). Modulation of respiratory rhythm in vitro: role of Gi/o protein-mediated mechanisms. *J Appl Physiol* 80(6):2120-33.
- Koshiya N, Smith JC (1999). Neuronal pacemaker for breathing visualized in vitro. *Nature* 400(6742):360-3.

- Liu Q, Wong-Riley MT (2002). Postnatal expression of neurotransmitters, receptors, and cytochrome oxidase in the rat pre-Botzinger complex. *J Appl Physiol* 92(3):923-34.
- Mantyh PW (2002). Neurobiology of substance P and the NK1 receptor. *J Clin Psychiatry* 63 Suppl 11:6-10.
- Manzke T, Guenther U, Ponimaskin EG, Haller M, Dutschmann M, Schwarzacher S, Richter DW (2003). 5-HT<sub>4</sub>(a) receptors avert opioid-induced breathing depression without loss of analgesia. *Science* 301(5630):226-9.
- Murakoshi T, Suzue T, Tamai S (1985). A pharmacological study on respiratory rhythm in the isolated brainstem-spinal cord preparation of the newborn rat. *Br J Pharmacol.* 86(1):95-104.
- Onimaru H, Homma I (2003). A novel functional neuron group for respiratory rhythm generation in the ventral medulla. *J Neurosci* 23:1478-86.
- Pagliardini S, Ren J, Greer JJ (2003). Ontogeny of the pre-Botzinger complex in perinatal rats. *J Neurosci* 23:9575-84.
- Pilowsky PM, Feldman JL (2001). Identifying neurons in the pre-Bötzing complex that generate respiratory rhythm: visualizing the ghost in the machine. *J Comp Neurol* 434:125-7.
- Rekling JC, Feldman JL. (1998). Pre-Bötzing complex and pacemaker neurons: hypothesized site and kernel for respiratory rhythm generation. *Annu Rev Physiol* 60:385-405.
- Roosterman D, Cottrell GS, Schmidlin F, Steinhoff M, Bunnett NW (2004). Recycling and resensitization of the neurokinin 1 receptor. Influence of agonist concentration and Rab GTPases. *J Biol Chem* 279(29), 30670-9.
- Smith JC, Liu G, Feldman JL (1988). Intracellular recording from phrenic motoneurons receiving respiratory drive in vitro. *Neurosci Lett* 88, 27-32.
- Smith JC, Ellenberger HH, Ballanyi K, Richter DW, Feldman JL (1991). Pre-Bötzing complex: a brainstem region that may generate respiratory rhythm in mammals. *Science* 254(5032):726-9.
- Smith JC, Ballanyi K, Richter DW (1992). Whole-cell patch-clamp recordings from respiratory neurons in neonatal rat brainstem in vitro. *Neurosci Lett.* 134:153-6.

- Smith JC, Butera RJ, Koshiya N, Del Negro C, Wilson CG, Johnson SM (2000). Respiratory rhythm generation in neonatal and adult mammals: the hybrid pacemaker-network model. *Respir Physiol* 122:131-47.
- Stornetta RL, Rosin DL, Wang H, Sevigny CP, Weston MC, Guyenet PG (2003). A group of glutamatergic interneurons expressing high levels of both neurokinin-1 receptors and somatostatin identifies the region of the pre-Bötzinger complex. *J Comp Neurol* 455:499-512.
- Stuart GJ, Dodt HU, Sakmann B. (1993). Patch-clamp recording from the soma and dendrites of neurons in brain slices using infra-red video microscopy. *Pflugers Arch* 423:511-8.
- Suzue T (1984). Respiratory rhythm generation in the in vitro brain stem-spinal cord preparation of the neonatal rat. *J Physiol* 354:173-83.
- Turcatti G, Zoffmann S, Lowe JA 3rd, Drozda SE, Chassaing G, Schwartz TW, Chollet A. (1997). Characterization of non-peptide antagonist and peptide agonist binding sites of the NK1 receptor with fluorescent ligands. *J Biol Chem* 272(34):21167-75.
- Wang X, Marvizon JC (2002). Time-course of the internalization and recycling of neurokinin 1 receptors in rat dorsal horn neurons. *Brain Res.* 944(1-2), 239-47.
- Yamamoto Y, Onimaru H, Homma I (1992). Effect of substance P on respiratory rhythm and pre-inspiratory neurons in the ventrolateral structure of rostral medulla oblongata: an in vitro study. *Brain Res* 599(2):272-6.

## CHAPTER V

### Role of Lbx1 in the formation of relay somatic sensory neurons in the developing medulla

---

The results published in this Chapter will be further elaborated on in order to submit possibly two manuscripts for publication, one on the expression of Lbx1 and the development of the medulla in *Lbx1*<sup>GFP/+</sup> and *Lbx1*<sup>GFP/GFP</sup> mice and another one, in combination with further electrophysiological recording experiments, on the respiratory defects in *Lbx1*<sup>GFP/GFP</sup> mice. Electrophysiological data provided on this chapter were performed by Dr. J. Ren. My contribution consisted in the planning and conducting the anatomical study in the *Lbx1*<sup>GFP/+</sup> and *Lbx1*<sup>GFP/GFP</sup> mice.

## 5.1 INTRODUCTION

In the developing central nervous system, the sequence of activation and inactivation of many transcription factors is fundamental for driving the early stages of neuronal development. This includes the early patterning of the nervous system, later stages of proliferation, neuronal differentiation, cell fate specification and lastly the settlement within a network and the acquisition of a specific neuronal phenotype. Data regarding combinatorial codes that specify and determine the identity of hindbrain neurons is limited in comparison to the large amount of experimental evidence obtained on spinal cord development (see Chapter I; reviewed in Shirasaki and Pfaff, 2002; Goulding and Pfaff, 2005). It is only in the past few years that a mapping of genes expressed at the level of different nuclei of the hindbrain has been actively pursued (reviewed Chatonnet et al., 2003; Wallen and Perlmann, 2003; Borday et al., 2004; Melton et al., 2004).

The medulla is an important centre for the generation and integration of processes related with autonomic behaviours of the cardiovascular, enteric and respiratory systems. It is also an important relay station for proprioceptive, nociceptive and visceral sensory processing information of the cranial nerve and contains several somatic, visceral and special motoneuronal groups controlling muscles in the face and upper trunk. In addition, there are a large number of ascending and descending axonal tracts running through the medulla that allow for information processing to and from supramedullary structures.

It is generally agreed that neuronal precursors in the brainstem develop in a pattern similar to the spinal cord, although the highly specialized functions of special sensory and motor structures require a more complex developmental program. In general, the ventral most part of the neuroepithelium, the basal plate, gives origin to the motor nuclei of the cranial nerves, whereas the alar plate, the dorsal portion of the neuroepithelium, gives origin to the sensory relay nuclei. From the alar plate, general somatic afferent (proprioceptive and nociceptive) and visceral afferent cell columns originate and develop into the Cn/Gr and spinal trigeminal (SpV) and the solitary tract (Stn) nuclei, respectively. In addition, from the dorsal most region of the alar plate, the IO formation is generated and migrates ventromedially along the submarginal stream to its

final destination. The special somatic afferent cells that constitute the vestibular (Ve) nucleus remain in the dorsal medulla.

In this study, we examined the potential role of the homeodomain transcription factor *Lbx1*, the vertebrate homologue of the *Drosophila ladybird* gene (Jagla et al., 1995; Dietrich et al., 1998) on the development of the mouse medulla. *Lbx1* is expressed caudal to r1 in postmitotic neurons of the alar plate in the hindbrain and spinal cord in mice and chicks (Jagla et al., 1995; Schubert et al., 2001). A subset of dorsal interneurons in the spinal cord, dI4-dI6 and dII<sub>A-B</sub>, are dependent on *Lbx1* for their specification and their neuronal identity (Gross et al., 2002; Muller et al., 2002). *Lbx1*<sup>+</sup> neurons later settle in the superficial laminae of the dorsal horn and become somatosensory association interneurons. The inactivation of *Lbx1* alters the developmental program resulting in *Lbx1* deficient spinal neurons acquiring a more dorsally derived commissural interneuron phenotype (Gross et al., 2002; Muller et al., 2002).

A recent report has also provided further evidence for the molecular mechanisms that regulate the neuronal phenotype in the *Lbx1*<sup>+</sup> spinal neurons. *Lbx1* is expressed in both excitatory glutamatergic and inhibitory GABAergic neurons in the embryonic spinal cord and *Lbx1* competes with the product of another homeobox gene, *Rnx/Tlx3*, to specify the GABAergic versus a glutamatergic neuronal phenotype (Cheng et al., 2005).

In this study we provide anatomical data on the expression of *Lbx1* in the developing medulla. We identified neuronal populations that depend on *Lbx1* for proper development and migration through embryonic gestation. We also show that in absence of *Lbx1*, proprioceptive and nociceptive sensory neurons in SpV and Cu/Gr nuclei acquire an abnormal phenotype and migratory pattern. In these regions, local inhibitory networks are disrupted and *Lbx1*<sup>-</sup> neurons partially acquire the identity of more dorsally generated general visceral relay neurons of the Stn. We also analyzed the respiratory related structures and their physiological properties in order to identify the defect responsible for respiratory deficiency at birth. The anatomy of the respiratory rhythm-generating centre, the preBötC, appears normal, although electrophysiological recordings in medullary slices show slow respiratory rhythmic activity and the presence of large amplitude ectopic bursts (non-respiratory related) originating from the XII nucleus. We

propose that respiratory defects within the medulla are the results of the abnormal networks within the dorsal medulla.

## 5.2 METHODS

### 5.2.1 GENERATION AND GENOTYPING OF *LBX1*<sup>GFP/GFP</sup> MICE

The generation of *Lbx1*<sup>GFP(neo)</sup> mice has been described previously (Gross et al., 2000). Identification of mutant offspring was performed by PCR genotyping of snap frozen tissue with the specific primers MKG396, CAGCTGCAGAAGCCAGGACTG; MKG321, CCGGACACGCTGAACTTGTGG; MKG333, ATGACTTCCAAGGAGGACGGCA). Amplification of mutant and wildtype *Lbx1* alleles generated diagnostic bands of 315 and 445 bp, respectively.

### 5.2.2 ANIMAL HANDLING

Timed pregnant mice at different gestational stages (E10 to E18) were anaesthetized with halothane (1.5% delivered in 95% O<sub>2</sub> and 5% CO<sub>2</sub>) and fetal mice were delivered and transcardially perfused with 4% paraformaldehyde in phosphate buffer (PB) at pH 7.2. Brainstems were dissected and post-fixed in the same fixative prior to embedding in agar and sectioning with a vibratome (VT1000S; Leica, Wetzlar, Germany). All procedures used in this study were approved by the Animal Welfare Committee at the University of Alberta.

### 5.2.3 IMMUNOHISTOCHEMISTRY

Mutant and wild-type mice within the same litter were processed together for comparisons. Transverse sections (50 μm) were serially collected in PBS and immunoreacted according to the following protocol. Sections were incubated with 1.0% BSA (Sigma) and 0.2-0.3% Triton X-100 in PBS for 60 minutes to reduce non-specific staining and to increase antibody penetration. Sections were incubated overnight with primary antibodies diluted in PBS containing 0.1% BSA and 0.2-0.3% Triton X-100. The following day, sections were washed in PBS and incubated with specific secondary antibodies diluted in PBS and 0.1% BSA for 2 hours (biotin-, Cy3-, Cy5 or Cy2-

conjugated DAR, DAG, DAR<sub>T</sub>, DAM; 1:200; all purchased from Jackson ImmunoResearch). Sections were further washed in PBS and those immunoreacted with fluorescent conjugated secondary antibodies were mounted and coverslipped with Fluorsave mounting medium (Calbiochem). When biotin conjugated secondary antibodies were used, sections were labelled using a peroxidase method. After washes in PBS, sections were incubated with peroxidase-conjugated ABC kit (1:100, Vector Laboratories) for a further 2 hours. The reaction was detected with 0.08% DAB and 0.007% H<sub>2</sub>O<sub>2</sub> in Tris-HCl buffer.

Primary antibodies used for this study were as follows; rabbit anti-GFP (1:500, Molecular Probes), chicken anti-green fluorescent protein (GFP) (1:500, Aves Labs, Tigard, OR), rabbit anti-neurofilament (NF)(1:2000, Chemicon, Temecula, CA), mouse anti-microtubule associated protein2 (MAP2, 1:2000, Sternberger Monoclonal Inc./Covance Research, Berkley, CA), rabbit anti-NK1R 1:1000, Advance Targeting System, San Diego, CA), goat anti-ChAT (1:300, Chemicon), rabbit anti-TH (1:2000, Chemicon), goat anti-5HT (1:1000, Chemicon), rabbit anti-SST (1:1000, Immunostar, Hudson, WI), rabbit anti-CR (1:2000, Chemicon), goat anti-CR (1:2000, Chemicon), rabbit anti-CB, (1:2000, Chemicon), rabbit anti-pax2 (PAX2, 1:500, Zymed Labs/Invitrogen, Burlington, ON), rabbit anti-FoxP2 (1:700, kindly provided by Dr.P.A.Gray), goat anti-Lmx1b (1:500, kindly provided by Dr.P.A.Gray), rabbit anti-Phox2b (1:500, kindly provided by Dr. J.F.Brunet).

#### **5.2.4 BRIGHT FIELD AND CONFOCAL IMAGING**

DAB-immunostained sections were analyzed with an Olympus BX40 microscope and images taken with a SPOTdigital Microscope camera (Carsen) connected to a computer running Image-Pro-Plus software (Media Cybernetics Inc). Acquired images were exported in TIFF format and brightness and contrast adjusted in Adobe Photoshop 7.0. Immunostained sections were examined and processed using a Zeiss100M microscope, LSM510 NLO laser and LSM510 software. For Cy2, Cy3 and Cy5 fluorescence, excitation was set to 488, 543 and 633 nm and emissions were collected with 505, 560 and 630 nm long-pass filters, respectively. Thin sections and multiple

sectioning acquisitions along the z-plane were performed to obtain a suitable signal through the depth of the section. Acquired images in JPEG format were then exported to Photoshop 7 for and brightness and contrast adjustment.

Measurements of areas of the spinal trigeminal tract (E18) and the extension of FoxP2<sup>+</sup> cells in the submarginal stream (E10-11) and MN pools (E18) were obtained from confocal acquired images. Surface areas of vagus, ambiguus and hypoglossal nuclei were measured bilaterally for each section and an average area was calculated for each animal using LSM510 software. For MN pools of E18 brainstems, a cell count was also performed and an average cell density determined for each pool. Nor/adrenergic cells immunolabeled for TH were counted in serial sections at E18 and an average of cells/nucleus calculated. Paired t-tests comparing *Lbx1*<sup>GFP/GFP</sup> mice to *Lbx1*<sup>GFP/+</sup> litter mates were applied to determine statistical significance at p<0.05.

## **5.2.5 IN VITRO EMBRYONIC MOUSE PREPARATIONS**

### **5.2.5.1 BRAINSTEM- SPINAL CORD- DIAPHRAGM PREPARATIONS**

Newborn pups (within 15 minutes of birth) were anesthetized with metofane. Fetuses (E18.5) were delivered from timed-pregnant mice anaesthetized with halothane (1.25-1.5% delivered in 95%O<sub>2</sub> and 5%CO<sub>2</sub>) and maintained at 37°C by radiant heat. The timing of pregnancies was determined from the appearance of sperm plugs in the breeding cages. New born pups and embryos were decerebrated and the brain stem-spinal cord with the diaphragm muscle attached was dissected following procedures similar to those established for perinatal rats (Smith et al., 1990; Greer et al., 1992). The neuraxis was continuously perfused at 27±1°C (perfusion rate 5 ml/minute, chamber volume of 1.5 ml) with Kreb's solution that contained (mM): 128 NaCl, 3.0 KCl, 1.5 CaCl<sub>2</sub>, 1.0 MgSO<sub>4</sub>, 24 NaHCO<sub>3</sub>, 0.5 NaH<sub>2</sub>PO<sub>4</sub>, and 30 D-glucose equilibrated with 95%O<sub>2</sub> - 5%CO<sub>2</sub> at 27° C (pH=7.4).

### **5.2.5.2 MEDULLARY SLICE PREPARATIONS**

Details of the preparation have been previously described (Smith et al. 1991). Briefly, the brain stem-spinal cords isolated from fetal mice were pinned down, ventral surface upward, on a paraffin-coated block mounted in a vibratome bath (Leica, VT1000S). The brain stem was sectioned serially in the transverse plane starting from the rostral medulla to within ~150  $\mu\text{m}$  of the rostral boundary of the preBötC, as judged by the appearance of the inferior olive. A single transverse slice containing the preBötC and more caudal reticular formation regions was then cut (400-500  $\mu\text{m}$  thick), transferred to a recording chamber and pinned down onto a Sylgard elastomer. The medullary slice was continuously perfused in physiological solution similar to that used for the brain stem-spinal cord preparation except for the potassium concentration, which was increased to 9 mM to depolarize neurons and thus stimulate the spontaneous rhythmic respiratory motor discharge (Smith et al. 1991).

### **5.2.6 RECORDING AND ANALYSIS**

Recordings of XII cranial nerve roots, C4 ventral roots, diaphragm EMG and neuronal population discharge within the ventrolateral medulla were made with suction electrodes. Signals were amplified, rectified, low-passed filtered and recorded on computer using an analog-digital converter (Digidata 1200, Axon Instruments) and data acquisition software (Axoscope, Axon Instruments). Mean values relative to control for the period of respiratory motoneuron discharge were calculated. Values given are means and standard deviations. Statistical significance was tested using paired difference student's t test; significance was accepted at P values lower than 0.05.

## 5.3 RESULTS

### 5.3.1 LBX1 EXPRESSION IN THE PRENATAL MEDULLA

The cytoarchitecture of *Lbx1*<sup>GFP/+</sup> mice, as revealed by thionin staining (data not shown), was similar to wild type mice. This is consistent with data from previous studies showing that the expression of one copy of *Lbx1* gene is sufficient to promote normal embryonic development (Gross et al., 2002; Muller et al., 2002). Thus, we compared the development of heterozygotes and null mice. *Lbx1* expression was visualized by analysis of GFP expression prior to birth (E18) in both heterozygotes (*Lbx1*<sup>GFP/+</sup>) and null (*Lbx1*<sup>GFP/GFP</sup>) mice. Immunohistochemical detection of GFP with a specific antibody improved the resolution for the detection of *GFP* expressing cells (Gross et al., 2002)).

In *Lbx1*<sup>GFP/+</sup> mice (Fig 5.1), *Lbx1/GFP* expression was prominent in the different subregions of the SpV (caudalis, interpolaris and the pontine oralis subnuclei) and Cn/Gr nuclei. In SpV, the caudally located subnucleus caudalis had strong GFP<sup>+</sup> expressing cells in the internal layers, likely corresponding to the stratum gelatinosum (layer II and III). More rostrally, in the nucleus interpolaris and oralis, where lamination does not occur, *Lbx1/GFP*<sup>+</sup> cells were evenly distributed within the subnuclei.

Scattered GFP<sup>+</sup> cells were also located within the area postrema (AP), Stn and in both ventral (MdV) and dorsal (MdD) medullary reticular formation. In particular, a cluster of GFP<sup>+</sup> cells was located within the ventral respiratory column in the region extending from the lateral reticular nucleus to the VII nucleus (Fig 5.1, top panel, arrowheads). More rostrally, GFP<sup>+</sup> cells were present in the pontine extension of the SpV (nucleus oralis), in the adjacent parvicellular reticular (PR) formation, the gigantocellular reticular nucleus and in the Ve.

The cytoarchitecture of *Lbx1*<sup>GFP/GFP</sup> expressing neuronal structures was severely disrupted at E18. In particular, the SpV was not organized in a layered C shaped pattern but rather arranged in densely packed groups of GFP<sup>+</sup> cells in the dorsolateral medulla (open arrowheads, Fig 5.1, bottom panel). Further, the cytoarchitecture of Gr/Cn and Stn was highly perturbed with GFP<sup>+</sup> cells within the nuclei being densely packed in a band of cells ventrolateral to the Cn and dorsal to the Stn rather than being interspersed. The

abnormal development of the dorsolateral medulla made it difficult to clearly differentiate the SpV nuclei from the dorsal medullary nuclei (Gr/Cn and external cuneate nucleus, Ecn) and Stn. In the ventral medulla, GFP<sup>+</sup> cell numbers were reduced through the extension of the ventral respiratory column (Fig 5.1, bottom panel, arrowheads). Inferior olive (IO) neurons in both *Lbx1*<sup>GFP/+</sup> and *Lbx1*<sup>GFP/GFP</sup> mice were not GFP<sup>+</sup>, although the cytoarchitecture of the olive appeared enlarged in the *Lbx1*<sup>GFP/GFP</sup> mice.

### 5.3.2 LBX1 EXPRESSION IN THE MEDULLA OF MICE DURING DEVELOPMENT

We analyzed expression of *Lbx1/GFP* in the brainstem of developing heterozygotes and null animals at different embryonic ages. Previous studies reported that expression of *Lbx1* in the dorsal spinal cord and hindbrain was detected in a single column of cells as early as E10 (Jagla et al., 1995). As previously reported, *Lbx1/GFP* expression in the E10 medulla was present in a column in the mantle layer (postmitotic neurons) adjacent to the sulcus limitans in *Lbx1*<sup>GFP/+</sup> mice throughout the rostrocaudal extent of the brainstem and spinal cord (Fig 5.2). At E11, the band of GFP<sup>+</sup> cells in the medulla of *Lbx1*<sup>GFP/+</sup> mice was enlarged and postmitotic neurons started migrating laterally and ventrally (data not shown). At E12, the newly generated GFP<sup>+</sup> cells were partially distributed within the dorsal medulla; a large number of GFP<sup>+</sup> cells were already migrating toward the lateral medulla to populate the presumptive region of the SpV nucleus. The ventral most portion of migrating GFP<sup>+</sup> cells was directed ventrally, running laterally to the differentiating MNs of XII and X nuclei. At E12, several contralateral fibres were detected all along the rostrocaudal extension of the brainstem.

At E14, GFP<sup>+</sup> cells in *Lbx1*<sup>GFP/+</sup> mice were located in a large band corresponding to the putative region of the SpV. Further, GFP<sup>+</sup> cells were present in the developing dorsal medulla, in the presumptive region of Stn, Cn and Gr nuclei. In the reticular formation, contralateral GFP<sup>+</sup> fibres were still detectable along the rostrocaudal extent of the brainstem and several GFP<sup>+</sup> cells were present ventral and ventrolateral to the XII nucleus and in the ventrolateral medulla, adjacent to the NA (Fig 5.2, arrowheads).

In *Lbx1<sup>GFP/GFP</sup>* mice, *GFP* was expressed at early stages of development in a similar fashion; a narrow band of *GFP*<sup>+</sup> cells located in the mantle layer with an extension similar to the one reported for *Lbx1<sup>GFP/+</sup>* mice (E10, Fig.5.2). At E12, *GFP*<sup>+</sup> cells in *Lbx1<sup>GFP/GFP</sup>* mice were still present in the dorsal mantle zone of the medulla in a single band. The distribution of migrating cells towards the putative region of the SpV nucleus was severely disrupted. *GFP*<sup>+</sup> cells migrating towards the dorsolateral surface of the medulla were grouped in the ventral most region of the *GFP* domain. More dorsally, only a few *GFP*<sup>+</sup> cells were identified. More medially, the ventromedial migrating cells identified in *Lbx1<sup>GFP/+</sup>* mice were absent or extremely reduced in number (Fig5.2, arrowheads). At E14, the SpV, Stn and Gr/Cn nuclei were severely disrupted by the inactivation of *Lbx1* during neuronal development. *GFP*<sup>+</sup> cells appeared in clusters within the Stn. A dense bundle of longitudinally migrating *GFP*<sup>+</sup> fibres was present in the ventrolateral medulla. Controlateral *GFP*<sup>+</sup> fibres were still present in *Lbx1<sup>GFP/GFP</sup>* mice, but the numbers of *GFP*<sup>+</sup> cells in the ventrolateral medulla were markedly reduced.

### **5.3.3 CYTOARCHITECTONICAL ABNORMALITIES IN THE BRAINSTEM OF *LBX1<sup>GFP/GFP</sup>* MICE**

To further characterize the anatomical abnormalities in the medulla of *Lbx1<sup>GFP/GFP</sup>* mice, we looked at the general neuronal cytoarchitecture of axonal tracts and dendrites via expression of NF (fig. 5.3, A-D). In *Lbx1<sup>GFP/GFP</sup>* mice (E18), fibres of the ascending and descending tracts were misrouted. In particular, the areas in which *GFP*<sup>+</sup> cells were tightly grouped in the dorsolateral medulla were devoid of fibres (Fig. 5.3). In the putative region of SpV, incoming fibres from the trigeminal ganglion were bundled in the space between groups of *GFP*<sup>+</sup> cells. Overall, the cross sectional area occupied by fibres in the SpV tract along the medulla of *Lbx1<sup>GFP/GFP</sup>* mice was reduced by 50.7% ( $\pm$  11.1 SD, n=3). In contrast, along the surface of the ventral medulla, strong immunoreactivity for NF showed the presence of compact localization of longitudinally oriented fibres.

SpV is a relay station for sensory information regarding pain and temperature from the face and mouth primarily through the sensory afferents of the trigeminal

ganglion cells along the SpV tract (Phelan and Falls, 1991; Benarroch, 2006). An antibody directed against to SubP was used to study the distribution of a portion of the incoming trigeminal fibres in *Lbx1*<sup>GFP/+</sup> and *Lbx1*<sup>GFP/GFP</sup> mice (Fig 5.3, E-H). SubP<sup>+</sup> fibres in *Lbx1*<sup>GFP/+</sup> mice were distributed along the SpV tract and within the ventrolateral medulla. From the SpV tract, bundles of fibres penetrated the region of the caudal and interpolaris subnuclei of the SpV tract and made contacts with trigeminal neurons. In *Lbx1*<sup>GFP/GFP</sup> mice, the area occupied by SubP<sup>+</sup> fibres was limited to the dorsalmost region of the putative SpV. SubP immunolabeling also demonstrated that SubP<sup>+</sup> fibres in the ventral most part of the SpV tract and their extension was limited in the *Lbx1*<sup>GFP/GFP</sup> mice in comparison to *Lbx1*<sup>GFP/+</sup> mice. Interestingly, from the perspective of abnormal breathing patterns described below, the staining for SubP<sup>+</sup> fibres that generate the fine network within the ventrolateral medulla was also reduced in *Lbx1*<sup>GFP/GFP</sup> mice.

#### **5.3.4 LBX1 EXPRESSION IS NECESSARY FOR THE PROPER DEVELOPMENT OF DORSAL INTERNEURONAL POPULATION IN THE DEVELOPING HINDBRAIN**

We next analyzed the expression of specific markers for dorsal neuronal populations in the developing hindbrain (Fig 5.4) to determine if *Lbx1* was specifying neuronal identity and neurotransmitter phenotype as reported for the spinal cord. We initially looked at the expression of the paired box transcription factor *Pax2* and the LIM homeodomain-containing gene *Lmx1b* in *Lbx1*<sup>GFP/+</sup> and *Lbx1*<sup>GFP/GFP</sup> mice. It has been previously shown that *Pax2* is a transcription factor associated with the expression of a GABAergic phenotype in the cerebellum and dorsal horn of the spinal cord (Burrill et al., 1997; Maricich and Herrup, 1999; Cheng et al., 2004). *Lmx1b* is expressed specifically in serotonergic medullary neurons, dopaminergic midbrain neurons, in dI5 dorsal spinal cord interneurons and forebrain neurons with a glutamatergic phenotype (Gross et al., 2002; Cheng et al., 2003; Ding et al., 2003; Cheng et al., 2004).

In the spinal cord, the neuronal populations expressing *Lbx1* (dI4, dI5, dI6 and dIL<sub>A-B</sub>; (Gross et al., 2002) also express *Pax2* (dI4 and dI6, dIL<sub>A</sub>) or *Lmx1b* (dI5, dIL<sub>B</sub>) according to their differentiation program (Gross et al., 2002; Muller et al., 2002; Cheng

et al., 2004). We therefore investigated the expression pattern of these markers in the brainstem of *Lbx1<sup>GFP/+</sup>* mice from E10 to E13 (Fig 5.4, left panel). Similar to what reported in the spinal cord, in the early stages of development (E10-11; Fig 5.4 A,C,E) the dorsal most domain of GFP<sup>+</sup> neurons coexpressed *Pax2* (in the region corresponding to dI4 interneurons), the intermediate domain coexpressed GFP and *Lmx1b* (dI5 interneurons) and the most ventral domain of the GFP<sup>+</sup> cells expressed *Pax2* (dI6 interneurons). Dorsal to the *Lbx1*/GFP<sup>+</sup> domain, another group of cells was GFP<sup>-</sup>/Lmx1b<sup>+</sup>, likely corresponding to the dI3 domain (asterisk in Fig 5.4E), whereas ventral to the GFP<sup>+</sup> domain, a large band of GFP<sup>-</sup>/Pax2<sup>+</sup> cells corresponded to the V0-V1 populations of ventral interneurons (arrowhead in Fig 5.4E).

At E12, similar to what occurs in the spinal cord, but slightly delayed, a second wave of neurogenesis occurred. The extension of the GFP<sup>+</sup> domain was enlarged and GFP<sup>+</sup>/Pax2<sup>+</sup> (dIL<sub>A</sub>) and GFP<sup>+</sup>/Lmx1b<sup>+</sup> (dIL<sub>B</sub>) were intermingled in the mantle layer adjacent to the neuroepithelium, with apparently no colocalization (Fig 5.4G). At E12, the population of GFP<sup>+</sup> cells adjacent to the midline expressed *Pax2* and they likely correspond to migrating dI6 cells, whereas dI4 and dI5 population migrated towards the lateral medulla. Ventrally migrating dI3 Lmx1b<sup>+</sup>/GFP<sup>-</sup> were interspersed with the laterally migrating dI4 and dI5 neurons, whereas GFP<sup>-</sup>/Pax2<sup>+</sup> ventral interneurons migrated ventrally to populate the ventral reticular formation. Also, a group of GFP<sup>-</sup>/Lmx1b<sup>+</sup> cells corresponding to the serotonergic population of the raphe nuclei were grouped adjacent to the ventral midline.

At E13 the putative region of the SpV was rich in GFP<sup>+</sup>/Pax2<sup>+</sup> cells intermingled with GFP<sup>+</sup>/Lmx1b<sup>+</sup> cells. A dense network of GFP<sup>+</sup>/Lmx1b<sup>+</sup>, GFP<sup>-</sup>/Lmx1b<sup>+</sup> and GFP<sup>+</sup>/Pax2<sup>+</sup> populated the developing reticular formation more ventrally (data not shown).

We then extended our analysis to the *Lbx1<sup>GFP/GFP</sup>* mice (Fig 5.4 right panel). In the early stages of development (E10-11), we could still identify the expression of GFP in the dI4, dI5 and dI6 neurons located in the mantle layer adjacent to the neuroepithelium of the developing hindbrain. At this stage of development, *Lbx1<sup>GFP/GFP</sup>* mice presented a major defect in the dI4 neuronal population. GFP<sup>+</sup> cells were generated but they did not coexpress *Pax2*, which was instead expressed in both dI6 and ventral interneuronal

populations. Expression for *Lmx1b* was still strongly present in dI3, dI5 and serotonergic precursors at E10 and E11 (Fig 5.4 B,D,F).

At E12, the late-born GFP<sup>+</sup> neurons were mostly expressing *Lmx1b*, although the intensity of the staining appeared to be weaker than in the dorsally derived neurons and in the same neuronal population in the *Lbx1<sup>GFP/+</sup>* mice. The only newly generated GFP<sup>+</sup>/Pax2<sup>+</sup> cells were located in the ventral most region of the GFP domain. At this stage of development, the densely packed group of GFP<sup>+</sup> cells migrating out of the ventral most region of the GFP domain, likely generated in the previous days, expressed mainly *Lmx1b* (arrow in Fig 5.4F). GFP<sup>+</sup>/Pax2<sup>+</sup> cells were almost absent in the whole hindbrain: the GFP<sup>+</sup>/Pax2<sup>+</sup> population in the medial medulla of *Lbx1<sup>GFP/+</sup>* mice (open arrow in Fig 5.4 G,H) was absent and a limited number of GFP<sup>+</sup>/Pax2<sup>+</sup> cells were present in the developing SpV and in the reticular formation.

These results suggest that the absence of Lbx1 expression alters the development of the dI4-dI6 and dIL<sub>A-B</sub> interneurons in the developing hindbrain. Specifically dI4 interneurons do not express *Pax2*; therefore they likely lose their GABAergic phenotype. In later stages of development (E12-13) Pax2<sup>+</sup> dI6 and dIL<sub>A</sub> neurons are defective as well, since by this time there is an almost complete absence of GFP<sup>+</sup>/Pax2<sup>+</sup> neurons.

In E18 *Lbx1<sup>GFP/+</sup>* mice, Pax2<sup>+</sup> cells were located extensively in the SpV, in the Cn, Gr and Stn nuclei, in the region lateral to the XII nucleus and in different regions of the reticular formation (MdD, MdV and PR; Fig. 5.5). No differences between *Lbx1<sup>+/+</sup>* and *Lbx1<sup>GFP/+</sup>* in Pax2 expression were detected (data not shown). In *Lbx1<sup>GFP/+</sup>* mice GFP was partially coexpressed with *Pax2* in SpV, in Gr/Cn nuclei and in scattered cells within Stn and the ventrolateral medulla, ventral to the nucleus ambiguus. Pax2<sup>+</sup> neurons in the medulla of *Lbx1<sup>GFP/GFP</sup>* mice were almost absent in the region corresponding to SpV and in the Cn/Gr nuclei. Pax2<sup>+</sup> cells were still present in the region lateral to the XII and in the medial reticular formation (Fig 5.5). Only a few Pax2<sup>+</sup> cells in the SpV and in the Cn/Gr nuclei coexpressed GFP. In the ventrolateral medulla, GFP<sup>+</sup> cells positive for Pax2 were not detected, although GFP<sup>+</sup>/Pax2<sup>+</sup> cells were still present.

These results demonstrate that GFP<sup>+</sup>/Pax2<sup>+</sup> originating from dI4, dI6 and dIL<sub>A</sub> populate SpV, Stn, Cn/Gr and the ventrolateral medulla in later stages of development.

Birth-dating studies by means of injection of single pulses of BrdU at E10.5, 11.5, 12.5 and 13.5 showed that earlier generated cells (E10.5) populated the region of Stn/Cn/Gr. Later generated cells populate the region of SpV and part of Stn (data not shown).

These results suggest that in *Lbx1<sup>GFP/GFP</sup>* mice a major defect occurs in the specification of GABAergic GFP<sup>+</sup>/Pax2<sup>+</sup> neurons generated in the dorsal medulla. The GFP<sup>+</sup> cells generated lose their GABAergic phenotype and migrate in aberrant position in the dorsolateral medulla, disrupting the cytoarchitecture of SpV, Cn/Gr and Stn.

### 5.3.5 INACTIVATION OF LBX1 ALTERS THE DEVELOPMENTAL PROGRAM OF INFERIOR OLIVE FORMATION

We also analyzed the expression of *FoxP2* in the developing hindbrain of *Lbx1<sup>GFP/+</sup>* and *Lbx1<sup>GFP/GFP</sup>* mice. *FoxP2* is part of the winged-helix/forkhead (*Fox*) transcriptional repressor gene family. It is expressed in the cerebral cortex, basal ganglia, thalamus, IO formation, cerebellum and a subpopulation of ventral interneurons in the adult and developing mice (Shu et al., 2001; Ferland et al., 2003; Lai et al., 2003).

In *Lbx1<sup>GFP/+</sup>* mice, *FoxP2* is weakly expressed in the floor plate of E10 and E11 mice (data not shown). At E12, migrating neurons along the submarginal stream strongly express *FoxP2* (Fig 5.6A-F). The majority of the FoxP2<sup>+</sup> cells corresponds to the IO neurons migrating from the dorsal lip where they originate towards to the floor plate where they settle (Bourrat and Sotelo, 1990). Some of the FoxP2<sup>+</sup> cells interrupt their tangential migration within the reticular formation and settled in it, as shown by the presence of FoxP2 immunoreactivity at later stages of development (E13, E18 Fig 5.6 G-R). Interestingly, scattered FoxP2<sup>+</sup> cells were also present in the region below the domain of newly generated dI5/dI6 neurons (Fig 5.6,C). At E13 and 18, FoxP2 immunoreactivity was mainly detected at the level of IO, in the MdV, in the perihypoglossal nuclei, in gigantocellular reticular nucleus and PR and in Ve (Fig 5.6, M-O).

In *Lbx1<sup>GFP/GFP</sup>* mice, FoxP2 immunoreactivity at E10-11 is similar to *Lbx1<sup>GFP/+</sup>* mice. At E12 the extension of FoxP2<sup>+</sup> cells distributed along the submarginal stream was wider than in *Lbx1<sup>GFP/+</sup>* mice (Fig 5.6, D-F). Furthermore, several FoxP2<sup>+</sup> cells were scattered in the region below to the dIL<sub>A-B</sub> GFP<sup>+</sup> domain. The area occupied by FoxP2<sup>+</sup>

cells appeared to be increased in comparison to the same region in *Lbx1*<sup>GFP/+</sup> mice (+222.6% in serial sections analyzed from one fetus). The morphology of these nuclei was different between heterozygotes and null mice. In *Lbx1*<sup>GFP/+</sup> mice, FoxP2 neurons follow a tangential migratory pathway (Fig 5.6C). In *Lbx1*<sup>GFP/GFP</sup> mice, some nuclei were tangentially oriented, whereas others were radially oriented, indicating the presence of a radial migration from the dIL<sub>A-B</sub> domain towards the ventrolateral medulla (Fig 5.6, F). At E13, the extension of the average area occupied by FoxP2<sup>+</sup> cells in the developing IO formation of *Lbx1*<sup>GFP/GFP</sup> mice was increased in comparison to the area occupied by FoxP2<sup>+</sup> cells in the *Lbx1*<sup>GFP/+</sup> mice (+207 % in serial sections analyzed from one fetus). The group of FoxP2<sup>+</sup> cells abnormally extended dorsally towards the XII nucleus and rostrally up to the level of the VII nucleus (Fig 5.6, J-L).

At E18, *FoxP2* is still expressed in the IO formation, lateral to the XII nucleus, in scattered cells in the reticular formation and in Ve and in Ecn. The appearance of the IO formation is still abnormal and the FoxP2<sup>+</sup> cells are widely expressed in the different subnuclei of the IO. Again, olivary FoxP2<sup>+</sup> cells abnormally extended rostrally in the pons at the rostrocaudal level of the VII nucleus (Fig 5.6, P-R).

These results suggest that the IO is affected by the inactivation of *Lbx1* in the ventral dI4-dI6 domains. Specifically, some neurons generated from the GFP domain may acquire a dorsal domain phenotype (dI1 and/or dI2), loose GFP expression and start expressing *FoxP2*, contributing to the formation of IO formation enlargement.

### **5.3.6 INACTIVATION OF LBX1 ALTERS THE DEVELOPMENTAL PROGRAM OF THE SOLITARY TRACT NUCLEUS**

The absence of *Lbx1* altered the developmental program of the dorsal structures in the medulla including the Stn, which had structural abnormalities and lack of well-defined borders (Fig 5.3). We identified Stn neurons by means of expression of the homeobox transcription factor *Phox2b* (Fig. 5.8) which is widely expressed in the autonomic nervous system and in the visceral and branchial motor nuclei through development (Pattyn et al., 1997).

At E10 and E11, *Phox2b* was expressed in the hindbrain of *Lbx1<sup>GFP/+</sup>* mice, in two major locations, in the region corresponding to the developing MNs (VII, XII, X and NA; (Pattyn et al., 2000b) and in the region corresponding to dI3, which gives origin to the neurons of Stn and AP (Fig 5.7 (Pattyn et al., 2000a). At E11, dorsally migrating MNs of the dorsal motor nucleus of the vagus nerve (X) and ventrally migration NA MNs were distinguishable from the developing Stn neurons by their coexpression of ChAT (asterisks in Fig 5.7A,B). In *Lbx1<sup>GFP/GFP</sup>* mice, *Phox2b* was present not only in developing branchial and visceral MNs and Stn neurons but also in the central portion of the GFP domain, likely corresponding to dI5 (*Lmx1b<sup>+</sup>*, fig 5.4) precursors. At E12 and E13, there was no colocalization between *Phox2b* and *Lbx1/GFP* in *Lbx1<sup>GFP/+</sup>* mice and *Phox2b<sup>+</sup>* cells were intermingled with dIL<sub>B</sub> neurons while migrating ventrally towards the putative location of the Stn. In *Lbx1<sup>GFP/GFP</sup>* mice, there was a large amount of colocalization between GFP and *Phox2b*. *Phox2b<sup>+</sup>/GFP<sup>+</sup>* cells were located in the mantle layer (suggesting that they are generated directly from the GFP domain), adjacent to the GFP<sup>+</sup> domain and interspersed with *Phox2b<sup>+</sup>/GFP<sup>-</sup>* cells and in the ventral band of earlier generated neurons (Fig 5.7 G-I,K,L) that lacked *Pax2* expression and was also *Lmx1b<sup>+</sup>*(Fig 5.4).

In the hindbrain of E18 *Lbx1<sup>GFP/+</sup>* mice (Fig 5.8), *Phox2b* was strongly expressed in AP, Stn, X, compact formation of NA, VII nucleus, PR formation and in scattered cells of the ventrolateral medulla, likely corresponding to the A1/C1 catecholaminergic group. The only neurons that coexpressed *Lbx1/GFP* and *Phox2b* were localized in the dorsal portion of PR (Fig 5.8; asterisk, PR) within the Ve, likely the spinal Ve (arrowhead in Fig 5.8D).

In *Lbx1<sup>GFP/GFP</sup>* mice, *Phox2b* expression delineated similar neuronal structures (AP, Stn, A1/C1, X, NA, VII, PR). Surprisingly, *Phox2b* was also extensively expressed in the larger cluster of GFP<sup>+</sup> cells in the putative region of SpV (arrows, Fig 5.8) and in the PR nucleus. In addition, the large cluster of cells in the Ve was absent. These results suggest that part of the GFP domain of the *Lbx1<sup>GFP/GFP</sup>* mice switch to a different phenotype. In particular, a portion of the GFP domain acquires a phenotype that is similar to the more dorsally generated dI3 cells.

Intrigued by the abnormal coexpression of *Phox2b* and *GFP*, we further investigated this area by analyzing the expression of calcium binding proteins and catecholaminergic marker tyrosine hydroxylase (TH) in *Lbx1<sup>GFP/+</sup>* and *Lbx1<sup>GFP/GFP</sup>* mice. Calcium binding proteins calbindin (CB) and calretinin (CR) are expressed in different and partially overlapping interneuronal population through the brainstem (Celio, 1990; Arai et al., 1991; Resibois and Rogers, 1992; Crockett et al., 1996). At E18, CB was expressed in *Lbx1<sup>GFP/+</sup>* mice in neurons within several nuclei (Fig 5.9) including the medial Stn, scattered neurons within the Cn/Gr nuclei and the reticular formation, IO, fibres and neurons within the SpV (caudalis and interpolaris subnuclei), Ve nucleus and in a dense cluster of neurons in the ventrolateral border of the XII nucleus. Colocalization of CB with *Lbx1/GFP* was limited to scattered cells in the dorsal portion of SpV, nucleus caudalis (Fig 5.9, top).

In *Lbx1<sup>GFP/+</sup>* mice, CR was expressed in partially complementary structures in the brainstem. In particular, clusters of cells strongly immunoreactive for CR were present in the lateral Stn, lateral reticular formation medial to SpV (Fig 5.9I, asterisk), region lateral to the XII nucleus and in PR. Scattered CR<sup>+</sup> neurons were also present in Cn/Gr, SpV and along the midline and in the ventrolateral medulla below the NA. CR<sup>+</sup> fibres were present in the IO formation. Colocalization of CR with GFP occurred only in scattered cells within Cn/Gr nuclei and in neurons located in the ventrolateral medulla (Fig5.9K, arrow).

In *Lbx1<sup>GFP/GFP</sup>* mice, the distribution of CB<sup>+</sup> and CR<sup>+</sup> neurons was markedly affected. CB<sup>+</sup> and CR<sup>+</sup> neurons and fibres were still present in the region lateral to XII and in the IO formation in a pattern similar to *Lbx1<sup>GFP/+</sup>* mice. The extension of CB<sup>+</sup> neurons within the Stn was strikingly enlarged in *Lbx1<sup>GFP/GFP</sup>* mice and apparently overlapped the abnormal extension of *Phox2b*<sup>+</sup> neurons observed in fig 5.9 (compare Fig5.9,E-H with Fig 5.8,K-M). In this location, similar to *Phox2b*<sup>+</sup> cells, CB<sup>+</sup> cells also colocalized with GFP in the central portion of the GFP<sup>+</sup> cluster in the putative SpV.

CR expression in both cell bodies and fibres was reduced in *Lbx1<sup>GFP/GFP</sup>* mice: CR<sup>+</sup> neurons were largely absent from the ventrolateral medulla and the lateral reticular formation adjacent to SpV. These neurons corresponded to, and colocalized with (data not shown), the Pax2<sup>+</sup> cells observed in Fig 5.5. Densely packed and strongly coexpressing CR<sup>+</sup>/GFP<sup>+</sup> cells were clustered in the two dorsal most groups of GFP<sup>+</sup>

clusters in the dorsolateral medulla just below the putative region of the Cn/Gr nuclei and the rostral region of the Stn that strongly expresses *Phox2b* and CB.

These results suggest that a reorganization of the interneuronal population occurs in the dorsolateral medulla of *Lbx1<sup>GFP/GFP</sup>* mice and that there is an ectopic expression of Phox2b<sup>+</sup>/CB<sup>+</sup> neurons in the aberrant structures generated in absence of *Lbx1* expression. Further, CR<sup>+</sup> neurons in the ventrolateral medulla and in the lateral reticular formation are either misrouted to a different location (e.g. in the GFP<sup>+</sup> clusters) or fail to generate properly in *Lbx1<sup>GFP/GFP</sup>* mice.

We also observed abnormalities in the pattern of CR and CB expression in the early stages of development (E11-E14) (Fig 5.10). In particular, the expression of CR in the dorsal developing medulla was reduced at E10.5 (data not shown) and at E11.5 (Fig5.10, bottom) and by E13.5 the CR<sup>+</sup> neurons normally expressed in the dorsolateral medulla were completely absent in *Lbx1<sup>GFP/GFP</sup>* mice. In contrast, CB<sup>+</sup> cells were more numerous in the dorsal developing medulla of E11.5 and E13.5. Strongly expressing CB<sup>+</sup> longitudinal fibres were also present in the ventrolateral medulla.

We conclude that these early developmental abnormalities in CR<sup>+</sup> and CB<sup>+</sup> expressing neurons explain some later abnormalities observed at E18. Specifically, the early reduction in CR<sup>+</sup> dorsally generated neurons (dI4-dI6 and dILA-B domains) and increased number of dorsally generated CB<sup>+</sup> neurons lead to the later abnormalities of Pax2<sup>+</sup> and Phox2b<sup>+</sup> expressing cells, respectively.

Since *Phox2b* has a key role in the specification of catecholaminergic phenotype in central and peripheral nervous system (Pattyn et al., 2000a; Qian et al., 2001; Brunet and Pattyn, 2002; Dauger et al., 2003), we further investigated nor/adrenergic neurons in the brainstem of E18 *Lbx1<sup>GFP/+</sup>* and *Lbx1<sup>GFP/GFP</sup>* mice by means of expression of TH, an enzyme that is specifically expressed in dopaminergic and nor/adrenergic neurons and its synthesis is induced by Phox2a and Phox2b (reviewed in (Pattyn et al., 2000a; Brunet and Pattyn, 2002)). *Phox2* genes are expressed in the developing hindbrain in all nor/adrenergic groups (TH<sup>+</sup>/dopamine  $\beta$  hydroxylase<sup>+</sup>, DBH<sup>+</sup>), in branchial and visceral MNs (choline acetyl transferase, ChAT<sup>+</sup>), and other neurons that do not express either TH/DBH or ChAT (Tiveron et al., 1996; Pattyn et al., 1997).

When we examined the expression of ChAT in *Lbx1<sup>GFP/GFP</sup>* mice we could not detect any difference in size of various motoneuronal pools in the medulla (data not shown), suggesting that GFP<sup>+</sup>/Phox2b<sup>+</sup> neurons are not transformed in ventrally derived Phox2b<sup>+</sup>/ChAT<sup>+</sup> neurons.

TH was present in the medulla within the ventrolateral medulla in the A1/C1 group, in the ventral bundle and dorsally in A2 and in C2/C3 groups in both *Lbx1<sup>GFP/+</sup>* and *Lbx1<sup>GFP/GFP</sup>* mice. Further, we observed scattered TH<sup>+</sup> nuclei along the midline, in the rostral medulla. More rostrally, in the caudal pons, we also observed TH<sup>+</sup> staining in scattered cells around the VII nucleus (corresponding to the A5 region) and in the locus ceruleus (A6 neurons) (Fig 5.11).

Staining for TH appeared more intense in *Lbx1<sup>GFP/GFP</sup>* mice, although at E18 we did not observe any coexpression of GFP and TH. When we further counted the TH<sup>+</sup> neurons through the brainstem, we did not observe significant changes in number of TH<sup>+</sup> cells in the A2, C2/C3 region of the medulla, although the numbers of TH<sup>+</sup> cells in these regions were slightly increased (122%, n=6, and 154%, n=4 increase). Surprisingly, TH<sup>+</sup> cells in the ventrolateral medulla (A1/C1), in the ventrolateral pons (A5), within the reticular formation (ventral bundle, vb) and along the midline were significantly increased in *Lbx1<sup>GFP/GFP</sup>* mice: 158.1% ( $\pm$  15.9 SD; n=6), 222.8% ( $\pm$  63.7 SD; n=3), 246.5% ( $\pm$ 95.2 SD; n=5), 288.0% ( $\pm$  157.5 SD; n=4), respectively.

These results suggest that Phox2b abnormalities induce an abnormal number of TH<sup>+</sup> cells in E18 *Lbx1<sup>GFP/GFP</sup>* mice in the ventrolateral medulla and in the reticular formation, but the ectopic Phox2b<sup>+</sup>/CB<sup>+</sup>/GFP<sup>+</sup> formation does not acquire a nor/adrenergic phenotype.

### 5.3.7 ANALYSIS OF THE RESPIRATORY RHYTHM GENERATING PATTERN GENERATED BY $LBX1^{GFP/+}$ AND $LBX1^{GFP/GFP}$ MICE

The majority of recordings were performed from *in vitro* preparations isolated from E18.5 mice delivered via caesarian section. This negated any potentially confounding problems associated with measurements from mutant newborn mouse preparations that may have had altered CNS function due to the hypoxia associated with postnatal hypoventilation.

*Brainstem-spinal cord-diaphragm preparations:* Suction electrode recordings of inspiratory motor discharge were made from the diaphragm muscle and/or XII nerve roots in brainstem-spinal cord-diaphragm preparations isolated from each embryo delivered to screen for potential mutants (i.e. abnormal respiratory motor pattern). A total of 13 putative  $Lbx1^{GFP/GFP}$  mice and 12 putative wild-type mice were analysed. In each case, genotyping of tissue isolated from the preparations confirmed the identity of wild type and  $Lbx1^{GFP/GFP}$  mice.

Figure 5.12A,B shows simultaneous suction electrode recordings of XII nerve discharge and diaphragm EMG from brainstem-spinal cord-diaphragm preparations. Preparations derived from  $Lbx1^{GFP/GFP}$  mice generated a fairly regular rhythmic respiratory motor discharge, however the mean interburst intervals were markedly longer in duration ( $29.1 \pm 8.4$ s; n=8) compared to wild-type preparations ( $5.2 \pm 0.85$ s; n=6). Further, long duration, non-respiratory bursts were occasionally observed.

The potassium concentration in the medium bathing  $Lbx1^{GFP/GFP}$  mice preparations was increased from 3 mM to 6 mM  $K^+$  to provide added excitatory drive (data not shown). Under the conditions of elevated potassium, the frequency of respiratory rhythmic bursting increased approximately two-fold, but remained significantly slower than wild-type preparations bathed in Kreb's solution containing physiological levels of extracellular  $K^+$  (3 mM). Further, the elevated potassium induced the increased production of non-respiratory bursting discharge patterns in  $Lbx1^{GFP/GFP}$  mice preparations.

*Medullary slice preparations:* Figure.5.12C,D shows recordings from the hypoglossal nerve and preBötC in medullary slice preparations isolated from  $Lbx1^{GFP/GFP}$

mice and wild type mice. A similar phenotype to that observed with brainstem-spinal cord-diaphragm preparations was observed in all 9 mutant preparations. The rhythmic neuronal discharge was regular, but the frequency of rhythmic bursting was significantly slower than in wild-type preparations. Further, there was a much higher prevalence of non-respiratory rhythmic bursting in medullary slices prepared from *Lbx1*<sup>GFP/GFP</sup> mice compared to control. The abnormal rhythmic discharge was observed in recordings of neurons within the preBötC, indicating that the defect originated within the respiratory rhythm generating centre, rather than simply reflecting a failure of transmission of inspiratory drive to motoneuron populations.

### **5.3.8 STRUCTURAL ANALYSIS OF THE RESPIRATORY RHYTHM GENERATING CENTRE IN THE MEDULLA OF *LBX1*<sup>GFP/+</sup> AND *LBX1*<sup>GFP/GFP</sup> MICE**

In order to investigate the possible neuroanatomical abnormalities that may explain respiratory defects in *Lbx1*<sup>GFP/GFP</sup> mice, we studied the expression of different neuronal markers within the medulla of *Lbx1*<sup>GFP/GFP</sup> and *Lbx1*<sup>GFP/+</sup> mice at E18 (Fig 5.13). ChAT identified the cholinergic neuronal pools of the NA, XII, VII and X nuclei. In *Lbx1*<sup>GFP/GFP</sup> mice the size and density of MNs in the nuclei was not affected, but the ventral MN pools (NA and VII nuclei) were shifted to a more dorsolateral position due to the presence of an increased amount of fibres within the ventral medulla and the abnormalities within the dorsal medulla.

NK1R and SST immunoreactivity in the ventrolateral medulla identifies the region of the preBötC (Gray et al., 1999; Guyenet et al., 2002; Pagliardini et al., 2003; Stornetta et al., 2003). The immunolabeling for NK1R and SST showed that preBötC was shifted in a more dorsolateral position, further away from the ventral surface of the medulla due to the aberrant migration of GFP<sup>+</sup> cells and fibres (Fig 5. 13). We also noticed that NK1R<sup>+</sup> and SST<sup>+</sup> cells in the preBötC area did not express GFP in either *Lbx1*<sup>GFP/+</sup> or *Lbx1*<sup>GFP/GFP</sup> mice. Interestingly, NK1R<sup>+</sup> cells were intermingled with GFP<sup>+</sup> cells in the ventrolateral medulla of *Lbx1*<sup>GFP/+</sup> mice and GFP<sup>+</sup> cells were consistently reduced through the ventrolateral medulla of *Lbx1*<sup>GFP/GFP</sup> mice, in particular at the level

of both preBötC and BötC. A further investigation of the phenotype of the GFP<sup>+</sup> cells located in the ventrolateral medulla showed that they were the previously identified Pax2<sup>+</sup> GABAergic/CR<sup>+</sup>/GFP<sup>+</sup> neurons in *Lbx1*<sup>GFP/+</sup> mice (Figs 5.5, 5.8 and 5.9).

These results suggest that the preBötC is likely normally developed in the *Lbx1*<sup>GFP/+</sup> mice, but several inhibitory, dorsally derived, cells in the preBötC and BötC regions are missing from the ventrolateral medulla. If these neurons have a functional role in respiratory rhythm modulation, is not known.

Raphe nuclei provide an important tonic modulation to the respiratory rhythm structures in the brainstem and spinal cord (Ellenberger and Feldman, 1994; Al-Zubaidy et al., 1996; Schwarzacher et al., 2002). Immunostaining for 5HT, that identifies the majority of raphe nuclei cells did not show any abnormality in the number and distribution of serotonergic neurons of the raphe nuclei (data not shown), supporting the data obtained with *Lmx1b* staining in the early stages of development (Fig 5.4). Interestingly TH<sup>+</sup> staining showed an aberrant number of nor/adrenergic cells in the ventral pons and medulla (A5 and A1/C1 neurons).

## 5.4 DISCUSSION

The aim of this study was to analyse *Lbx1* expression pattern during hindbrain development, determine the phenotype of *Lbx1*<sup>+</sup> neurons, elucidate the influence of *Lbx1* on brainstem development and the possible mechanisms involved in the early post-natal death caused by respiratory distress in *Lbx1*<sup>GFP/GFP</sup> mice. Here we show that *Lbx1* is necessary for the proper development of relay sensory neurons within SpV and Cn/Gr. Inactivation of *Lbx1* switched the fate of *Lbx1*<sup>+</sup> neurons into dorsally derived Stn and IO neurons, causing the generation of ectopic clusters of GFP<sup>+</sup> neurons lateral to the Stn and a major disruption of the cytoarchitecture of the medulla in *Lbx1*<sup>GFP/GFP</sup> mice.

### 5.4.1 EXPRESSION OF LBX1 IN THE MEDULLA AND CYTOARCHITECTONICAL ABNORMALITIES IN *LBX1*<sup>GFP/GFP</sup> MICE

We initially analyzed the expression of *Lbx1/GFP* in E18 *Lbx1*<sup>GFP/+</sup> and *Lbx1*<sup>GFP/GFP</sup> mice and the cytoarchitectonical defects induced by inactivation of *Lbx1*. *Lbx1* is necessary for the proper development of SpV and the Cn/Gr nuclei, two major relay stations for somatic sensory afferent processing. In *Lbx1*<sup>GFP/GFP</sup> mice, we observed a complete disruption of the cytoarchitecture of SpV and Cn/Gr nuclei at E18. We also identified abnormalities in the IO formation, and migratory defects in the GFP<sup>+</sup> neurons that in *Lbx1*<sup>GFP/+</sup> mice populate the reticular formation.

*Lbx1* inactivation also affected the distribution of trigeminal afferent fibres that innervate SpV (SpV tract). These axonal tracts were aberrantly located and significantly smaller through the brainstem. One cause for this defect could be that sensory ganglia innervating SpV are abnormal: this possibility though is quite unlikely since *Lbx1* is not expressed in ganglion cell and an analysis of sections counterstained with thionin did not reveal any morphological abnormality. Although we can not exclude that some finer defects occur at the ganglion level, we propose that the abnormal developmental program in *Lbx1*<sup>GFP/GFP</sup> mice alters the migratory pathway of sensory afferent into the SpV. Similarly, it was previously shown that the sensory afferents growing into the spinal cord were affected in *Lbx1*<sup>GFP/GFP</sup> mice and the expression of molecules that direct growing

axons (netrin-1, ephrin 5A) were downregulated in GFP<sup>+</sup> dorsal horn neurons (Gross et al., 2002). Further studies will be necessary to determine if the inactivation of *Lbx1* induces an abnormal expression of developmental cues necessary for the proper innervation in the brainstem as well, or the defects in the SpV tract are the consequence of abnormalities in the distribution of SpV neurons in the developing medulla of *Lbx1*<sup>GFP/GFP</sup> mice.

We also observed an ectopic cluster of longitudinally oriented GFP<sup>+</sup> fibres in the ventrolateral medulla that was present as early as E13-14 and that consequently shifted the ventrally located neurons in a more dorsolateral position. Since the spinal cord of *Lbx1*<sup>GFP/GFP</sup> mice contains an increased number of ascending commissural neurons in the spinal cord (Gross et al., 2002), it is likely that these fibres represent the rostral extension of the ventral funiculus. Further experiments with anterograde dyes in the commissural neurons will be necessary to ascertain the origin of these longitudinal fibres.

#### **5.4.2 CHARACTERIZATION OF LBX1 NEURONS IN THE MEDULLA OF LBX1<sup>GFP/+</sup> AND LBX1<sup>GFP/GFP</sup> MICE**

In order to identify the origin of Lbx1/GFP<sup>+</sup> cells in *Lbx1*<sup>GFP/+</sup> and *Lbx1*<sup>GFP/GFP</sup> mice and to decipher the developmental abnormalities in the mutants, we looked at the early development of the medulla and combined the expression of *Lbx1/GFP* with several TFs known to be specifically expressed in precursor cells of either spinal cord or brainstem (Pattyn et al., 2000a; Pattyn et al., 2000b; Cheng et al., 2004; Ding et al., 2004; Cheng et al., 2005). We therefore classified the post-mitotic dorsal interneurons prior to their migratory process in 6 classes, similarly to what has been proposed in the developing spinal cord (Gross et al., 2000; Muller et al., 2002).

Thus, Lbx1/GFP<sup>+</sup> cells in wild type and *Lbx1*<sup>GFP/+</sup> mice constitute the domains corresponding to the early-born dI4-dI6 interneurons (E10-11) and to the late-born dIL<sub>A-B</sub> interneurons (E12-13).

When we analyzed the expression of GFP in *Lbx1*<sup>GFP/GFP</sup> mice during the early stages of development, we observed five major defects: i) abnormal migratory pathways were evident as early as E12; ii) Pax2 was down regulated in dI4, dIL<sub>A</sub> and to a lesser

extent in dI6 neuronal population; iii) *Lmx1b* was still present in dI3 dI5 and dIL<sub>B</sub> neuronal populations, even though the intensity of the staining in dIL<sub>B</sub> neurons appeared slightly weaker in comparison to the adjacent dI5 and dI3 neurons; iv) the extension of the distribution of cells immunopositive for FoxP2 appeared to be increased in the E12 embryos; v) ectopic expression of *Phox2b* was present in the dI5 and dIL<sub>A-B</sub> neurons.

We were intrigued by the abnormal expression of *FoxP2* and *Phox2b* in the medulla of *Lbx1<sup>GFP/GFP</sup>* mice. *FoxP2* is a transcription factor expressed in neurons of the IO formation (Lai et al., 2003), in a subpopulation of motoneurons and a population of ventral interneurons in the spinal cord (Shu et al., 2001) and other neuronal structures in the midbrain and forebrain (Ferland et al., 2003; Lai et al., 2003; Takahashi et al., 2003). Its expression begins in the presumptive IO neurons while migrating along the submarginal stream, therefore their site of origin is not identifiable by means of FoxP2 immunoreactivity. Nonetheless, it is well established that IO neurons are generated in the dorsal neuroepithelium and then migrate tangentially to the medullary surface along the submarginal stream until they reach the ventral midline, where they settle (Bourrat and Sotelo, 1990; Bloch-Gallego et al., 2005). At present, no other studies have examined in full detail *FoxP2* expression in the developing medulla, therefore we cannot exclude that some of these neurons derive from other neuronal precursors, either dorsally or ventrally located, similarly to what occurs in spinal ventral interneurons (Shu et al., 2001).

The enlarged distribution of FoxP2<sup>+</sup> cells in the submarginal stream and the enlargement of the IO formation prior to birth suggest that there is an increased production of FoxP2<sup>+</sup> neurons, likely occurring in the dorsal medulla, that do not migrate in a tight stream, but are rather dispersed. Interestingly, despite the enlargement of the IO formation at E18, we could not distinguish any abnormality when we immunolabelled IO formation for CR and CB. Thus, independently from their origin, FoxP2<sup>+</sup> neurons acquire a phenotype that likely corresponds to the location in which they settle.

Although we did not notice any colocalization of GFP and FoxP2 within the same cell, it is intriguing to speculate that some of the extranumerary FoxP2<sup>+</sup> cells are generated within the GFP<sup>+</sup> domain of the *Lbx1<sup>GFP/GFP</sup>* mice, lose their GFP<sup>+</sup> expression and acquire the fate of dorsal lip interneurons: this possibility is suggested by the presence of a high number of radially oriented FoxP2<sup>+</sup> nuclei in apposition to the newly

generated GFP domain and by the fact that, in the spinal cord of *Lbx1<sup>GFP/GFP</sup>* mice, dI4 and dI5 neurons switch their neuronal identity to more dorsally derived dI2 (possibly corresponding to the domain of origin of IO neurons) and dI3 neurons, respectively. To test this hypothesis, further experiments with early markers of differentiation for IO neurons will be necessary. Recently the developmental origin of rhombic lip derivatives has been investigated and it has been shown that IO neurons derive from a class of progenitor cells that are *Math1<sup>-</sup>/Ptf1a<sup>+</sup>* (Hoshino et al., 2005; Wang et al., 2005). Therefore the detection of *Ptf1a* or other specific markers for developing IO neurons could provide insight in the abnormalities we observed in the IO formation of *Lbx1<sup>GFP/GFP</sup>* mice.

We also investigated the expression of *Phox2b<sup>+</sup>* neurons in *Lbx1<sup>GFP/+</sup>* and *Lbx1<sup>GFP/GFP</sup>* mice. These results suggest that in the early stages of development *Phox2b<sup>+</sup>* is expressed only in few *Lbx1/GFP<sup>+</sup>* cells in the dIL<sub>A-B</sub>, similarly to what reported in the spinal cord, where the homologous gene *Phox2a* is expressed in a subset of dI5 neurons (Ding et al., 2004). These neurons may constitute one subpopulation of *GFP/Lbx1<sup>+</sup>/Phox2b<sup>+</sup>* neurons that are sparse in the reticular formation (mainly located medial to SpV in the region surrounding the VII nucleus, in the region dorsal to the rostral Stn in the PR and in the dense cluster of *GFP<sup>+</sup>* cells within the vestibular nucleus) and that were previously identified, but not fully characterized, as non-cholinergic/non-adrenergic in the medulla of post-natal mice (Tiveron et al., 1996).

The ectopic expression of *Phox2b* in the GFP domain of *Lbx1<sup>GFP/GFP</sup>* mice through development likely takes origin from neurons in dI5 and dIL<sub>A-B</sub> domains that settle in the putative region of SpV and, rostrally in the PR formation. These results suggest that some of the neurons in the GFP domain switch their neuronal identity to more dorsally derived dI3 neurons.

The analysis of TH, CB and CR expression showed that the acquisition of a new neuronal identity might only be partial. In fact, the ectopic *Phox2<sup>+</sup>/GFP<sup>+</sup>* cells in the putative region of SpV did not acquire a TH<sup>+</sup> phenotype. This is quite surprising given that previous experiments in which *Phox2* genes were overexpressed in chick embryos, neural crest cells and dorsal root ganglia demonstrated that *Phox2* genes can induce the development of ectopic neurons that express TH, DBH, ChAT and VChAT (Stanke et al.,

1999). Specifically, TH and DBH have specific binding sites for *Phox2a* and *Phox2b* promoters and *Phox2a* and *Phox2b* can activate both enzymes (Zellmer et al., 1995; Lo et al., 1999).

A possible explanation for our results could be that the expression of *Phox2b* would induce the selective activation of only DBH (Yang et al., 1998) and thus we would not see a nor/adrenergic phenotype in GFP<sup>+</sup> neurons by simply labelling our tissue with TH. However, this seems unlikely since *Phox2b*<sup>-/-</sup> mutants show a reduction in the expression of both DBH and TH (Pattyn et al., 1999; Dauger et al., 2003) and overexpression of *Phox2b* induces the expression of both (Zellmer et al., 1995; Lo et al., 1999).

It is more likely that the ectopic *Phox2b*<sup>+</sup> cells we identified in the *Lbx1*<sup>GFP/GFP</sup> mice are the result of a switch of neuronal fate into: i) abnormally developed dI3 derived nor/adrenergic neurons (*Phox2b*<sup>+</sup>/TH<sup>-</sup>); ii) an overexpression of the previously identified, but not fully characterized *Phox2*<sup>+</sup>/DBH<sup>-</sup>/ChAT<sup>-</sup> neurons distributed in the postnatal medulla, some of them located lateral to Stn and in the PR formation (Tiveron et al., 1996); iii) neurons that temporarily express TH and DBH in the early stages of development and then expression is down regulated by E18. Further experiments aimed to test the expression of TH and DBH in the early stages of development will be necessary to test this hypothesis.

These results are interesting in terms of the regulation of hindbrain cell fate specification. *Phox2* genes have been implicated in the acquisition of the phenotype of nor/adrenergic neurons and branchial and visceral MNs in the CNS (reviewed in Brunet et al, 2002). dI3 and dI4-5 domains derive from the same class of *Mash1* progenitors and their differentiation is influenced by dorsoventral patterning cues, which then induce the expression of different TFs in post-mitotic neuronal precursors. Both *Phox2b* and *Lbx1* are expressed in post-mitotic neurons in the developing medulla in complementary populations. It is possible that *Lbx1* antagonizes the induction of a noradrenergic phenotype in the *Mash1*<sup>+</sup> ventrally derived neurons. Therefore the inactivation of *Lbx1* could induce a partial respecification of dI4-dI6 and dIL neurons into the more dorsally derived dI3 *Phox2b*<sup>+</sup> neurons. The absence of TH and DBH expression could be explained by the fact that a specific combinatorial code of transcription factors is

necessary for the complete acquisition of a noradrenergic phenotype. For example, *GATA2* (in chicks) and *GATA3* (in mice) are TF downstream of *Mash1*, *Phox2a* and *Phox2b* (Tsarovina et al., 2004); when inactivated, they reduced the expression of TH and DBH, but when overexpressed in chick neural crest, *GATA2* generates ectopic neurons in the sympathetic ganglia that do not express a noradrenergic phenotype (Tsarovina et al., 2004). Therefore it is possible that ectopic expression of *Phox2b* is not sufficient in the *Lbx1<sup>GFP/GFP</sup>* mice to completely switch their neuronal fate to nor/adrenergic neurons.

Another TF involved in the development of Stn and SpV neurons is *Rnx/Tlx3*. This homeodomain TF was reported to be expressed in the dI3 and dI5 and dIL neurons of hindbrain and spinal cord (Shirasawa et al., 2000; Qian et al., 2001; Qian et al., 2002). Both *Rnx/Tlx3* and *Tlx1* are necessary for the proper development of SpV and *Rnx/Tlx3* antagonizes the effect of *Lbx1*, with an independent mechanism, in order to specify glutamatergic versus GABAergic phenotype in the spinal cord (Cheng et al., 2005).

It will be therefore necessary to further discover the combinatorial code expressed by dI3 precursor and the compare it with the several derived nor/adrenergic and non-nor/adrenergic populations in order to identify the neuronal fate that ectopic *Phox2b<sup>+</sup>/GFP<sup>+</sup>* cells acquired in *Lbx1<sup>GFP/GFP</sup>* mice.

The observation that a larger number of A1/C1 and A5 neurons are generated in the *Lbx1<sup>GFP/GFP</sup>* mice may suggest that these neurons have a slightly diverse differentiation program compared with the dorsally located nor/adrenergic neurons. Although several genes have been implicated with A5 group neuronal development (Hirsch et al., 1998; Guo et al., 2005; Huang et al., 2005; Viemari et al., 2005), a limited amount of data is present in the literature regarding the specification and origin of the A1/C1 neuronal group. Further studies are necessary to identify the genetic traits of the different nor/adrenergic populations in order to explain their diverse identity and alternative migration patterns.

Thus, from these data, we propose that inactivation of *Lbx1* induces a loss of the GABAergic phenotype in the dI4-dI6 and dIL<sub>A-B</sub> neurons and the *Lbx1<sup>-</sup>* deficient neurons acquire a more dorsally derived phenotype of dI3 (*Phox2b<sup>+</sup>*) and possibly dI2 (*FoxP2<sup>+</sup>*) phenotype. The newly formed neurons acquire a migratory pattern that is similar to the

dorsally derived neurons, therefore generating a larger IO formation, and altering the cytoarchitecture of dorsally located neuronal structures (Stn, Cn/Gr and SpV).

#### **5.4.3 ANALYSIS OF THE VENTROLATERAL MEDULLA AND THE RESPIRATORY FUNCTION IN $LBX1^{GFP/+}$ AND $LBX1^{GFP/GFP}$ MICE**

Newborn  $Lbx1^{GFP/GFP}$  mice die during the early postnatal period from respiratory distress (Gross et al., 2000). We therefore investigated the physiological and anatomical properties of the medulla of  $Lbx1^{GFP/GFP}$  mice in order to identify the specific respiratory defect. Data from *in vitro* models demonstrated that the defect could be explained by abnormal neuronal activity within the brainstem. The motor patterns generated by the  $Lbx1^{GFP/GFP}$  perinatal preparations were clearly different than that generated in wild-type preparations of the same age. The frequency of the respiratory rhythm was markedly reduced and there was a propensity for the generation of long-duration ectopic bursts that were not related to the respiratory cycle. Both of these characteristics are typical of what is observed in *in vitro* preparations isolated from earlier stage embryos (Greer et al., 1992). The long-duration motor bursts are generated in embryonic rodent spinal cords from the time when motor axons first emerge from the spinal cord (Greer et al., 1992; Nakayama et al., 1999; Ren and Greer, 2003). These synchronous bursts of motor discharge propagate along the neuraxis from the medulla to sacral spinal cord. Typically, the propensity for generating synchronous motor bursts declines with gestational age and is much less prevalent late in gestation when organized respiratory and locomotor patterns are well established.

The electrophysiological data support the hypothesis that a loss of  $Lbx1$  expression results in a lethal perturbation of central respiratory rhythmogenesis in newborn mice. Data from *in vitro* (Smith et al., 1991) and *in vivo* (Solomon et al., 1999; Gray et al., 2001) models strongly suggest that the preBötC is a major contributor to the genesis of respiratory rhythm. A detailed understanding of the cellular mechanisms underlying rhythm and pattern generation with the ventrolateral medulla remains to be elucidated. However, the primary conditioning excitatory drive that maintains the oscillatory state arises from activation of glutamatergic receptors (Greer et al., 1991;

Funk et al., 1993). Further conditioning is provided by a diverse group of neuromodulators including GABA, serotonin, noradrenaline, opioids, prostaglandins, Substance P and acetylcholine (Lagercrantz, 1987; Moss and Inman, 1989; Ballanyi et al., 1999). The loss of *Lbx1* expression could result in the loss, or perturbation of function, of rhythmogenic neurons in the preBötC that results in the abnormally slow rhythms. Alternatively, *Lbx1* expression may be necessary for providing the appropriate conditioning drive from neurons impinging on rhythmogenic neurons within the preBötC.

Anatomically, neurons in the preBötC region can be identified by means of NK1R and SST immunolabelling. The analysis of these two markers in combination with GFP detection in the ventrolateral medulla of *Lbx1<sup>GFP/GFP</sup>* mice suggests that preBötC neurons do not express *Lbx1/GFP* in either *Lbx1<sup>GFP/+</sup>* or *Lbx1<sup>GFP/GFP</sup>* mice. Further, preBötC neurons are present in the mutants and they express their phenotypic markers. Although we cannot rule out the possibility that preBötC neurons have some defects in their physiological properties caused by the inactivation of *Lbx1*, we excluded the possibility that preBötC neurons do not form in the *Lbx1<sup>GFP/GFP</sup>* mice. From the anatomical analysis of the ventrolateral medulla at E18 with different neuronal markers we noted that preBötC NK1<sup>+</sup>/SST<sup>+</sup> neurons were embedded in a dense network of GFP<sup>+</sup>/Pax2<sup>+</sup>/CR<sup>+</sup> neurons in *Lbx1<sup>GFP/+</sup>* mice, and this network was depleted in the preBötC region of *Lbx1<sup>GFP/GFP</sup>* mice. At present, we cannot demonstrate that these neurons have a role in the generation of respiratory rhythm frequency and pattern, but experimental evidences exist for a role of GABAergic modulation of preBötC and other respiratory neurons in the VRG (Feldman and Smith, 1989; Shao and Feldman, 1997; Pierrefiche et al., 1998; Kuwana et al., 2006).

The proposed reduction of GABAergic cells in the ventral respiratory column and consequently the abnormal inhibitory innervation on preBötC neurons does not explain the abnormal and slow respiratory rhythmic activity recorded in medullary slices and brainstem spinal cord preparation. The respiratory output recorded in *Lbx1<sup>GFP/GFP</sup>* mice is probably the consequence of a very complex reorganization, not only of the identity of precursor neurons but also of the networks that operate within the respiratory centres and between the sensory systems and the respiratory centre. It will be therefore necessary to study the respiratory network at different levels, Firstly, it will be necessary to test if the

application of different neuromodulators is sufficient to restore normal breathing: GABA and nor/adrenaline transmission will be tested because of the neuroanatomical results in *Lbx1<sup>GFP/GFP</sup>* mice. Further, an investigation of properties of respiratory neurons, both at the level of the VRG (preBötC included) and at the level of XII MNs, will be necessary to test if abnormal inputs determine the reduction in rhythm frequencies and the occurrence of long duration, non-respiratory bursts. For this purpose, the use of TMR-SubP in conjunction with the fluorescence emitted by *Lbx1/GFP<sup>+</sup>* neurons in both *Lbx1<sup>GFP/+</sup>* and *Lbx1<sup>GFP/GFP</sup>* mice will facilitate the recording and analysis of respiratory and non-respiratory neurons.

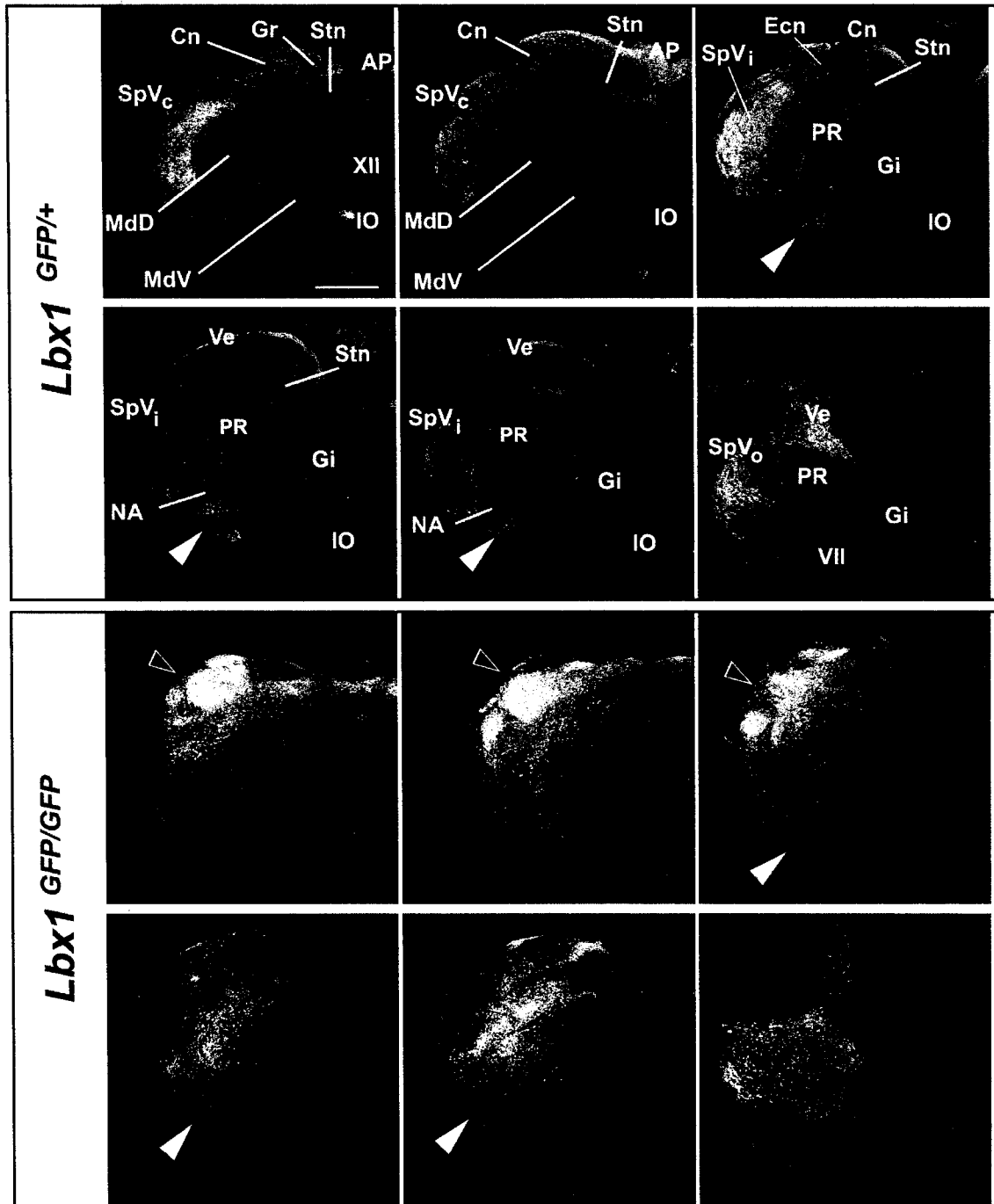
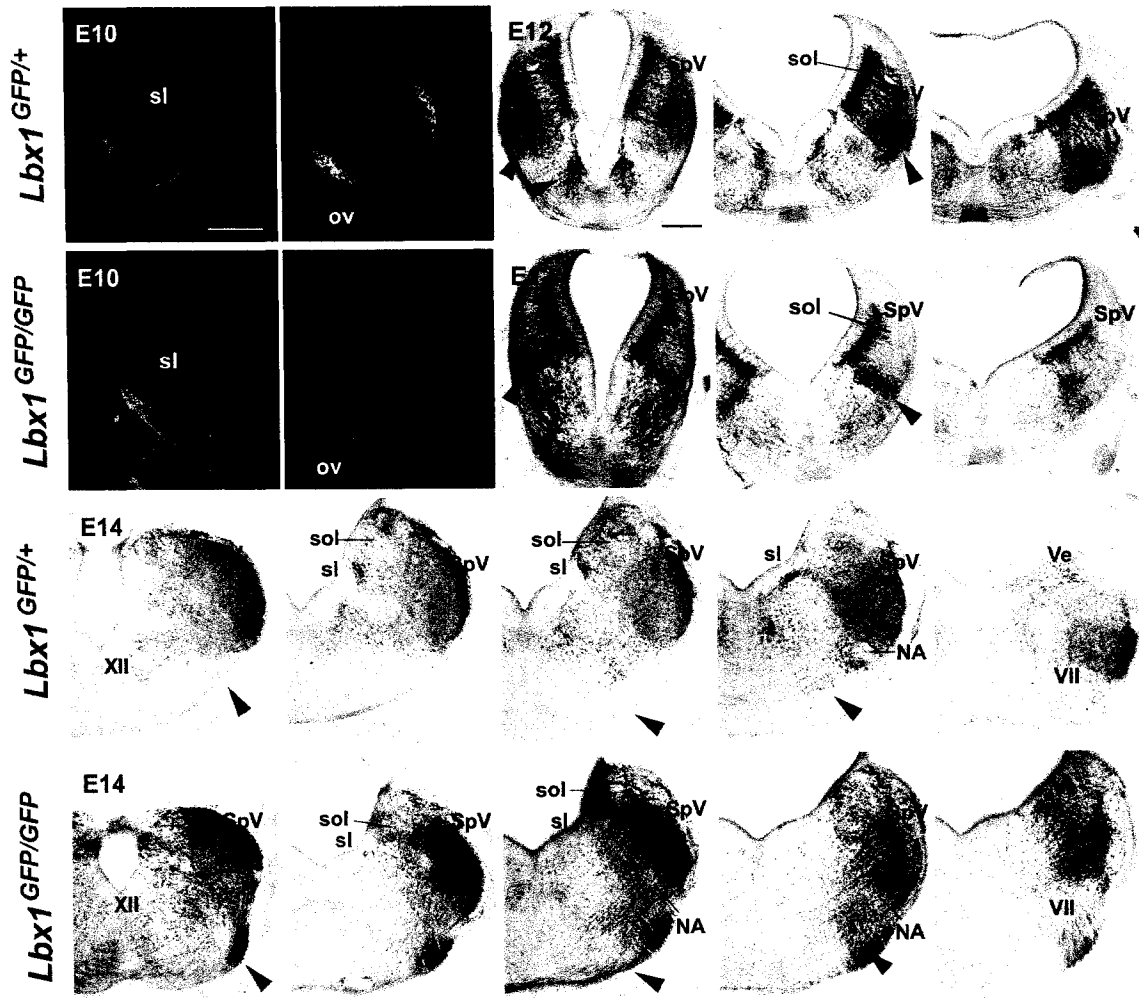


**Figure 5.1** Expression of GFP in *Lbx1*<sup>GFP/+</sup> *Lbx1*<sup>GFP/GFP</sup> mice at E18. Serial caudo-rostral transverse sections of the medulla of *Lbx1*<sup>GFP/+</sup> (top panel) and *Lbx1*<sup>GFP/GFP</sup> (bottom panel) mice at E18. In *Lbx1*<sup>GFP/+</sup> mice, Lbx1/GFP is expressed in the SpV caudalis (SpVc), interpolaris (SpVi) and oralis (SpVo), in the Cn and Gr nuclei, in the AP, in the Stn, in scattered cells in MdV and MdD and, more rostrally, in ECn, in PR and

the gigantocellular reticular (Gi) formations and in the Ve. In the *Lbx1*<sup>GFP/GFP</sup> mice, GFP is expressed in the putative region of SpV (open arrowheads), Cn, Gr, AP and in scattered cells in MdV and MdD, in Gi and PR. Note the different cytoarchitecture of the sensory systems (SpV, Cn and Gr). Calibration bar: 400µm.

### Next Page

**Figure 5.2 GFP expression in the medulla of *Lbx1*<sup>GFP/+</sup> and *Lbx1*<sup>GFP/GFP</sup> mice during development.** Serial caudo-rostral transverse sections of the medulla at E10, E12 and E14. **E10** (top left), GFP expression is present in a single column of postmitotic neurons through the medulla of both *Lbx1*<sup>GFP/+</sup> and *Lbx1*<sup>GFP/GFP</sup> mice. **E12** (top right), GFP<sup>+</sup> cells in *Lbx1*<sup>GFP/GFP</sup> are present in a narrow band adjacent to the alar plate and migrate out in two directions: one laterally towards the lateral surface of the developing medulla, and one medio-ventrally. In the *Lbx1*<sup>GFP/GFP</sup> mice, GFP<sup>+</sup> cells are reduced from the surface of the dorsolateral medulla and migrate laterally in a narrow band at the ventral end of the GFP<sup>+</sup> domain (arrowheads). Medially GFP<sup>+</sup> cells are dispersed in the reticular formation (arrowheads). **E14** (bottom), GFP<sup>+</sup> cells are distributed within the dorsal medulla (in the putative regions of SpV), Stn and in the ventrolateral medulla. In *Lbx1*<sup>GFP/GFP</sup> mice, presumptive SpV contains a dense group of GFP<sup>+</sup> cells not distributed in a layered and organized pattern. Calibration bars, E10, 500µm; E12,14, 200µm;



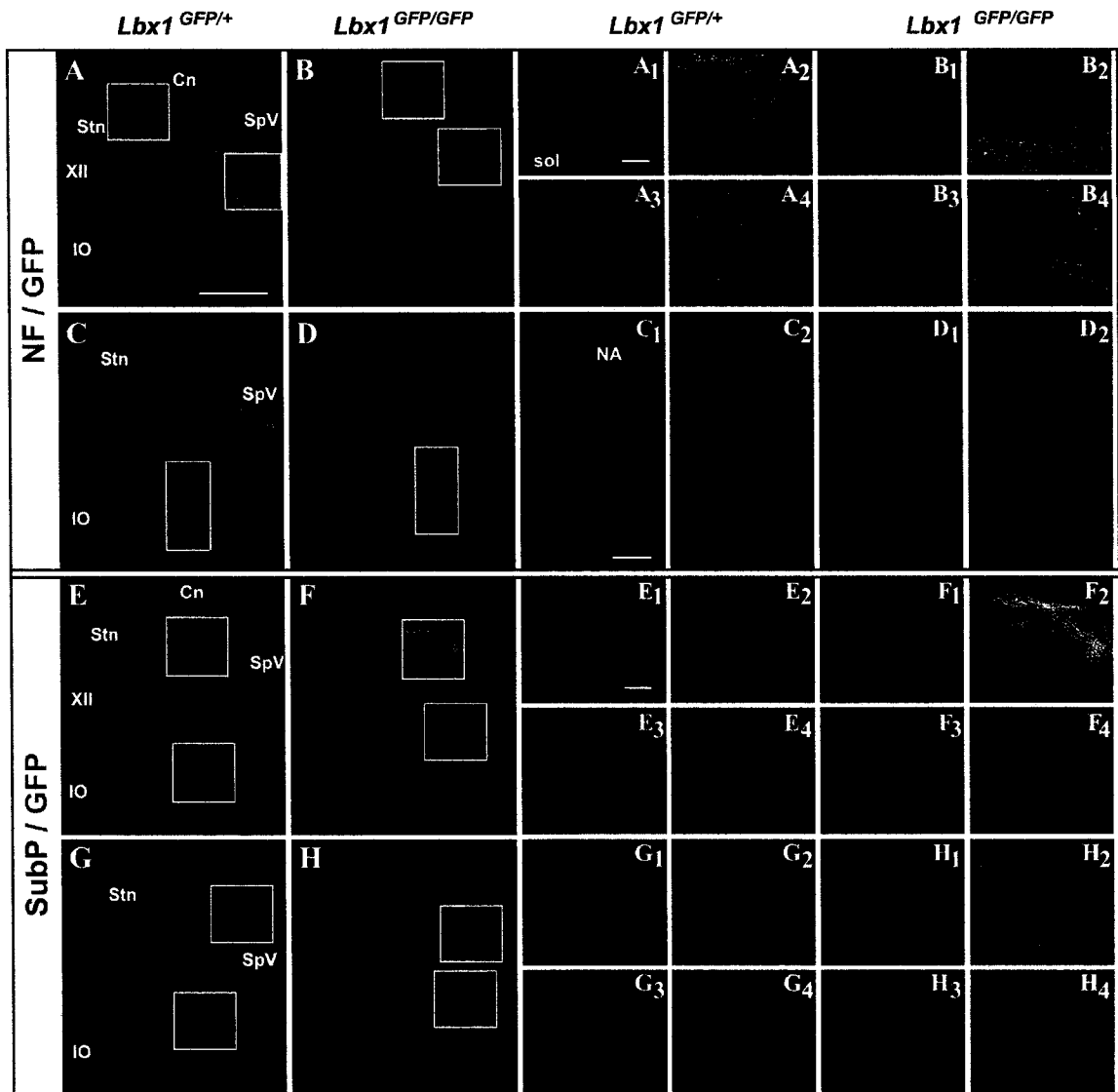
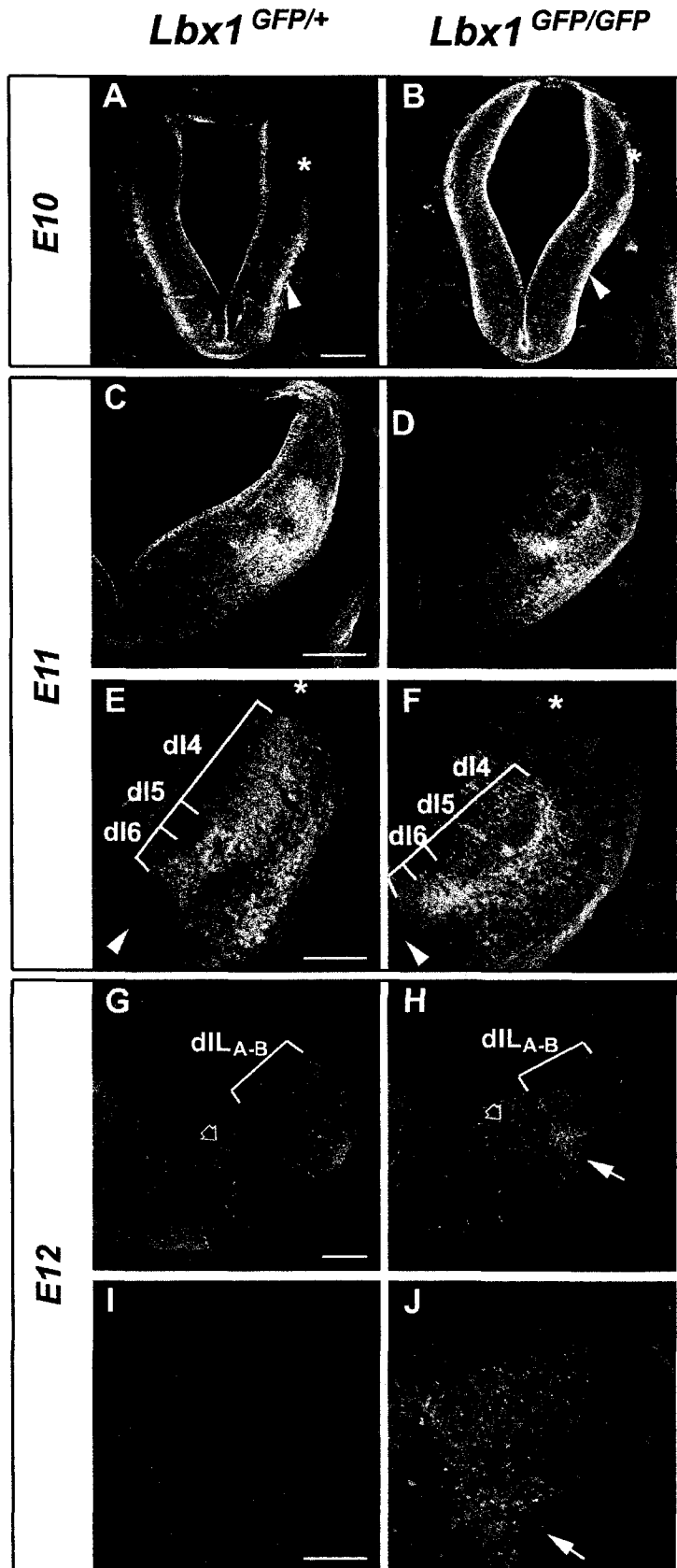


**Figure 5.3 Cytoarchitectural abnormalities in the medulla of *Lbx1*<sup>GFP/GFP</sup> mice at E18.** Top panel, NF (red) and GFP (green) expression at two different levels of the medulla in *Lbx1*<sup>GFP/+</sup> and at *Lbx1*<sup>GFP/GFP</sup> mice at E18. A<sub>1</sub>,B<sub>1</sub> (NF only), A<sub>2</sub>,B<sub>2</sub> (NF and GFP) are details of the dorsal medulla (top left box in A and B, respectively). A<sub>3</sub>,B<sub>3</sub> (NF only), A<sub>4</sub>,B<sub>4</sub> (NF and GFP) are details of SpV (bottom right box in A and B, respectively). C<sub>1</sub>,D<sub>1</sub> (NF only), C<sub>2</sub>,D<sub>2</sub> (NF and GFP) are details of the ventrolateral medulla (boxes in C and D, respectively). Note the altered orientation of NF<sup>+</sup> fibres within the Cn and SpV nuclei due to the abnormal distribution of GFP<sup>+</sup> cells in the medulla of *Lbx1*<sup>GFP/GFP</sup> mice (A<sub>1</sub> to B<sub>4</sub>). Abnormal axonal distribution is also present in the ventrolateral medulla where several tangentially oriented axons are located along the

medullary surface (C<sub>1</sub> to D<sub>2</sub>). **Bottom panel**, Expression of Substance P (red) and GFP (green) at two different levels of the medulla in *Lbx1<sup>GFP/+</sup>* and at *Lbx1<sup>GFP/GFP</sup>* mice at E18. In *Lbx1<sup>GFP/+</sup>* SubP<sup>+</sup> fibres are distributed along the surface of the spinal trigeminal tract and several fibres are detected within the ventrolateral medulla and in the Stn. In *Lbx1<sup>GFP/GFP</sup>* mice incoming fibres in the spinal trigeminal tract are only distributed in the dorsalmost region of the putative SpV. E<sub>1</sub>,F<sub>1</sub>,G<sub>1</sub>,H<sub>1</sub> (SubP only), E<sub>2</sub>,F<sub>2</sub> G<sub>2</sub>,H<sub>2</sub> (SubP and GFP) are details of the dorsal SpV (top box in E,F,G and H, respectively). E<sub>3</sub>,F<sub>3</sub>,G<sub>3</sub>,H<sub>3</sub> (SubP only), E<sub>4</sub>,F<sub>4</sub>,G<sub>4</sub>,H<sub>4</sub> (SubP and GFP) are details of the ventrolateral medulla (bottom box in E,F,G, and H, respectively). Overall expression of SubP is reduced in the medulla, both in the ventrolateral medulla and the Stn. Calibration bars, A-H, 500 µm; A<sub>1</sub>-B<sub>4</sub>, 100 µm; C<sub>1</sub>-D<sub>2</sub>, 100 µm; E<sub>1</sub>- H<sub>4</sub>, 100 µm.

### Next Page

**Figure 5.4 GFP (green), Pax2 (blue) and Lmx1b (red) expression in the medulla of *Lbx1<sup>GFP/+</sup>* (left) and *Lbx1<sup>GFP/GFP</sup>* mice (right) at E10 (A,B), E11 (C-F) and E12 (G-K).** GFP is expressed in the dI4-dI6 and dIL<sub>A-B</sub> dorsal interneurons. *Lmx1b* is expressed in the dI3 (asterisks) and dI5 and dIL<sub>A</sub> dorsal interneuronal population, *Pax2* is expressed in the dI4, dI6, dIL<sub>B</sub> and in ventral interneuronal populations (arrowheads in E,F). In *Lbx1<sup>GFP/GFP</sup>* mice, *Pax2* is absent in dI4 and dIL<sub>A</sub> interneurons (F,H). Pax2<sup>+</sup>/GFP<sup>+</sup> cells are missing in the medial medulla (open arrows in G,H) and in the ventral medulla the majority of GFP<sup>+</sup> cells are Lmx1b<sup>+</sup> (arrows in H,J) Calibration bars, A-B,C-D,G-H, 200µm; E,F,I J, 100µm.



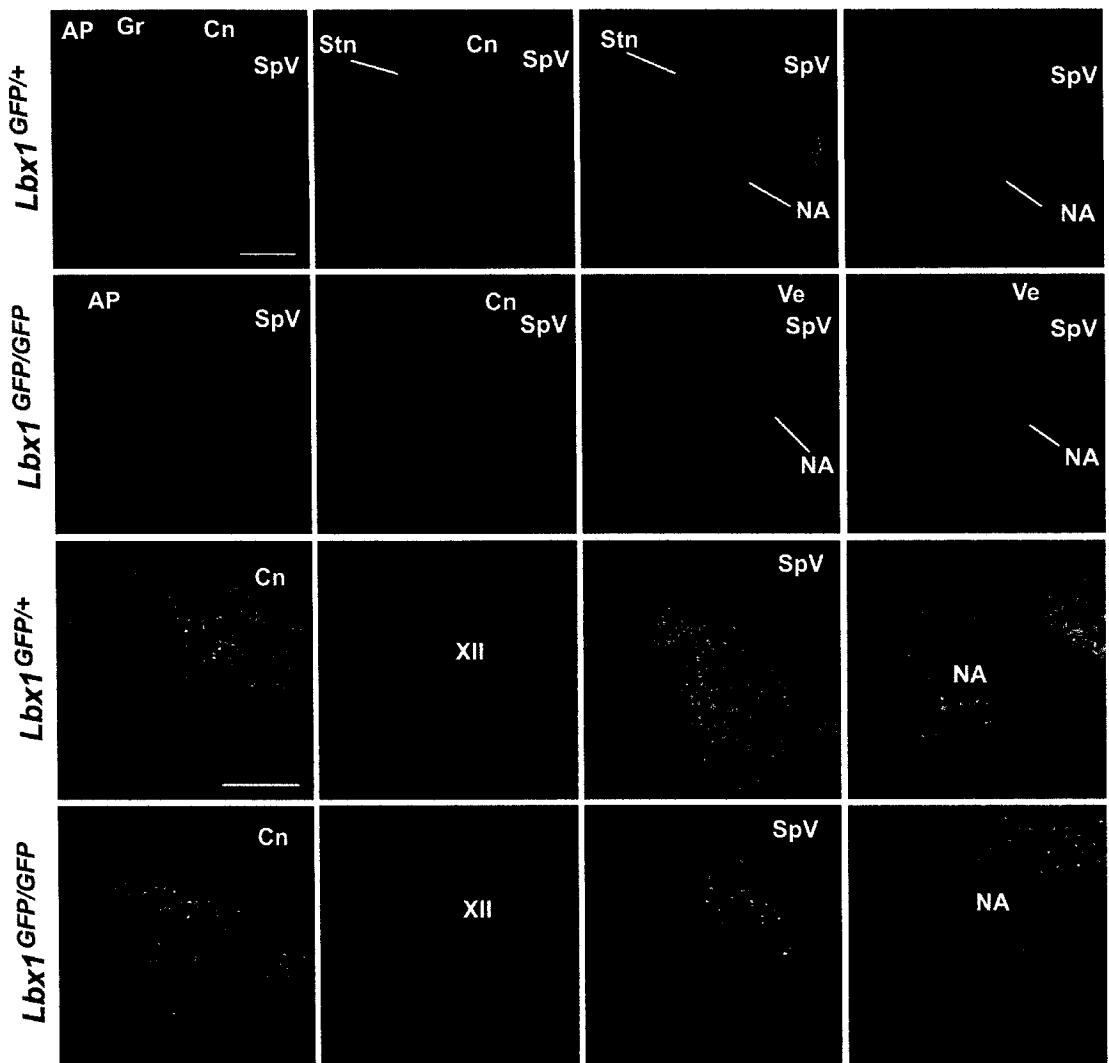
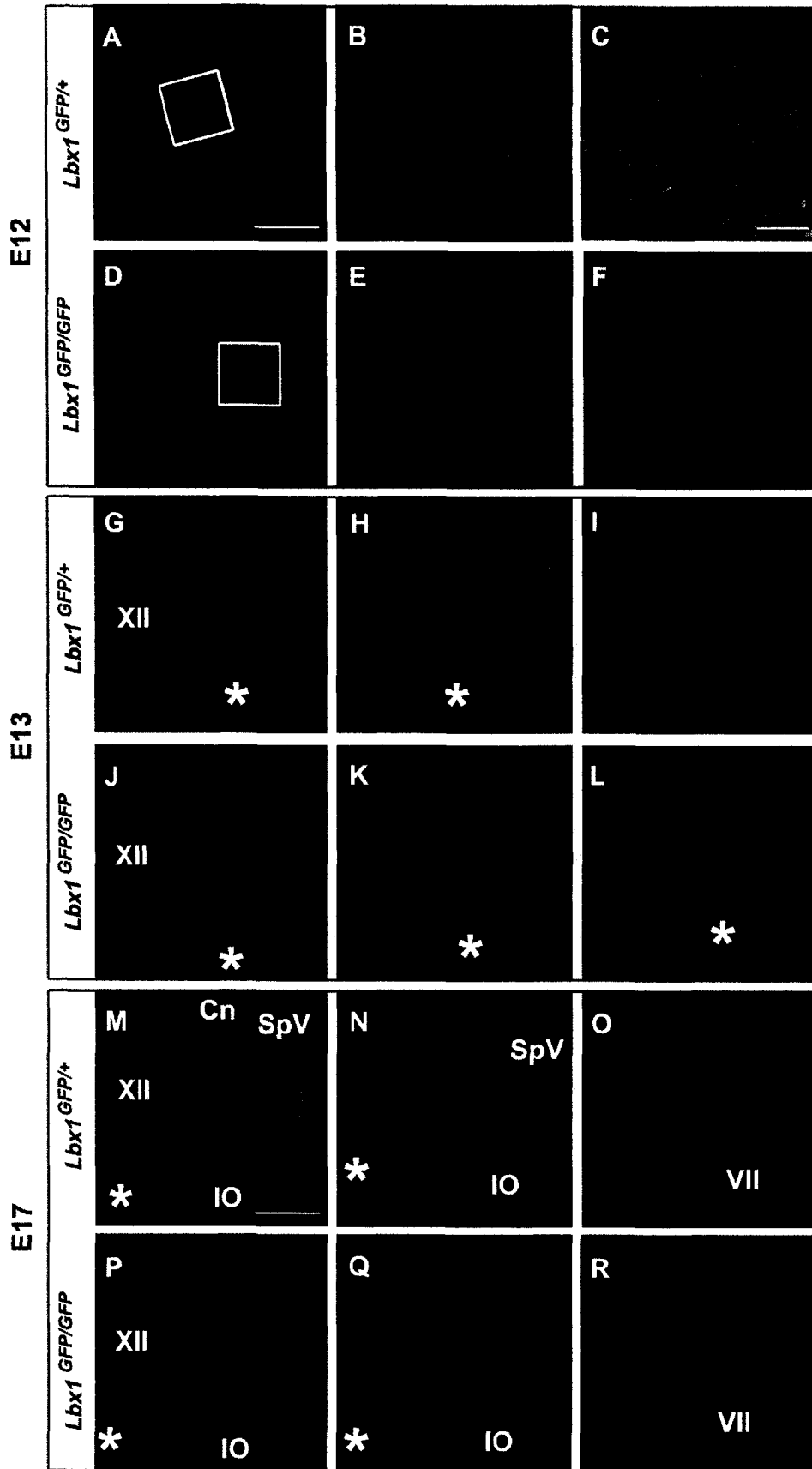


**Figure 5.5** GFP (green) and *Pax2* (red) expression in the medulla of *Lbx1*<sup>GFP/+</sup> and *Lbx1*<sup>GFP/GFP</sup> mice at E18. Serial caudo-rostral transverse sections of the medulla of *Lbx1*<sup>GFP/+</sup> and *Lbx1*<sup>GFP/GFP</sup> mice at E18. In *Lbx1*<sup>GFP/+</sup> mice *Pax2* is expressed in cells located in the medial reticular formation and lateral to XII nucleus, in the SpV, Gr/Cn, Stn nuclei and in the ventrolateral medulla. It colocalizes with *Lbx1*/GFP in the Cn/Gr nuclei, in the SpV and in a subpopulation of *Pax2*<sup>+</sup> cells in the ventrolateral medulla. In the *Lbx1*<sup>GFP/GFP</sup> mice *Pax2* is expressed in the medial reticular formation and lateral to XII nucleus, only scattered cells are present in the SpV, Gr/Cn, Stn nuclei and in the ventrolateral medulla. GFP<sup>+</sup>/*Pax2*<sup>+</sup> cells are almost absent. Calibration bars, first and third row, 500µm; second and fourth row, 200µm.

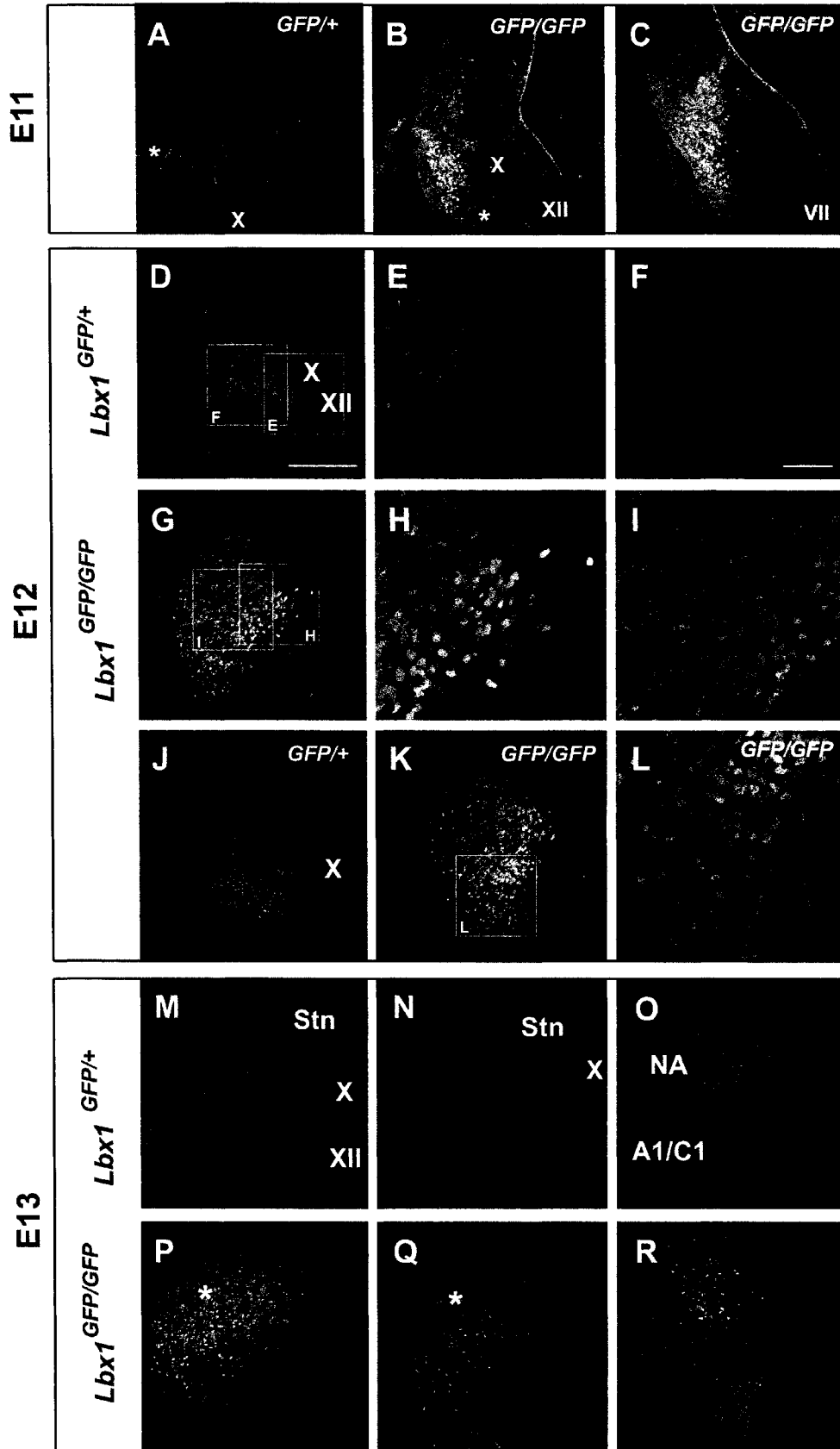


### Previous page

**Figure 5.6 GFP (green) and FoxP2 (red) expression in the medulla of *Lbx1*<sup>GFP/+</sup> and *Lbx1*<sup>GFP/GFP</sup> mice at E12, E13 and E17.** Serial caudo-rostral transverse sections of the medulla of *Lbx1*<sup>GFP/+</sup> and *Lbx1*<sup>GFP/GFP</sup> mice. (A-F) At E12 FoxP2 is expressed in tangentially migrating IO neurons in the developing medulla. C,F are details from boxes in A and D, respectively. Note the different orientation of the nuclei in C and F. (G-L) At E13 the developing IO in *Lbx1*<sup>GFP/GFP</sup> mice appears enlarged in comparison to *Lbx1*<sup>GFP/+</sup> mice (asterisks). (M-R) At E18 the defect in the IO is still evident (asterisks); IO is enlarged and it extends further rostrally (O,R). Calibration bars, A,B,D,E,G-L, 200µm; C,F, 50µm; M,R, 500 µm.

### Next page

**Figure 5.7 GFP (green), *Phox2b* (red) and ChAT (blue) expression in the medulla of *Lbx1*<sup>GFP/+</sup> and *Lbx1*<sup>GFP/GFP</sup> mice at E11, E12 and E13.** (A-C) At E11 *Phox2b* is expressed in dI3 neurons in *Lbx1*<sup>GFP/+</sup> mice (A) and in dI3 and dI5 neurons and in X, XII,VII and NA motoneurons (asterisk) in *Lbx1*<sup>GFP/GFP</sup> mice (B, caudal and C, rostral medulla. (D-L) At E12, *Phox2b* is expressed in scattered cells in the dIL domain of *Lbx1*<sup>GFP/+</sup> mice medulla (F), whereas in *Lbx1*<sup>GFP/GFP</sup> mice the colocalization of GFP and *Phox2b* is almost complete (I). E,H are details of *Phox2b*<sup>+</sup> neurons of X from E,H boxes in images D and G respectively. J,K represent *Phox2b* expression in more rostral sections and L is a detail of K (box in K). (M-R) Expression of *Phox2b* at E13 at two different rostrocaudal level (M,P and N,Q respectively). *Phox2b*<sup>+</sup>/*GFP*<sup>-</sup> cells accumulate in the presumptive Stn neurons. In *Lbx1*<sup>GFP/GFP</sup> mice *Phox2b*<sup>+</sup>/*GFP*<sup>+</sup> neurons are located lateral to the developing Stn region (asterisks in P,Q). Images in O,R represent details of the ventrolateral medulla where A1/C1 and NA neurons are settling in. Calibration bar, A-D,G,J,K,M-R, 200µm; E,F,H,I,L, 50µm.



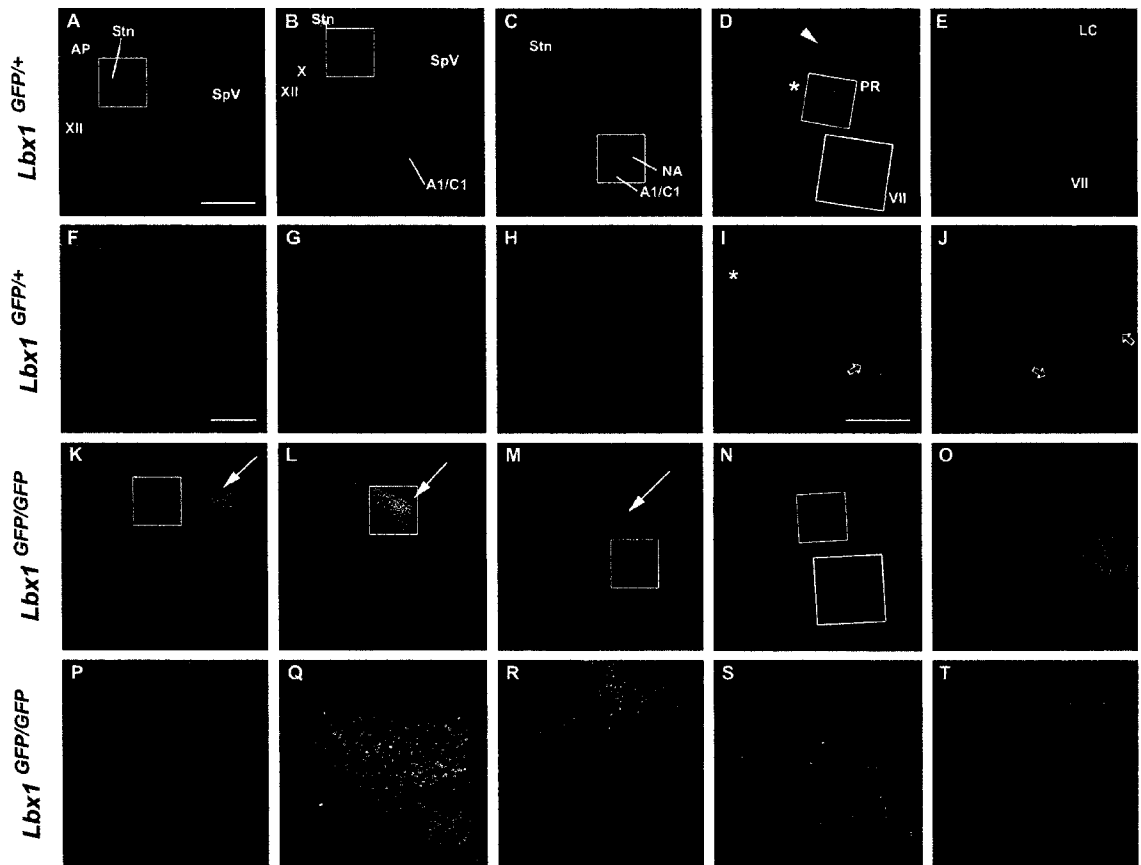


**Figure 5.8** GFP (green) and *Phox2b* (red) expression in the medulla of *Lbx1*<sup>GFP/+</sup> (A-J) and *Lbx1*<sup>GFP/GFP</sup> mice (K-T) at E18. Serial caudo-rostral transverse sections of the medulla of *Lbx1*<sup>GFP/+</sup> and *Lbx1*<sup>GFP/GFP</sup> mice. In *Lbx1*<sup>GFP/+</sup> mice *Phox2b* is expressed in neurons of the Stn, AP, PR formation, motoneurons in NAc and VII nuclei, catecholaminergic neurons in the ventrolateral medulla (A1/C1), A5 neurons and locus ceruleus (LC). Colocalization with GFP/*Lbx1* is only present in the dorsal (asterisks in D,I) and central (open arrow in I) PR formation, within the Ve nucleus (arrowhead in D) and in scattered cells around the facial nucleus (open arrows in J). In *Lbx1*<sup>GFP/GFP</sup> mice *Phox2b* is expressed in similar regions. In addition, *Phox2b* is coexpressed with GFP in a large number of cells within the central portion of the putative region of SpV (arrows in K-M) and in the PR formation (N). Details in F-I and P-S correspond to boxes shown in A-D and K-N, respectively. J and T are details of the VII nucleus in D and N respectively. Calibration bar, A-E, K-O, 500  $\mu$ m; F-H,P,Q,S, 100  $\mu$ m; I,J,R,T, 200  $\mu$ m.

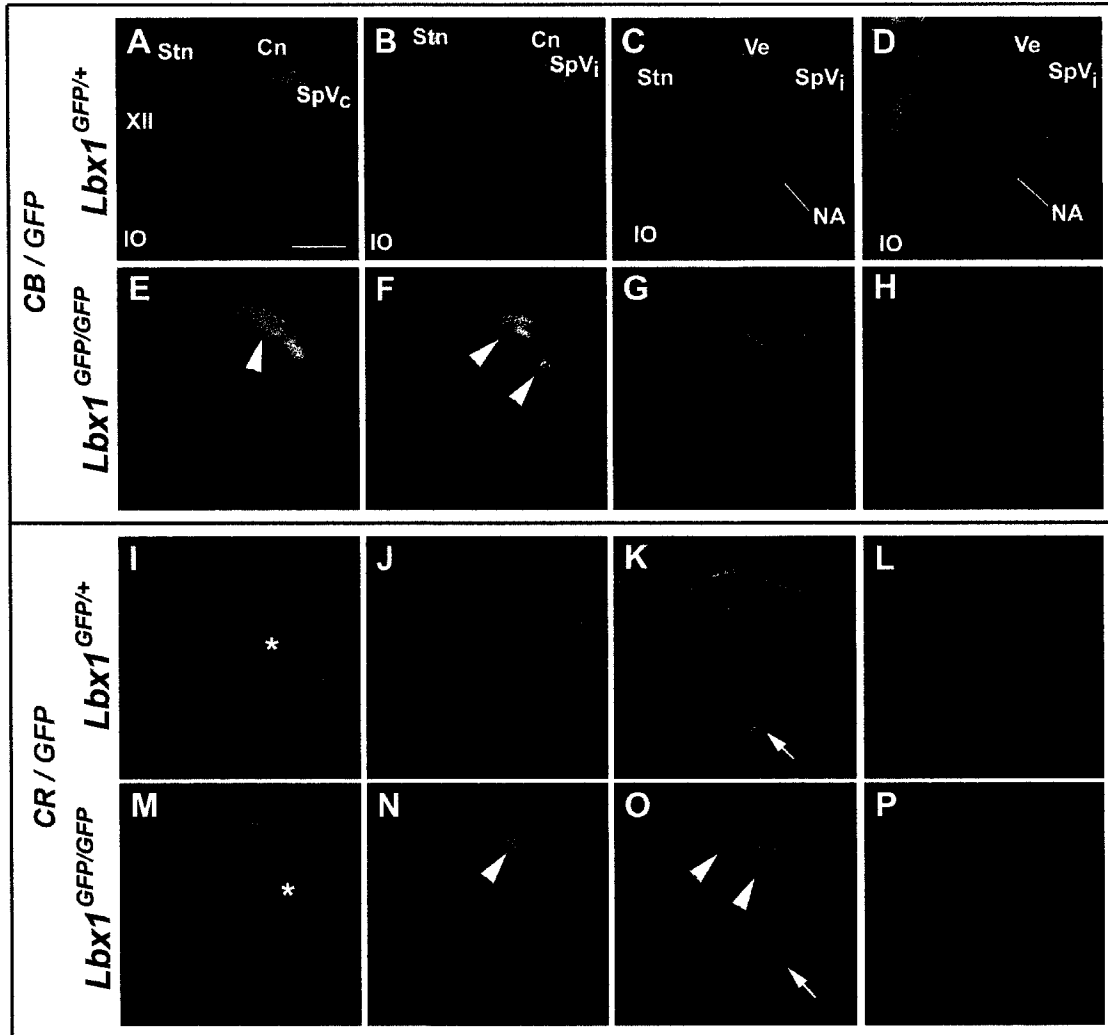


**Figure 5.9** GFP (green), Calbindin (CB, red, top panel) and calretinin (CR, red, bottom panel) expression in the medulla of *Lbx1<sup>GFP/+</sup>* and *Lbx1<sup>GFP/GFP</sup>* mice at E18. Serial caudo-rostral transverse sections of the medulla originally immunostained for both CR and CB. The staining for CB and CR has been splitted in two different panels and CB and CR have been represented with the same pseudocolor (red) to allow for better comparison. In *Lbx1<sup>GFP/+</sup>* mice CB and CR are expressed in neurons within the Stn, Cn/Gr, the region lateral to XII nucleus, in scattered cells in the medulla and Ve. Note the enlarged extension of CB expression in the Stn and in the GFP<sup>+</sup> domains (arrowheads in E,F) and the absence of CR<sup>+</sup> in the lateral reticular formation (asterisks in I,M) and in the ventrolateral medulla (arrows in K,M). Several GFP<sup>+</sup> cells in the GFP<sup>+</sup> clusters are also CR<sup>+</sup> (arrowheads in N,O) Calibration bar, 500µm.

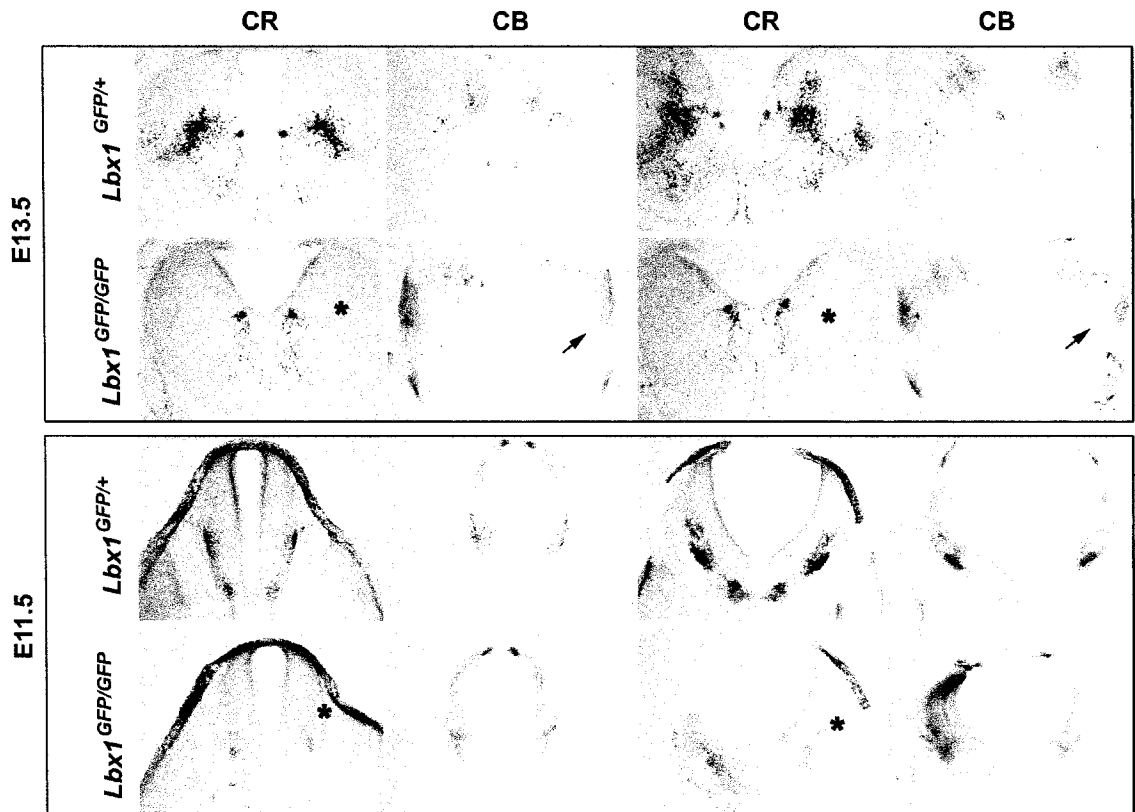


**Figure 5.10** Calretinin (CR, first and third column) and Calbindin (CB, second and fourth column) expression in the medulla of  $Lbx1^{GFP/+}$  and  $Lbx1^{GFP/GFP}$  mice at E13.5 (top panel) and E11.5 (bottom panel). Adjacent transverse sections of two caudo-rostral level of the medulla of  $Lbx1^{GFP/+}$  and  $Lbx1^{GFP/GFP}$  mice. CR expression in the medulla of E11.5 and E13.5 mice is reduced in  $Lbx1^{GFP/GFP}$  mice. Note the absence of laterally migrating neurons at E13.5 (asterisks). CB expression in the medulla of E13.5 is increased in the laterally migrating neurons in  $Lbx1^{GFP/GFP}$  mice (arrows). Note the intense staining of longitudinally oriented fibres in the developing ventrolateral medulla  $Lbx1^{GFP/GFP}$  mice (ventral to arrows).

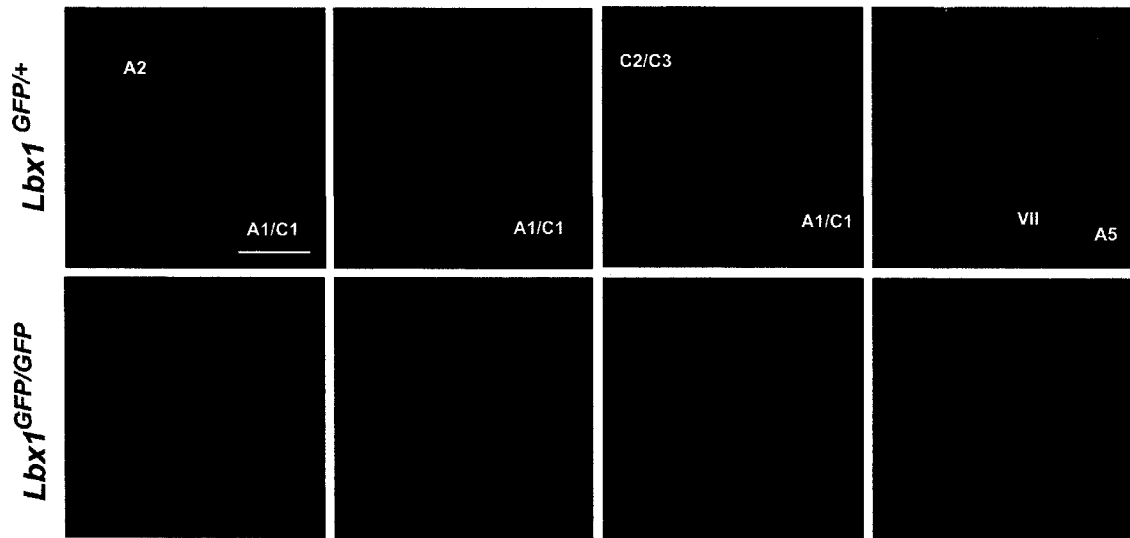


**Figure 5.11** GFP (green) and TH (red) expression in the medulla of *Lbx1*<sup>GFP/+</sup> and *Lbx1*<sup>GFP/GFP</sup> mice at E18. Serial caudo-rostral transverse sections of the medulla of *Lbx1*<sup>GFP/+</sup> and *Lbx1*<sup>GFP/GFP</sup> mice immunostained for TH. Note the intense labelling in the nor/adrenergic structures. In A1/C1 and A5 group there is a statistically significant increase in TH<sup>+</sup> neurons. Calibration bar, 500  $\mu$ m.

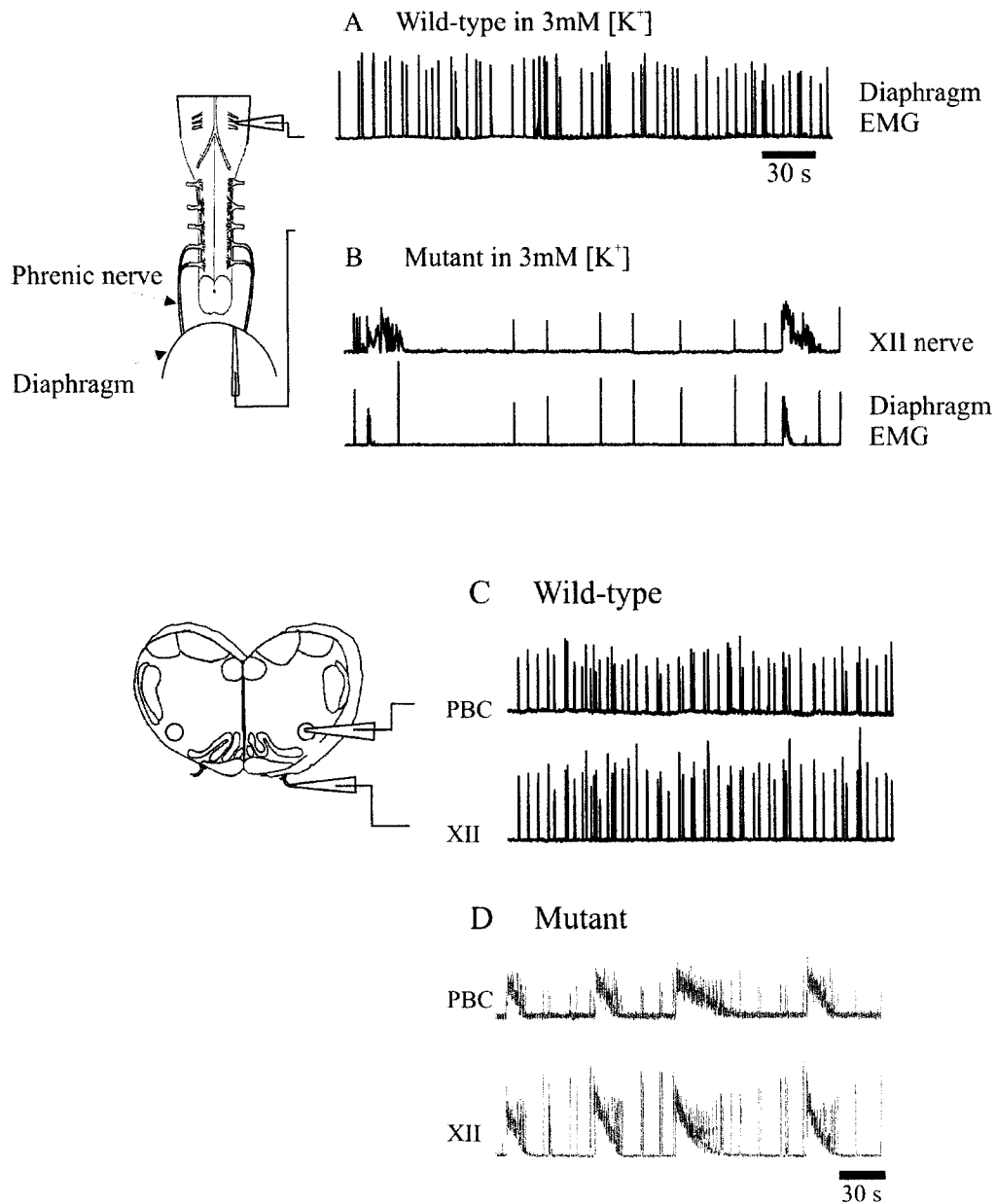


**Figure 5.12 Respiratory discharge patterns generated in the brainstem-spinal cord-diaphragm preparations (top) and in the medullary slice preparations of wild-type (A,C) and mutant (B,D) animals at E18.** Top, rectified and integrated suction electrode recordings of diaphragm EMG and XII nerve from E18 wild type and *Lbx1*<sup>GFP/GFP</sup> mice. Bottom, rectified and integrated suction electrode recordings were made from preBötC and XII nerve from E18 wild type and *Lbx1*<sup>GFP/GFP</sup> mice. Note the occurrence of large amplitude and long duration burst in both preparations in the preBötC, XII nerve and diaphragm.

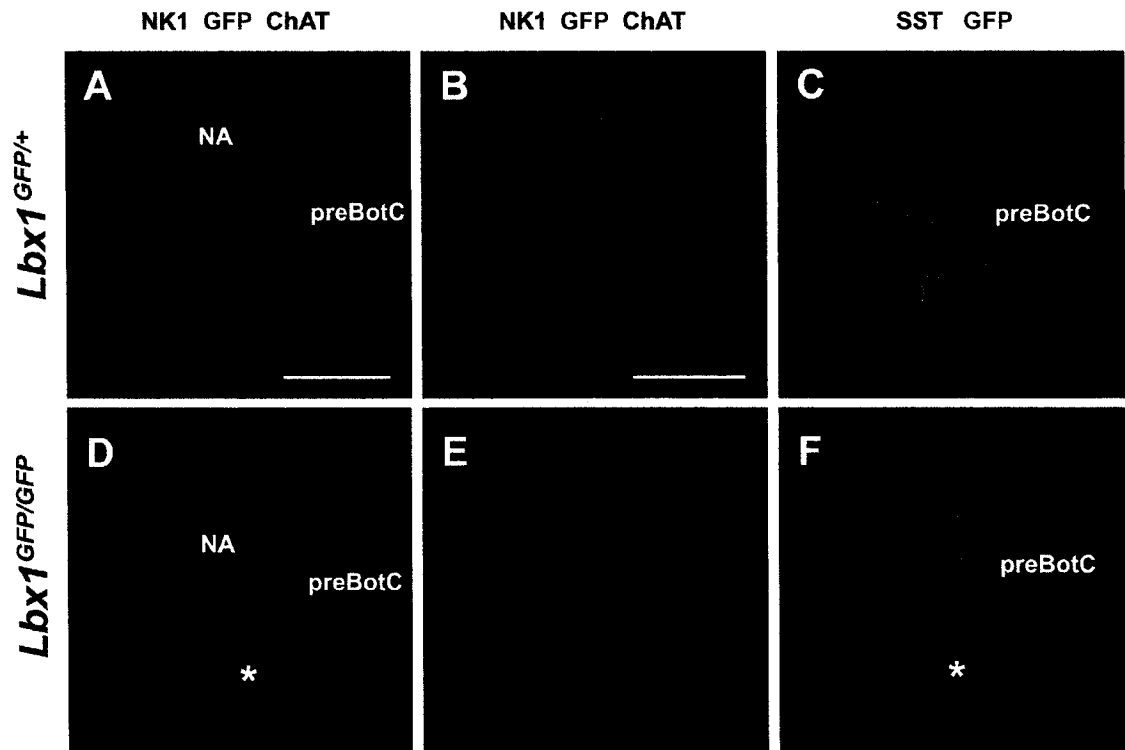


**Figure 5.13** GFP (green, A-F), NK1R (red, A,B,D,E), ChAT (blue, A,B,D,E) and SST (red, C,F) expression in the ventrolateral medulla of *Lbx1*<sup>GFP/+</sup> and *Lbx1*<sup>GFP/GFP</sup> mice at E18. PreBötC neurons (NK1R<sup>+</sup>/ChAT<sup>-</sup> and SST<sup>+</sup>) are present in both *Lbx1*<sup>GFP/+</sup> and *Lbx1*<sup>GFP/GFP</sup> mice. B and E are details of preBötC neurons from A and D respectively. Note the reduction in GFP<sup>+</sup> neurons within the network of the ventrolateral medulla (asterisks). Calibration bars, A,C,D,F, 200  $\mu$ m; B,E, 100 $\mu$ m.

## 5.5 REFERENCES

- Al-Zubaidy ZA, Erickson RL, Greer JJ (1996) Serotonergic and noradrenergic effects on respiratory neural discharge in the medullary slice preparation of neonatal rats. *Pflugers Arch* 431:942-949.
- Arai R, Winsky L, Arai M, Jacobowitz DM (1991) Immunohistochemical localization of calretinin in the rat hindbrain. *J Comp Neurol* 310:21-44.
- Ballanyi K, Onimaru H, Homma I (1999) Respiratory network function in the isolated brainstem-spinal cord of newborn rats. *Prog Neurobiol* 59:583-634.
- Benarroch EE (2006) Pain-autonomic interactions. *Neurol Sci* 27 Suppl 2:S130-133.
- Bloch-Gallego E, Causeret F, Ezan F, Backer S, Hidalgo-Sanchez M (2005) Development of precerebellar nuclei: instructive factors and intracellular mediators in neuronal migration, survival and axon pathfinding. *Brain Res Brain Res Rev* 49:253-266.
- Borday C, Wrobel L, Fortin G, Champagnat J, Thaeron-Antono C, Thoby-Brisson M (2004) Developmental gene control of brainstem function: views from the embryo. *Prog Biophys Mol Biol* 84:89-106.
- Bourrat F, Sotelo C (1990) Migratory pathways and selective aggregation of the lateral reticular neurons in the rat embryo: a horseradish peroxidase in vitro study, with special reference to migration patterns of the precerebellar nuclei. *J Comp Neurol* 294:1-13.
- Brunet JF, Pattyn A (2002) Phox2 genes - from patterning to connectivity. *Curr Opin Genet Dev* 12:435-440.
- Burrill JD, Moran L, Goulding MD, Saueressig H (1997) PAX2 is expressed in multiple spinal cord interneurons, including a population of EN1+ interneurons that require PAX6 for their development. *Development* 124:4493-4503.
- Celio MR (1990) Calbindin D-28k and parvalbumin in the rat nervous system. *Neuroscience* 35:375-475.
- Chatonnet F, Dominguez del Toro E, Thoby-Brisson M, Champagnat J, Fortin G, Rijli FM, Thaeron-Antono C (2003) From hindbrain segmentation to breathing after

- birth: developmental patterning in rhombomeres 3 and 4. *Mol Neurobiol* 28:277-294.
- Cheng L, Chen CL, Luo P, Tan M, Qiu M, Johnson R, Ma Q (2003) *Lmx1b*, *Pet-1*, and *Nkx2.2* coordinately specify serotonergic neurotransmitter phenotype. *J Neurosci* 23:9961-9967.
- Cheng L, Samad OA, Xu Y, Mizuguchi R, Luo P, Shirasawa S, Goulding M, Ma Q (2005) *Lbx1* and *Tlx3* are opposing switches in determining GABAergic versus glutamatergic transmitter phenotypes. *Nat Neurosci* 8:1510-1515.
- Cheng L, Arata A, Mizuguchi R, Qian Y, Karunaratne A, Gray PA, Arata S, Shirasawa S, Bouchard M, Luo P, Chen CL, Busslinger M, Goulding M, Onimaru H, Ma Q (2004) *Tlx3* and *Tlx1* are post-mitotic selector genes determining glutamatergic over GABAergic cell fates. *Nat Neurosci* 7:510-517.
- Crockett DP, Maslany S, Egger MD (1996) Synaptophysin immunoreactivity and distributions of calcium-binding proteins highlight the functional organization of the rat's dorsal column nuclei. *Brain Res* 707:31-46.
- Dauger S, Pattyn A, Lofaso F, Gaultier C, Goridis C, Gallego J, Brunet JF (2003) *Phox2b* controls the development of peripheral chemoreceptors and afferent visceral pathways. *Development* 130:6635-6642.
- Dietrich S, Schubert FR, Healy C, Sharpe PT, Lumsden A (1998) Specification of the hypaxial musculature. *Development* 125:2235-2249.
- Ding YQ, Yin J, Kania A, Zhao ZQ, Johnson RL, Chen ZF (2004) *Lmx1b* controls the differentiation and migration of the superficial dorsal horn neurons of the spinal cord. *Development* 131:3693-3703.
- Ding YQ, Marklund U, Yuan W, Yin J, Wegman L, Ericson J, Deneris E, Johnson RL, Chen ZF (2003) *Lmx1b* is essential for the development of serotonergic neurons. *Nat Neurosci* 6:933-938.
- Ellenberger HH, Feldman JL (1994) Origins of excitatory drive within the respiratory network: anatomical localization. *Neuroreport* 5:1933-1936.
- Feldman JL, Smith JC (1989) Cellular mechanisms underlying modulation of breathing pattern in mammals. *Ann N Y Acad Sci* 563:114-130.

- Ferland RJ, Cherry TJ, Preware PO, Morrisey EE, Walsh CA (2003) Characterization of Foxp2 and Foxp1 mRNA and protein in the developing and mature brain. *J Comp Neurol* 460:266-279.
- Funk GD, Smith JC, Feldman JL (1993) Generation and transmission of respiratory oscillations in medullary slices: role of excitatory amino acids. *J Neurophysiol* 70:1497-1515.
- Goulding M, Pfaff SL (2005) Development of circuits that generate simple rhythmic behaviors in vertebrates. *Curr Opin Neurobiol* 15:14-20.
- Gray PA, Rekling JC, Bocchiaro CM, Feldman JL (1999) Modulation of respiratory frequency by peptidergic input to rhythmogenic neurons in the preBotzinger complex. *Science* 286:1566-1568.
- Gray PA, Janczewski WA, Mellen N, McCrimmon DR, Feldman JL (2001) Normal breathing requires preBotzinger complex neurokinin-1 receptor-expressing neurons. *Nat Neurosci* 4:927-930.
- Greer JJ, Smith JC, Feldman JL (1991) Role of excitatory amino acids in the generation and transmission of respiratory drive in neonatal rat. *J Physiol* 437:727-749.
- Greer JJ, Smith JC, Feldman JL (1992) Respiratory and locomotor patterns generated in the fetal rat brain stem-spinal cord in vitro. *J Neurophysiol* 67:996-999.
- Gross MK, Dottori M, Goulding M (2002) Lbx1 specifies somatosensory association interneurons in the dorsal spinal cord. *Neuron* 34:535-549.
- Gross MK, Moran-Rivard L, Velasquez T, Nakatsu MN, Jagla K, Goulding M (2000) Lbx1 is required for muscle precursor migration along a lateral pathway into the limb. *Development* 127:413-424.
- Guo H, Hellard DT, Huang L, Katz DM (2005) Development of pontine noradrenergic A5 neurons requires brain-derived neurotrophic factor. *Eur J Neurosci* 21:2019-2023.
- Guyenet PG, Sevigny CP, Weston MC, Stornetta RL (2002) Neurokinin-1 receptor-expressing cells of the ventral respiratory group are functionally heterogeneous and predominantly glutamatergic. *J Neurosci* 22:3806-3816.

- Hirsch MR, Tiveron MC, Guillemot F, Brunet JF, Goridis C (1998) Control of noradrenergic differentiation and Phox2a expression by MASH1 in the central and peripheral nervous system. *Development* 125:599-608.
- Hoshino M, Nakamura S, Mori K, Kawauchi T, Terao M, Nishimura YV, Fukuda A, Fuse T, Matsuo N, Sone M, Watanabe M, Bito H, Terashima T, Wright CV, Kawaguchi Y, Nakao K, Nabeshima Y (2005) Ptf1a, a bHLH transcriptional gene, defines GABAergic neuronal fates in cerebellum. *Neuron* 47:201-213.
- Huang L, Guo H, Hellard DT, Katz DM (2005) Glial cell line-derived neurotrophic factor (GDNF) is required for differentiation of pontine noradrenergic neurons and patterning of central respiratory output. *Neuroscience* 130:95-105.
- Jagla K, Dolle P, Mattei MG, Jagla T, Schuhbauer B, Dretzen G, Bellard F, Bellard M (1995) Mouse Lbx1 and human LBX1 define a novel mammalian homeobox gene family related to the Drosophila lady bird genes. In: *Mech Dev*, pp 345-356.
- Kuwana S, Tsunekawa N, Yanagawa Y, Okada Y, Kuribayashi J, Obata K (2006) Electrophysiological and morphological characteristics of GABAergic respiratory neurons in the mouse pre-Botzinger complex. *Eur J Neurosci* 23:667-674.
- Lagercrantz H (1987) Neuromodulators and respiratory control in the infant. *Clin Perinatol* 14:683-695.
- Lai CS, Gerrelli D, Monaco AP, Fisher SE, Copp AJ (2003) FOXP2 expression during brain development coincides with adult sites of pathology in a severe speech and language disorder. *Brain* 126:2455-2462.
- Lo L, Morin X, Brunet JF, Anderson DJ (1999) Specification of neurotransmitter identity by Phox2 proteins in neural crest stem cells. *Neuron* 22:693-705.
- Maricich SM, Herrup K (1999) Pax-2 expression defines a subset of GABAergic interneurons and their precursors in the developing murine cerebellum. *J Neurobiol* 41:281-294.
- Melton KR, Iulianella A, Trainor PA (2004) Gene expression and regulation of hindbrain and spinal cord development. *Front Biosci* 9:117-138.
- Moss IR, Inman JG (1989) Neurochemicals and respiratory control during development. *J Appl Physiol* 67:1-13.

- Muller T, Brohmann H, Pierani A, Heppenstall PA, Lewin GR, Jessell TM, Birchmeier C (2002) The homeodomain factor *lhx1* distinguishes two major programs of neuronal differentiation in the dorsal spinal cord. *Neuron* 34:551-562.
- Nakayama K, Nishimaru H, Iizuka M, Ozaki S, Kudo N (1999) Rostrocaudal progression in the development of periodic spontaneous activity in fetal rat spinal motor circuits in vitro. *J Neurophysiol* 81:2592-2595.
- Pagliardini S, Ren J, Greer JJ (2003) Ontogeny of the pre-Botzinger complex in perinatal rats. *J Neurosci* 23:9575-9584.
- Pattyn A, Goridis C, Brunet JF (2000a) Specification of the central noradrenergic phenotype by the homeobox gene *Phox2b*. *Mol Cell Neurosci* 15:235-243.
- Pattyn A, Hirsch M, Goridis C, Brunet JF (2000b) Control of hindbrain motor neuron differentiation by the homeobox gene *Phox2b*. *Development* 127:1349-1358.
- Pattyn A, Morin X, Cremer H, Goridis C, Brunet JF (1997) Expression and interactions of the two closely related homeobox genes *Phox2a* and *Phox2b* during neurogenesis. *Development* 124:4065-4075.
- Pattyn A, Morin X, Cremer H, Goridis C, Brunet JF (1999) The homeobox gene *Phox2b* is essential for the development of autonomic neural crest derivatives. *Nature* 399:366-370.
- Phelan KD, Falls WM (1991) The spinotrigeminal pathway and its spatial relationship to the origin of trigeminospinal projections in the rat. *Neuroscience* 40:477-496.
- Pierrefiche O, Schwarzacher SW, Bischoff AM, Richter DW (1998) Blockade of synaptic inhibition within the pre-Botzinger complex in the cat suppresses respiratory rhythm generation in vivo. *J Physiol* 509 ( Pt 1):245-254.
- Qian Y, Shirasawa S, Chen CL, Cheng L, Ma Q (2002) Proper development of relay somatic sensory neurons and D2/D4 interneurons requires homeobox genes *Rnx/Tlx-3* and *Tlx-1*. *Genes Dev* 16:1220-1233.
- Qian Y, Fritsch B, Shirasawa S, Chen CL, Choi Y, Ma Q (2001) Formation of brainstem (nor)adrenergic centers and first-order relay visceral sensory neurons is dependent on homeodomain protein *Rnx/Tlx3*. *Genes Dev* 15:2533-2545.
- Ren J, Greer JJ (2003) Ontogeny of rhythmic motor patterns generated in the embryonic rat spinal cord. *J Neurophysiol* 89:1187-1195.

- Resibois A, Rogers JH (1992) Calretinin in rat brain: an immunohistochemical study. *Neuroscience* 46:101-134.
- Schubert FR, Dietrich S, Mootoosamy RC, Chapman SC, Lumsden A (2001) Lbx1 marks a subset of interneurons in chick hindbrain and spinal cord. *Mech Dev* 101:181-185.
- Schwarzacher SW, Pestean A, Gunther S, Ballanyi K (2002) Serotonergic modulation of respiratory motoneurons and interneurons in brainstem slices of perinatal rats. *Neuroscience* 115:1247-1259.
- Shao XM, Feldman JL (1997) Respiratory rhythm generation and synaptic inhibition of expiratory neurons in pre-Botzinger complex: differential roles of glycinergic and GABAergic neural transmission. *J Neurophysiol* 77:1853-1860.
- Shirasaki R, Pfaff SL (2002) Transcriptional codes and the control of neuronal identity. *Annu Rev Neurosci* 25:251-281.
- Shirasawa S, Arata A, Onimaru H, Roth KA, Brown GA, Horning S, Arata S, Okumura K, Sasazuki T, Korsmeyer SJ (2000) Rnx deficiency results in congenital central hypoventilation. *Nat Genet* 24:287-290.
- Shu W, Yang H, Zhang L, Lu MM, Morrisey EE (2001) Characterization of a new subfamily of winged-helix/forkhead (Fox) genes that are expressed in the lung and act as transcriptional repressors. *J Biol Chem* 276:27488-27497.
- Smith JC, Ellenberger HH, Ballanyi K, Richter DW, Feldman JL (1991) Pre-Botzinger complex: a brainstem region that may generate respiratory rhythm in mammals. *Science* 254:726-729.
- Solomon IC, Edelman NH, Neubauer JA (1999) Patterns of phrenic motor output evoked by chemical stimulation of neurons located in the pre-Botzinger complex in vivo. *J Neurophysiol* 81:1150-1161.
- Stanke M, Junghans D, Geissen M, Goridis C, Ernsberger U, Rohrer H (1999) The Phox2 homeodomain proteins are sufficient to promote the development of sympathetic neurons. *Development* 126:4087-4094.
- Stornetta RL, Rosin DL, Wang H, Sevigny CP, Weston MC, Guyenet PG (2003) A group of glutamatergic interneurons expressing high levels of both neurokinin-1

- receptors and somatostatin identifies the region of the pre-Botzinger complex. *J Comp Neurol* 455:499-512.
- Takahashi K, Liu FC, Hirokawa K, Takahashi H (2003) Expression of *Foxp2*, a gene involved in speech and language, in the developing and adult striatum. *J Neurosci Res* 73:61-72.
- Tiveron MC, Hirsch MR, Brunet JF (1996) The expression pattern of the transcription factor *Phox2* delineates synaptic pathways of the autonomic nervous system. *J Neurosci* 16:7649-7660.
- Tsarovina K, Pattyn A, Stubbusch J, Muller F, van der Wees J, Schneider C, Brunet JF, Rohrer H (2004) Essential role of Gata transcription factors in sympathetic neuron development. *Development* 131:4775-4786.
- Viemari JC, Maussion G, Bevingut M, Burnet H, Pequignot JM, Nepote V, Pachnis V, Simonneau M, Hilaire G (2005) *Ret* deficiency in mice impairs the development of A5 and A6 neurons and the functional maturation of the respiratory rhythm. *Eur J Neurosci* 22:2403-2412.
- Wallen A, Perlmann T (2003) Transcriptional control of dopamine neuron development. *Ann N Y Acad Sci* 991:48-60.
- Wang VY, Rose MF, Zoghbi HY (2005) *Math1* expression redefines the rhombic lip derivatives and reveals novel lineages within the brainstem and cerebellum. *Neuron* 48:31-43.
- Yang C, Kim HS, Seo H, Kim CH, Brunet JF, Kim KS (1998) Paired-like homeodomain proteins, *Phox2a* and *Phox2b*, are responsible for noradrenergic cell-specific transcription of the dopamine beta-hydroxylase gene. *J Neurochem* 71:1813-1826.
- Zellmer E, Zhang Z, Greco D, Rhodes J, Cassel S, Lewis EJ (1995) A homeodomain protein selectively expressed in noradrenergic tissue regulates transcription of neurotransmitter biosynthetic genes. *J Neurosci* 15:8109-8120.

## **CHAPTER VI**

### **General Discussion**

The main purpose of the work reported in this thesis was directed toward elucidating key developmental issues concerned with the respiratory rhythm-generating center located in the rodent ventrolateral medulla. Specifically, the first project of my thesis aimed to determine the birth date, the settlement, and the inception of functional activity of preBötC neurons in the developing embryonic rat (Chapter II). The second project aimed to determine the anatomical defects in an animal model for PWS (Chapter III) that may account for the breathing and other behavioral abnormalities associated with the developmental anomaly. In the third project, I developed a novel experimental approach to further evaluate electrophysiological properties of NK1R<sup>+</sup> preBötC neurons, thought to be critical for inspiratory rhythmogenesis, in the perinatal period (Chapter IV). The last project initially set out to determine the anatomical abnormalities that could explain the severe respiratory dysfunction at birth in *Lbx1*<sup>GFP/GFP</sup> mice. The study subsequently expanded into a detailed study of *Lbx1* expression and its role in determining neuronal cell fate and neurotransmitter phenotype throughout the medulla (Chapter VI).

## **6.1 ONTOGENY OF PREBÖTZINGER COMPLEX NEURONS IN PERINATAL RATS**

Since the publication of the study conducted by Smith and collaborators (1991), the region of the preBötC has been a major focus of research in the field of respiratory neurobiology. A large number of studies directed to elucidating mechanisms governing respiratory rhythm regulation have been performed using rodent perinatal in vitro preparations because of their ability to generate spontaneous respiratory-like rhythmic activity (Suzue, 1984). Although maturational changes in the respiratory network occur with development, these perinatal experimental preparations provide the necessary experimental approach for understanding the basic mechanisms underlying the generation and modulation of respiratory rhythms. It is therefore of fundamental importance to understand the developmental process underlying respiratory rhythm generation for the

interpretation of experimental results obtained in these models. Further, abnormalities of respiratory control during the newborn period are of major clinical significance.

Respiratory-like activity has been detected by means of ultrasound recordings and phrenic nerve recordings in utero in several mammalian species (Rigatto, 1992, 1996; Kobayashi et al., 2001; Cosmi et al., 2003). By birth, the respiratory network is already functional and, in normal conditions, able to support life and maintain adequate oxygen levels in the body.

Previous studies in rodents have demonstrated maturational changes of electrophysiological properties within the neuronal respiratory network (reviewed in Hilaire and Duron, 1999; Greer et al., 2006). The majority of these studies focused on the establishment of a respiratory motor output (phrenic nerve activity, diaphragm contractions, plethysmographic recordings (Di Pasquale et al., 1992; Greer et al., 1992; Onimaru and Homma, 2002; Ren and Greer, 2003; Viemari et al., 2003), but we realized that there was a lack in the current literature of experimental data that focused on the specific development of preBötC neurons in the medulla. Further, no combined anatomical and physiological data concerning preBötC were yet available. This was the aim of work in Chapter II (Pagliardini et al., 2003).

We provided anatomical and electrophysiological data regarding the ontogeny of the preBötC neurons in rats. Previous data showed that rhythmic activity could be recorded from XII and C4 nerve roots in the early stages of rat development (Di Pasquale et al., 1992; Greer et al., 1992; Ren and Greer, 2003). A rhythmic activity, likely of spinal origin and non-respiratory related, could be detected as early as E13.5. This non-respiratory activity could be identified by the characteristics of their bursts, having large amplitude, long duration and not being accompanied by a diaphragm contraction (Onimaru and Homma, 2002). This activity is the result of cholinergic, glycinergic and GABAergic-mediated networks, which gradually develop and switch to a more mature glutamatergic (non-NMDA) mediated activity (Ren and Greer, 2003) and subsequently disappear. In the later stages of gestation (E16-E18) another spontaneous rhythmic activity emerges; this activity is of medullary origin and likely respiratory related, characterized by smaller bursts, shorter duration and accompanied by diaphragm

contractions (Di Pasquale et al., 1992; Greer et al., 1992; Onimaru and Homma, 2002; Ren and Greer, 2003). Our recordings from medullary slice preparation showed that a respiratory like rhythm emerged around E17 within the preBötC. With progression of embryonic development, the frequency and amplitude of inspiratory discharge increases and the variability of respiratory cycles diminishes. By E20, the characteristics of respiratory rhythmic activity are similar to the ones recorded in neonatal animals.

We also showed that, contrary to previous reports (Ptak et al., 1999), respiratory frequency can be modulated by SubP as early as E17. This effect is the result of the emergence of NK1R expression on respiratory neurons in the preBötC. SubP is able to increase respiratory rhythm in both brainstem-spinal cord and medullary slice preparation, similarly to the data obtained in the neonatal period (Monteau et al., 1996; Viemari et al., 2003).

By means of BrdU injections we determined the birth date of NK1R<sup>+</sup> preBötC neurons. Previous studies on the ontogeny of the medulla identified the genesis of lower medullary neurons (Altman and Bayer, 1980; Phelps et al., 1990). Given the heterogeneity of neuronal populations in the ventrolateral medulla, Altman and Bayer's study (1980) provided general birthdating data on the mixed neuronal population located in the ventrolateral medulla without identifying and birth dating the specific neuronal phenotypes. This study (Chapter II; (Pagliardini et al., 2003) provided specific information on the ontogeny and settlement of NK1R<sup>+</sup> neurons within the preBötC region. Specifically we identified the time frame in which the majority of neurons were generated (E12.5-13.5), the time of settlement in the ventrolateral medulla (E16-17) and provided specific information on the growth changes of preBötC neurons during the late stages of gestation.

Using NK1R and SST immunoreactivity in combination with BrdU incorporation, we identified the region corresponding to the preBötC and its NK1R<sup>+</sup>/SST<sup>+</sup> neurons as early as E17. The lack of expression of NK1R during earlier stages of development limited our studies to the developmental stage of settlement and inception of functional activity. We were unable to track cells during their division and migration because no other marker, to our knowledge, could identify preBötC neurons in earlier stages of

development. Therefore our study cannot provide any information on the developmental origin of preBötC neurons in terms of either rostrocaudal (rhombomere location) or dorsoventral (precursor domain in the ventricular layer) location of the neuronal progenitors.

Once the expression of early markers for preBötC neurons (i.e. a combinatorial code of specific developmentally expressed TFs or other specific markers) will be identified, it will be possible to: i) study early stages of preBötC neurons development (identification of progenitor domain, migratory pattern, establishment of synaptic connections within the respiratory network); ii) analyze the abnormalities, if present, induced by the selective inactivation of genes (in knockout or conditional knock out mice) that specify the identity of preBötC neurons.

These studies will be important for characterizing the developmental program occurring more generally in the medulla that promotes for such a high heterogeneity of neurons and neuronal networks coexisting in the reticular formation. They will also be fundamental in order to correlate possible defects in the preBötC with pathologies with known and unknown etiology that determine respiratory deficiency (SIDS, for example).

Following the publication of our study (Pagliardini et al., 2003), another group has looked at the ontogeny of the preBötC in the mouse embryo (Thoby-Brisson et al., 2005). Thoby-Brisson and colleagues showed that the mouse preBötC is functionally active by E15. They confirmed that preBötC neurons commence expressing NK1R at the time when respiratory rhythmic activity commences, that respiratory rhythms, similarly to what happens in the neonatal period, are sustained by a glutamatergic non-NMDA mediated synaptic transmission and that respiratory activity can be modulated by SubP and  $\mu$ OR agonists. These data are in accordance with what we have shown in Chapter II, since the development of the mouse embryo is delayed by a couple of days with respect to the rat. Interestingly, they also showed that by E15 preBötC pacemaker neurons could be identified by electrophysiological recordings, providing further evidence for a possible role of preBötC neurons in the early establishment of respiratory rhythm generation.

The region of pFRG/RTN has been proposed to be an alternative site to respiratory rhythm generation in the neonatal period (Onimaru et al., 2006b; Onimaru et

al., 2006a) or, alternatively, a region responsible for expiratory rhythm generation (Janczewski and Feldman, 2006; Onimaru et al., 2006b) in juvenile and adult rats. Our study did not aim to investigate the ontogeny of the pFRG, although we detected a peak of neurogenesis at E11 in the region around the facial nucleus, likely corresponding to the RTN/pFRG neurons. These data suggest therefore that the neurogenesis of RTN/pFRG could occur before the generation of preBötC neurons.

Since a specific marker for RTN/pFRG does not exist at present, it is impossible to determine the anatomical boundaries and the developmental process occurring in this region. Further analyses of the phenotype and other physiological properties of the RTN/pFRG neurons are now necessary in order to specifically identify this neuronal population.

Recent imaging studies in the rat fetal period (Onimaru and Homma, 2005) indicate that within a respiratory cycle, inspiratory burst activity is initially generated in the preBötC and then spreads to the parafacial area in the early stages of development (E17-18), whereas in older animals (E18-20 and neonatal period) the pFRG/RTN area is active before the preBötC region (Onimaru and Homma, 2003, 2005). The authors suggest that in the early stages of development preBötC neurons drive respiratory rhythm activity, whereas in the late gestation and in the neonatal period pFRG/RTN is the principal respiratory rhythm generator. Further studies will be necessary to establish the exact nature of neurons corresponding to pFRG/RTN in terms of physiological, pharmacological and anatomical properties both in the adult and in the perinatal period. Once specific markers for the respiratory neurons within this region exist, it will be possible to conduct further studies on the ontogeny of RTN/pFRG neurons, the organization of functional connections with the preBötC and their relative contribution to the establishment of respiratory rhythms in the fetal period.

Further, the presence of neurons with pacemaker properties in the preBötC region and their susceptibility to neuromodulators as early as the commencement of the respiratory drive (Pagliardini et al., 2003; Thoby-Brisson et al., 2005) suggest that preBötC neurons may indeed have a critical role in the establishment of respiratory rhythms. If a reconfiguration of the network occurs within few days from the

establishment of respiratory rhythms, it still has to be demonstrated. Further studies aimed to identify, record and selectively block either the preBötC or the RTN/pFRG region will be necessary to determine the relative contribution of the RTN/pFRG to the respiratory (inspiratory/expiratory) activity in the late stages of gestation.

## 6.2 ANALYSIS OF DEVELOPMENTAL ABNORMALITIES IN THE MEDULLA OF *NDN*<sup>*tm2Stw*</sup> MICE

In chapter II we laid the foundation for interpreting and analyzing data obtained on the medulla, and in particular on the preBötC region, in the early stages of embryonic development. We acquired knowledge on the NK1/SST expression pattern in the preBötC during development and we determined the time of inception of respiratory rhythms, their stabilization and the effects of neuromodulators on the preBötC in the prenatal period. We used this novel information to study abnormalities in mutant animals that show respiratory defect at birth (Chapter III and Chapter V).

The *Ndn*<sup>*tm2Stw*</sup> mouse studied in chapter III is an animal model for PWS. Although the function of neccdin has not been completely identified, several pieces of evidence show that neccdin is expressed predominantly in postmitotic neurons, it is implicated in cell cycle regulation and terminal neuronal differentiation (Kuwako et al., 2004), it interacts with several cell cycle regulatory transcription factors (Taniura et al., 1998; Kobayashi et al., 2002), homeodomain transcription factors (Masuda et al., 2001), cytoskeletal proteins (Lee et al., 2005) and the TrkA and p75 low affinity neurotrophin receptors (Andrieu et al., 2003; Kuwako et al., 2004).

The strain of *Ndn*<sup>*tm2Stw*</sup> mouse that we analyzed dies at birth due to a central respiratory defect (Ren et al., 2003). We investigated the cytoarchitectural, anatomical and electrophysiological properties of the developing medulla to determine whether there were defects within the preBötC or synaptic inputs that regulate respiratory rhythmogenesis. Consistent with the role of neccdin in axonal growth and elongation (Lee et al., 2005), we identified several defects in the medulla and spinal cord of *Ndn*<sup>*tm2Stw*</sup> mice. Among these defects, defasciculation and irregular projections of axonal tracts, aberrant neuronal migration, and a major defect in the cytoarchitecture of the cuneate/gracile nuclei, including dystrophic axons were the main abnormalities in these animals.

Recent evidence has confirmed that the defects we observed in the sensory pathway within axonal tracts of the gracile/cuneate nuclei and funiculi are likely

determined by a distal degeneration of NGF-dependent dorsal root ganglia axons caused by the inactivation of *Necdin* (Takazaki et al., 2002; Kuwako et al., 2005).

In *Ndn<sup>tm2Srw</sup>* mice, we also observed a reduction in size of several motoneuronal pools in the spinal cord and the medulla. These results can be likely explained by the evidence that *necdin* interacts with and promotes activation of p75 and TrkA neurotrophin receptors, having then a regulatory role on apoptosis and survival of NGF-dependent motoneurons (Tcherpakov et al., 2002; Kuwako et al., 2004; Kuwako et al., 2005).

We analyzed in detail the VRG of the *Ndn<sup>tm2Srw</sup>* mice and we could not identify a clear defect within the preBötC neurons by means of NK1R and SST immunoreactivity. Interestingly, axonal tracts immunoreactive for 5HT and SubP, two major neuromodulators acting on preBötC neurons (Chapter I), appeared to be abnormal. 5HT<sup>+</sup> and SubP<sup>+</sup> fibers within the ventrolateral medulla were swollen and enlarged in mutants, suggesting the presence of axonal defects also in neurons that provide neuromodulatory drive to the preBötC. Exogenous application of neuromodulators alleviated the long periods of slow respiratory rhythms and apnea, but some instability of rhythmogenesis persisted. These results suggest that *Necdin* has an important role on proper neuronal development and, as a consequence, function of the respiratory rhythm generating center and/or the neuronal structures responsible for the neuromodulatory drive to the preBötC.

Further analysis at an ultrastructural level in the preBötC region will be critical in order to determine if defects exist in the cytoskeletal structure or in the synaptic machinery of respiratory neurons of *Ndn<sup>tm2Srw</sup>* mice. Furthermore, single cell recording of pacemaker neurons, possibly via identification with TMR-SubP application (chapter IV), will be able to elucidate the physiological properties underlying the respiratory abnormalities that have been previously described (Ren et al., 2003).

In fact, since application of neuromodulators is not sufficient to maintain a regular respiratory rhythmic activity, it is possible that major abnormalities exist within preBötC neurons, either at the post-synaptic level (altered response to synaptic inputs) or at the level of axonal transmission within the respiratory network (an inability to transmit adequate signals to follower neurons). We might in fact speculate that *necdin* could interact not only with TrkA and p75 receptors (Andrieu et al., 2003; Kuwako et al.,

2004), but also with other receptors located on the membrane of preBötC neurons and therefore the absence of *necdin* could alter their electrophysiological properties and determine abnormal respiratory rhythm activity.

The presence of an increased number of TH<sup>+</sup> neurons in several catecholaminergic groups was striking. We do not have experimental data to propose that abnormalities in the nor/adrenaline system may be responsible for the respiratory defects, since brainstem spinal cord and medullary slice preparations that were devoid of the proposed noradrenergic structures responsible for neuromodulation of the respiratory activity (A5 and A6 neurons) were still abnormal. We also did not focus on these pontine regions, but limited our analysis to the medulla; therefore the nor/adrenergic groups A1/C1, A2, C2/C3 and the TH<sup>+</sup> neurons within the ventral bundle and along the midline. A recent report proposes that the A1/C1 nor/adrenergic group, usually implicated in cardiovascular regulation, may influence respiratory frequency (Zanella et al., 2005). Preliminary experiments aimed to block the noradrenergic inputs on the preBötC neurons of *Ndn*<sup>tm2Sfw</sup> mice did not yield any results consistent with this hypothesis (Ren, personal communication), suggesting that the abnormalities in the hindbrain catecholaminergic system are likely not implicated in respiratory modulation.

A recent publication also showed that *necdin* interacts with Dlx2 (distal-less homeobox) homeodomain protein (Kuwayama et al., 2006), which is involved in the differentiation and migration of GABAergic neurons in the forebrain and hindbrain (Panganiban and Rubenstein, 2002). In a different strain of *Necdin* deficient mice, absence of *necdin* during embryonic development determines a reduction in numbers of differentiating GABAergic neurons in the developing forebrain (Kuwayama et al., 2006), likely caused by a reduction of transcriptional activation of Dlx homeodomain proteins. In our study we did not test the possibility of abnormalities in the GABAergic system that modulates respiratory activity.

These novel data, are quite interesting because they propose a role for *necdin* in the early stages of development, in particular at the moment of neuronal specification and acquisition of a neuronal phenotype. It will be interesting to study what happens to the neuronal progenitors and differentiating neurons in both the ventral (V0-V3 and MN) and

dorsal (dII-6) hindbrain neuronal progenitors and precursors in the absence of *neccin*. The possibility that *neccin* interacts with specific transcription factors to determine the acquisition of particular neuronal phenotypes could contribute to explain the abnormalities we detected in both the MN pools and the catecholaminergic neurons at the end of gestation. Further analysis of *neccin* interaction with other TFs important in the hindbrain neuronal phenotype specification and the study of their expression in control and *Ndn<sup>tm2Stw</sup>* mice in the period between E10 and E13 will be critical in determining the function of *neccin* in the development of the medulla.

### **6.3 TAGGING OF NK1R<sup>+</sup> PREBÖTZINGER COMPLEX NEURONS WITH TMR-SUBSTANCE P**

A major obstacle in the analysis of properties of pacemaker neurons in the preBötC region is determined by the heterogeneity of the tissue in which they are embedded. Pacemaker neurons are in fact a subpopulation of respiratory preBötC neurons intermingled in a neuronal network represented by other respiratory-related neurons, cardiovascular catecholaminergic and non-catecholaminergic neurons and motoneurons of the external formation of the nucleus ambiguus.

At present, the best marker available to identify a subpopulation of preBötC neurons is NK1R (Gray et al., 1999; Guyenet et al., 2002; Pagliardini et al., 2003). Experimental evidences show that NK1R is expressed in the preBötC neurons of perinatal and rats (Gray et al., 1999; Liu et al., 2001; Guyenet et al., 2002; Pagliardini et al., 2003), mice (Blanchi et al., 2003; Thoby-Brisson et al., 2005), goats (Wenninger et al., 2004a; Wenninger et al., 2004b) and humans (Benarroch et al., 2003).

At present no mutant mice in which NK1R<sup>+</sup> cells tagged with a fluorescent protein (e.g. GFP) have been generated. Therefore the current approach for identifying pacemaker preBötC neurons within a live medullary slice preparation consist in the analysis of voltage dependent properties and persistence of bursting behavior in absence of synaptic transmission (Thoby-Brisson et al., 2000; Thoby-Brisson and Ramirez, 2001; Del Negro et al., 2002; Pena et al., 2004; Pena and Ramirez, 2004; Del Negro et al., 2005) or alternatively in presence of voltage or calcium sensitive dyes (Koshiya and Smith, 1999; Onimaru and Homma, 2003, 2005).

In Chapter IV (Pagliardini et al., 2005), we developed a new method to identify NK1R<sup>+</sup> preBötC neurons in medullary slice preparations. We demonstrated that tagging preBötC neurons with TMR-SubP is a useful tool for identifying respiratory neurons. As mentioned in Chapters I and II, not all NK1R<sup>+</sup> neurons in the preBötC region are rhythmogenic and not every respiratory neuron in the preBötC region is NK1R<sup>+</sup>. It must be noted, however, that the majority of NK1R<sup>+</sup> neurons are respiratory. This technique therefore provides researchers with a fast, economical and efficacious tool to select

primarily respiratory neurons, a small proportion of them with pacemaker properties, in medullary slice preparations.

Since NK1R is expressed in preBötC neurons as early as E17 in rats and continues throughout life, this method will provide a useful tool to further study rhythmogenic properties of both embryonic and postnatal respiratory neurons. The majority of studies of rhythmogenic properties has been in fact conducted in the early postnatal period (Thoby-Brisson et al., 2000; Thoby-Brisson and Ramirez, 2001; Del Negro et al., 2002; Pena et al., 2004; Pena and Ramirez, 2004; Del Negro et al., 2005). A comprehensive understanding of the development of the respiratory centers will require analyzing rhythmogenic properties of respiratory neurons in the embryonic tissue. Although the probability of recording from pacemaker neurons is still limited, the tagging approach can be efficacious to reduce the time for searching respiratory neurons with rhythmogenic properties. Furthermore, the use of TMR-SubP in acutely prepared slices has several advantages: i) it requires a short incubation time before the commencement of the experiment; ii) application of TMR-SubP does not affect the viability of the tissue and it does not affect rhythmogenic properties, since the activity of the slice returned to baseline after washout; iii) the identification for tagged neurons does not required an expensive and elaborated imaging system and further image averaging or signal amplification is not required.

This approach can also be used in mice, in particular in genetically modified mice that present respiratory defects in the perinatal period, in order to easily identify and study pacemaker properties of preBötC neurons, provided that mutant animals still express NK1R in the preBötC neurons. Further analysis of physiological properties on pacemaker neurons will in fact be necessary to establish specific abnormalities in both *Ndn<sup>tm2Stw</sup>* mice and *Lbx1<sup>GFP/GFP</sup>* mice. Further, since some of the RTN/pFRG neurons directly respond to SubP and likely are NK1R<sup>+</sup> (Yamamoto et al., 1992), TMR-SubP tagging could be a powerful tool to study the activity of these neurons in the rostral medulla and their interaction with pacemaker neurons in the preBötC.

We further envisioned a possible development for this technique: if we were able to tag NK1R<sup>+</sup> cells with a fluorescent probe in freshly dissociated neurons from the

embryonic ventrolateral medulla, we would be able to isolate them by means of fluorescent activated cell sorting (FACS) and culture them in appropriate conditions. Previous studies have shown the neurons of the ventrolateral medulla isolated in the perinatal period can survive for several weeks in culture and still show responses to neurotransmitters and chemical stimuli such as pH and CO<sub>2</sub> (Fitzgerald et al., 1992; Rigatto et al., 1992). When the heterogeneous cell population that constitutes the ventrolateral medulla is acutely dissociated, several electrophysiological properties can also be analyzed (Rybak et al., 2003; Ptak et al., 2005). Therefore if we were successful in selecting only NK1R neurons from the ventrolateral medulla we would be able to use this purified primary culture in order to assess biochemical and pharmacological properties. This approach would have the advantage of isolating a relatively pure population of respiratory related neurons (even though heterogeneous in their electrophysiological properties), therefore providing an alternative tool to study properties related (and not) to respiratory rhythm generation at the level of single cell or the whole population.

Preliminary data with this approach have shown few limitations though:

i) The cell sorter machines available at the University of Alberta are able to isolate cells that have been tagged with fluorescent probes that absorb and emit at specific wavelengths. Unfortunately, there is not a laser for the detection of TMR probes; therefore the study had to be carried out with the weaker, but still specific Oregon Green 488-SubP.

ii) The use of FACS technique requires that cells are in a suspension, therefore in primary neuronal cultures this can occur only following acute dissociation and not after several days in culture (neurons would not survive a second trypsinization and plating). This limitation determined that the sorting protocol had to occur following the isolation of tissue and cell dissociation. At this point, cells are very vulnerable, therefore the death rate is high; furthermore, the dissociation procedure not only eliminates extracellular matrix but also temporarily alters the receptor expression on the cell surface and the receptor-mediated internalization machinery. Despite changing several experimental procedures for isolation and dissociation of medullary neurons, we were not able to

obtain a strong and consistent internalization of Oregon Green 488-SubP. This is in contrast with some results recently presented (Johnson, 2006), in which a heterogeneous population of medullary neurons, cultured for several days, was able to specifically internalize TMR-SubP: these results suggest that the isolation protocol is a critical step in the feasibility of our procedure. We recently overcame this problem by using an antibody against NK1R that specifically recognizes an epitope on the extracellular surface of the receptor; therefore, an application of the primary antibody followed by the incubation with a fluorescent-conjugated secondary antibody, allowed us for the detection of specific staining in a subpopulation of neurons of the ventrolateral medulla.

iii) In the ventrolateral medulla, the population of NK1R<sup>+</sup> neurons is quite heterogeneous; respiratory related neurons and NA motoneurons represent two major groups that express NK1R. Thus, in order to obtain the proposed neuronal culture we have to eliminate motoneurons from our sorted population. A feasible procedure would be to select other markers, specific for either respiratory neurons or NA motoneurons that are expressed on the cell surface of the membrane of these cells, double label the heterogeneous population and sort the cells according to the specific markers. We tested this possibility by using antibodies against the extracellular portion of p75 and TrkC receptors that are specifically expressed on NA motoneurons in the perinatal period (we used 20-21 in our preparation) (Ringstedt et al., 1993; Lamballe et al., 1994; Chen et al., 1996; Helke et al., 1998). At this point we were able to isolate two fluorescent neuronal populations: one single labeled for NK1R and the other one single/double labeled for NK1R and p75 or TrkC. The analysis of mRNA expressed in the two labeled neuronal populations by RT-PCR with several markers (NK1R, SST, ChAT,  $\beta$ tubulin, 5HT<sub>4</sub> and 5HT<sub>4A</sub> receptors) revealed that the NK1R<sup>+</sup> neuronal population is either an artifact, a group of glial cells, or represent a subgroup of cells that are dying since the only mRNA that they actually contain is  $\beta$ tubulin, whereas the NK1R<sup>+</sup>/p75<sup>+</sup>/TrkC<sup>+</sup> neurons contain all the markers tested, therefore they still contain NK1R<sup>+</sup>/SST<sup>+</sup> neurons that are allegedly the respiratory neurons that we hoped to isolate.

These preliminary results showed that it is possible to isolate freshly dissociated neurons from the ventrolateral medulla, sort them with the FACS technique and culture

them. This method has though to be further modified in order to specifically separate MNs from the respiratory related neurons that are the object of our study.

#### **6.4 DEVELOPMENTAL ABNORMALITIES IN THE MEDULLA OF MICE LACKING THE EXPRESSION OF THE HOMEODOMAIN TRANSCRIPTION FACTOR *LBX1***

The last project I undertook during my PhD research work (Chapter V) consisted in examining the development of the hindbrain of a genetically modified mouse in which the gene for the transcription factor *Lbx1* has been inactivated by the insertion of the sequence for the green fluorescent protein (Gross et al., 2000). This study was initiated as a collaborative work with the laboratory directed by Dr. Goulding at the Salk Institute. Specifically, *Lbx1* mice die shortly after birth and we tested the hypothesis that this was due to a central respiratory defect. Electrophysiological data from in vitro fetal preparations demonstrated an abnormal respiratory drive. This led to a much more extensive study analyzing the expression pattern of *Lbx1* during hindbrain development and abnormalities induced by inactivation of *Lbx1*. We also characterized different dorsal neuronal populations in the early stages of neuronal differentiation and analyzed the changes of neuronal identity induced by *Lbx1* inactivation.

Our results showed that *Lbx1* is necessary for the proper development of dI4-dI6 and late-born dIL dorsal interneurons and, by inactivating this TF, part of the Cn/Gr neurons and the majority of SpV neurons followed a different neurodevelopmental program and acquired an abnormal phenotype in part resembling the one of Stn and IO formation neurons.

These results provided further information on the specific action of *Lbx1* on hindbrain development. We were able to classify dorsally derived interneurons in different domains according to their TFs expression, similarly to what has been previously shown in the spinal cord (Gross et al., 2000; Muller et al., 2002). *Lbx1* is not expressed in preBötC neurons in the developing medulla, thus our study did not provide further information on the combinatorial code that identifies preBötC neurons. These

results support the hypothesis that preBötC neurons derive from a ventrally derived domain (Paul Gray, personal communication).

The study on *Lbx1* expressing cells showed that several Lbx1/GFP<sup>+</sup> neurons settled in the ventrolateral pons and medulla, adjacent to and within the respiratory structures of cVRG, rVRG, preBötC, BötC and pFRG/RTN. Do these Lbx1/GFP<sup>+</sup> neurons have a respiratory related function? Are these Lbx1/GFP<sup>+</sup> neurons responsible for some neuromodulatory activity on the respiratory network? We have no experimental data to prove it or even to suggest it. In fact, due to the manifest abnormalities observed in the medulla of *Lbx1*<sup>GFP/GFP</sup> mice, the defects on the respiratory rhythms could just be the consequence of abnormal development of the medulla.

Our results showed that some GFP<sup>+</sup> neurons are indeed embedded with preBötC neurons and in *Lbx1*<sup>GFP/GFP</sup> mice these neurons are almost absent. A further analysis of the phenotype of these neurons showed that they are CR<sup>+</sup>, Pax2<sup>+</sup> and GABA<sup>+</sup>. Are they responsible for providing GABAergic inputs on the preBötC? Are they some subtype of inhibitory respiratory neurons located in the VRG? Further single cell analysis of GFP<sup>+</sup> neurons in medullary slice preparation of *Lbx1*<sup>GFP/+</sup> mice will be necessary to determine their involvement in the respiratory network.

It is possible that *Lbx1* is involved in the regulation of specification of proprioceptive sensory networks in the medulla, similarly to *Phox2b* in the visceral sensory networks (Pattyn et al., 2000; Brunet and Pattyn, 2002). Therefore, if *Lbx1* neurons in the ventral medulla actually interact with the respiratory networks, they could have a role in the integration of sensory inputs that act on the neuronal networks that operates to control respiratory rhythm activity.

## 6.5 CONCLUSIONS

In conclusions, we laid the foundations for the study of the development of respiratory control in experimental animals in normal and pathological conditions. The study of the maturation of the mammalian respiratory system is an important area of research in respiratory neurobiology in consideration of the clinical relevance associated with the gain of a methodical understanding of normal and pathological respiratory regulation during the newborn period. Acquiring a comprehensive knowledge on the basic respiratory regulation mechanisms and the developmental changes that occur in the fetal and perinatal period can have considerable implications in the management of respiratory-related pathologies with known and unknown etiology, such as apnea of prematurity, sleep apnea, sudden infant death syndrome and genetically determined disease (CCHS, Rett Syndrome, PWS).

Further, the discovery of the combinatorial code that identify preBötC neurons and other respiratory related neurons in the VRG will be a fundamental progress in the field of respiratory neurobiology since it will give further tools to analyze the contribution of specific neuronal populations to the neural control of breathing.

## 6.6 REFERENCES

- Altman J, Bayer SA (1980) Development of the brain stem in the rat. I. Thymidine-radiographic study of the time of origin of neurons of the lower medulla. *J Comp Neurol* 194:1-35.
- Andrieu D, Watrin F, Niinobe M, Yoshikawa K, Muscatelli F, Fernandez PA (2003) Expression of the Prader-Willi gene *Necdin* during mouse nervous system development correlates with neuronal differentiation and p75<sup>NTR</sup> expression. *Gene Expr Patterns* 3:761-765.
- Benarroch EE, Schmeichel AM, Low PA, Parisi JE (2003) Depletion of ventromedullary NK-1 receptor-immunoreactive neurons in multiple system atrophy. *Brain* 126:2183-2190.
- Blanchi B, Kelly LM, Viemari JC, Lafon I, Burnet H, Bevenegut M, Tillmanns S, Daniel L, Graf T, Hilaire G, Sieweke MH (2003) *MafB* deficiency causes defective respiratory rhythmogenesis and fatal central apnea at birth. *Nat Neurosci* 6:1091-1100.
- Brunet JF, Pattyn A (2002) *Phox2* genes - from patterning to connectivity. *Curr Opin Genet Dev* 12:435-440.
- Chen EY, Mufson EJ, Kordower JH (1996) TRK and p75 neurotrophin receptor systems in the developing human brain. *J Comp Neurol* 369:591-618.
- Cosmi EV, Anceschi MM, Cosmi E, Piazze JJ, La Torre R (2003) Ultrasonographic patterns of fetal breathing movements in normal pregnancy. *Int J Gynaecol Obstet* 80:285-290.
- Del Negro CA, Koshiya N, Butera RJ, Jr., Smith JC (2002) Persistent sodium current, membrane properties and bursting behavior of pre-botzinger complex inspiratory neurons in vitro. *J Neurophysiol* 88:2242-2250.

- Del Negro CA, Morgado-Valle C, Hayes JA, Mackay DD, Pace RW, Crowder EA, Feldman JL (2005) Sodium and calcium current-mediated pacemaker neurons and respiratory rhythm generation. *J Neurosci* 25:446-453.
- Di Pasquale E, Monteau R, Hilaire G (1992) In vitro study of central respiratory-like activity of the fetal rat. *Exp Brain Res* 89:459-464.
- Di Pasquale E, Tell F, Monteau R, Hilaire G (1996) Perinatal developmental changes in respiratory activity of medullary and spinal neurons: an in vitro study on fetal and newborn rats. *Brain Res Dev Brain Res* 91:121-130.
- Fitzgerald SC, Willis MA, Yu C, Rigatto H (1992) In search of the central respiratory neurons: I. Dissociated cell cultures of respiratory areas from the upper medulla. *J Neurosci Res* 33:579-589.
- Gray PA, Rekling JC, Bocchiaro CM, Feldman JL (1999) Modulation of respiratory frequency by peptidergic input to rhythmogenic neurons in the preBotzinger complex. *Science* 286:1566-1568.
- Greer JJ, Smith JC, Feldman JL (1992) Respiratory and locomotor patterns generated in the fetal rat brain stem-spinal cord in vitro. *J Neurophysiol* 67:996-999.
- Greer JJ, Funk GD, Ballanyi K (2006) Preparing for the first breath: prenatal maturation of respiratory neural control. *J Physiol* 570:437-444.
- Gross MK, Moran-Rivard L, Velasquez T, Nakatsu MN, Jagla K, Goulding M (2000) Lbx1 is required for muscle precursor migration along a lateral pathway into the limb. *Development* 127:413-424.
- Guyenet PG, Sevigny CP, Weston MC, Stornetta RL (2002) Neurokinin-1 receptor-expressing cells of the ventral respiratory group are functionally heterogeneous and predominantly glutamatergic. *J Neurosci* 22:3806-3816.
- Helke CJ, Adryan KM, Fedorowicz J, Zhuo H, Park JS, Curtis R, Radley HE, Distefano PS (1998) Axonal transport of neurotrophins by visceral afferent and efferent neurons of the vagus nerve of the rat. *J Comp Neurol* 393:102-117.

- Hilaire G, Duron B (1999) Maturation of the mammalian respiratory system. *Physiol Rev* 79:325-360.
- Janczewski WA, Feldman JL (2006) Distinct rhythm generators for inspiration and expiration in the juvenile rat. *J Physiol* 570:407-420.
- Johnson SM (2006) PreBötzinger Complex neurokinin-1 receptor expressing neurons in primary cell culture. *Oxford Conference on Modeling and Control of Breathing: Integration in Respiratory Control from Genes to Systems*.
- Kobayashi K, Lemke RP, Greer JJ (2001) Ultrasound measurements of fetal breathing movements in the rat. *J Appl Physiol* 91:316-320.
- Kobayashi M, Taniura H, Yoshikawa K (2002) Ectopic expression of neccdin induces differentiation of mouse neuroblastoma cells. *J Biol Chem* 277:42128-42135.
- Koshiya N, Smith JC (1999) Neuronal pacemaker for breathing visualized in vitro. *Nature* 400:360-363.
- Kuwajima T, Nishimura I, Yoshikawa K (2006) Neccdin promotes GABAergic neuron differentiation in cooperation with *Dlx* homeodomain proteins. *J Neurosci* 26:5383-5392.
- Kuwako K, Taniura H, Yoshikawa K (2004) Neccdin-related MAGE proteins differentially interact with the E2F1 transcription factor and the p75 neurotrophin receptor. *J Biol Chem* 279:1703-1712.
- Kuwako K, Hosokawa A, Nishimura I, Uetsuki T, Yamada M, Nada S, Okada M, Yoshikawa K (2005) Disruption of the paternal neccdin gene diminishes TrkA signaling for sensory neuron survival. *J Neurosci* 25:7090-7099.
- Lamballe F, Smeyne RJ, Barbacid M (1994) Developmental expression of *trkC*, the neurotrophin-3 receptor, in the mammalian nervous system. *J Neurosci* 14:14-28.
- Lee S, Walker CL, Karten B, Kony SL, Tennese AA, O'Neill MA, Wevrick R (2005) Essential role for the Prader-Willi syndrome protein neccdin in axonal outgrowth. *Hum Mol Genet* 14:627-637.

- Liu YY, Ju G, Wong-Riley MT (2001) Distribution and colocalization of neurotransmitters and receptors in the pre-Botzinger complex of rats. *J Appl Physiol* 91:1387-1395.
- Masuda Y, Sasaki A, Shibuya H, Ueno N, Ikeda K, Watanabe K (2001) Dlxin-1, a novel protein that binds Dlx5 and regulates its transcriptional function. *J Biol Chem* 276:5331-5338.
- Monteau R, Ptak K, Broquere N, Hilaire G (1996) Tachykinins and central respiratory activity: an in vitro study on the newborn rat. *Eur J Pharmacol* 314:41-50.
- Muller T, Brohmann H, Pierani A, Heppenstall PA, Lewin GR, Jessell TM, Birchmeier C (2002) The homeodomain factor *lhx1* distinguishes two major programs of neuronal differentiation in the dorsal spinal cord. *Neuron* 34:551-562.
- Onimaru H, Homma I (2002) Development of the rat respiratory neuron network during the late fetal period. *Neurosci Res* 42:209-218.
- Onimaru H, Homma I (2003) A novel functional neuron group for respiratory rhythm generation in the ventral medulla. *J Neurosci* 23:1478-1486.
- Onimaru H, Homma I (2005) Developmental changes in the spatio-temporal pattern of respiratory neuron activity in the medulla of late fetal rat. *Neuroscience* 131:969-977.
- Onimaru H, Kumagawa Y, Homma I (2006a) Respiration-related rhythmic activity in the rostral medulla of newborn rats. *J Neurophysiol*.
- Onimaru H, Homma I, Feldman JL, Janczewski WA (2006b) Point:Counterpoint: The parafacial respiratory group (pFRG)/pre-Botzinger complex (preBotC) is the primary site of respiratory rhythm generation in the mammal. *J Appl Physiol* 100:2094-2098.
- Pagliardini S, Ren J, Greer JJ (2003) Ontogeny of the pre-Botzinger complex in perinatal rats. *J Neurosci* 23:9575-9584.

- Pagliardini S, Adachi T, Ren J, Funk GD, Greer JJ (2005) Fluorescent tagging of rhythmically active respiratory neurons within the pre-Botzinger complex of rat medullary slice preparations. *J Neurosci* 25:2591-2596.
- Panganiban G, Rubenstein JL (2002) Developmental functions of the Distal-less/Dlx homeobox genes. *Development* 129:4371-4386.
- Pattyn A, Goridis C, Brunet JF (2000) Specification of the central noradrenergic phenotype by the homeobox gene Phox2b. *Mol Cell Neurosci* 15:235-243.
- Pena F, Ramirez JM (2004) Substance P-mediated modulation of pacemaker properties in the mammalian respiratory network. *J Neurosci* 24:7549-7556.
- Pena F, Parkis MA, Tryba AK, Ramirez JM (2004) Differential contribution of pacemaker properties to the generation of respiratory rhythms during normoxia and hypoxia. *Neuron* 43:105-117.
- Phelps PE, Brennan LA, Vaughn JE (1990) Generation patterns of immunocytochemically identified cholinergic neurons in rat brainstem. *Brain Res Dev Brain Res* 56:63-74.
- Ptak K, Di Pasquale E, Monteau R (1999) Substance P and central respiratory activity: a comparative in vitro study on foetal and newborn rat. *Brain Res Dev Brain Res* 114:217-227.
- Ptak K, Zummo GG, Alheid GF, Tkatch T, Surmeier DJ, McCrimmon DR (2005) Sodium currents in medullary neurons isolated from the pre-Botzinger complex region. *J Neurosci* 25:5159-5170.
- Ren J, Greer JJ (2003) Ontogeny of rhythmic motor patterns generated in the embryonic rat spinal cord. *J Neurophysiol* 89:1187-1195.
- Ren J, Lee S, Pagliardini S, Gerard M, Stewart CL, Greer JJ, Wevrick R (2003) Absence of Ndn, encoding the Prader-Willi syndrome-deleted gene necdin, results in congenital deficiency of central respiratory drive in neonatal mice. *J Neurosci* 23:1569-1573.
- Rigatto H (1992) Maturation of breathing. *Clin Perinatol* 19:739-756.

- Rigatto H (1996) Regulation of fetal breathing. *Reprod Fertil Dev* 8:23-33.
- Rigatto H, Fitzgerald SC, Willis MA, Yu C (1992) In search of the central respiratory neurons: II. Electrophysiologic studies of medullary fetal cells inherently sensitive to CO<sub>2</sub> and low pH. *J Neurosci Res* 33:590-597.
- Ringstedt T, Lagercrantz H, Persson H (1993) Expression of members of the trk family in the developing postnatal rat brain. *Brain Res Dev Brain Res* 72:119-131.
- Rybak IA, Ptak K, Shevtsova NA, McCrimmon DR (2003) Sodium currents in neurons from the rostroventrolateral medulla of the rat. *J Neurophysiol* 90:1635-1642.
- Suzue T (1984) Respiratory rhythm generation in the in vitro brain stem-spinal cord preparation of the neonatal rat. *J Physiol* 354:173-183.
- Takazaki R, Nishimura I, Yoshikawa K (2002) Necdin is required for terminal differentiation and survival of primary dorsal root ganglion neurons. *Exp Cell Res* 277:220-232.
- Taniura H, Taniguchi N, Hara M, Yoshikawa K (1998) Necdin, a postmitotic neuron-specific growth suppressor, interacts with viral transforming proteins and cellular transcription factor E2F1. *J Biol Chem* 273:720-728.
- Tcherpakov M, Bronfman FC, Conticello SG, Vaskovsky A, Levy Z, Niinobe M, Yoshikawa K, Arenas E, Fainzilber M (2002) The p75 neurotrophin receptor interacts with multiple MAGE proteins. *J Biol Chem* 277:49101-49104.
- Thoby-Brisson M, Ramirez JM (2001) Identification of two types of inspiratory pacemaker neurons in the isolated respiratory neural network of mice. *J Neurophysiol* 86:104-112.
- Thoby-Brisson M, Telgkamp P, Ramirez JM (2000) The role of the hyperpolarization-activated current in modulating rhythmic activity in the isolated respiratory network of mice. *J Neurosci* 20:2994-3005.
- Thoby-Brisson M, Trinh JB, Champagnat J, Fortin G (2005) Emergence of the pre-Botzinger respiratory rhythm generator in the mouse embryo. *J Neurosci* 25:4307-4318.

- Viemari JC, Burnet H, Bevengut M, Hilaire G (2003) Perinatal maturation of the mouse respiratory rhythm-generator: in vivo and in vitro studies. *Eur J Neurosci* 17:1233-1244.
- Wenninger JM, Pan LG, Klum L, Leekley T, Bastastic J, Hodges MR, Feroah T, Davis S, Forster HV (2004a) Small reduction of neurokinin-1 receptor-expressing neurons in the pre-Botzinger complex area induces abnormal breathing periods in awake goats. *J Appl Physiol* 97:1620-1628.
- Wenninger JM, Pan LG, Klum L, Leekley T, Bastastic J, Hodges MR, Feroah TR, Davis S, Forster HV (2004b) Large lesions in the pre-Botzinger complex area eliminate eupneic respiratory rhythm in awake goats. *J Appl Physiol* 97:1629-1636.
- Yamamoto Y, Onimaru H, Homma I (1992) Effect of substance P on respiratory rhythm and pre-inspiratory neurons in the ventrolateral structure of rostral medulla oblongata: an in vitro study. *Brain Res* 599:272-276.
- Zanella S, Roux JC, Viemari JC, Hilaire G (2005) Possible modulation of the mouse respiratory rhythm generator by A1/C1 neurones. *Respir Physiol Neurobiol*.